MAINLINE

MAINtenance, renewal and Improvement of rail transport iNfrastructure to reduce Economic and environmental impacts

Collaborative project (Small or medium-scale focused research project)

Theme SST.2011.5.2-6.: Cost-effective improvement of rail transport infrastructure

Deliverable 2.2:
Degradation and intervention modelling techniques

Grant Agreement number: 285121 SST.2011.5.2-6.

Start date of project: 1 October 2011 Duration: 36 months

Lead beneficiary of this deliverable: SETRA

Due date of deliverable: 31/12/2012 Actual submission date: 06/06/2013

Release: Final

Project co-funded by the European Commission within the 7th Framework Programme		
Dissemination Level		
PU	Public	X
PP	Restricted to other programme participants (including the Commission Services)	
RE	Restricted to a group specified by the consortium (including the Commission Services)	
CO	Confidential, only for members of the consortium (including the Commission Services)	

Abstract of the MAINLINE Project

Growth in demand for rail transportation across Europe is predicted to continue. Much of this growth will have to be accommodated on existing lines that contain old infrastructure. This demand will increase both the rate of deterioration of these elderly assets and the need for shorter line closures for maintenance or renewal interventions. The impact of these interventions must be minimized and will also need to take into account the need for lower economic and environmental impacts. New interventions will need to be developed along with additional tools to inform decision makers about the economic and environmental consequences of different intervention options being considered.

MAINLINE proposes to address all these issues through a series of linked work packages that will target at least €300m per year savings across Europe with a reduced environmental footprint in terms of embodied carbon and other environmental benefits. It will:

- Apply new technologies to extend the life of elderly infrastructure
- Improve degradation and structural models to develop more realistic life cycle cost and safety models
- Investigate new construction methods for the replacement of obsolete infrastructure
- Investigate monitoring techniques to complement or replace existing examination techniques
- Develop management tools to assess whole life environmental and economic impact.

The consortium includes leading railways, contractors, consultants and researchers from across Europe, including from both Eastern Europe and the emerging economies. Partners also bring experience on approaches used in other industry sectors which have relevance to the rail sector. Project benefits will come from keeping existing infrastructure in service through the application of technologies and interventions based on life cycle considerations. Although MAINLINE will focus on certain asset types, the management tools developed will be applicable across a broader asset base.

Partners in the MAINLINE Project

UIC, FR; Network Rail Infrastructure Limited, UK; COWI, DK; SKM, UK; University of Surrey, UK; TWI, UK; University of Minho, PT; Luleå tekniska universitet, SE; DB Netz AG, DE; MÁV Magyar Államvasutak Zrt, HU; Universitat Politècnica de Catalunya, ES; Graz University of Technology, AT; TCDD, TR; Damill AB, SE; COMSA EMTE, ES; Trafikverket, SE; SETRA, FR; ARTTIC, FR; Skanska a.s., CZ.

WP2 in the MAINLINE Project

The main objectives of work package WP2 'Degradation and structural models to develop realistic life cycle cost and safety models' are the following:

- To identify and model important degradation phenomena and processes for selected railway assets for the purpose of LCC and LCA analysis.
- To quantify the influence of intervention strategies on degradation time profiles.
- To develop performance time profiles for selected asset types.
- To validate the developed degradation and performance models through case studies.

 Copyright © MAINLINE Consortium

Table of Contents

 Copyright © MAINLINE Consortium

 Copyright © MAINLINE Consortium

Table of Figures

 Copyright © MAINLINE Consortium

 Copyright © MAINLINE Consortium

Table of Tables

 Copyright © MAINLINE Consortium

Glossary

Abbreviation / acronym	Description
DoW	Description of Work
DRF	Dose Response Function
IM	Infrastructure Manager
LCAT	Life Cycle Assessment Tool
RRSRH	Rail Rock Slope Risk Apraisal
RSHI	Rock Slope Hazard Index
SSHI	Soil Slope Hazard Index
WP	Work Package

 Copyright © MAINLINE Consortium

1. Executive summary

1.1 Basis

The first deliverable of WP2 (D2.1: Degradation and Performance Specification for Selected Assets) constitutes the baseline for D2.2. Deliverable D2.1 was completed in February 2012.

1.2 Important definitions

The following definitions are highlighted:

- Deterioration describes how the condition of the asset gets worse.
- Degradation is a summary of deterioration and damage.
- Performance profile is a time dependent representation of previous and future load and resistance distribution of an asset. Performance profiles can be benchmarked against an acceptable level of performance.

1.3 Target reader

The target reader of this deliverable is a structural engineer experienced in assessment and/or inspection of railway infrastructural elements.

1.4 Content

The main chapters of this deliverable cover deterioration models for:

- Track (plain line only) – chapter 5
- Metallic bridges (two types) – chapter 6
- Cuttings (in soil only) – chapter 7
- Corrosion and coatings – chapter 8
- Tunnels with masonry linings and concrete linings – chapter 9

 Copyright © MAINLINE Consortium

2. General remarks

The project 'MAINtenance, renewaL and Improvement of rail transport iNfrastructure to reduce Economic and environmental impacts' (in short MAINLINE) is an integrated project within the 7th Framework Programme. It has been financed on the basis of the contract SST.2011.5.2-6 between the European Community represented by the Commission of the European Communities and International Union of Railways (UIC) acting as coordinator of the project.

The main objectives of the project are:

- apply new technologies to extend the life of elderly infrastructure
- improve degradation and structural models to develop more realistic life cycle cost and safety models
- investigate new construction methods for the replacement of obsolete infrastructure
- investigate monitoring techniques to complement or replace existing examination techniques
- develop management tools to assess whole life environmental and economic impact

The present report D2.2 - Degradation and intervention modelling techniques has been prepared within the work package WP2 (from month M4 to month M15) of the MAINLINE project, named 'Degradation and structural models to develop realistic life cycle cost and safety models', one of the eight work packages WP1-WP8 dealing with relevant tasks for maintenance, renewal and improvement of rail transport infrastructure to reduce economic and environmental impacts.

WP2 interacts with WP1, WP4 and WP5. The interaction with WP1 consists of inputs for degradation and performance models that will be developed within WP1 and will also be utilised within WP2. The two-way interaction with WP4 is focused on identifying model parameters for the degradation and structural models that would benefit (in terms of the confidence with which they can be specified in models) through monitoring and examination. The main outputs from WP2 in terms of time-dependent performance profiles will be passed on to WP5.

An overview of the general organisation of the project is presented below together with the list of all the partners in the work package WP2.

 Copyright © MAINLINE Consortium

General organisation of the project

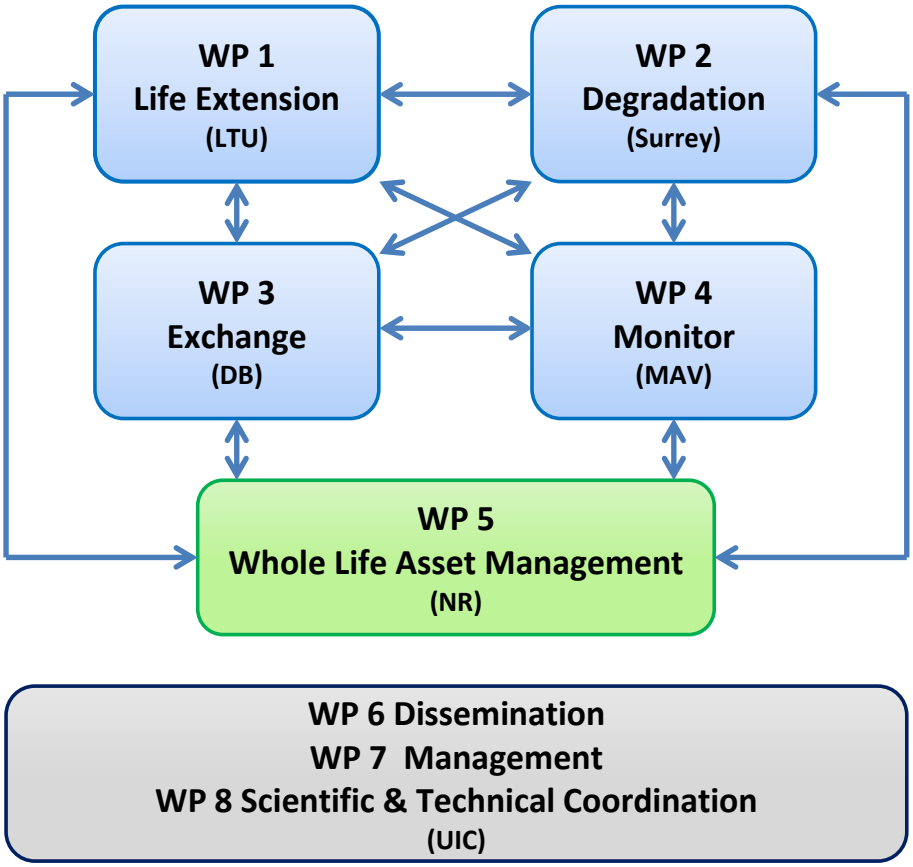

Figure 2-1 General organisation of the project. UIC, Surrey, MAV and NR are listed below. DB is Deutche Bahn AG (Germany) and LTU is Lulea Tekniska Universitet (Sweden).

Part n°	WP2 Partners	Country
1	UNION INTERNATIONALE DES CHEMINS DE FER - UIC	FR
2	NETWORK RAIL INFRASTRUCTURE LTD	UK
3	COWI A/S	DK
4	SINCLAIR KNIGHT MERZ	UK
5	UNIVERSITY OF SURREY	UK
6	TWI LIMITED	UK
10	MAV MAGYAR ALLAMVASUTAK ZARTKORUEN MUKODO RT	HU
12	TECHNISCHE UNIVERSITAET GRAZ	AT
17	SERVICE D'ETUDES SUR LES TRANSPORTS, LES ROUTES ET LEURS AMENAGEMENTS	FR

Copyright © MAINLINE Consortium

3. Acknowledgments

This present report has been prepared within the work package WP2 of the MAINLINE project by the following team of contractors with University of Surrey as the work package leader:

- Network Rail (NR), United Kingdom
- Sinclair Knight Merz (SKM), United kingdom
- University of Surrey (Surrey), United Kingdom
- TWI Limited (TWI), United kingdom
- MAV Magyar Allamvasutak Zartkoruen Mukodo RT (MAV), Hungary
- Technische Universitaet Graz (TUGraz), Austria
- Service d'Etudes sur les Transports, les Routes et leurs Aménagements (SETRA), France

The guidance of the WP2's scientific leader Professor Marios Chryssanthopoulos of University of Surrey was greatly appreciated.

 Copyright © MAINLINE Consortium

4. Introduction

4.1 Background and motivation

Deliverable D2.1 “Degradation and performance specification for selected assets“ has specified relevant degradation and performance states for selected assets to be given special focus in the MAINLINE project which aims at the enhancement of degradation and performance models to provide a step change in safe, cost effective management and/or life extension of these assets.

The following asset types have been identified as focus areas:

- Cuttings (soil and rock),
- Metallic bridges,
- Tunnels with concrete and masonry linings,
- Plain line (total track superstructure) and switches of crossings,
- Retaining walls.

These assets have been analyzed in terms of scientific and technical knowledge and available data. The objective of deliverable D2.2 is to provide the principles of deterioration models and intervention effects for defining time performance profiles (deliverable D2.3) that will be used in Workpackage WP5. Consequently, the work has been focused on assets that were able to give sufficient data for the LCAT tool (WP5).

In order to successfully create a Life Cycle Asset Tool (LCAT) it is essential to have extensive data from which projections of the performance of the asset can be made; without such data, a useful LCAT system is impossible to build. Recent research has shown that there are limitations to the data available for some assets types, as described below. In this context, data refers to degradation and performance models, as well as laboratory and field observations on degradation states over time collected through experimental studies or in-service inspections.

4.1.1 Data on Cuttings

There is extensive data available, from Network Rail in UK, on Soil Cuttings which has formed the basis for performance modelling. In the first instance only cuttings in cohesive soils have been dealt with, but the analysis could be extended to granular soils in a future development.

Rock cuttings are found to be very varied in nature and their failure mechanisms are difficult to evaluate. Although there is data on rock cuttings, also available from Network Rail, it is not easy to analyse because of its complexity. For this reason we recommend that rock cuttings are not taken forward for the LCAT development. Rock cuttings are therefore not analysed in this document.

 Copyright © MAINLINE Consortium

4.1.2 Data on Metallic bridges

In view of the varied structural forms of metallic bridges, it is recommended that the performance of a limited sub-set of bridge types is pursued at this stage. The two common forms selected are steel 'half-through' bridges of spans 5-15 m, and steel trusses of span 15-50 m.

4.1.3 Data on Tunnels

Some data on masonry-lined tunnels is available from Network Rail in UK and this has been assessed for inclusion in the LCAT model. With regard to concrete-lined tunnels, modelling techniques that have been developed and validated for reinforced concrete bridge can be adapted but the availability of field degradation data pertaining to tunnels per se is limited. In this respect, validation of models appears difficult but will be kept under review during development of the LCAT.

4.1.4 Data on Track

Extensive data on track performance from the Austrian railway network has been collected and analysed by TU Graz. This has been used in this document for forecasting the performance of track but, in the first instance, only plain track will be assessed, with switches and crossings treated in a possible future development.

4.1.5 Retaining walls

There is no evidence that data on retaining walls is collected systematically in any European countries and therefore it is not possible to develop deterioration and performance profiles for these assets. We recommend that retaining walls is dropped as an asset type to be modelled.

4.2 Scope of deliverable D2.2

It is therefore recommended that, in the first instance, deterioration data and models are developed for:

- Cuttings (in soil only),
- Metallic bridges (two types),
- Tunnels with masonry linings and concrete linings,
- Track (plain line only)

Nevertheless, for all the asset types mentioned in D2.1, there is a high probability for knowledge increase within a 3 year period and useful validation data may become available.

For the four asset types listed above degradation models, where available, are presented in this deliverable, whereas associated performance characteristics and limit states have been addressed in deliverable ML-D2.1 (2012). Furthermore, the temporal and spatial characteristics of the degradation mechanisms are investigated in order to facilitate the

 Copyright © MAINLINE Consortium

development of performance profiles for the selected asset types. It is important to make the distinction here between condition-governed and capacity-governed performance profiles. For the former, the degradation profiles can be eventually used as performance profiles; for the latter, additional steps are required involving structural analysis and assessment, e.g. evaluating the bending resistance of a bridge girder with thickness loss due to corrosion. In that sense, the present deliverable presents models that can be valuable for deliverable D2.3 that will be dedicated to the development of performance profiles.

The above tasks are performed with due attention to the overall aim of WP2 that is to develop and validate the required degradation and performance time-dependent models, including appropriate intervention strategies for realistic LCC and LCA analysis to be carried out in WP5.

4.3 References

ML-D2.1 (2012), Degradation and performance specification for selected assets, Deliverable 2.1, MAINLINE project, SST.2011.5.2-6, 31/01/2012, 113 pp.

 Copyright © MAINLINE Consortium

5. Tracks (TU Graz)

5.1 Track quality and deterioration

Reducing the experiences of track engineers to a common denominator, it can be stated that a good track behaves well, while a poorer one deteriorates faster. Expressed in mathematical terms, this means that the quality loss is a function of the actual track quality. This is described by a differential equation showing that the quality behaviour over time follows an exponential function:

$$Q(t) = Q_i \exp(b\,t) \tag{5.1}$$

It is obvious that the initial quality at the point of time zero defines the quality behaviour to an enormous degree. Unfortunately this simple function is not so simple since the deterioration rate *b* is also a function including the influence of all boundary conditions such as transport volume, superstructure, and substructure… It is also a fact that maintenance actions increase quality without resulting as a 'new track'. The loss of quality compared to the initial one is thereby a question of the intervention levels. The quality behaviour over time ends up in a model describing quality behaviour over time (Fig.5.1).

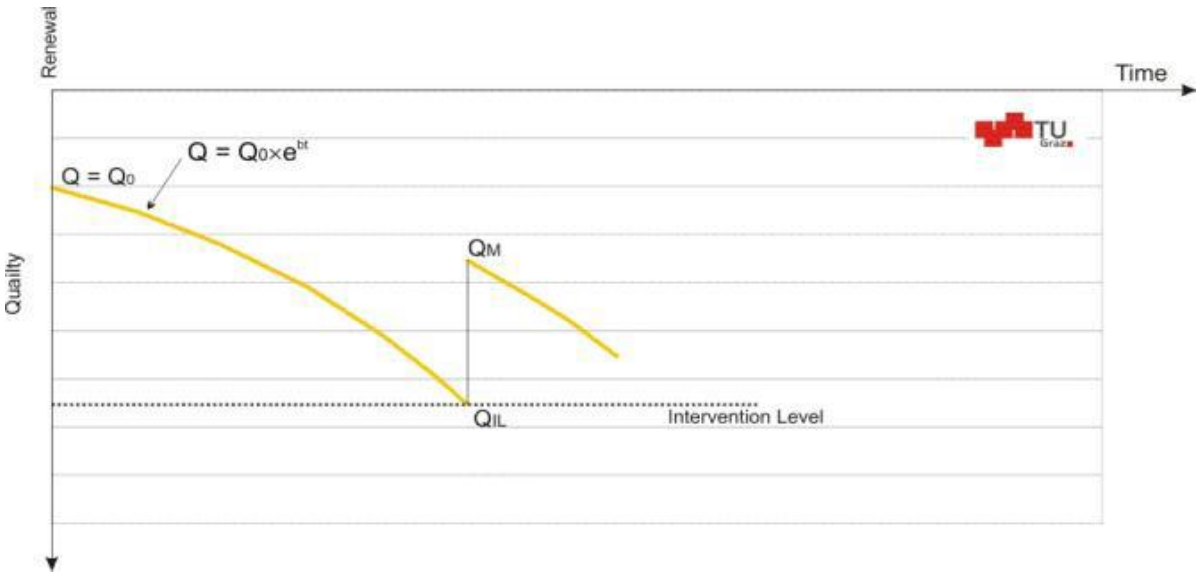

Figure 5-1 Track quality index – theoretical curve.

The theoretical curve of Fig.5.1 can be easily explained: the better the quality, the less the dynamic forces. Lower forces lead to minor problems while higher ones caused by track irregularities increase the growth of these track failures. Nevertheless this requires to be checked. Thus, before going further, it is important to be precise about what is meant by track quality.

5.1.1 Track quality

A background to track engineering is given in Esveld (2001) and Lichtberger (2005).In general riding quality for tracks is characterized by standard deviations. Indeed, the vertical standard deviation or a mix of vertical and horizontal standard deviations is used to describe the roughness of a track and thus riding quality and riding comfort. Therefore the intervention level is a comfort driven value not a safety limit.

 Copyright © MAINLINE Consortium

However, it is obvious that the quality demand for riding comfort depends on the train speed. For low speed levels a specific standard deviation leads to a better riding comfort than for high speed levels. This influence is not reflected within a standard deviation. Speed dependent threshold values are therefore necessary. The approach described in this chapter is based on another riding quality index, so called MDZ (for Mechanized Tamping Train in German). This index describes the roughness of a track or the riding quality based on accelerations in the car body. More precisely, within this quality data the differences of the accelerations in a short distance are summed up and referred to a point as a gliding mean value for 100 m of track length. The ideal track can be calculated for a zero MDZ index value.

$$\mathrm{MDZ} = V^{0.65}\,\frac{1}{L}\sum_{0}^{L}\mathrm{Diff}\left(\sqrt{v^2+\left(h+\Delta^2 u\right)^2}\right) \qquad (5.2)$$

with

- MDZ: riding quality
- V: speed [m/s]
- L: gliding influence length [m]
- v: vertical track failure [mm]
- h: horizontal track failure [mm]
- Δu: super-elevation failure [mm]

This value allows to take into account all track irregularities (vertical and horizontal ones). Failures cause accelerations in the train; recalculating the riding quality for different train speeds is thus possible. To make the results of this Austrian research comparable with international approaches, all the evaluations have been based on vertical standard deviation (mainly used in Europe) and MDZ. The results do not differ significantly, but some details can be more easily identified with the MDZ quality index.However, maintenance planning requires knowledge about the development of this index over time. This knowledge is the prerequisite to switch towards more preventive and less corrective maintenance activities.

5.1.2 Fitting track quality

To handle all the data available and the discrepancies among data structures and data recording and analysis, it is necessary to implement all track data to a data warehouse, i.e. recording car data, operational data of the track sections, information on the type and age of the track components, information on the executed maintenance, data on the position of turnouts, stations, embankments and cuts, alignment information, sub-soil information... All these data are organized in the warehouse and time rows are therefore available from year 2000 onwards.

Based on the riding quality data of the recording car, all exponential functions (Eq.5.1) and thus, the real behaviour of track, were calculated every 5 m covering the whole core network of the Austrian Federal Railways (OeBB) with 3,800 km track length and resulting in about 3 million functions. In Fig.5.2, the deterioration of track quality at one specific track position is depicted over a period from 2001 to 2007. The theoretical exponential function is in good accordance with the real track behaviour since the measured track indexes (dots) are well fitted by Eq.5.1. The vertical lines present the tamping actions.

 Copyright © MAINLINE Consortium

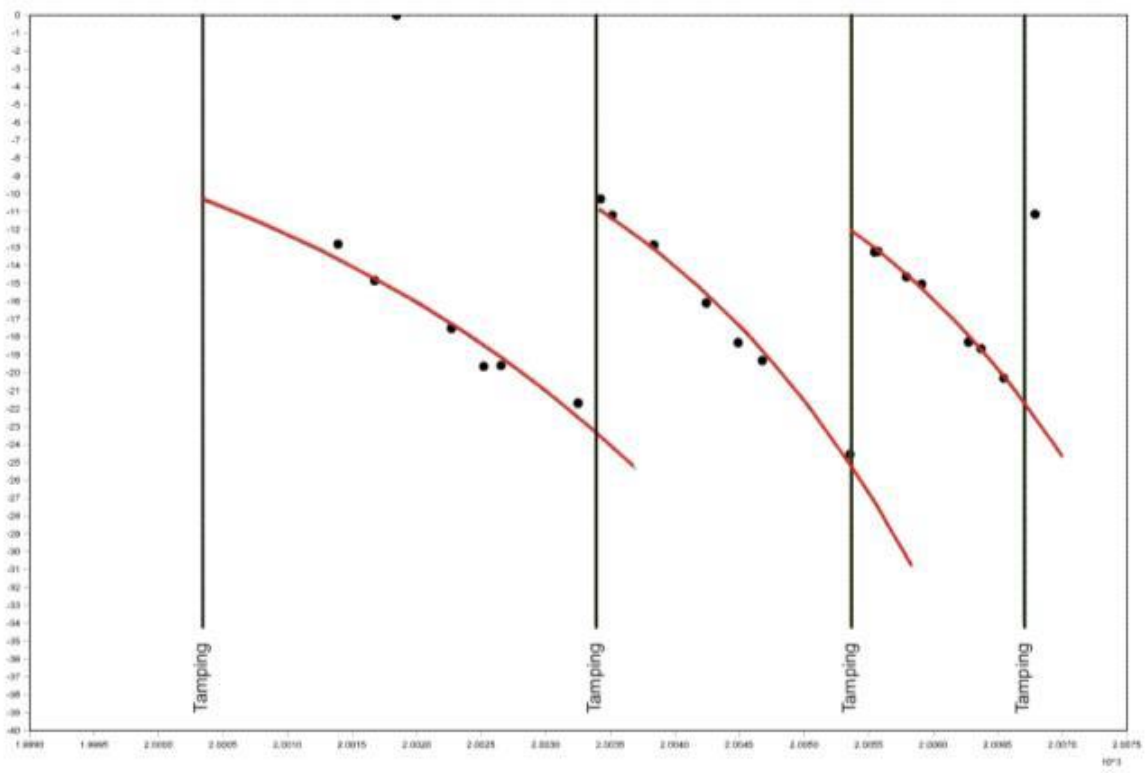

Figure 5-2 Track quality behaviour – practical experience.

Nevertheless, the deterioration rate b depends on many parameters: transport load, train speed, sub-grade quality, track superstructure, functionality of dewatering system... Therefore, the rate of deterioration varies within a wide range for different track sections.

The above database allows the analysis of the deterioration function in identifying interrelations between the rates of deterioration and the different track conditions. But, the most important result is that track quality behaviour is non-linear, thus justifying a posteriori the choice of an exponential function.

5.1.3 Initial track quality

There is a high influence of the initial track quality as shown schematically in Fig.5.3.

High initial qualities lead to low track irregularities, resulting in lower dynamic forces and hence on slower deterioration. However, a high initial quality can be delivered by a general renewal only. If all track components are replaced, all of them will get back to their initial quality levels and will provide a high initial quality for the entire system track. If only some individual components are replaced, new components will be mixed with old ones and different quality levels will be merged, resulting in a lower global quality track level.

 Copyright © MAINLINE Consortium

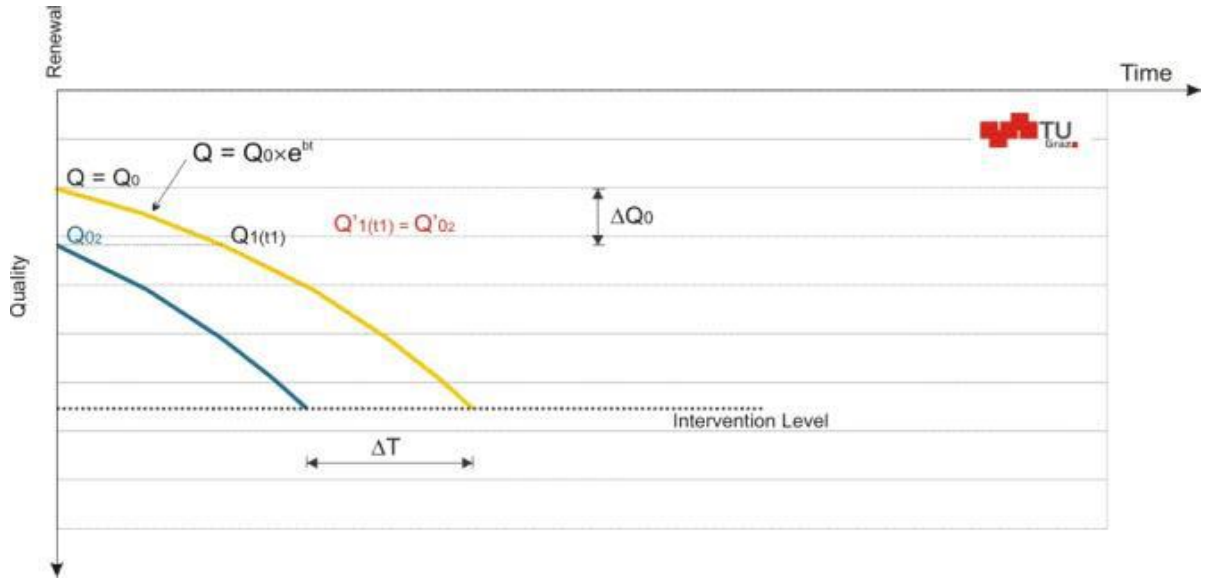

Figure 5-3 Influence of initial track quality.

5.1.4 Threshold quality levels

Intuitively, threshold levels can be determined by optimizing installation/replacement costs (for high initial quality) versus reduced maintenance costs could be a solution. This is nevertheless not so simple because the level of the initial quality and the maintenance activities are both influencing the service lifetime of the track: high initial quality leads to long service life, but earlier maintenance activities will maintain the quality close to the original one. A maintenance action will be efficient if it is performed a long time before a failure stamps into the superstructure (Fig.5.4).

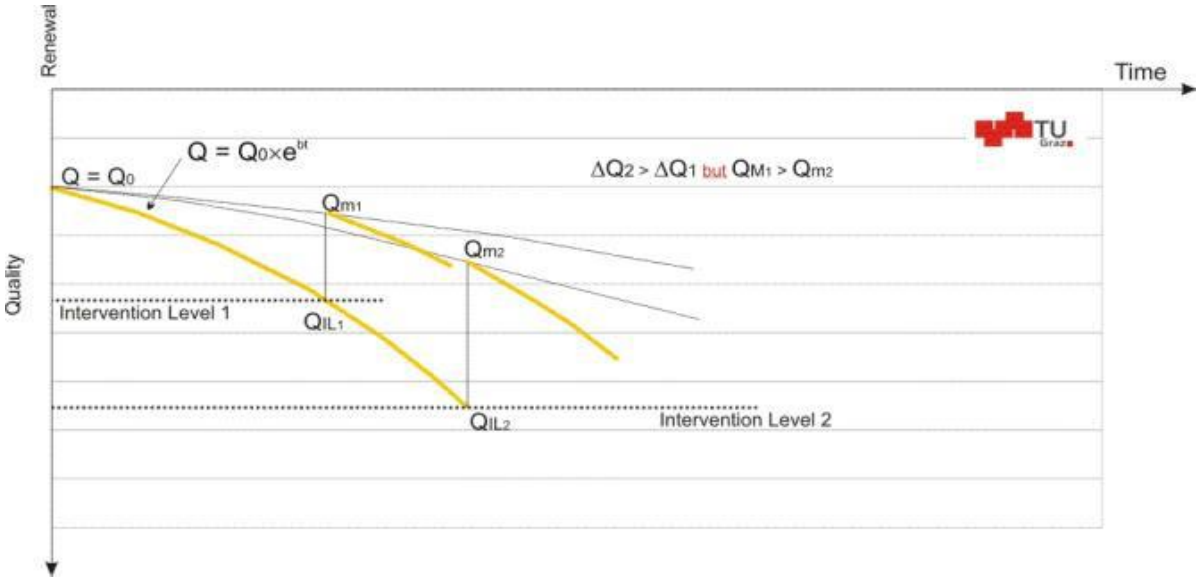

Figure 5-4 Influence of threshold values.

It is also possible to optimize deterioration versus an increased maintenance demand. Again, this may be not appropriate since the threshold values affect the service life of the track. A constant high intervention level reduces deterioration but unfortunately service life as well. Thus a so-called “conform intervention level” is proposed, based on the idea that the intervention level itself must depend on track age (Fig.5.5). In order to generate low

 Copyright © MAINLINE Consortium

deterioration of track at the early stage, the intervention level is enforcing high quality levels. This reduction of deterioration can be transposed into additional service life by accepting a lower but still acceptable track quality at the end of the track lifetime.

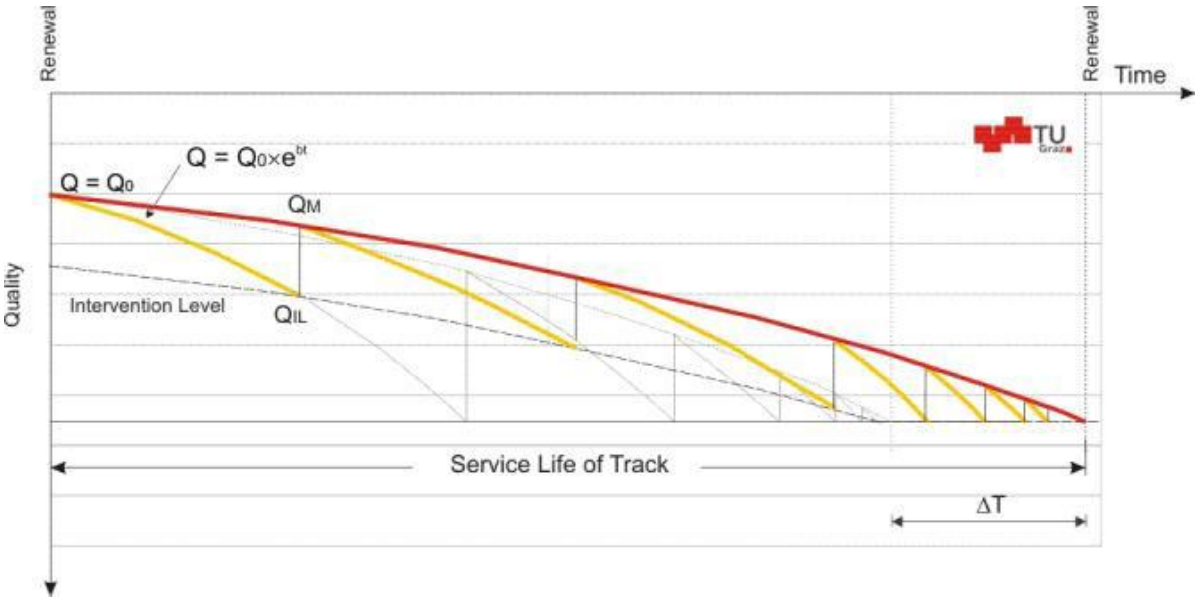

Figure 5-5 Influence of a conform threshold value.

Experience from track operation underlines that the quality of a shared corridor is defined by the fastest train, but quality is also determined by operation, axle loads, construction of superstructure... Thus the question of a proper maintenance regime arises. Even if optimisation from a technical point of view could be challenging, total track costs must be taken into account to deliver reliable and economically feasible track solutions. These solutions will differ significantly due to different edge track conditions.

5.2 Track costs

The influencing parameters shown on Fig.5.6 affect the track quality, maintenance demands and service life, but also the track cost.

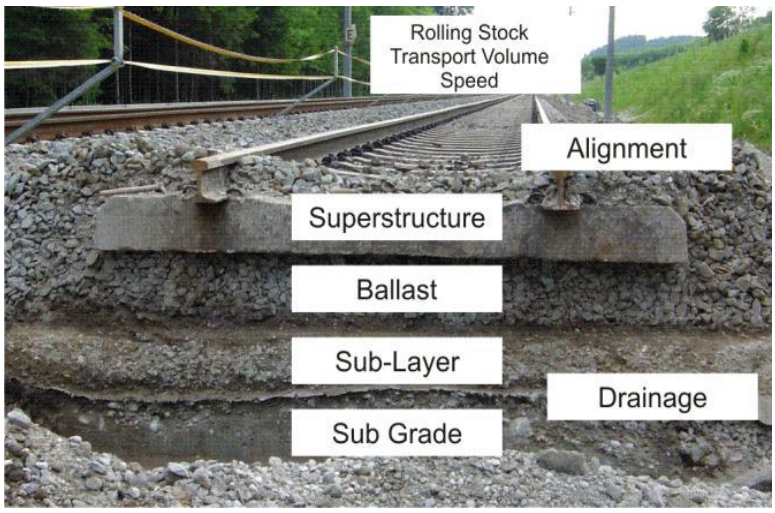

Figure 5-6 Track system.

Fig.5.7 describes the results of track cost analyses in Austria, in shared corridors for an axle load of 22.5 tons over different numbers of trains per day and track. It must be noticed that for the mixed rail transport system in Austria (far distance passenger trains, regional, trains, far distance freight trains, local freight trains) the average weight of a train is only 450 tons. The composition of the total lifecycle cost of a track is depending on the number of trains per

 Copyright © MAINLINE Consortium

day and on track, depicting the average annual costs. In addition to the direct costs of infrastructure interventions, due to the dense use of the Austrian network, track-work causes delays, diverted trains and/or cancelled trains. The resulting costs, called costs of operational hindrances, are integrated in the lifecycle costs.

The analysis of track costs of OeBB (Fig.5.7) shows some significant results concerning the major categories of life cycle costs of track. Half of the total lifecycle costs are fixed costs associated with depreciation1 of the track structure, increasing with decreasing traffic. Up to a third of the total lifecycle costs are related to operational hindrances. For dense lines maintenance costs (direct costs) do not exceed 17%.

However, for tracks facing less operation (less than 70 trains per day and track of double tracks lines) costs of operational hindrances are negligible. This distribution of costs indicates that reducing the lifecycle cost of highly utilised track needs investments for a high initial quality, as this quality extends the service life.

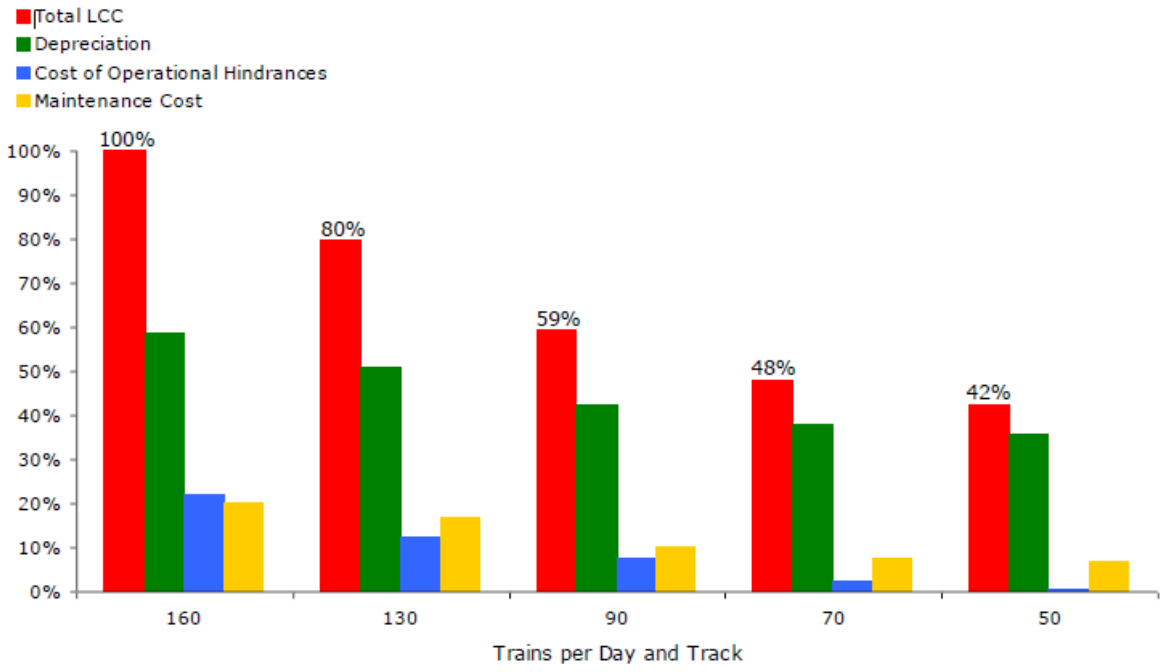

Figure 5-7 Track costs over transport volume.

Regardless of traffic volume, maintenance costs are a small portion of the lifecycle costs compared to depreciation.

On Fig.5.8 different maintenance regimes are discussed on the basis of a dense line (160 trains per day and direction). If permanent slow orders are accepted to extend the service life of the track, the costs of operational hindrances increases. The total cost increases in this case, although the service life is extended: depreciation costs are decreasing.

[1] As regulations of depreciation differs from country to country only costs of track renewal are covered by depreciation while all other costs are summed up to the maintenance costs.

 Copyright © MAINLINE Consortium

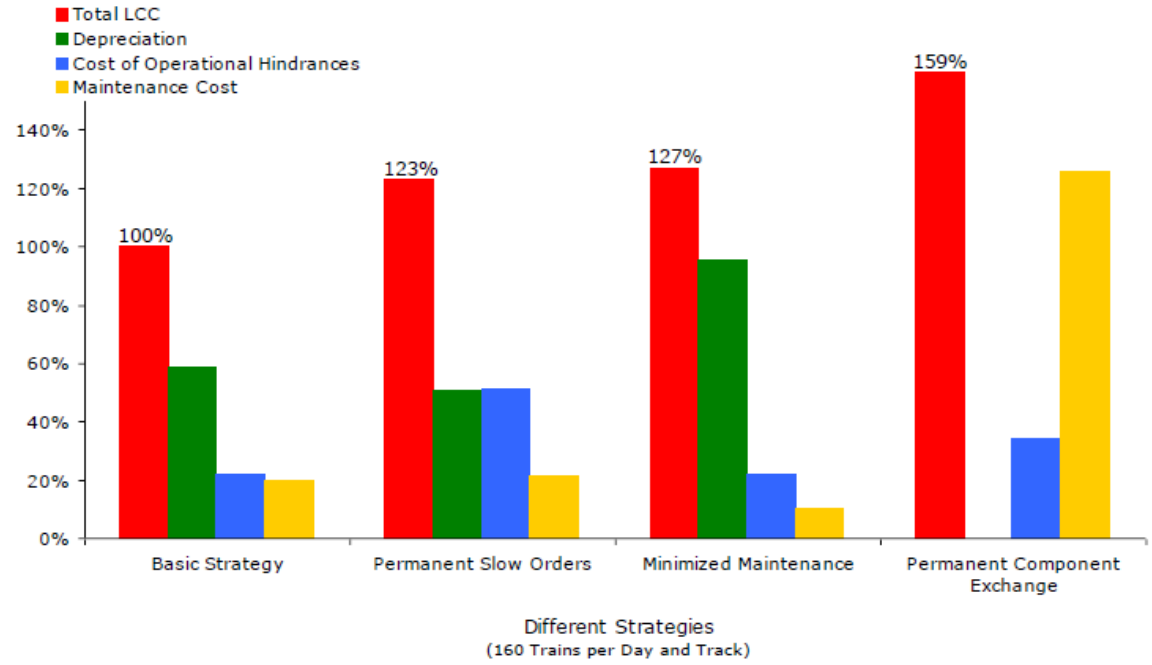

Figure 5-8 Costs of different managements.

Reducing maintenance costs consists in cutting costs at the lowest level: this only provides small savings. Furthermore reducing already low maintenance costs includes the risk of reducing the service life and therefore of increasing total costs.

All these results are strong hints for the economic efficiency in investing for quality and proper maintenance activities. Short-term savings in maintenance will be overcompensated by long-term additional costs. However, these general statements must be proven on different investment and maintenance options, based on track analyses and cost figures. Thus the targets of track renewal and track maintenance can be defined in a simple way:

- the only target of track renewal is to create high initial quality;
- the only target of maintenance action is to transform this quality into service life.

A low initial quality cannot be compensated by maintenance activities for delivering an appropriate service life. In turn, poor maintenance can compromise the value of the track renewal.

5.3 High quality tracks at low costs

The objective in this section is to identify technical solutions for cost-efficient tracks. Therefore all the proposed investment and maintenance actions have to be economically justified. As re-investment is the most costly part of the track management and shows the largest impact on long-term track behaviour, investment strategies are prior-ranked. A 5% rate calculation is used to deliver a cautious evaluation. In order to evaluate the track renewal options, technical consequences of various qualities have been studied and summed up in a list of cost drivers, due to their impact on the total costs:

 Copyright © MAINLINE Consortium

1. The most important cost driver is the initial quality. This especially means the sub-grade quality. Sub-grade quality dominates the behaviour of track. Therefore an excellent substructure quality is a prerequisite for any optimisation;

2. If a sub-grade is badly affected, the dewatering system is less efficient and water is kept in the track. Dewatering devices are integrated parts of the technical track system;

3. Ballast is the critical component that limits the service life of the track. Optimisation within the superstructure requires a good ballast quality[2]. This analysis indicates that sustainable track designs require lower stresses in the ballast bed;

4. The number of turnouts is a main cost driver. The type of trains on shared corridors result in a high number of turnouts, as the number needs to increase with increasing differences of train speeds. In Europe 0.9 turnouts per main track kilometre of shared corridors are usual. Total cost of turnouts reach values 11 to 13 times higher than open track, counted in cost per through going length;

5. Within the alignment the radius is the cost driver, while the gradient seems to have less importance. Especially radii less than 300 m increase track cost three times compared to straight sections;

6. Traffic load has an impact on track costs. However, as long as the track superstructure is designed to carry the load, higher loads have generally small impacts on track costs. High costs occur if a weak superstructure is designed. In general the increase of track costs (in percentage terms) is less than the increase in transport volume (also in percentage terms);

7. This indicates preference for installing heavy track structures;

8. Different qualities of rolling stock result in differences in track costs of up to ±10%. Austria and United Kingdom implemented track access charges for different quality levels of traction units.

A lifecycle cost optimisation based on track behaviour, as described above, allows identification of investment and maintenance strategies.

5.3.1 Sub-grade and dewatering system

As mentioned previously, weak sub-grade is the major cost driver. The annual expenditure for track surface maintenance dramatically increases if old, historically weak embankments are overloaded. Sub-grade rehabilitation is a common method enforcing existing roads to modern needs. To this end a number of technologies have been developed replacing the top sub-grade layer by specially mixed gravel, brought in by work trains, combined with water-

[2]Many railway companies,e.g. in Switzerland have defined different quality demands regarding the ballast according to the number of trains. In Germany and France the best ballast is used for the high speed lines.

 Copyright © MAINLINE Consortium

cleaning the old ballast or edge-sharpening of the ballast particles, producing the required gravel by crushing the old ballast and supply fresh ballast. It must be emphasized that optimisation of track is only possible if sub-grade and dewatering system conditions meet their requirements.

To demonstrate the economic efficiency, track behaviour of sections on different sub-grade qualities have been compared. Really poor sub-grade and drainage conditions on high loaded shared corridors leads to reduced service life, dramatically increased maintenance and even to permanent slow orders ensuring an acceptable (not good) riding quality. The far right bars of Fig.5.9 depict this described poor case in its cost consequences. Note that total life cycle cost increase by the factor 9.5 due to the sub-grade and drainage condition[3]. Thus the additional investment in sub-grade rehabilitation lowers total track cost in a big scale. For lines with lower transport volume these economic values decrease. The calculations show, that implementing an additional sub-layer can be proposed in general with the exception of branch lines operated by few passenger and/or light freight train only.

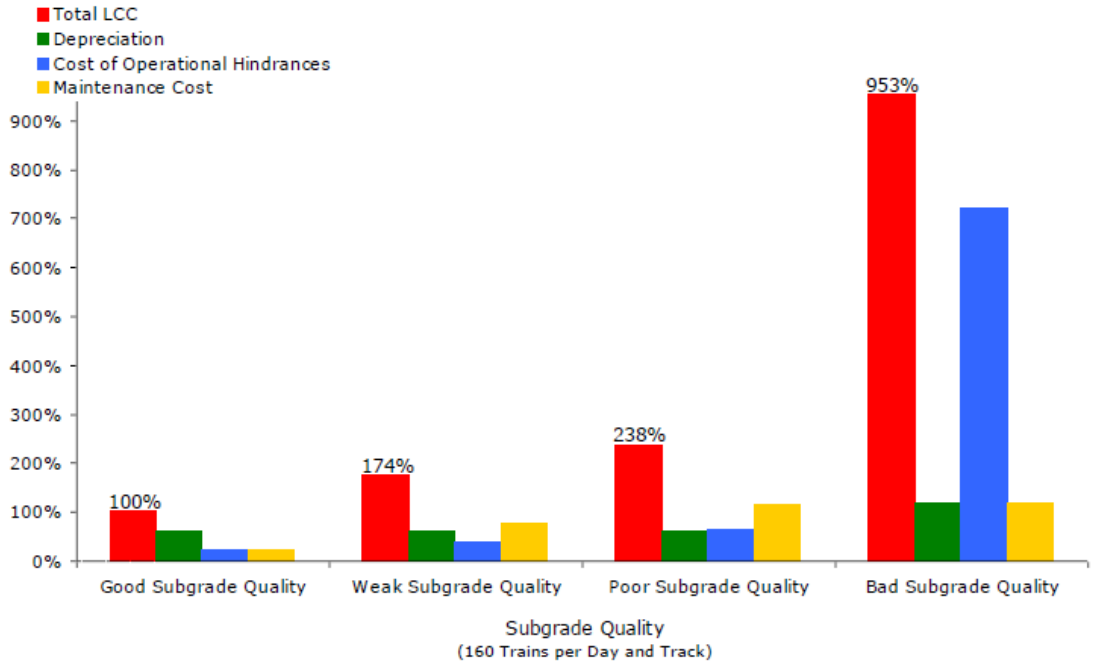

Figure 5-9 Consequences of poor sub-soil.

Another example shows the importance of dewatering of track (Fig.5.10).

[3] This evaluation is based on existing track sequences, meanwhile repaired.

 Copyright © MAINLINE Consortium

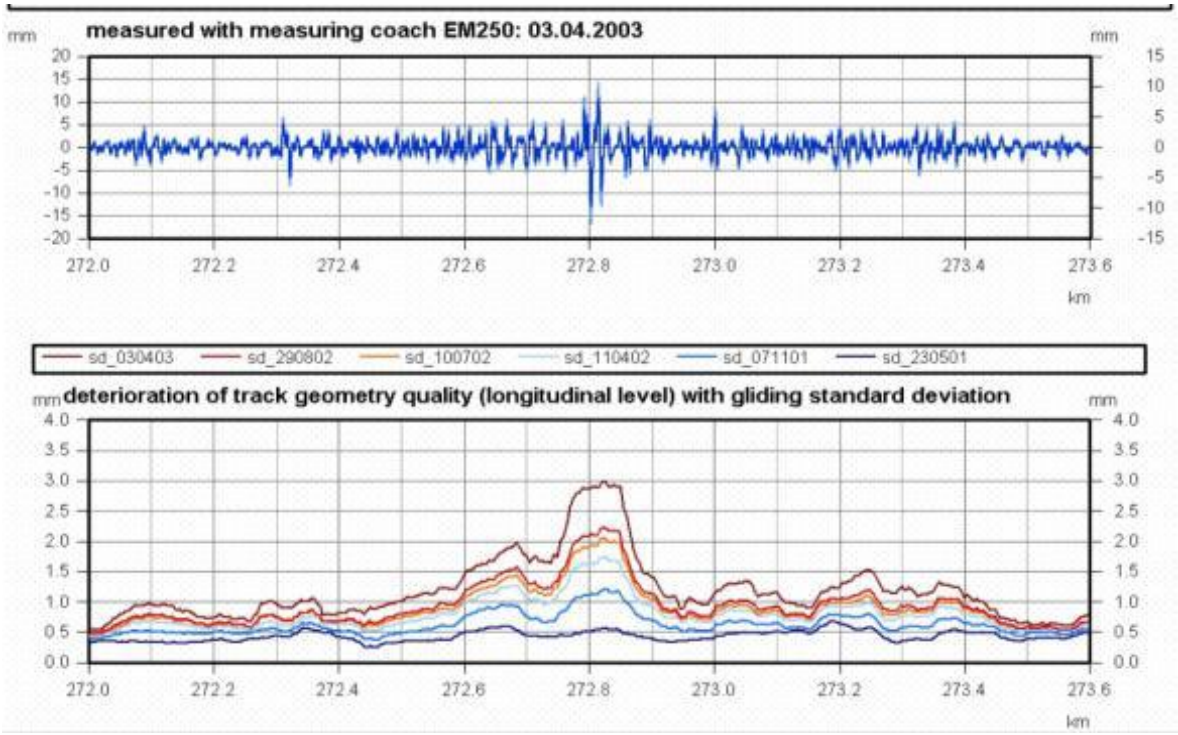

Figure 5-10 Consequences of poor drainage.

In Fig.5.10, vertical standard deviation of a 5 year old track is shown. A single failure occurs in the middle of the section. The reason is water. It was found, that the water was not even in track but just in the ditch. This reduces the loading capacity of sub-grade locally leading to the single failure highlighted by the recording car measurements. Furthermore, high attention must be paid in maintenance to keep the existing drainage systems in a functional condition. The budget spent for these measures is negligible compared to the consequences of doing nothing.

5.3.2 Ballast

Track and laboratory tests show just 3% to 5% of a concrete sleeper is effectively in contact with the ballast surface after tamping. This percentage increases to 9% using a dynamic track stabiliser. Even before the next tamping, and thus after operational wear of ballast, a maximum of 12% contact area is observed only. The hard-to-hard situation in this contact area causes only a few, highly overloaded contact points, which form the starting points for a limited number of “force-paths” through the ballast structure rather than allowing the entire ballast structure to act as a sleeper-support. Edges and corners are quickly cracked off, leading to unpredictable initial settlements. As the number of “force-paths” varies for neighbouring sleepers, the sleepers settle differently, causing initial failures. An increase of the rate of deterioration is the consequence. This is the main reason for the need of high quality ballast, such as basalt or granite.

Additionally the stresses in the ballast bed can be minimized. Under sleeper pads (USP) are used to better match the delicate contact interface between hard concrete and hard ballast. Using USP - tested at OeBB for open track for more than ten years and under turnouts for six years - the contact area increases to 35%. Test sections proved that ballasted track with under sleeper pads form a more stable superstructure, requiring less maintenance and providing longer service lives. Both characteristics increase the availability of track, an important fact, as availability becomes more and more crucial in dense used track sections.

 Copyright © MAINLINE Consortium

Elastic footing of sleepers has therefore proven to be highly successfully. The economic evaluation lead to a new regulation, stating that track carrying more than 10 million tons per year is to be equipped with USP within the next regular renewal, track as well as turnouts.

5.3.3 Type of Superstructure

As mentioned previously, the relatively small additional costs for a heavier track lead to the proposal of standard track design for main lines consisting 60E1 rails on concrete sleepers.

Additional and branch lines are equipped with 54E2 or 49E1. All these rails have a steel grade of R260. Due to the high side wear in narrow curves head hardened rails are in use ate radii less than 500 m. Due to the problems of rail contact fatigue, head checking, head hardened rails with a steel grade of R350HT are foreseen in wider curves as well.

5.3.4 Maintenance

Since 2003 a new method for track maintenance known as “integrated maintenance” is in use. Within this new maintenance action levelling-lining-tamping, track stabilizing, and rail grinding are executed in the same track possession. Analyses of track behaviour shows, that reducing dynamic forces by correcting track failures and rail unevenness reduces the degradation rate of track. The rate b is reduced by 20%, thus tamping cycles can be increased, leading to an economic efficiency of this new maintenance action. Unfortunately, the savings in total figures are small, as generally optimizing maintenance can only lead to relatively small savings compared to investment in quality, due the cost distribution given in Fig.5.7. However, the necessary costs are also lower and the savings are realized in a shorter period.

Understanding track behaviour more in detail, corrective maintenance can be substituted by more preventive work, causing less logistic costs and reduced operational hindrances. Furthermore preventive maintenance allows a higher efficiency in track machinery use.

5.4 Summary

Track deterioration can be modelled with an exponential function. Once a deterioration model is calibrated, it is possible to predict when tamping and other maintenance actions will be necessary by forecasts based on recent track quality measurements.

It is intuitive that high quality levels discussed require high quality track machinery for all track-work.

Evaluations of innovative track designs always need in situ tests together with scientific understanding of how the track structure and individual components and materials perform. However, scientific knowledge about quality behaviour enables shorter test periods and thus earlier estimations of maintenance demands, service lives, and therefore life cycle costs.

Several economically proven proposals for shared corridors are presented regarding:

- investment:
    - Cyclic track regime based on general renewal and subsequent maintenance

 Copyright © MAINLINE Consortium

  - Track quality behaviour based track regime
  - Implementation of an additional sub-layer to strengthen the track system within a regular track renewal (wherever necessary)
  - Installation of heavy superstructure with proper rails, concrete sleepers and good ballast
  - Implementation of under sleeper pads on high loaded track sections

- maintenance:
  - Non-acceptance of permanent slow orders (wherever dense traffic is operated)
  - Avoiding short time savings by reduction of maintenance, accepting loss of track quality as causing high long term costs
  - Keeping high attention on functional dewatering systems
  - Implementing a conform intervention level

All these measures lead to high quality tracks. Such tracks are sustainable showing long service lives and,at the same time, relatively low maintenance demands. The key for achieving this sustainability is a long lasting high quality level of track. A high availability and low life cycle costs are further benefits of a high quality track regime. However, implementing such track regimes needs investment first.

It is underlined that the high quality levels discussed requires high quality track machinery for maintenance actions as well as for track relaying and, wherever necessary, sub-layer installation.

However, the key for prognoses of track deterioration is to identify the impact of the various track parameters on the deterioration rate b. An entire prediction model can be designed in presenting the rage of the variation of the deterioration rate b for the main track parameters. This will be the main focus of the work to be executed within WP5. This chapter aims to describe the background of a track quality prediction model, its necessary differences due to the varying reaction of track to different boundary conditions.

5.5 References

Esveld, Coenraad (2001): Modern Rail Technology, Delft University of Technology, 2nd Ed, 653pp, ISBN 90-8004-324-3-3. An excerpt of 87pp can be downloaded from http://www.esveld.com/MRT_Selection.pdf

Lichtberger Bernard (2005): Track Compendium. Track System-Substructure-Maintenance-Economics. Eurail Press 2nd Ed, 622 pp, ISBN 978-3-7771-0421-8. (Originally in German as “Handbuch Gleis”, 3rd Ed, 2010. 656 pp, ISBN 978-3-7771-0400-3.)

 Copyright © MAINLINE Consortium

Veit P. (2007), “Track Quality – Luxury or Necessity?”, RTR, Renewal and Maintenance, 8-10, July 2007

Marschnig St., Veit P (2006), “Projekt Strategie LCC“, Betriebserschwerniskosten; TU Graz.

6. Metallic bridges (TWI+MAV)

6.1 Fatigue in old metallic bridges

The steel production and construction technology developed quickly towards the end of the 19th century. Testing methods to examine relevant properties such as toughness, fatigue and corrosion were developed in the 20th century but these related to modern steels rather than old steels of existing structures. In addition, railway authorities adopted specific rules to specify the materials used for iron railway bridges only from 1900 (Pipinato et al. 2012). The lack of standardisation in the industry beforehand resulted in a wide variety of metals such as grey cast iron, wrought iron, mild steel and contemporary steel product being used.

In the context of joining technology, the technique of riveting is no longer used in bridges, which is also highlighted in MAINLINEML-D2.1 (2012). Thus, information in codes for riveted structures is not very detailed. From the materials point of view, although the majority of the old bridges that still remain today are made of steel, a number of bridges made from wrought iron are still in service. The knowledge in regard to wrought iron bridges though is not as extensive as for steel bridges. Nevertheless, there is evidence that fatigue endurance between steel and wrought iron structures is similar (SB4.6.2 2007).

One of the most relevant concerns about steel and metal bridges stands on the repair and maintenance of existing structures. The remaining service life of steel bridges is substantially limited by fatigue damage and in order to ensure the safety of these bridges it is often necessary to inspect the structure. According to a survey carried out for the purposes of the ML-D2.1 report (2012), several documents, such as Ril 804.8001, Network Rail's guide to hidden details, Trafikverket's handbook for bridge inspection and the Sustainable Bridges SB-4.6 (2007), are used to assess the degradation in metallic bridges due to fatigue.

6.1.1 Fatigue as a dominant failure mode

Fatigue is not a new phenomenon; it has puzzled researchers for more than 200 years, especially due to the use of metal in structures such as bridges. Fatigue plays a significant role in undermining bridge resistance and, thus, several authors have conducted research in this field of expertise. August Wöhler (1819-1914) was the first to study fatigue and propose an empirical approach. Between 1852 and 1870, Wöhler and his colleagues conducted fatigue investigations on train axles and produced diagrams with the stress on the vertical axis and the number of cycles on the horizontal axis. A linear decreasing response of the component's fatigue life was thereby possible to be detected and the diagrams became known as Wöhler-diagrams or S-N diagrams. The S-N method is still the most widely used today. Fatigue failures can occur both in a detail of a component or a whole structure due to repeated loading at load levels lower than the design load. The phenomenon of fatigue failure can be explained by microscopic cracks occurring in the material and weakening the structure.

One of the largest databases of bridge failures has been established by Imhof (Imhof 2004), which has now been updated by incorporating the latest incidents from 2004 onwards and can be easily accessed via the web (Bridge Forum 2009). In addition, a database of 164 failures of metallic bridges formed the evaluation which was carried out in terms of identifying the factors contributing to the failure or collapse, the modes of failure or collapse as well as

 Copyright © MAINLINE Consortium

an analysis of the structural form of the bridges (Imam and Chryssanthopoulos 2010). 34% of the 164 cases were railway bridges and 73 (47%) were classified as 'no collapse' cases and the dominant failure mode for non-collapsed metallic bridges was found to be fatigue (67%). This justifies the significant attention paid to the phenomenon by bridge engineers. It also suggests that fatigue failure is picked up at an early enough stage through inspections (and/or that the level of redundancy in metallic bridges with respect to fatigue detail failure is satisfactory) so that it does not result in collapse.

The causes resulting in fatigue cracking have also been investigated in more detail. The majority of the fatigue cracking observed was attributed to out-of-plane distortions in welded structures, unanticipated connection fixity and secondary stresses in riveted structures and poor quality material/welding. Furthermore, according to the statistics, truss bridges are more susceptible to total collapse failures and girder bridges to failure that do not necessarily result in total collapse. The majority of non-collapse metallic bridges are girder bridges (40%), whereas the majority of collapse bridges are truss bridges (Imam and Chryssanthopoulos 2010). Arguably, failures can be detected more promptly in girder bridges (and redundancy of such bridges is higher), thus preventing total bridge collapse. On the other hand, many truss bridges are 'fracture critical', which is the term used in the US to indicate a bridge that is likely to fail when a single member fails (i.e. no redundancy).

6.1.2 Fatigue critical details in metallic bridges

The estimation of the residual life of a structure is achieved by evaluating the residual fatigue strength of critical components. A catalogue of fatigue critical details in steel bridges is, therefore, of high importance for the assessment procedure. Such a catalogue has been developed during the "Bridge Fatigue Guidance" (BriFaG) research project (BriFaG 2011) and comprises a large number of fatigue damage cases which have been reported for various types of bridge details. The majority of collected damage cases were found to be of the type caused by secondary load effects. In most cases, unforeseen (or overlooked) interaction between different members and load-carrying systems in the bridge, often combined with poor detailing, have been the main causes of fatigue cracking. In some cases, a complex stress state may also exist in some structural details.

However, design codes and evaluation specifications generally provide very little guidance on the way this kind of fatigue damage should be accounted for or prevented. In BriFaG, special attention is directed to the increasing heavy load traffic and to strengthening aspects to improve the service life of existing orthotropic bridges. Furthermore, the fatigue behaviour of connections of vertical stiffeners to bridge girders or secondary beams is also investigated.

The fatigue life of a connection or detail is commonly defined as the number of load cycles that causes cracking of a component. The most important factors governing the fatigue life of structures are the severity of the stress concentration and the stress range of the cyclic loading. The fatigue life of a structure (member or connection) is often represented by an Sr-N curve, which defines the relationship between the constant-amplitude stress range Sr (σ_{max}-σ_{min}) and fatigue life N (number of cycles), for a given detail or category of details. The effect of the stress concentration for various details is reflected in the differences between the Sr-N curves.

A number of specific details in steel bridges have been identified as being especially susceptible to cracking with a list of expected fracture locations (Xanthakos 1994) being summarized in Table 6.1.

Table 6-1 Expected fracture locations in steel bridges (Massarelli and Baber 2001)

General Detail Type	Specific Location
Groove welds	Flange and web groove welds
	Longitudinal stiffener groove welds
Welded cover plates on tension flanges	Toe weld or weld throat at midwidth of flange at the end of cover plates with end welds
	End of longitudinal welds on cover plates without end welds
Attachment plates welded to flange or web	Welded splices
	Flanges or webs repaired with doubler plates
Diaphragm connections	Ends of welded connection plates on girder webs where the plate is not attached to flanges
	Ends of riveted connection plates on girder webs where the angles are not connected to the flanges.
End connections of floor beams	Coped and blocked flanges at floor beam ends
	Connection plates and angles
Floor beam brackets	Bracket connections to girder webs
Top and bottom lateral bracing connections	Gusset plate bracing connections to girders
	Gusset plate to diaphragm connection plates
Transverse stiffeners	End of cut-short stiffeners
Tack welds	Between gussets and main members
	Between bearing plates and beam flanges
	Between bolted connection angles and webs
Plug welds	Misplaced drilled holes
	Repair locations

In regard to riveted railway bridges, in particular, most fatigue cracks detected on this type of bridges have been attributed to deformation-induced stresses resulting from out-of-plane motions of the different bridge member and connection components which were overlooked when designing these old bridges (Imam et al. 2006). The fatigue damage has been mainly concentrated on riveted connections, in particular stringer-to-cross-girder connections between longitudinal and transverse members of these bridges (Al-Emrani 1999).

6.1.3 Fatigue aggressors, consequences and detection methods

The primary aggressors for the degradation mechanism of fatigue are attributed to traffic loading, environmental effects and poor designing. The older the bridges are, the more a bridge accumulates partial damage from service load cycles. Depending on the type of structure, the initial fatigue damages to be evaluated during inspection can be caused by different reasons. Initial damages can be caused:

- during fabrication, welding or riveting,
- due to unfavourable design with regard on fatigue, poor detailing,
- due to stresses and deformations unforeseen in design, or

 Copyright © MAINLINE Consortium

- because the state of knowledge was too low

If a sufficient safety level for the bridge in question cannot be shown by means of calculation, static and dynamic measurements shall be used. Measurement is appropriate in the fatigue assessment, for example if:

- there are doubts about the acting static system,
- effects with consequences on the fatigue safety not known during design occurred,
- effects of increased loads or additional lanes on the fatigue safety have to be assessed,
- secondary stresses led to fatigue damage, measurements are needed to assess the reasons

Although during the very important visual inspection almost all damages are detected, non-destructive testing (NDT) is recently being increasingly applied. The most common monitoring and inspection techniques used to assess degradation due to fatigue are: visual inspection, dye penetration, electromagnetic techniques, acoustic emission monitoring and theoretical estimations are the main methods. Table 6.2 shows available non-destructive testing methods proposed for old riveted metallic bridges that are used for detection of fatigue damages.

Table 6-2 Non-destructive testing methods for detection of fatigue (Helmerich et al 2006)

Method	Damage to be detected	Comment on effectiveness of the equipment
Visual inspection	Surface cracks	With help of magnifying glass and training
Magnetic particle test	Surface cracks	Only for magnetic materials
Dye penetrant test	Surface cracks	Good alternative for magnetic particle test, also for non magnetic materials
Radiography	Crack detection also in sandwiched elements	Experts with permission required
Ultrasonic test	Only the first layer can be assessed	Not applicable for puddle iron
Eddy current technique	Cracks in rivet holes	Not currently applied
Acoustic emission technique	Active cracks	Not applied for detection (insufficient research), only for monitoring of detected cracks

Fatigue failures take decades to initially develop but progress to failure is then relatively quick. Remaining fatigue capacity must be enough until critical parts can be exchanged and the trigger point for intervention is the presence of cracking. Damage due to cyclic loadings is a result of gradual enlargement of fatigue cracks during the tensile part of the loading cycle; once a crack reaches a certain critical size, catastrophic failure of the affected cross-section ensues (Pipinato et al. 2012). In order to maintain these bridges in service reinforcement techniques are needed to prevent fatigue cracking whilst increasing bridge safety.

The consequences of failure are a good indicator of the importance of a bridge structure. As suggested in recent reports from the Standing Committee on Structural Safety (SCOSS), utilising the ‘3Ps’, pertaining to people, process and product, can help describe and categorise the contributory factors which may lead to failure. The ‘3Ps’ emphasise the wide range of influences in designing and constructing structures and ensure that ‘human factors’ are a key component of any risk assessment (SCOSS 2007).

 Copyright © MAINLINE Consortium

6.2 General concepts applied for fatigue assessment

In the life of a bridge the question that may arise is: for how long can it be preserved for the future? That defines the remaining fatigue life up to the point when the probability of occurrence of cracks of vital structural members exceeds a given limit. The estimation of the remaining life of the structure is achieved by evaluating the residual fatigue strength of critical components. These critical components which are designed to survive a single load may fail if the load is repeated a large number of times. This failure behaviour is classified as fatigue failure. In general, the following 6 general concepts for fatigue verifications are widely accepted (SB-5.2.S1 2007):

- Verification with particular fatigue tests using prototypes
- S-N-curve concept with detail classes based on nominal stresses
- Geometrical stress method using reference S-N-curves
- Local notch stress method using local elastic stresses
- Local notch strain method using local stresses and strains
- Fracture mechanics analysis.

The verification with particular fatigue tests is supported by experimental investigations, the local notch strain method using local stresses and strains is based on the analysis of the crack initiation, the fracture mechanics concept depends on crack propagation analysis whereas the other 3 concepts are based on service life assessment, as described below.

6.2.1 Verification using fatigue tests with prototypes

The verification of the fatigue resistance is performed with S-N-curves that are experimentally determined using original or representative components. The material, the geometry and the manufacturing of the component as well as the loading sequence and environmental conditions of the tests configuration have to be as close as possible to reality to achieve results of acceptable reliability. The residual service life is determined by a damage accumulation model, e.g. Palmgren-Miner, on the basis of the S-N-curves derived experimentally.

6.2.2 S-N-curve concept with detail categories based on nominal stresses

The application of the S-N-curve concept is based on nominal stresses. The nominal stress is defined as the stress in the parent material or in a weld adjacent to a potential crack location calculated in accordance with elastic theory and excluding all stress concentration effects. The nominal stress as specified can be a direct stress, a shear stress, a principal stress or an equivalent stress. It is derived from the loads applied on the net sections of a structure or member. A stress increase due to geometry or the effects of other imperfections are not included in this nominal stress concept.

 Copyright © MAINLINE Consortium

6.2.3 Geometrical stress method using reference S-N-curve

The concept of the geometrical stress method is very similar to the S-N-curve concept and has mainly been developed for welded structures. For complex structures, the nominal stresses cannot be determined using elementary structural models. The stresses need to be determined on the basis of more advanced structural models (slab theory, theory of sheets or shell theory). These stresses are calculated for critical locations where the crack may occur and are defined as structural stresses.

6.2.4 Local notch stress method using local elastic stresses

The local notch stress method is based on the elastic calculation of local stresses at the tip of a crack that is assumed to occur during the fabrication process, e.g. welding. The amplification of stresses by notch effects has to be considered. The determination of stresses is typically carried out by FE-analysis (Finite Element Analysis), BE-analysis (Boundary Element Analysis) or by applying K_t-values taken from literature. Due to the fact that the linear elastic material law offers only an approximate estimation of the stresses for constant amplitude fatigue limit under a pure alternating stress range, the concept is only applicable for the alternating endurance limit of the member (R=-1). In this case, the local stresses calculated are compared with the alternating material properties. The influence of roughness and the size effect are considered in the analysis. A generalisation of the concept is realised referring to the proportionality of local elastic stresses to nominal stresses which enable a transfer of S-N-curves of the nominal stress concept to local elastic stresses. Therefore, the average stress relation and the service life can be estimated using the S-N-curve method.

6.2.5 Local notch strain method using local stresses and strains

The local notch strain method refers to a characteristic function and to characteristic values of a material which is subjected to elastic-plastic deformations due to cyclic loads along a single axis. The results are cyclic stress-strain curves and strain-life-curves. The curves are determined experimentally or estimated empirically and described analytically. They account for material characteristics as well as effects from fabrication, size and environment. The characteristic loads as input in the local notch strain method are local stresses and strains. A correlation between loads on the structure and local elastic-plastic strains is guaranteed by load-strain curves. They are derived by numerical calculations, e.g. FE-analysis, or formulae for their approximation. The outcomes are local elastic-plastic stress-strain-curves calculated for a specific loading event. They are closed σ-ε-hysteresis curves which are evaluated with respect to their damage effect. The results are S-N-curves or Gaßner-curves for crack initiation. The magnitude of the initial crack length can be taken from literature.

The local notch strain method can be applied for notched or un-notched as well as welded or non-welded members.

6.2.6 Fracture mechanics analysis

The fracture mechanics analysis is used to determine the remaining fatigue life after a macroscopic crack has been developed. The relevant information for this analysis approach is:

 Copyright © MAINLINE Consortium

- Under which circumstances could crack propagation occur?
- Is it possible to intercept the growth of the crack?
- When will unstable fracture occur?

The fatigue life assessment using fracture mechanics is based on the relationship observed between the range of the stress intensity factor, ΔK, and the crack growth rate of fatigue cracks, da/dN. A simplified approach to estimate crack propagation is the equation of Paris and Erdogan:

$$\frac{da}{dN} = C\,\Delta K^{m} \tag{6.1}$$

C, *m* are material properties (crack growth constants), *da*/*dN* is the crack propagation (*da*) per load cycle (*dN*) respectively the crack extension. Δ*K* the range of the stress intensity factor, given by:

$$\Delta K = K_{\max} - K_{\min} \tag{6.2}$$

K_{max} is the maximum stress intensity in each cycle and K_{min} is the minimum stress intensity in each cycle.

Since the crack growth rate is related to ΔK^{m} raised to an exponent, the exponent *m* having typically a magnitude of 3-4, it is important that Δ*K* should be known accurately if an acceptable reliability of prediction of crack propagation has to be achieved. The input parameters for the materials properties *C* and *m* have to be obtained by representative material tests of the member being investigated. If *da*/*dN* versus Δ*K* is displayed for an actual crack in a double-logarithmic diagram, an approximate sigmoidal curve results as shown in Fig.6.1. Below a certain threshold range of the stress intensity factor, ΔK_{th}, no crack growth occurs. For intermediate values of Δ*K*, the growth rate is idealised by a straight line.

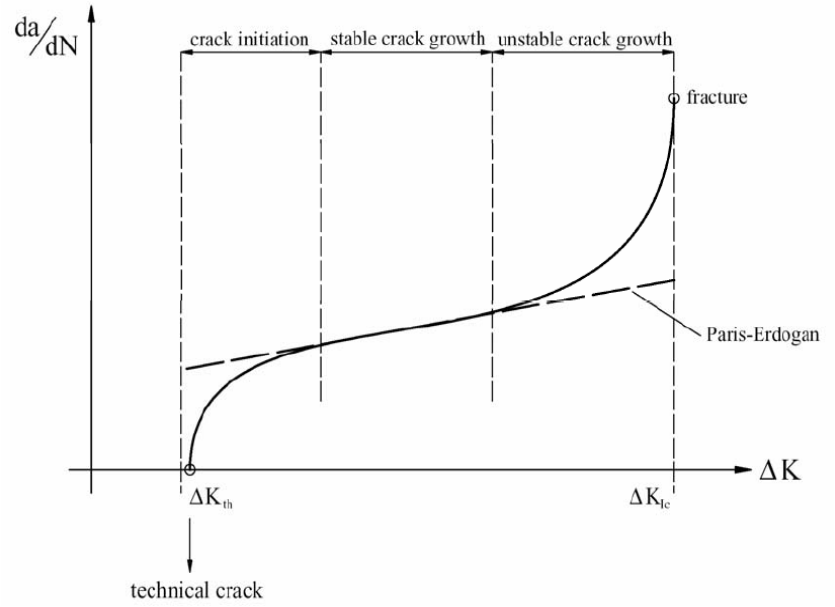

Figure 6-1 Crack propagation rate da/dN in dependence on the range of the stress intensity ΔK

 Copyright © MAINLINE Consortium

For a crack in a certain structural member, the following equation for ΔK can be derived:

$$\Delta K = \Delta\sigma\sqrt{\pi a}\, Y(a)\, M_k(a) \tag{6.3}$$

where:

- a: crack length derived from the cracks' geometry
- $Y(a)$: stress intensity correcting function depending on crack configuration
- $M_k(a)$: stress intensity correcting function of welded components
- $\Delta\sigma$: stress range

Since $\Delta\sigma$, $Y(a)$ and $M_k(a)$ are not constant the estimation of service life has to be carried out incrementally using the following equation which is applicable for cracks with a crack depth greater than 0.1 mm to 1 mm:

$$N = \int_{a_0}^{a_c} \frac{1}{\left(\frac{da}{dN}\right)} = \int_{a_0}^{a_c} \frac{1}{C\left(\Delta\sigma\sqrt{\pi a}\, Y(a)\, M_k(a)\right)^m}\, da \tag{6.4}$$

a_0 (initial crack depth) and a_c (final crack depth corresponding to failure) are used in order to predict the fatigue strength of a cracked member, assuming that the remaining life depends on crack growth starting from a pre-existing initial crack of known size. This crack has to be detected during an inspection or equivalent measures first and the size of the initial crack has to be determined. Independently from the assessment concept, the local sequence of loading during service life mainly influences the fatigue strength.

6.2.7 Remaining life

The fatigue endurance of material with no initiation factors such as welds, holes and sharp notches present will improve with mechanical properties. The first stage in the fatigue process is influenced by the internal structure of the material. Through a shortened initiating phase by stress raisers the effect of the mechanical properties will be less influencing and cracks starts to grow direct from defects. In order to determine the remaining life of structures due to fatigue, the most applied method is Palmgren-Miner's rule, Palmgren (1924), Miner (1945). Palmgren-Miner's rule is a linear approach to determine the accumulated damage caused by variable stress cycles. The damage at a certain stress range is proportional to the number cycles. The fatigue endurance N_i at a constant stress range $\Delta\sigma_i$ indicates the space for the available cycles to occur. The influence of the number of cycles at a certain stress range have affected a detail is compared to the allowable, n_i/N_i, and the fatigue life ends when $\sum n_i/N_i = 1$. The values of N_i are determined from Wöhler curves for the corresponding value of $\Delta\sigma_i$ (Fig.6.2).

 Copyright © MAINLINE Consortium

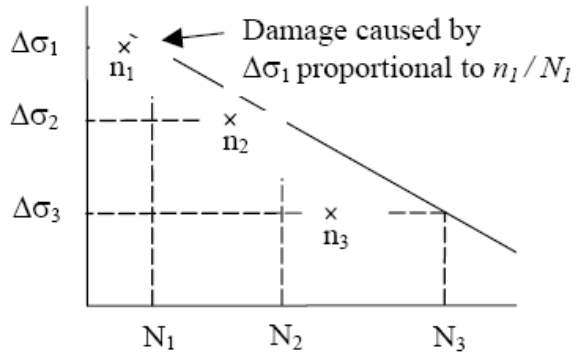

$$\sum_{i=1}^{n} \frac{n_i}{N_i} = \frac{n_1}{N_1} + \frac{n_2}{N_2} + \cdots + \frac{n_n}{N_n} = 1$$

Figure 6-2 The Palmgren-Miner rule for calculation of accumulated damage

6.3 Fatigue assessment models and parameters

During the last decades, the inspection of the existing bridge stock and the condition assessment procedures have been increasingly well organised. However, the assessment of fatigue safety was not included in the design at the turn of the 19th to 20th century. Furthermore, changes in the structure after repair or strengthening measures within the last hundred years were not indicated in the drawings and information got lost.

In 1993 the technical committee 6 of the European convention of Constructional Steelwork (ECCS) created the working group “Remaining fatigue life” with the objective to produce a guideline for fatigue assessment on steel structures (ECCS 2004). For the clarification of how endurance of details and calculation of remaining life are accomplished in codes, the European code EN 1993-1-9 (Eurocode3 2003) is often chosen.

There have already been attempts to develop models for the estimation of consequences of bridges failures (Imhof 2004; Wong et al. 2005; Stein and Sedmera 2006, Imam and Chryssanthopoulos, 2012). Considering these consequences is essential in both qualitative and quantitative risk-based design and assessment. Risks of structures in service should be examined to determine more appropriate assessment, inspection and strengthening/repair criteria. In order to make accurate assessments of existing railway bridges information on the behaviour of bridges exposed to fatigue as well as the behaviour of old materials due to cyclic exposure is essential. Furthermore, weld-related cracking and the presence of geometrical discontinuities at bolts and bolted connections are also of concern in relation to the phenomenon of fatigue.

Fatigue is the most common cause of failure in structures consisting of metallic material. Conducting endurance assessments of bridges is of great importance to understand the process of how fatigue develops in material and structures. In specified components and details critical to fatigue loading, the remaining fatigue life is estimated by means of the Palmgren-Miner damage accumulation rule (Miner 1945). Miner’s rule is a linear approach to determine the accumulated damage. Although the Miner’s rule is not exact, it will provide a safe estimation for the majority of stress spectra applied.

The design codes for fatigue use the principles of Wöhler curves (S-N curve), with an allowable stress range decreasing with the number of load cycles. The stress ranges a

 Copyright © MAINLINE Consortium

section or a detail are exposed to are obtained by load models placed on a bridge, representing cars' or trains' static and dynamic response. The numbers of load cycles a component can endure are thereby determined from these models. When vehicles pass a bridge, components in the bridge with different lengths and positions will be exposed to fatigue loading differently. A primary structure will experience the vehicles passing as a more isolated event, while a cross beam/stringer will be loaded by every axle of the passing vehicle. This fact makes different parts in a bridge more exposed to accumulation of fatigue damage than others. For fatigue assessment, the procedure requires the knowledge of the fatigue cycles applied to the different details. The number of cycles for the different stages in the fatigue process can vary significantly from hundred to millions of cycles depending on stress range, stress initiation factors, material properties and so forth.

6.3.1 Frameworks/guidelines

For the estimation of the current fatigue resistance and the remaining fatigue life, assessment frameworks such as the procedure proposed by Helmerich et al (2006), which incorporates information about old materials and non-destructive testing methods for evaluation of details, have been developed. This step-by-step fatigue assessment procedure is divided into four different phases, and the participation of experts, non-destructive methods, measurements and the analysis of the material are all assigned to different stages of the assessment (Helmerich et al 2006). The proposed fatigue assessment procedure is based on the general procedure developed by the Joint Committee for Structural Safety (JCSS) (JCSS 2001) and consists of the following proposed phases (ECCS 2004):

1. *Preliminary evaluation*: Information from visual inspection, including, for example, information from Bridge Management Systems (BMS) and own inspection on site.

2. *Detailed investigation*: Information on the structure and loadings are updated using specific tools as refined calculation models or more realistic traffic loads.

3. *Expert investigation*: A refined static model is used for probabilistic evaluation and fracture mechanics for establishing final decisions. Advanced NDT may be used in cross sections specified with the updated model.

4. *Remedial measures*: A final report summarises the results of all working steps. All remedial measures, possible from the technical point of view are proposed.

The proposed stepwise procedure (Figure 6.3) can assist in identifying the best strategy to extend the lifetime and postpone investments in new bridges.

 Copyright © MAINLINE Consortium

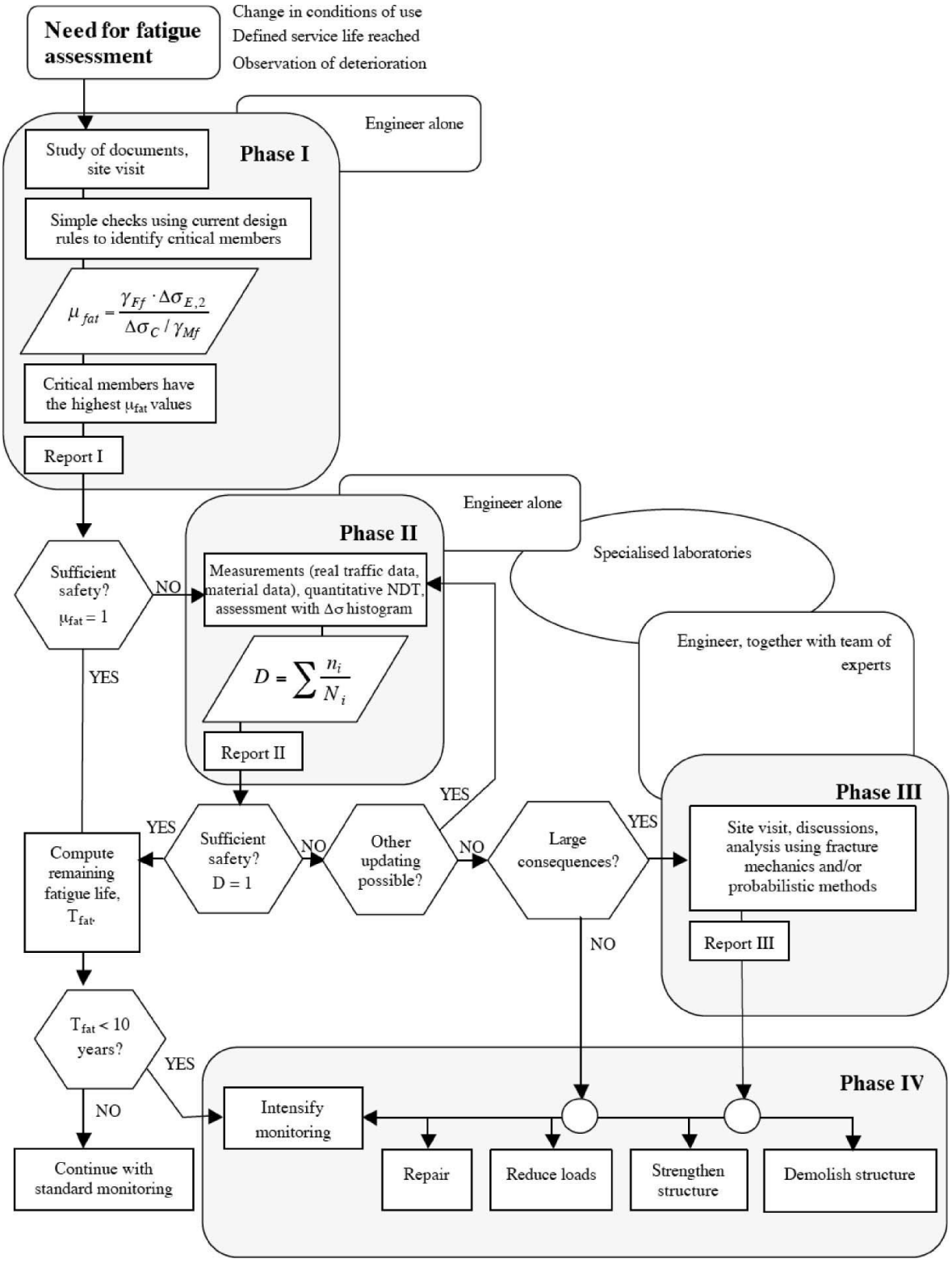

Figure 6-3 Stepwise procedure for fatigue assessment (Helmerich et al. 2006)

Table 6-3 Physical dimensions to measure and sensors used (Helmerich et al 2006)

Measurement task	Preferred sensors	Accuracy
Local strain distribution in cross sections with assumed high stress level or cross sections with changes, caused by damages,	Strain gauges Mechanical strain measurement Fibre optical sensors (integral sensors Fabry–Perot Sensors, Brag-grid sensors)	2 μ 0.5–1 μ depending on type of fibre sensor and application
Actual static system	System of strain gauges Dynamic measurement system	
Influence of temperatures	Temperature sensor (resistance based) Thermocouples (Semiconductors)	~0.1°C (depending on the max. temperature range)
Inclination	Inclinometer	Depending on chosen max. angle (see producer, ~0.1%)
Displacements or settlement	Potentiometer Inductive measurement Laser based system Hydrostatic levelling/force transducer	0.1%, depending on displacement 0.1%, depending on displacement 0.3 mm+influence of measured distance ~0.1% depending on max. force
Dynamic characteristics: Acceleration Eigenfrequencies	Accelerators Strain transducer	0.05–1% depending on force

The procedure, which enables practising engineers to find a most effective solution for the further use of the bridge, clarifies whether a bridge is safe without any further measures or needs to be reinforced or demolished. Table 6.3 provides an overview on physical dimensions to measure and the sensors used.

In general, measurements are used to obtain information from the real structure in fatigue relevant strain concentration regions with the minimum amount of sensors, e.g.:

- strain distribution in high loaded cross sections,
- function of elements, as anchors or braking trusses,
- evaluation of the actual zero axis,
- secondary stresses,
- moments in fixed supports or restraint,
- movement in bearings,
- measurement of strains in theoretical zero elements,
- local strain concentrations in connections assumed to be hinges/joints.

6.3.2 Probabilistic approaches

Another approach to providing fatigue assessment solutions for metallic railway bridges is the use of probabilistic methods. This method allows uncertainties to be taken into account and provides a framework for estimates of remaining lives to be assessed depending on the required level of confidence and target reliability.

The most widely used method to carry out an initial fatigue assessment for a structure with many fatigue susceptible details is, as described above, the S-N method which is based on the S-N curve of the fatigue detail in question and is used in combination with Miner's rule. In the specific case when a fatigue crack has been detected in a detail, the use of fracture mechanics principles is preferred which allows explicit prediction of fatigue crack growth.

 Copyright © MAINLINE Consortium

A probabilistic approach for the fatigue assessment of riveted railway bridges was proposed by Imam et al (2006), with a finite element model of a typical short-span riveted railway bridge being the focus of investigation (Imam et al 2006). The approach consists of a 3 steps methodology:

1. Global analysis of the bridge in order to identify the most fatigue-critical details,

2. Annual response spectra for a critical connection were developed under a historical load model (represent past traffic) and the BS 5400 medium traffic,

3. The remaining fatigue life (through the probability of the fatigue failure) of the connection was estimated for different target failure probabilities.

The strength of the approach stands on the randomised variables incorporated to capture the loading uncertainties (for present and historical rail traffic) as well as the material and modelling uncertainties (dealt with by literature and case studies). Riveted railway bridges have shown less of a tendency for fatigue damage development over the years when compared to their welded successors according to the work carried out using this proposed approach. For the fatigue assessment, a historical load model was developed in collaboration with Network Rail in order to represent train loading in the period from 1900 until 1970, whilst the BS 5400 medium traffic model (BS 5400 1980) was adopted for the period from 1970 onwards (Imam et al 2006).

For the purposes of the probabilistic analyses, variability in terms of loading, resistance and modelling were taken into account. The randomised variables used are listed below and described in more detail (including their characteristics and values) in Table 6.4:

- Loading – dynamic amplification of the statistically calculated stresses and the train frequency,

- Resistance – S-N curve and cumulative damage model,

- Modelling – ratio between actual and calculated stresses.

Table 6-4 Variables taken into account for the probabilistic analyses (Imam et al 2006).

Variable	Mean	CoV	Distribution
C	9.33×10^{13}	0.30	Lognormal
m	4	-	Deterministic
Δ	0.90	0.30	Lognormal
DAF	1.10	0.14	Normal
α	0.80	0.14	Normal
n_i	From annual response spectrum	0.14	Lognormal

- C: constant in S-N curve depending on material,

- m: inverse of slope of S-N curve,

- Δ: damage limit,

- DAF: dynamic amplification factor,

 Copyright © MAINLINE Consortium

- α : ratio of measured to calculated stresses,
- n_i: number of applied cycles,
- CoV: coefficient of variation

In the proposed probabilistic approach, the failure probability, which is a function of time, is calculated by Monte Carlo simulation using 10^6 samples. According to the approach, the behaviour of the material at or below the fatigue limit plays a major part in high cycle fatigue life estimation of railway bridges. The report concludes that fatigue damage in the last 30 years has been taking place at far higher annual rates than in the preceding 70 years, which is depicted on the cumulative damage evolution of one of the most fatigue-critical bridge connections investigated.

At a more general level, Liu and Frangopol considered parameter uncertainties in reliability-based life-cycle maintenance cost optimization of deteriorating bridges (Liu and Frangopol 2004). A genetic algorithm (GA) based procedure is presented for optimal life-cycle maintenance planning of deteriorating bridges while considering condition, safety, and cumulative maintenance cost over the intended service life. A multi-linear computational model is used to describe the deterioration process under no maintenance and under maintenance interventions. Three parameters are used to depict the deteriorating performance profile under no maintenance, i.e., initial performance index P_0, time to damage initiation T_i, and a constant deterioration rate a, as shown in Figure 6.4.

A maintenance intervention has some effects on the deterioration profile of bridge components; these effects can be characterized by a set of parameters including immediate performance improvement c, time delay in deterioration T_d, reduction in deterioration rate d, and duration of maintenance effect T_{pd}. The effects, according to Liu and Frangopol (2004) can be described as:

(a) instant improvement of performance index upon application,

(b) delay of performance deterioration upon application, and

(c) alleviation of performance deterioration, followed by complete loss of maintenance functionality after a period of effective time.

 Copyright © MAINLINE Consortium

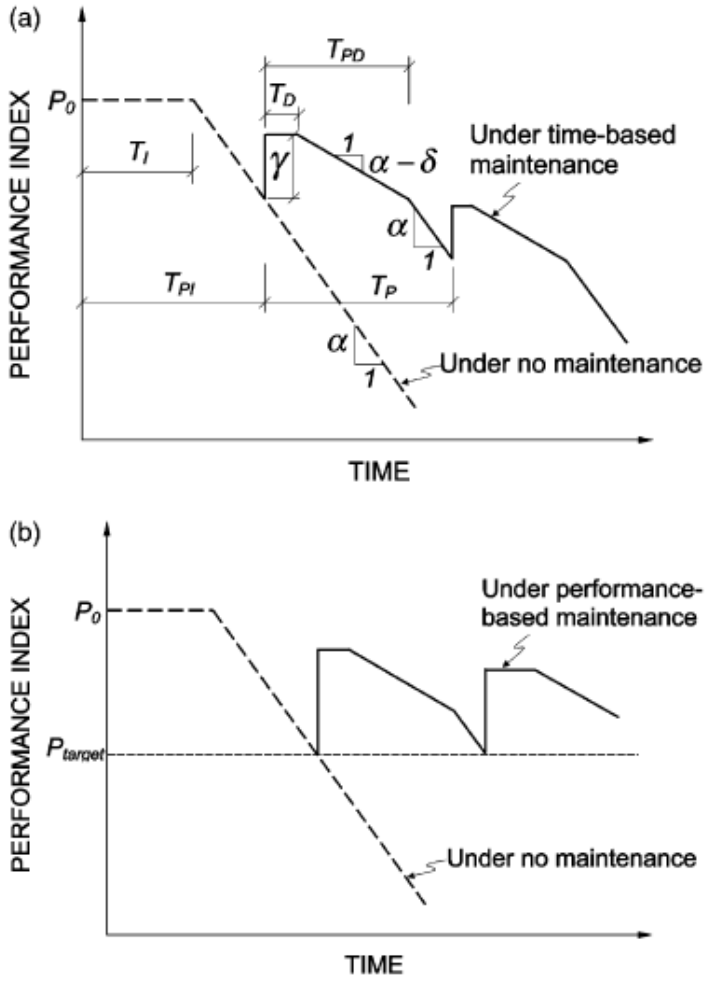

Figure 6-4 Multi-linear performance profile model under no maintenance and under (a) time-based and (b) performance-based maintenance interventions (Liu and Frangopol 2004)

The optimal maintenance planning problem deals with cost-effective allocation of maintenance efforts so that a preferred balance among condition, safety, and life-cycle maintenance cost objectives can be obtained. The main objective is to obtain a set of optimized trade-off maintenance solutions while:

- minimizing the largest (i.e. worst) condition index during the service life,
- maximizing the smallest (i.e. worst) safety index during the service life,
- minimizing the present value of cumulative lifecycle maintenance cost;
- subject to specific condition index and safety index values.

The proposed approach (Liu and Frangopol 2004) incorporates the visual inspection based condition index, the structural assessment based safety index, and cumulative life-cycle maintenance cost which are simultaneously considered in the optimisation process. The conclusion that can be drawn from this study is that the effects of uncertainties in deterioration processes as well as in maintenance interventions on evaluation of the condition, safety, and life-cycle maintenance cost can be significant and therefore need to be appropriately considered in the maintenance planning optimization. This approach could be

adapted for fatigue assessment purposes, noting that, in this case, the deterioration rates should be represented by non-linear functions.

6.3.3 Other approaches

Further approaches have been developed based on reliability theory in order to incorporate the high degree of uncertainty associated with evaluating bridges in fatigue. Such a methodology is the one developed by Tobias and Foutch (1997) for the fatigue evaluation of riveted girder railway bridges. The approach allows for the inclusion of uncertainties associated with strengths, bridge responses and loadings. These inclusions allow fatigue endurance predictions to be more qualified and give a broader idea of the potential lives of bridges. For the development of the fatigue model proposed, three primary tasks were identified (Tobias and Foutch 1997):

1. the calculation of fatigue loadings for each type of freight to cross a bridge,

2. the determination of fatigue strengths for a bridge,

3. the evaluation of these two variables to estimate remaining life.

Fatigue strengths and fatigue loadings are described by probability distributions, which are evaluated using a performance function. This allows for the calculation of failure probabilities when multiple random variables (loading and resistance) are involved. Furthermore, several parametric studies were conducted using the proposed fatigue model. The model enables the evaluation of a bridge in fatigue using two sets of probability distributions and a performance function that is a modified form of Miner's damage law. The studies illustrated the efficacy of a reliability-based method for fatigue evaluation.

Subsequent studies employed variations of some important variables to study their effects. These parameters included (Tobias and Foutch 1997):

- the allowable freight car loading,

- the centre-to-centre (c-c) truck spacing of unit freight cars,

- the variance in fatigue resistances,

- the variance in car and axle loadings,

- the length of the span.

According to further reports surrounding the degradation mechanism of fatigue on metallic bridges and the associated parameters affecting the rate of fatigue growth, these factors are found to be dominant (Halfpenny 2001):

- **Stress or strain range**. Stress or strain range has the most important influence; from the SN curve, it is evident that fatigue life drops exponentially as the stress cycle range increases

 Copyright © MAINLINE Consortium

- **Mean stress**. The mean stress (residual stress) also affects the rate of fatigue damage. If a mean tensile stress is applied to a crack, then the crack is being forced open and any stress cycles applied will therefore have a more pronounced effect.

- **Surface quality and surface treatments**. Since the fatigue cracks usually initiate from a pre-existing defect at the surface of a component, the quality of the surface will greatly influence the chance of a crack initiating. Surface treatments can be applied to improve the fatigue resistance of a component.

6.4 Intervention strategies

6.4.1 Typical types of interventions

Fatigue damage appears as a fatigue crack in details with the highest sensitivity to fatigue. Design of remedial measures has to be done carefully, because the strengthening of a detail can lead to changes in notch cases or load distribution and consequently remedial measures can lead to additional fatigue-sensitive details. The typical fatigue details differ between welded and riveted structures. Only if the reason for a fatigue crack is identified, for example by calculations or by intensifying monitoring, then a proper solution can be applied as remedial measure. Remedial measures are (Helmerich *et al.* 2006):

- reducing loads;

- repair;

- strengthening;

- demolishing the structure.

The type of intervention selected is determined considering the following factors:

1. cause of damage

2. remaining service life

3. frequency and type of future inspections

4. construction constraints

Fatigue strength can be improved significantly by providing a smooth transition between connected elements. A flange attachment, for example, can be improved from a Category E to a Category B detail by providing a radius transition and grinding the weld smooth. The fatigue strength of a transverse groove weld can be improved from a Category C to a Category B by removing the weld reinforcement and grinding the weld smooth. Other important considerations are to avoid intermittent welds on backup bars and discontinuous backup bars.

Some of the same treatments or modifications of a structural detail are used in both repairs and retrofits. The distinction can be made that a repair is intended to arrest the propagation of an existing fatigue crack, while a retrofit is intended to upgrade the fatigue resistance and

 Copyright © MAINLINE Consortium

prevent the future occurrence of fatigue cracking. Retrofits are usually carried out at details similar to those that have previously caused cracking. The choice of method depends on the circumstances of the fatigue cracking and may depend on the availability of certain skills and tools from local contractors who would perform the repairs. Techniques can generally be categorized into three major categories (Dexter and Ocel 2013):

i. Surface treatments

ii. Repair of through-thickness cracks

iii. Modification of the connection or the global structure.

6.4.2 Surface treatments

Weld toe surface treatments include grinding, gas tungsten arc (GTA, also called plasma remelting) of the weld toe, and impact treatments are included in this type of intervention. These techniques can be used as "weld improvement" retrofit methods to increase the fatigue strength of uncracked welds. Once the treatment is applied to welds that have already been in service, the remaining fatigue life is at least as long as that provided by original detail when new (assuming the stress-range histogram stays relatively constant). In other words, the damaging effect of prior fatigue loading cycles is removed (Dexter and Ocel 2013).

Reshape by grinding

Grinding can be used to totally remove portions of a detail containing small cracks, particularly cracks at the edges of flanges or other plates. Typical examples of this technique are Disc Grinding and Burr Grinding.

Gas Tungsten Arc (GTA) remelting

GTA remelting is an autogenous welding operation along the weld toe and the base metal. This is accomplished by manually moving a gas shielded tungsten electrode at a constant speed along the weld toe and just melting the metal without addition of new filler metal.

Impact treatments

Impact treatments work by introducing compressive residual stress near the weld toe. Because the compressive residual stress lowers the effective tensile stress range locally on crack-like defects, it is most effective when conducted under dead load.

Hammer peening is a simple and effective technique for weld improvement. The method uses an air hammer with a blunt tip (commonly used by welders to remove slag from welds) to plastically deform the weld toe creating a compressive state of stress where tensile residual stress was produced during the welding process. This lowers the tensile stress range the weld toe experiences under live load and extends the fatigue life.

As an alternative to hammer peening, ultrasonic impact treatment (UIT) is an attractive option. Hammer peening is a noisy and physically enduring task. Ultrasonic impact is relatively quiet, and the equipment is much easier to handle.

 Copyright © MAINLINE Consortium

6.4.3 Repair through-thickness cracks

Hole drilling

Hole drilling is perhaps the most widely used repair method for fatigue cracks. The hole drilling method requires placing a hole at the tip of the crack, removing the sharp notch at the crack tip.

Vee-and-weld

Vee-and-weld is a method of weld repair for long, through-thickness cracks. Once a crack is identified, material is removed along the crack length, through three-quarter the thickness of the section that is cracked in the shape of a V. The V-shaped groove is then filled with weld metal, and the process is repeated on the other side of the section, so the entire crack is replaced by weld.

Adding doubler/splice plates

Another technique that can be used to repair through-thickness cracks is doubler or splice plates, hereafter referred to as doubler plates or doublers. Doubler plates add material to either increase a cross-section or provide continuity at a cracked cross-section. The philosophy of doublers for fatigue crack repair is to add cross-sectional area, which in turn reduces stress ranges.

Post-tensioning

Crack closure concepts can be used to slow down or eliminate fatigue crack growth. Post-tensioning forces can be applied to cracked beam sections, forcing crack faces to close together and push the effective stress range into the compression regime to hinder additional crack growth. A limited amount of research has verified the validity of this retrofit.

6.4.4 Modify the detail

When the stress range in a repaired region must be reduced for a repair to be effective, such as in a weld repair made at a location where there originally was no weld, then a detail modification is required. Typical examples may be (Dexter and Ocel 2013):

- adding doubler plates to increase the cross-sectional area;
- changing the overall geometry of the connection to reduce stress in the joint;

6.5 Summary

This chapter presents a review of fatigue as a deterioration phenomenon in metallic bridges, with particular attention to the critical elements of the structure, the fatigue aggressors, consequences and detection methods. The general concepts associated with the fatigue assessment are outlined and modelling frameworks and approaches that consider the properties and parameters affecting performance are identified and described. Several guidelines, frameworks and probabilistic approaches have been developed for the estimation

of consequences of bridges failures as well as the prediction of the vital parameter of the remaining life of the structure.

The remaining service life of steel bridges is limited by fatigue damage and in order to ensure the safety of these bridges it is often necessary to inspect the structure using traditional as well as more advanced techniques (NDT methods incorporating sensors). Key inputs (parameters) associated with such types of models have been highlighted in this report; the uncertainties of these parameters, in particular in terms of fatigue loading, resistance and modelling, are often taken into account by the use of probabilistic analyses as presented in this report.

The report makes reference to typical intervention strategies applied to address fatigue related issues in metallic bridges and provides a link between the degradation phenomenon and intervention triggers and modelling techniques.

6.6 References

Al-Emrani M., (1999), Stringer-to-Floor-Beam Connections in Riveted Railway Bridges – An Introductory Study of Fatigue Performance, publ. S99:4, Technical Report, Chalmers University of Technology, Sweden

ASCE (1982), Committee on Fatigue and Fracture Reliability of the Structural Division, "Fatigue Reliability 1-4", Journal of the Structural Division, ASCE, Vol. 108, No. ST1, pp. 3-88

Bien J., Helmerich R., Kubiak Z, (2009), Condition Assessment of Old Railway Bridges, a Scientific Cooperation between Berlin and Wroclaw, Proceedings of the Third International Congress on Construction History, 2009

Bridge Forum, (2009), Bridge collapse database. University of Cambridge, UK. www.bridgeforum.org/dir/collapse

BriFag (2011), BriFag – Bridge Fatique Guidance. Meeting sustainable design and assessment. An EC project within the Research fund for Coal and Steel (RFCS) 2008-2011

BS 5400, (1980), Steel, Concrete and Composite Bridges: Part 10: Code of Practice for Fatigue, British Standards Institute, London

Dexter R. J., and Ocel J. M. (2013), Manual for Repair and Retrofit of Fatigue Cracks in Steel Bridges, FHWA Publication No. FHWA-IF-13-020, US Department of Transportation, 2013

ECSS. WG-A (2008), Assessment of Existing Steel Structures: Recommendations for Estimation of Remaining Fatigue Life

ECSS. WG-A, TC6 (2004), Assessment of Existing Steel Structures, final draft 09/2004 (ECCS: Brussels)

Eurocode 3. (2003), Design of steel structures – part 1-9, Fatigue, EN 1993-1-9:2003, 2003 (CEN: Brussels)

 Copyright © MAINLINE Consortium

Halfpenny A., (2001), A practical discussion on fatigue, Environmental Engineering; Sep 2001, Vol. 14 Issue 3, p21

Helmerich et al (2006), Assessment of existing steel structures. A guideline for estimation of the remaining fatigue life, Structure and Infrastructure Engineering, Vol. 3, No. 3

Imam B M and Chryssanthopoulos M K (2010), A review of metallic bridge failure statistics, IABMAS 2010.

Imam B M and Chryssanthopoulos M K (2012).Causes and consequences of bridge failures, Structural Engineering International, 22(1),pp. 93-98

Imam B.M., Righiniotis T.D. and M.K. Chryssanthopoulos (2008), Probabilistic Fatigue Evaluation of Riveted Railway Bridges, Journal of Bridge Engineering, ASCE, 13(3), pp. 237-244.

Imam B.M., Righiniotis T.D. and M.K. Chryssanthopoulos (2006), Fatigue reliability of riveted connections in railway bridges. 3rd International ASRANet Colloquium, 2006

Imhof, D, (2004). Risk assessment of existing bridge structures.PhD Thesis. University of Cambridge, UK.

JCSS (Joint Committee on Structural Safety), (2001). Probabilistic Assessment of Existing Structures, Rilem publication, 2001

Liu M. and Frangopol D. M., (2004). Optimal bridge maintenance planning based on probabilistic performance prediction, Engineering Structures, vol. 26, issue 7, pp. 991-1002

Massarelli P. and Baber T., (2001). Fatigue reliability of steel highway bridge details, Final Report, Virginia Transportation Research Council, 2001

Matar, E. (2007), Evaluation of Fatigue Category of Riveted Steel Bridges Connections, Structural Engineering International 1

Miner, A., (1945). Cumulative Damage in Fatigue. Journal of Applied Mechanics, 12, pp159-164.

ML-D2.1 (2012). Degradation and performance specification for selected assets, Deliverable 2.1, MAINLINE project, SST.2011.5.2-6, 31/01/2012, 113 pp.

Munse, H., (1992). Estimating the remaining life of riveted railway bridges. Rep. Study Conducted for AAR, Assn. of Am. Railroads, III.

Palmgren, Arvid (1924). Die Lebensdauer von Kugellagern.(The Life Length of Roller Bearings. In German) Zeitschrift des Vereines Deutscher Ingenieure (VDI Zeitschrift), ISSN 0341-7258, Vol 68, No 14, 5 April 1924, pp 339-341.Equation (11) in the paper reads: $m_1/n_1 + m_2/n_2 + m_3/n_3 + \ldots = 1$. Here m_1 is the actual number of loadings for a specific load case and $n_1$is the number of loadings up to failure if only that load case is applied.

Pipinato, A, Pellegrino, C, Modena, C., (2012). Fatigue Behaviour of Steel Bridge Joints Strengthened with FRP Laminates, Modern Applied Sciences, vol. 6, No 10

 Copyright © MAINLINE Consortium

Standing Committee on Structural Safety (SCOSS), (2007).The Standing Committee on Structural Safety. 16th Biennial Report, London.

Stein, S. &Sedmera, K. (2006).Risk-Based Management Guidelines for Scour at Bridges with Unknown Foundations. NCHRP Web-Only Document 107, National Cooperative Highway Research Program, Transportation Research Board.

SB-4.6 (2007) Improved Assessment Methods for Static and Fatigue Resistance of Old Steel Railway Bridges. Background document D4.6, Sustainable Bridges, www.sustainablebridges.net

SB-5.2 (2007) Guideline for Monitoring of Steel Railway Bridges, Background document D5.2., Sustainable Bridges, www.sustainablebridges.net

SB-LRA (2007) Guideline for Load and Resistance Assessment of Existing European RailwayBridges (2007), SB-LRA document, Sustainable Bridges,www.sustainablebridges.net

Tobias D H, Foutch D A, (1997) 'Reliability-Based Method for Fatigue Evaluation of Railway Bridges', Journal of Bridge Engineering, Vol. 2, No. 2, pp53-60.

Xanthakos, P. P. (1994). Theory and Design of Bridges. New York: John Wiley and Sons, 1994.

Wong, S.M., Onof, C.J., Hobbs, R.E. (2005). Models for evaluating the costs of bridge failure. Proceedings of the Institution of Civil Engineers, Bridge Engineering 158(BE3): 117-128.

 Copyright © MAINLINE Consortium

7. Soil cuttings (SKM+NR)

7.1 Introduction

This chapter will report on the development of a deterioration and intervention modelling approach for railway cuttings across Europe. Both soil and rock cuttings are considered within the MAINLINE Project, and as such both types are covered in the literature review sections of this chapter. Due to the restrictions on time and resource in the preparation of this deliverable, efforts have been focussed on developing a modelling approach for soil cuttings. It is intended that this modelling approach could be adapted and extended to use on rock cutting assets at a later stage.

This chapter will build upon work done to date within other MAINLINE Work Packages and therefore a summary of the key findings related to the deterioration and intervention modelling of railway cuttings is provided in the sections below. These findings, along with further research undertaken into deterioration and intervention modelling techniques including a review of previous modelling work undertaken by Network Rail have informed the modelling approach that has been developed under this deliverable.

7.1.1 Input from Deliverable 2.1

Chapter 6 of the preceding MAINLINE deliverable 'D2.1 Degradation and Performance Specification' (MAINLINE.2.1 2012) presented and discussed a range of damage and deterioration mechanisms relevant to soil and rock cuttings. These are summarised in Table 7.1.

Table 7-1 Summary of damage and deterioration mechanisms for cuttings

Soil cuttings	Water ingress
	Weathering
	Long-term creep
	Erosion
	Supporting structure deterioration
	Landslides
	Excavations
	Mining subsistence
Rock cuttings	Weathering
	Climatic influences
	Discontinuities - natural
	Discontinuities - construction
	Failure of slope support systems

D2.1 also reported on the findings of a questionnaire issued to a range of European railway infrastructure owners. It was found that observed earthwork deterioration trends varied widely across questionnaire responses. The large number of variables involved in earthwork condition, including geometry, geology, environmental and external factors means that the rate of deterioration can vary on an asset by asset basis. The sensitivities of earthwork stability to climate change effects were also discussed.

 Copyright © MAINLINE Consortium

D2.1 found that earthwork deterioration rates are generally dependant on the age of an earthwork, and that the deterioration trends within the first 20 years of construction may be significantly different to the longer term deterioration trends. The focus of the MAINLINE Project is on elderly infrastructure assets, and as such the focus will be on longer term deterioration trends.

7.1.2 Input from Deliverable 1.1

D1.1 reported on the benchmarking of new technologies to extend the life of elderly rail infrastructure and included the following table outlining 3 new technologies related to earthworks (Table 7.2).

Table 7-2 New technologies for extending the life of elderly earthworks, as reported in D1.1

Fell et al (2005)

New Technology	Pros	Cons	Reference
Slope stability analysis for progressive failures	- More accurate predictions	- More complicated calculations	Bernander (2011)
Lime-cement columns	- Stabilizes the ground	- Need special equipment to apply	Larsson et al (2012)
Vertical drains	- Stabilizes the ground	- Need special equipment to apply	Hansbo (1997), Müller (2010)

These identified new technologies will be considered alongside the more traditional life extension techniques in chapter 7.3 of the present report, which describes interventions and their effect on condition.

7.1.3 Input from Deliverable 4.1

D4.1 reported on current monitoring and examination practices in relation to the degradation models. The following parameters were identified as being of high importance when monitoring the condition of a cutting (Table 7.3).

Table 7-3 Important parameters to be considered during monitoring of cuttings as reported in D4.1

Physical parameters	• Slope height • Failure frequency • Slope angle • Launching features • Ditch catchment
Climatic conditions	• Annual precipitation • Seepage/water • Aspect
Geological conditions	• Undercuttings • Durability/weathering • Inter bedded/ character • Slope • Joint conditions • Vegetation • Tension crack

The report identified regular visual examinations as being among the most cost-effective means of ensuring safety and longevity of cuttings. Such inspections involve careful examination of all parts of the cutting and its adjacent environment and must be carried out

 Copyright © MAINLINE Consortium

by a suitably trained person. Although cost effective, this observational method does have limitations in its accuracy as it can only report on visual features on the surface of the cutting and is affected by human error and inconsistencies between different assessors. The limitations of the visual examination method described above have led to the development and application of a wide range of new monitoring techniques for cuttings which are also reported in D4.1. A summary table of the cutting monitoring and examination techniques covered in D4.1 is presented in Table 7.4.

Table 7-4 Summary of cutting monitoring and examination techniques considered in D4.1

MAINLINE Project
WP4: Monitoring and Examination Techniques
D4.1: Report on assessment of current monitoring and examination practices in relation to the degration

Section 3. Cuttings

DM / M&E	Water presence	Washout	Long term creep	Scour	Failure of supporting structures	Erosion	Landslides and rockfalls	Vegetation
Visual Inspection	✓	✓	✓	✓	✓	✓	✓	✓
Inclinometers			✓		✓		✓	
Laser Scanning (LiDAR)	✓			✓	✓		✓	✓
Time Domain Reflectometry	✓						✓	
GPS			✓		✓		✓	
Interferometry							✓	
Acoustic Monitoring		✓			✓	✓	✓	
Video/image Analysis		✓		✓	✓		✓	✓

Refer to the full report for full details of the data outputs, advantages and disadvantages of each technique.

7.1.4 Input from Deliverable 5.5

D5.5 concerns the development of the MAINLINE LCAT and is strongly linked with the present deliverable as the deterioration models developed here will need to be incorporated into the cuttings model within the LCAT. At the time of writing this report D5.5 was in the early stages of production, however the following points have emerged from preliminary documentation and the kick-off workshop which will inform the development of the cutting deterioration and intervention model:

- It is anticipated that the prototype LCAT developed in D5.5 will work at single asset level, but with the capability to be up-scaled for use across a network or population of assets in the future. The deterioration and intervention model should therefore also be developed at single asset level.

- It is likely that the LCAT will be built in Excel, so it is intended to develop a deterioration modelling approach that could be implemented in Excel in order to maximize flexibility and compatibility.

 Copyright © MAINLINE Consortium

- The model should be flexible enough for use by different infrastructure managers across Europe, and should have the capability to allow the user to made adjustments, for example to the number or weighting of parameters, or to deterioration rates.

7.2 Condition Assessment Methods

In order to model the deterioration of a cutting it is necessary to first establish a measure of condition that can be repeatedly obtained and tracked over time. As discussed in D4.1, condition assessment may arise from either visual examinations, or from intrusive ground investigations and monitoring equipment. These methods provide data outputs related to a number of different aspects of stability and failure modes, which must be combined in some appropriate way in order to obtain an indication of overall asset condition.

7.2.1 Method of condition data collection

As discussed in D4.1, condition data for earthworks might be collected by either monitoring or examination techniques. The Network Rail approach to condition rating uses an examination method in order to obtain the input parameters for the SHHI algorithm. However in other parts of Europe monitoring data may be collected more extensively

The data obtained from monitoring is more detailed, reliable and quantitative, compared to the subjective and qualitative observations that arise from visual examinations. As such, the type of data that is available will define the level of condition assessment and deterioration modelling than can be undertaken.

Furthermore, there may be differences in the cutting assessment and condition scoring systems used across Europe as a result of regional differences in experience, preference and particular problems that are related to that region, for example sensitive soils in Sweden.

The authors of this chapter have only had access to the cutting assessment systems used by Network Rail in the UK, and so these systems are reviewed in Sections 7.2.2 and 7.2.3. It would be desirable to review any equivalent systems that may be in use in other parts of Europe; however this information has not been made available to the MAINLINE Consortium to date, and the authors are not aware of any such systems. Following review of the SSHI algorithm, the authors of this chapter have also developed an alternative approach to assessing the condition of a cohesive soil cutting which is presented in chapter 7.2.4. This is a prototype for a more generalised algorithm that might be more readily adapted to suit different regions and authorities within the European Union and may therefore be more appropriate for use in the MAINLINE Project.

7.2.2 Soil Slope Hazard Index (SSHI)

In 2003 Network Rail commissioned Babtie Group (Babtie 2003) to develop a system to facilitate quick and repeatable inspection of railway earthworks (both soil cuttings and embankments) to enable impartial assessment of their condition. This resulted in the development of the Soil Slope Hazard Index and associated algorithm. A measure of earthwork condition such as the SSHI is required in order to monitor deterioration over time, and as such an understanding of how the SSHI was derived will help inform what input parameters are suitable for use in the deterioration profiles to be developed under the present deliverable. Babtie Group produced a report on the principles and requirements of

 Copyright © MAINLINE Consortium

the SSHI algorithm and how they were achieved (Babtie 2003). The key points of this report are discussed in the following sub sections.

Input Parameters and Failure Mechanisms.

The parameters that are recorded from site, and that form inputs to the SSHI algorithm relate to a range of 5 different failure mechanisms, as well as the size, geometry and geology of the earthwork. The input parameters can be broken down into three categories:

1. Evidence of past, on-going or imminent failures, such as toe bulge or tension cracks.

2. Factors that could influence the likelihood of future failure, even if no failure has yet occurred, such as the geology of the slope, surcharging at the top of a cutting or the slope angle.

3. Factors that could influence the magnitude of a slope failure, i.e. the slope height.

The first two sets of parameters are specific to one or more individual failure modes, whereas the slope height will be the same for each failure mode. General descriptions of the 5 soil cutting failure modes considered in the SSHI algorithm are provided in Table 7.5.

Table 7-5 Soil Cutting Failure Mechanisms used in the SSHI (Babtie 2003)

Failure Mechanism	General Description
Deep Rotational	Rotational or quasi-rotational failure affecting whole slope and crest. May include heave of track formation.
Shallow Translational	Shallow failure parallel to slope usually of weathered mantle.
Earthflow	Groundwater seepage causing saturation and plastic flow of cutting face.
Washout	Surface water flow from adjacent ground leading to erosion of cutting face and deposition in cess.
Burrowing	Burrowing activity leading to settlement of cutting slope and deposition of spoil on cutting slope and cess.

Fundamentals of the Algorithm

The SSHI algorithm is based on the following key principles:

- **Semi-Qualitative** – The SSHI system gives a semi-qualitative indication of general condition. It is not an analytical process, but rather based on simple manipulation of empirical observations.

- **Transparent** – The system has been designed to be as transparent as possible

- **Assesses failure modes independently** – the system has been designed to allow changes in the condition for each failure mode to be monitored between inspections. An asset is given 5 SSHI scores corresponding to the 5 failure modes.

- **Assesses Overall Earthwork Condition** – the system has been designed to differentiate between Poor, Marginal and Serviceable Conditions. The overall classification of the earthwork is based on the worst SSHI across the 5 failure modes.

 Copyright © MAINLINE Consortium

The earthwork only need to be classified as Poor for one failure mode in order to be considered in a Poor condition.

Failure Scores and Earthwork Condition Scores

For each failure mode an earthwork is assigned two separate failure scores, together with an earthwork height factor, which combine to generate the SSHI:

- **Actual failure score** – Determined for each failure mode on the basis of relevant actual failure indicators, which indicate that failure has happened in the past, is happening at present or is imminent.

- **Potential failure score** – Determined for each failure mode on the basis of relevant potential failure indicators, which indicate the potential for future failure to occur.

- **Earthwork Height Factor –** A single number for an earthwork based on its height.

The SSHI is derived based on the combination of actual, potential and earthwork height scores. These actual, potential and earthwork scores are themselves derived from site observations that are recorded on an inspection data sheet during regular earthwork examinations. Each of the inspection parameters recorded on the data sheet was assigned a corresponding actual or potential score following a series of development and review stages carried out by Babtie, including sample assessments and engineering reviews. As such, the relevant significance of various inspection parameters to the condition of the earthwork was determined.

The inspection parameters and their assigned earthwork, actual and potential scores are shown in Table 7.6-8 (TRL 2000). Note that shaded cells indicate Actual Failure Parameters and numbers marked with * contribute to both Actual and Potential Score.

 Copyright © MAINLINE Consortium

Table 7-6 Network Rail Soil Cutting Inspection Sheets with Parameter Scores (1/3)

STABILITY INDICATORS FOR SOIL CUTTINGS	STABILITY INDEX PARAMETER	OBSERVED/MEASURED VALUE	REF CUT	EARTHWORKS FACTOR	ROTATIONAL	TRANSLATIONAL	EARTHFLOW	WASHOUT	BURROWING
Slope Geometry	Slope Angle and Slope Height	<15 degrees, <3m High	A1	L	0	0	0	0	0
		15 to <25 degrees, <3m High	A2	L	5	10	5	5	5
		25 to <35 degrees, <3m High	A3	L	10	20	15	10	10
		>35 degrees, <3m High	A4	L	40	50	20	15	20
		<15 degrees, 3m to <10m High	A5	M	0	0	0	0	0
		15 to <25 degrees, 3m to <10m High	A6	M	5	10	5	5	5
		25 to <35 degrees, 3m to <10m High	A7	M	10	20	15	10	10
		>35 degrees, 3m to <10m High	A8	M	40	50	20	15	20
		<15 degrees, >10m High	A9	H	0	0	0	0	0
		15 to <25 degrees, >10m High	A10	H	5	10	5	5	5
		25 to <35 degrees, >10m High	A11	H	10	20	15	10	10
		>35 degrees, >10m High	A12	H	40	50	20	15	20
	Slope angle adjacent to earthwork (i.e. Sidelong Ground)	(-)ve	B1		0				
		(+)ve <5 degrees	B2		3				
		(+)ve 5 to 15 degrees	B3		6				
		(+)ve >15 degrees	B4		9				
	Retaining walls 1m high or greater	None	C1		**0**	**0**			
		<1m high but>20m length	C2		**0**	**0**			
		No evidence of distress	C3		**0**	**0**			
		Minor distress (spalling, pointing etc)	C4		**10**	**10**			
		Cracking / evidence of lateral	C5		**35**	**35**			
		Evidence of Repairs	C6		**35**	**35**			
	Construction activity	None	D1		0	0			
		Removal of material from crest	D2		0	0			
		Addition of fill <1m high	D3		0	0			
		Addition of fill between 1m & 5m high	D4		10	5			
		Addition of fill >5m high	D5		20	10			
		Removal of material from toe	D6		20	20			
Minimum slope to track separation	Distance between sleeper ends and toe of cutting	Cutting cess width >6m	E1						**-70***
		Cutting cess width 3-6m	E2						**-25***
		Cutting cess width 1-3m	E3						
		Cutting cess width<1m	E4						
Adjacent Geology	BGS Geological Strata Shown within 0.2km of Earthwork limits (if more than one of these is present, use the cumulative score)	No drift	F0						
		Boulder Clay	F1		3	3			
		Blown Sand	F2				10	10	15
		Alluvium	F3		6	3	6	6	15
		Terrace Deposits	F4				3	3	10
		Sand and Gravel	F5				3	3	10
		Peat	F6				3	3	0
		Head Deposits	F7		9	9	6	6	0
		Laminated Clay	F8		9	9			
		Landslip	F9		20	20			
		Made Ground	F10						
		Solid							
		Manchester Marl	F11		3	3			
		Mercia Mudstone	F12		3	3			
		Shale/Mudstone Carboniferous	F13						
		Other Competent	F20						
Slope Crest	Width	Crest to boundary <1.5m	G1						
		Crest to boundary 1.5-3m	G2						
		Crest to boundary >3m	G3						

Copyright © MAINLINE Consortium

Table 7-7 Network Rail Soil Cutting Inspection Sheets with Parameter Scores (Part 2 of 3)

STABILITY INDICATORS FOR SOIL CUTTINGS	STABILITY INDEX PARAMETER	OBSERVED / MEASURED VALUE	REF CUT	EARTHWORKS FACTOR	ROTATIONAL	TRANSLATIONAL	EARTHFLOW	WASHOUT	BURROWING
Slope Composition at Crest	Predominant Material Type	Very Weak or Weak Rock	H1		0	0	0	0	0
		Coarse granular	H2		0	0	5	4	10
		Fine granular	H3		3	0	10	8	30
		Mixed granular/cohesive	H4		6	5	5	4	20
		Cohesive (low - intermediate plasticity)	H5		9	5	0	0	0
		Cohesive (high – very high plasticity)	H6		12	10	0	0	0
		Unknown	H7		8	5	5	4	10
Slope Composition at Toe	Predominant Material Type	Very Weak or Weak Rock	I1		0	0	0	0	0
		Coarse granular	I2		0	0	5	4	10
		Fine granular	I3		3	0	10	8	30
		Mixed granular/cohesive	I4		6	5	5	4	20
		Cohesive (low - intermediate plasticity)	I5		9	5	0	0	0
		Cohesive (high - very high plasticity	I6		12	10	0	0	0
		Unknown	I7		8	5	5	4	10
Associated Drainage	Slope face drainage conditions	Face dry	J1		0	0	0	0	
		Functioning drainage	J2		0	0	4	0	
		Blocked drainage	J3		5	5	8	6	
		Marshy areas on slope	J4		10	10	12	12	
		Surface issues on lower slope	J5		15	15	24	12	
		Surface issues on upper slope	J6		15	15	20	12	
	Drainage of adjacent land	None	K1		0	0	0	0	
		Natural water course within 20m of slope crest	K2		10	10	8	8	
		Artificial water course within 20m of slope crest	K3		0	0	0	0	
	Adjacent catchment size	>50 Ha	L1		0	0	9	9	
		10 –50 Ha	L2		0	0	6	6	
		1-10 Ha	L3		0	0	3	3	
		< 1Ha	L4		0	0	0	0	
	Adjacent catchment gradient	> 25^{o}	M1		0	0	10	20	
		5-25^{o}	M2		0	0	5	15	
		< 5^{o}	M3		0	0	2	5	
		Slopes away from structure	M4		0	0	0	0	
	Catchment Surface	Rough Grass	N1				0	0	
		Grazed Pasture	N2				0	0	
		Ploughed	N3				2	2	
		Wooded/Large Scrub	N4				2	2	
		Other	N5				3	3	
		Residential	N6				5	5	
		Industrial/Hardstanding	N7				5	5	
	Catchment Geology	Permeable	P1				0	0	
		Impermeable	P2				5	5	
		Mixed	P3				2	2	

Copyright © MAINLINE Consortium

Table 7-8 Network Rail Soil Cutting Inspection Sheets with Parameter Scores (Part 3 of 3)

STABILITY INDICATORS FOR SOIL CUTTINGS	STABILITY INDEX PARAMETER	OBSERVED / MEASURED VALUE	REF CUT	EARTHWORKS FACTOR	ROTATIONAL	TRANSLATIONAL	EARTHFLOW	WASHOUT	BURROWING
Associated	Slope crest drainage	None Visible	Q1				5	10	
		French Drain	Q2				0	0	
		V Channel	Q3				0	0	
		U Channel	Q4				0	0	
		Size >0.25 m^2	Q5				0	0	
		Size 0.1m^2 to 0.25m^2	Q6				0	0	
		Size < 0.1m^2	Q7				0	0	
		Gradient <5^0	Q8				0	0	
		Gradient 5^0 to 15^0	Q9				0	0	
		Gradient >15^0	Q10				0	0	
		Free Draining	Q11				0	0	
		Partially blocked	Q12				5	10	
		Blocked	Q13				15	20	
	Slope Crest concentration features	Multiple Narrow – Well Defined	R1					10	
		Single Narrow – Well Defined	R2					20	
		Multiple - Shallow	R3					5	
		Single - Shallow	R4					10	
		None	R5					0	
	Slope erosion	Multiple – well defined	S1					**70**	
		Multiple – poorly defined	S2					**30**	
		Single – well defined	S3					**30**	
		Single – poorly defined	S4					**20**	
		None	S5					**0**	
	Cess Drainage	None	T1		3	3	3	3	
		Present clear running	T2		0	0	0	0	
		Present unknown condition	T3		0	0	0	0	
		Flooding apparent	T4		6	6	6	6	
		Blocked/Impaired	T5		10	10	10	10	
Movement Indicators (Overall Failure)	Slope form of Earthwork	Uniform toe	U1		**0**	**0**	**0**		
		Terracing in midslope	U2		**10**	**10**	**5**		
		Hummocky ground in midslope	U3		**10**	**10**	**5**		
		Toe bulging	U4		**25**	**25**	**15**		
		Uniform Crest	U5		**0**	**0**	**0**		
		Stepped Crest	U6		**30**	**30**	**15**		
	Geomorphology of Adjacent Land	Deep-seated landslips	V1		30	30			
		Hummocky Ground / Solifluction Lobes	V2		10	10			
		No Significant Features	V3		0	0			
	Track Movements (vis. to naked eye)	Track Heave	W1		**70**		**70**		
		No Significant Features	W2		**0**		**0**		
	Attitude of mature trees / fence lines / signals	Vertical	X1		**0**	**0**	**0**		
		Random	X2		**0**	**0**	**0**		
		Bent tree trunks (convex upslope)	X3		**0**	**0**	**0**		
		Bent tree trunks (convex downslope)	X4		**10**	**10**	**6**		
		Predominantly tilted downslope (<10 degrees off vertical)	X5		**10**	**10**	**6**		
		Predominantly tilted downslope (>10 degrees off vertical)	X6		**10**	**10**	**6**		
		Tilted upslope near cutting crest	X7		**10**	**10**	**6**		

In turn, this enables both the final results and the scores that are applied to the individual parameters to be more transparent. The scores are combined to generate the SSHI for each failure mode as shown in Table 7.9.

 Copyright © MAINLINE Consortium

Table 7-9 Derivation of the SSHI Score (Babtie 2003)

i) The Actual failure score and Potential failure score are determined for each of the five failure modes by adding the scores for the relevant parameters. The scores for each are then ranked as High, Medium or Low on the following basis:

Actual Failure Score	Ranking	Potential Failure Score
<30	Low	<45
30 – 69	Medium	45 – 69
>69	High	>69

ii) The Earthworks Factor is determined based on the slope height as follows:

Slope Height	**Earthworks Factor**
< 3 metres	Low
3 – 10 metres	Medium
> 10 metres	High

Based on the ranking of the three factors as High, Medium or Low, the following operation is carried out:

Factor	**High**	**Medium**	**Low**	
Actual Failure Factor (derived by adding up individual scores for actual failure indicators)	6	3	1	**+**
Potential Failure Factor (derived by adding up individual scores for potential failure indicators)	4	2	1	
Earthworks Height Factor	1.6 (slope height > 10m)	1.3 (slope height = 3 – 10m)	1 (slope height < 3m)	**x**
				= SSHI

The SSHI scores are banded into 3 Earthwork Conditions, Poor, Marginal and Serviceable as shown in Fig.7.1.

 Copyright © MAINLINE Consortium

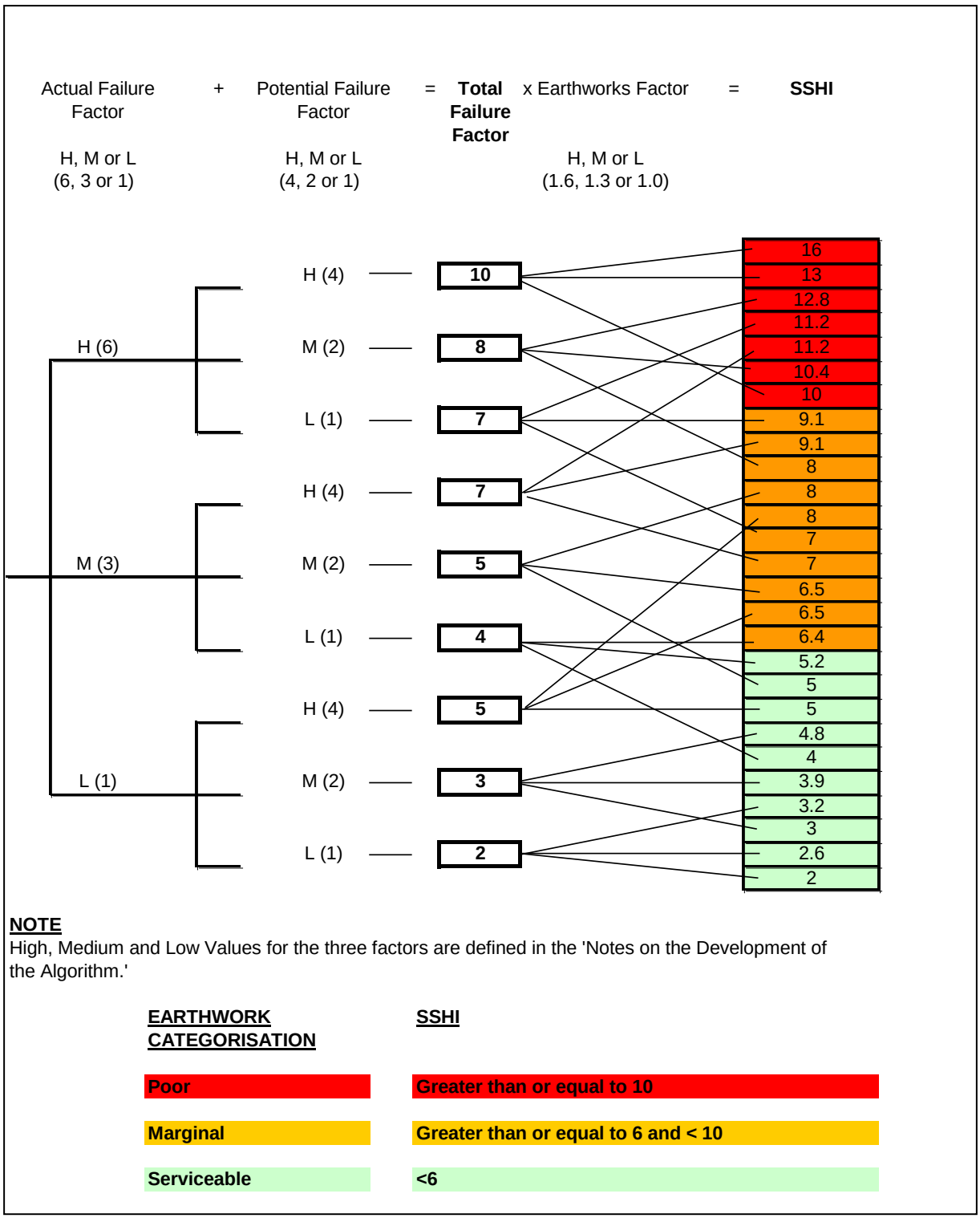

Figure 7-1 SSHI Failure Flow Diagram (Babtie 2003)

Validation of the SSHI algorithm

The following validation exercises were carried out during the development of the SHHI algorithm:

 Copyright © MAINLINE Consortium

i) Sample SSHI assessments were compared with an alternative assessment, the Risk Evaluation Matrix (REM), carried out by the examining engineer. The engineers assessment could then be compared with the earthwork categorisation as a result of the SSHI algorithm.

ii) All sites recorded as Poor on the REM and a proportion of others were assessed by senior earthwork examiners, providing a more robust indication of the state of an earthwork.

iii) A large number of poor sites (both from the REM and from the algorithm) were examined by Network Rail's Earthworks Manager and Babtie's Technical Director to reassess their condition.

At each stage discrepancies between the SSHI condition assessment and the alternative assessments were identified, and the algorithm was reviewed and adjusted as appropriate in order to improve confidence in the outputs.

7.2.3 Rock Slope Hazard Index (RSHI) (TRL 2000) and Rail Rock Slope Risk Appraisal (RRSRA) (McMillan & Manley 2003)

As the characteristics and behaviour of rock cuttings are very different to that of soil cuttings, Network Rail use a different condition scoring index for these assets, known as the Rock Slope Hazard Index (RSHI). Unlike the SSHI the RSHI was not developed specifically for Network Rail assets, but is a more general rock slope assessment method.

The RSHI system was developed by TRL to aid in identifying potentially hazardous slopes. It was developed for use in the assessment of highway rock slopes and is based around quick and standardised field data collection containing estimates of geotechnical, geometric and remedial work factors (Babtie 2003). Parameter values were derived for each input factor as a result of extensive research and calibration, in order to reflect the influence of each factor on rock slope hazard. These input parameters are combined with highway traffic flow data in a calculation procedure in order to derive the RSHI value.

Network Rail adapted the RSHI scoring for use on its assets by making a couple of minor additions, namely with the addition of ravelling failure as well as variations to trap and rock volume parameter tables to take account of railway cutting scenarios. This modified algorithm is officially named the Rail Rock Slope Risk Assessment (RRSRA) however is commonly still referred to as RSHI in Network Rail literature. From this point onwards in the text, the term RSHI is used to refer to the railway rock cutting assessment process developed by Network Rail, rather than the original TRL system.

<u>Input Parameters and Failure Mechanisms</u>
The RSHI algorithm calculates a score for each of the four failure mechanisms applicable to rock slopes:

- Planar Failure
- Wedge Failure
- Toppling Failure
- Ravelling Failure

 Copyright © MAINLINE Consortium

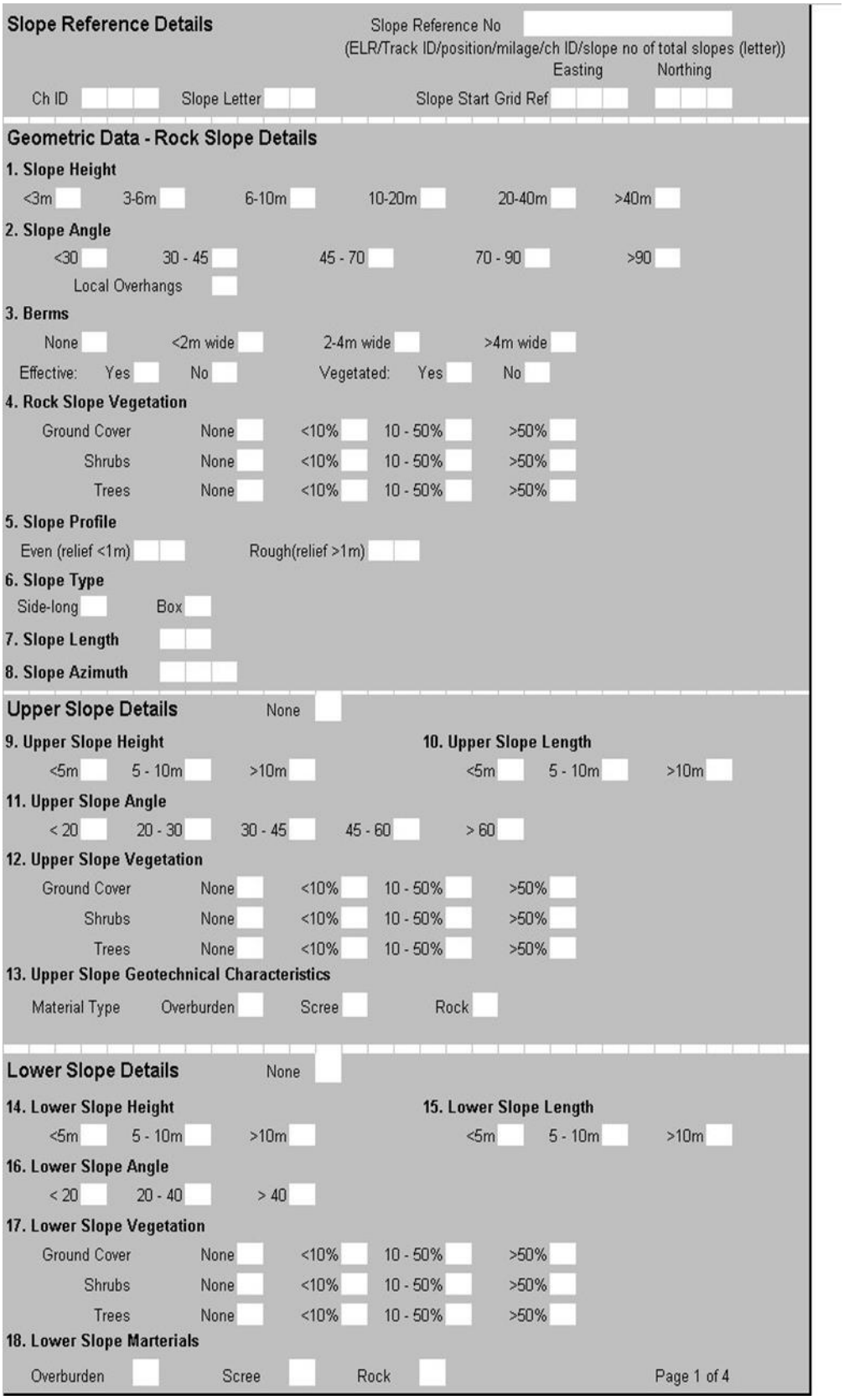

Slope Reference Details

Slope Reference No
(ELR/Track ID/position/milage/ch ID/slope no of total slopes (letter))

Easting Northing

Ch ID Slope Letter Slope Start Grid Ref

Geometric Data - Rock Slope Details

1. Slope Height

<3m 3-6m 6-10m 10-20m 20-40m >40m

2. Slope Angle

<30 30 - 45 45 - 70 70 - 90 >90

Local Overhangs

3. Berms

None <2m wide 2-4m wide >4m wide

Effective: Yes No Vegetated: Yes No

4. Rock Slope Vegetation

Ground Cover	None	<10%	10 - 50%	>50%
Shrubs	None	<10%	10 - 50%	>50%
Trees	None	<10%	10 - 50%	>50%

5. Slope Profile

Even (relief <1m) Rough(relief >1m)

6. Slope Type

Side-long Box

7. Slope Length

8. Slope Azimuth

Upper Slope Details None

9. Upper Slope Height

<5m 5 - 10m >10m

10. Upper Slope Length

<5m 5 - 10m >10m

11. Upper Slope Angle

< 20 20 - 30 30 - 45 45 - 60 > 60

12. Upper Slope Vegetation

Ground Cover	None	<10%	10 - 50%	>50%
Shrubs	None	<10%	10 - 50%	>50%
Trees	None	<10%	10 - 50%	>50%

13. Upper Slope Geotechnical Characteristics

Material Type Overburden Scree Rock

Lower Slope Details None

14. Lower Slope Height

<5m 5 - 10m >10m

15. Lower Slope Length

<5m 5 - 10m >10m

16. Lower Slope Angle

< 20 20 - 40 > 40

17. Lower Slope Vegetation

Ground Cover	None	<10%	10 - 50%	>50%
Shrubs	None	<10%	10 - 50%	>50%
Trees	None	<10%	10 - 50%	>50%

18. Lower Slope Marterials

Overburden Scree Rock

Page 1 of 4

Figure 7-2 RSHI data sheet (Part 1 of 4)

 Copyright © MAINLINE Consortium

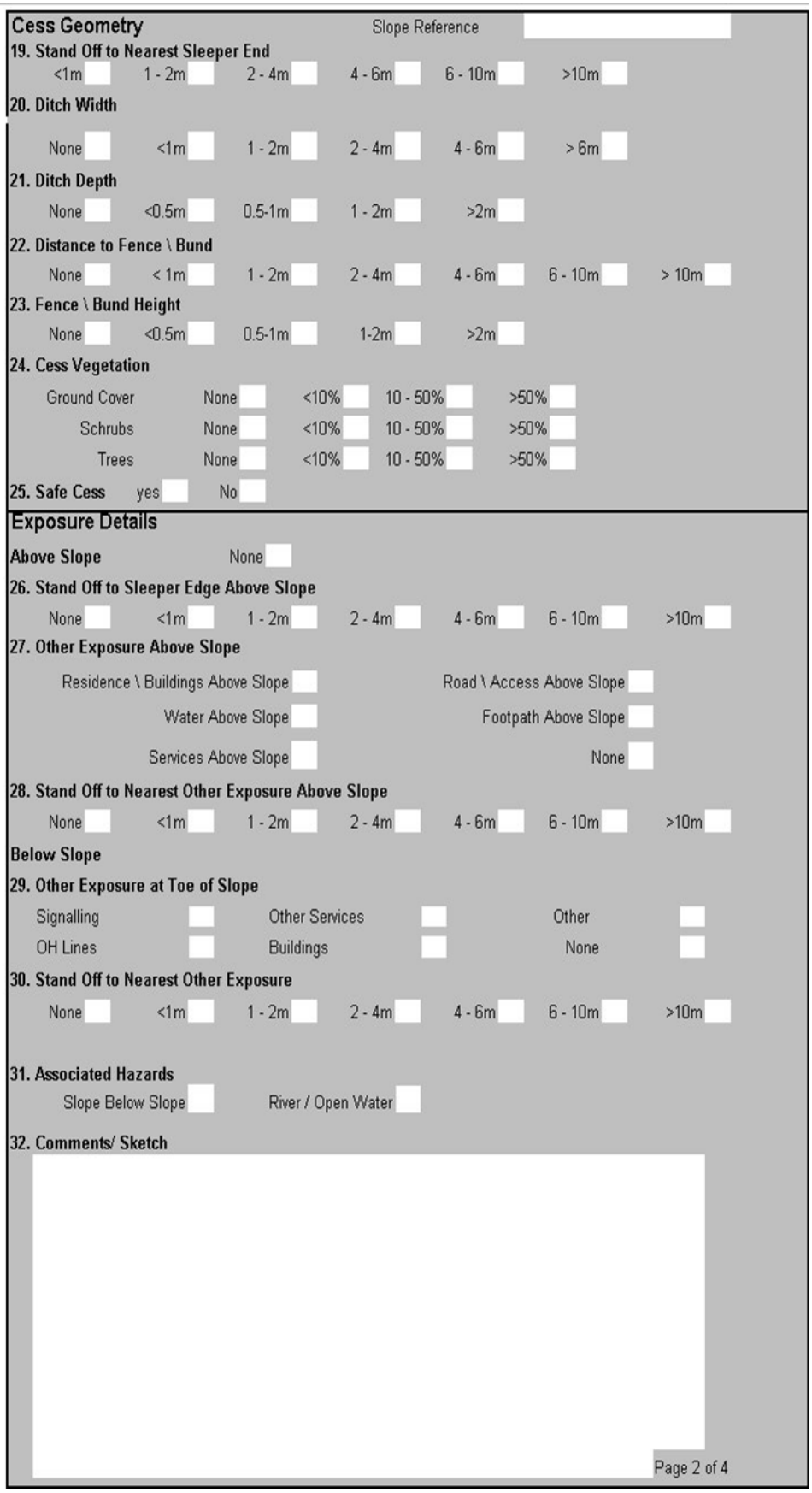

Cess Geometry Slope Reference

19. Stand Off to Nearest Sleeper End
<1m 1 - 2m 2 - 4m 4 - 6m 6 - 10m >10m

20. Ditch Width
None <1m 1 - 2m 2 - 4m 4 - 6m > 6m

21. Ditch Depth
None <0.5m 0.5-1m 1 - 2m >2m

22. Distance to Fence \ Bund
None < 1m 1 - 2m 2 - 4m 4 - 6m 6 - 10m > 10m

23. Fence \ Bund Height
None <0.5m 0.5-1m 1-2m >2m

24. Cess Vegetation

Ground Cover	None	<10%	10 - 50%	>50%
Schrubs	None	<10%	10 - 50%	>50%
Trees	None	<10%	10 - 50%	>50%

25. Safe Cess yes No

Exposure Details

Above Slope None

26. Stand Off to Sleeper Edge Above Slope
None <1m 1 - 2m 2 - 4m 4 - 6m 6 - 10m >10m

27. Other Exposure Above Slope
Residence \ Buildings Above Slope Road \ Access Above Slope
Water Above Slope Footpath Above Slope
Services Above Slope None

28. Stand Off to Nearest Other Exposure Above Slope
None <1m 1 - 2m 2 - 4m 4 - 6m 6 - 10m >10m

Below Slope

29. Other Exposure at Toe of Slope
Signalling Other Services Other
OH Lines Buildings None

30. Stand Off to Nearest Other Exposure
None <1m 1 - 2m 2 - 4m 4 - 6m 6 - 10m >10m

31. Associated Hazards
Slope Below Slope River / Open Water

32. Comments/ Sketch

Page 2 of 4

Figure 7-3 RSHI data sheet (Part 2 of 4)

 Copyright © MAINLINE Consortium

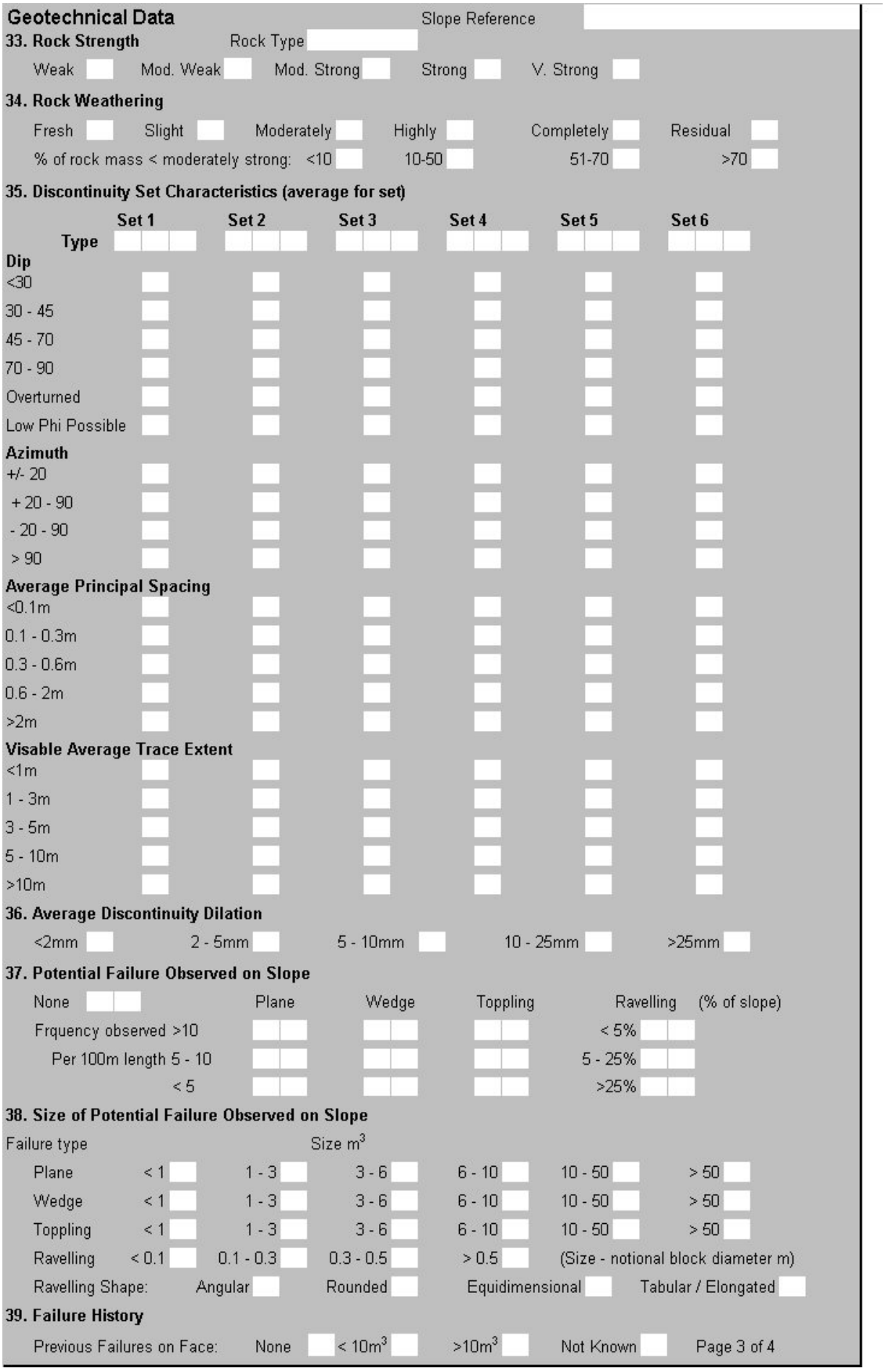

Geotechnical Data Slope Reference

33. Rock Strength Rock Type

Weak | Mod. Weak | Mod. Strong | Strong | V. Strong

34. Rock Weathering

Fresh | Slight | Moderately | Highly | Completely | Residual

% of rock mass < moderately strong: <10 | 10-50 | 51-70 | >70

35. Discontinuity Set Characteristics (average for set)

	Set 1	Set 2	Set 3	Set 4	Set 5	Set 6
Type						
Dip						
<30						
30 - 45						
45 - 70						
70 - 90						
Overturned						
Low Phi Possible						
Azimuth						
+/- 20						
+ 20 - 90						
- 20 - 90						
> 90						
Average Principal Spacing						
<0.1m						
0.1 - 0.3m						
0.3 - 0.6m						
0.6 - 2m						
>2m						
Visable Average Trace Extent						
<1m						
1 - 3m						
3 - 5m						
5 - 10m						
>10m						

36. Average Discontinuity Dilation

<2mm | 2 - 5mm | 5 - 10mm | 10 - 25mm | >25mm

37. Potential Failure Observed on Slope

	None	Plane	Wedge	Toppling	Ravelling (% of slope)
Frquency observed	>10				< 5%
Per 100m length	5 - 10				5 - 25%
	< 5				>25%

38. Size of Potential Failure Observed on Slope

Failure type	Size m^3					
Plane	< 1	1 - 3	3 - 6	6 - 10	10 - 50	> 50
Wedge	< 1	1 - 3	3 - 6	6 - 10	10 - 50	> 50
Toppling	< 1	1 - 3	3 - 6	6 - 10	10 - 50	> 50
Ravelling	< 0.1	0.1 - 0.3	0.3 - 0.5	> 0.5	(Size - notional block diameter m)	

Ravelling Shape: Angular | Rounded | Equidimensional | Tabular / Elongated

39. Failure History

Previous Failures on Face: None | < $10m^3$ | > $10m^3$ | Not Known

Page 3 of 4

Figure 7-4 RSHI data sheet (Part 3 of 4)

 Copyright © MAINLINE Consortium

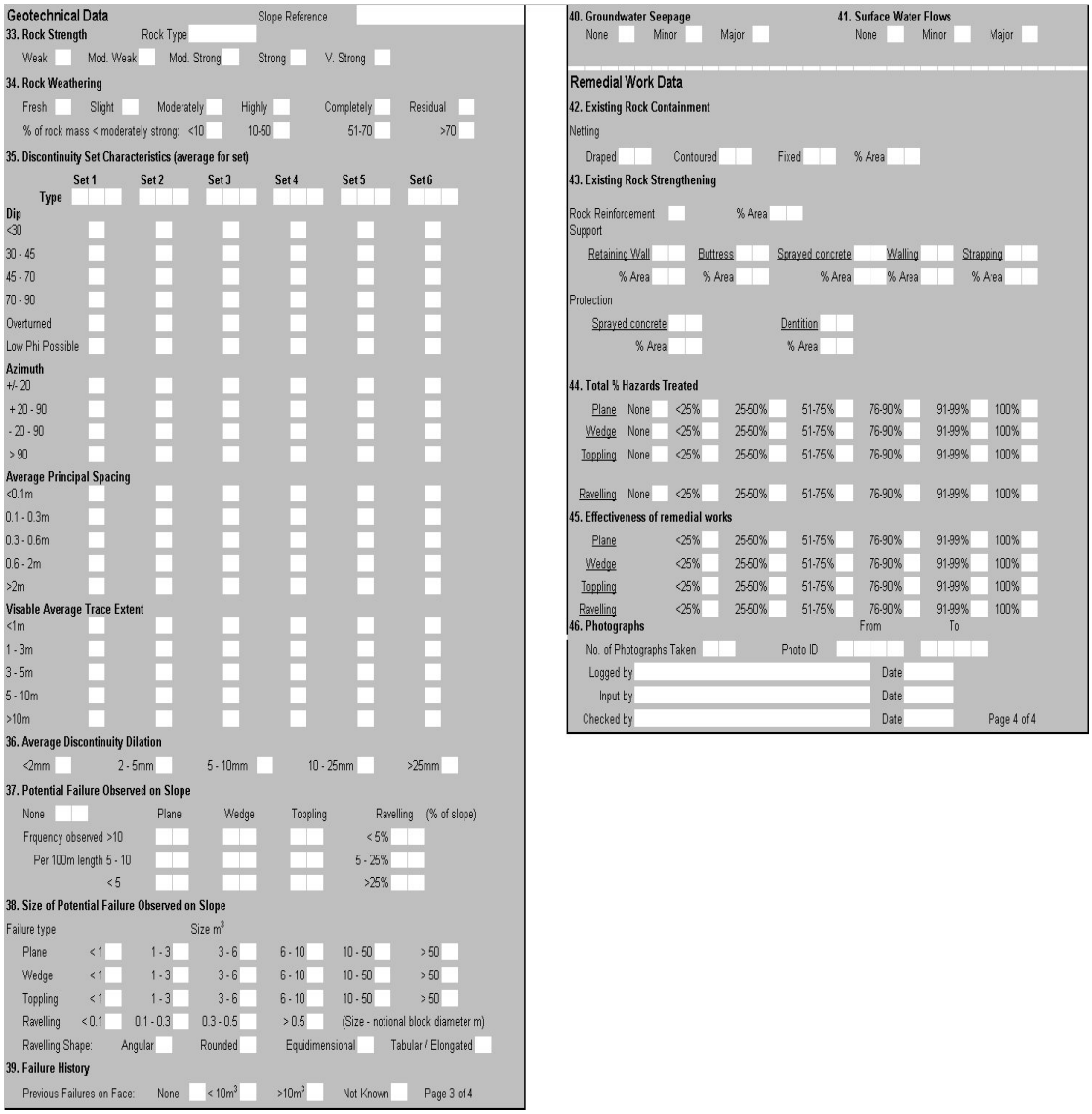

Figure 7-5 RSHI data sheet (Part 4 of 4)

The overall Earthworks Condition is derived from the combined score across the different failure modes. This is fundamentally different to the SSHI which takes the Earthworks Condition to be the highest score from a single failure mechanism.

Weighted values are assigned to each data parameter collected during site inspection and recorded on a data sheet. The inspection data sheet is provided on Fig.7.2-5.

The RSHI calculation differentiates between 2 types of input parameter:

- Primary Parameters – these establish the potential for rock fall. Within the algorithm they indicate calculation paths or add in to the calculation at appropriate stages.

- Secondary Parameters – these influence the likelihood, scale, severity and consequence of a rock fall event.

 Copyright © MAINLINE Consortium

RSHI calculation

The RSHI calculation is carried out by third party software and us such there is limited visibility of the calculation steps and parameter weightings. For some factors each recorded data element has a specific corresponding parameter value. However for other factors, the relationship between recorded data elements and RSHI parameter values is more complex, and is dependent on combinations of data collection options. As far as possible the parameter weightings have been derived from published relationships and research. However in areas where published data is lacking some assumed parameters have been adopted based on the expertise and experience of the RSHI development team. A schematic of the RSHI calculation procedure is provided in Fig.7.6.

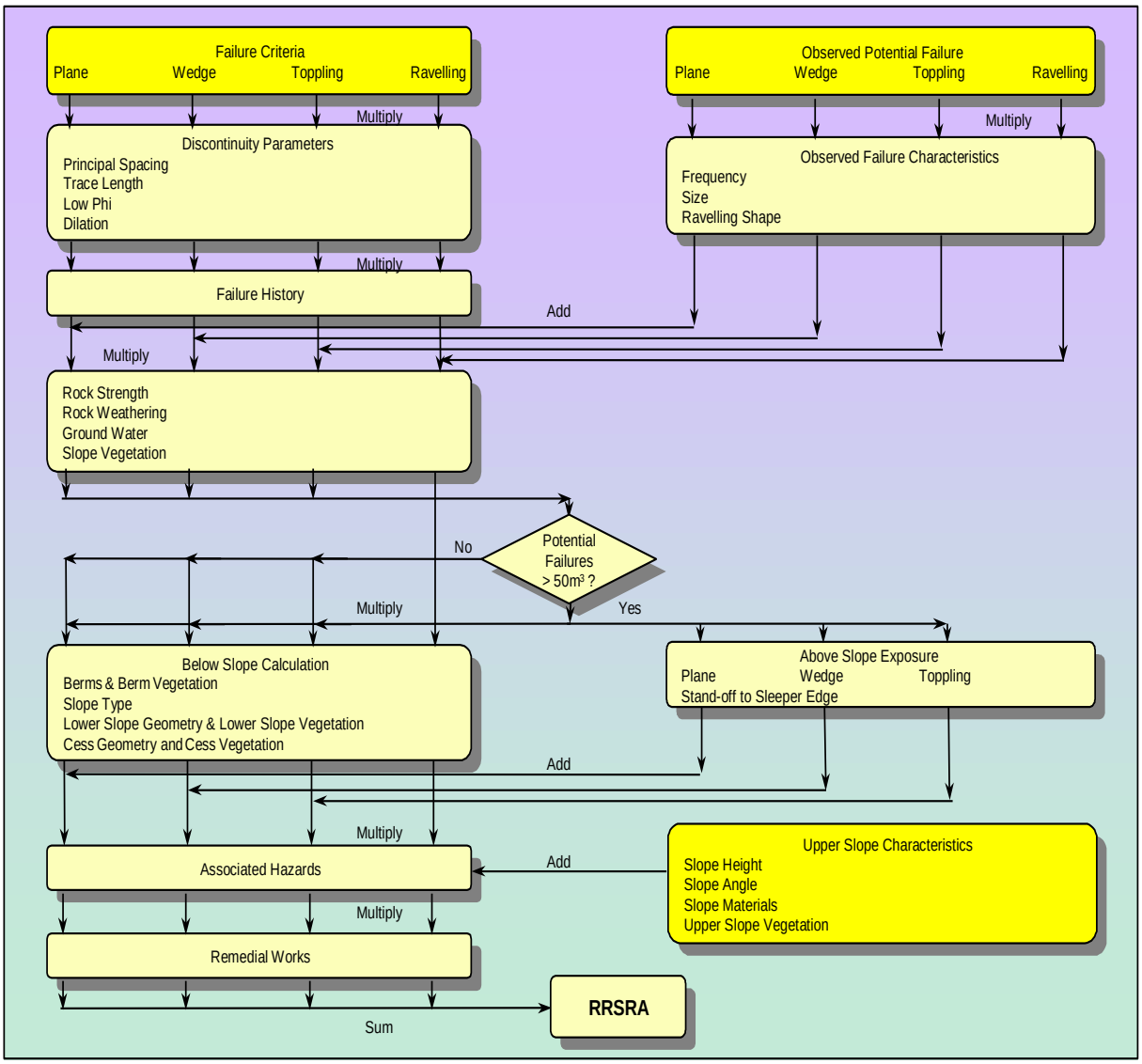

Figure 7-6 Schematic of RRSRA Calculation Procedure (McMillan & Manley, 2003)

As with SSHI, the RSHI score is used to categorise the cutting into three condition categories: Serviceable, Marginal or Poor. The range of RSHI values in each Earthwork categorisation band are as follows:

 Copyright © MAINLINE Consortium

- Serviceable ≤ 10
- Marginal > 10, < 100
- Poor ≥100, ≤200

Top Poor is not a defined category within RSHI, but is used as an additional prioritisation and applies to RSHI scores of > 200.

As can be seen in Fig.7.6, the effect of interventions is captured directly in the calculation of the RSHI. This is discussed further in Section 7.4.

7.2.4 Generalised soil slope condition assessment algorithm

Following review of the SSHI and RSHI algorithms, SKM have identified some possible limitations to their application within the deterioration models to be developed for the MAINLINE LCAT.

They have been developed based on UK experience alone and may not be suited to the assessment of earthworks in other European regions.

There is the possibility of some double accounting within the SSHI algorithm, for example the additive effects of poor drainage and observed surface water, which may limit accuracy of condition scoring. In reality there are complex cause and effect relationships between the base values and observed condition parameters, as well as between the observed values themselves as illustrated in Fig.7.7. If these interdependencies are ignored when calculating condition then there is a danger of double counting the contribution to condition score. However the complexity of the interdependencies means that it is not practical to attempt to model them all. The challenge is to account for the major interdependencies without making the model too complex.

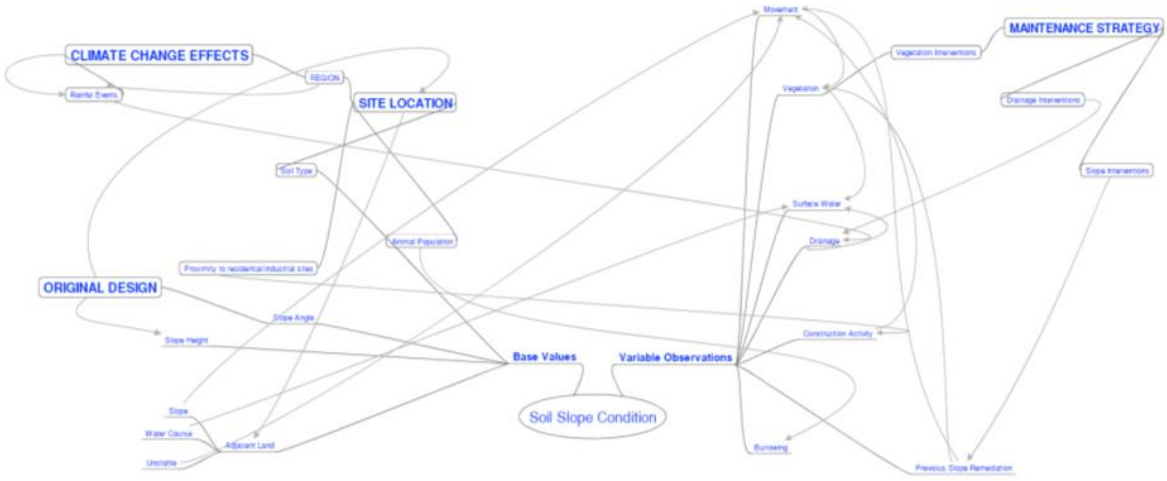

Figure 7-7 Flow Map showing interaction between soil cutting condition input variables.

The specific nature of some of the input parameter values may not be compatible with examination data available in other European counties.

Simultaneous monitoring of SSHI scores for the 5 different failure modes, and counting only the most onerous as the overall condition may not be the most appropriate way to deal with the inter relationships between degradation mechanisms. The SSHI model treats failure modes separately but in reality there is clearly interaction between them.

SKM have therefore looked for the means and methods to suggest a more generalised algorithm that can be readily adapted to suit different regions and authorities within the European Union. Due to the time and resource restraints, efforts have been focussed on developing a prototype condition assessment algorithm for cohesive soil cuttings only. If this is the preferred condition assessment approach to be taken forward, following feedback from other European infrastructure managers and WP5 partners, then the prototype algorithm could be further developed and extended to cover other soil types and rock cuttings.

The algorithm presented herein has been developed by SKM, and incorporates the experience and expertise of the SKM Geotechnical Engineering team, who have reviewed the SSHI algorithm that has been developed by Network Rail. It builds upon the principles and research that is embedded within the SSHI and utilises a similar suite of input parameters. The prototype algorithm has also been reviewed by Network Rail, whose comments have been incorporated.

Input Parameters

The generalised algorithm is based on a suite of input parameters that can be independently defined and then inter-related through their relative impact on cutting stability. The identified building blocks are:

- Slope geology and geometry (base values)
- Degradation observations and their inter-relationships (assessment values)

A full list of the input data required for the generalised algorithm is provided in Table 7.10.

Descriptions of the input parameters, their weightings and interdependencies are provided in the following sections.

Base Values

The stability of any cutting slope, in terms of geotechnical design, is based on the following fundamental elements:

- Soils deposits which constitute the slope and the ground underlying it
- The height of the cutting
- The shear strength (effective stress parameters) of the deposits
- The angle at which the slope is formed
- The steady state groundwater profile developed behind the cut face

When considering the practicalities of assessing extensive lengths of cutting it is presumed that, except in isolated cases, no measurement of shear strength and groundwater profiles will be available to the engineer. The assessor is therefore left with a limited number of what

 Copyright © MAINLINE Consortium

are termed herein as 'Base Values', against which subsequent deterioration/degradation can be observed and measured:

- Soil Type
- Slope Angle
- Slope Height

An additional element that can be included in this set of Base Criteria is the general landform that exists above the cutting. It is recognised by most practitioners that without the presence of water soil mechanics would be a relatively straightforward discipline. Ground sloping towards the top of a cutting will clearly increase surface water flow towards the cutting, and also potentially sub-surface flow; steeply rising ground to the rear of a cutting can also contribute to the overall effective cutting height. So a fourth element can be ascribed to the Base Criteria:

- Adjacent landform

Table 7-10 Input parameters required for generalised cohesive slope assessment algorithm (prototype)

Slope Base Value Inputs				
	Soil Type (ST)		Soil Type	
			ST1	Cohesive (C)
			ST2	Grandular (G)
			ST3	Interbedded (I)
	Slope Angle Factor (SAF)		Slope Angle	
			SAF1	< 15°
			SAF2	15° - 25°
			SAF3	25° - 35°
			SAF4	> 35°
	Slope Height Factor (SHF)		Slope Height	
			SHF1	< 3m
			SHF2	3m - 10m
			SHF3	> 10m
	Adjacent Land Factor (ALF)		Adjacent Land Slope	
			ALF1	-ive slope
			ALF2	No slope
			ALF3	+ive slope
			Adjacent Land Features	
			ALFA	Slope Only
			ALFB	Slope + Water Course
			ALFC	Slope + Unstable Land
			ALFD	Slope + W.C. + U.L.
Slope Assessment Inputs				
	Movement Assessment (MA)		Movement Feature 1	
			MA1	Track Heave
			MA2	Toe Bulging
			MA3	Crest Slump
			MA4	Midslope Hummocks
			MA5	Toe Debris
			Movement Feature 2	
			MAA	Track Heave
			MAB	Toe Bulging
			MAC	Crest Slump
			MAD	Midslope Hummocks
			MAE	Toe Debris
	Vegetation Assessment (VA)		Vegetation Feature 1	
			VA1	Slope Base is Sparse
			VA2	Abundant Grass
			VA3	Occasional Trees
			VA4	Frequent Trees
			VA5	Tilted Trees
			Vegetation Feature 2	
			VAA	Slope Base is Sparse

 Copyright © MAINLINE Consortium

			VAB	Slope Cracked (>3mm)
			VAC	Abundant Grass
			VAD	Occasional Trees
			VAE	Frequent Trees
			VAF	Tilted Trees
	Surface Water Assessment (SWA)		Surface Water Feature 1	
			SWA1	Surface Flow
			SWA2	Erosion Channels
			SWA3	Marshy Ground
			SWA4	Toe Ponding
			SWA5	Toe Fines Accumulating
			SWA6	Crest Erosion
			Surface Water Feature 2	
			SWAA	Surface Flow
			SWAB	Erosion Channels
			SWAC	Marshy Ground
			SWAD	Toe Ponding
			SWAE	Toe Fines Accumulating
			SWAF	Crest Erosion
	Drainage Assessment (DA)		Drainage Feature 1	
			DA1	Comp rehensive
			DA2	Crest Blocked
			DA3	Slope Blocked
			DA4	Toe Blocked
			DA5	No Drains
			Drainage Feature 2	
			DAA	Comprehensive
			DAB	Crest Blocked
			DAC	Slope Blocked
			DAD	Toe Blocked
			DAE	No Drains
	Burrowing Assessment (BA)		Burrows	
			BA1	Occasional Small
			BA2	Occasional Large
			BA3	Frequent
	Construction Activity Assessment (CA)		Construction Activity	
			CA1	None
			CA2	Crest Stockpile
			CA3	Toe Excavation
			Construction Activity	
			CAA	None
			CAB	Crest Stockpile
			CAC	Toe Excavation
	Previous Remediation (PR)		Previous Remediation	
			PR1	No Remediation
			PR2	Part Remediation
			PR3	Full Remediation

Soil Type

Across any country, and any region of that country, a multitude of soil deposits are normally encountered. In this instance, with the intention of only applying broad categorisation, consideration is focussed on whether a soil is primarily cohesive, primarily granular or interbedded. The soil types are described in Table 7.11.

Table 7-11 Soil Types used in generalised slope assessment algorithm

Soil Type	Description
Cohesive (C)	In general terms cohesive soils have low effective (long term) shear strength, giving rise to stability being achieved through cutting to relatively shallow angles. Historically railway cuttings were cut at much steeper angles than is now known to be required for long term stability. Delay of failure for several decades in some instances was as a result of the time taken for the ground to develop a steady state groundwater table; removal of spoil to form the cutting led to ground stress relief which induced suction in the as formed cutting.
Granular (G)	Granular soils have inherently high effective strength which is apparent almost immediately during construction; any over steepened slope is likely to fail during cut slope formation. These soils are also relatively free draining, so as opposed to

 Copyright © MAINLINE Consortium

	cohesive soils, shallow drains are not that beneficial in maintaining stability.
Interbedded (I)	Interbedded soils present a number of characteristics that can generate increased rates of degradation, when compared to slpes formed of one soil type ie granular or cohesive. Overall stability will be governed by the weaker deposit (cohesive). However instability can be increased by granular soils (permeable) overlying cohesive soils (impermeable). This form of slope will potentially give rise to perched water tables, which without drains installed to intercept water egressing on to the slope surface, could give rise to erosion and subsequently to undermining of the face of the slope.

The soil type will drive the weightings assigned to the subsequent base value input parameters, as well as the logic driving the algorithm. The prototype generalised algorithm has been developed for a cohesive cutting as an example, and therefore the weighted values given herein are specific to the cohesive soil type cuttings. Some description of how the values might be altered for different soil types is also provided.

Slope Angle Factor (SAF)

As explained in Table 7.9, it is anticipated that cohesive and interbedded slopes will maintain stability at lower angles than will be the case for granular soils. Consequently higher factors would be assigned to cohesive and interbedded slopes than to granular slopes, reflecting their increased likelihood of instability. stability

Slope Height Factor (SHF)

Simply stated the higher the slope the greater the volume of soil that is susceptible to downslope movement. Granular slopes are more liable to translational sliding (shallow slips) than the deeper rotational slips classically observed in cohesive slopes. They are also more prone to downslope erosion/ravelling due to the effects of heavy rainfall or surface water flow. As previously cited the interbedded soil can also encourage surface degradation or undercutting of the overall slope. It is recommended that higher values than those assigned to cohesive slopes should be used for granular and interbedded slopes.

Adjacent Landform Factor (ALF)

The ground to the rear of any cut slope will have a varying degree of influence on the overall long term slope performance because of the following issues:

The area of the catchment. The greater the area of the catchment sloping towards the cutting, the greater the potential volume of water that will, unless intercepted, flow down the face of the cut.

The slope of the ground. The steeper the adjacent land, the faster the rate of flow and the consequent greater likelihood of erosion. It can also be surmised that any sub-surface ground water flow will also be towards the cut face, and with increasing gradient of the ground the greater the possibility of any steady state groundwater profile being near to the cut face. Conversely where the ground to the rear is level, or sloping away from the cutting, there is no real expectation of surface flow over the face of the cut and groundwater profiles are likely to be more remote from the slope face.

The proximity of any water courses. If a water course is nearby there is always the danger that this may overtop and flood the surrounding area. This inevitably leads to a higher risk of

 Copyright © MAINLINE Consortium

flow on to the cut slope and potential for erosion. It should be noted that even in the case of fairly level catchment water flows on to the cut face are likely to arise.

The degree of instability of the surrounding ground. Where the nature of the surrounding land is that in itself it is unstable then there is a greater possibility of destabilisation of the cut slope. Similarly where ground to the rear is steeply rising the overall perceived height oif the cutting is larger and this again will contribute to greater potential for lowering the overall factor of safety of the earthwork.

Base Value (BV) Calculation

The Base Value (BV) is calculated by summating the scores for Slope Angle, Slope Height and Adjacent Landform. The calculation for a cohesive slope is outlined in Fig.7.8.

Base Value (C_{BV})

C_{BV}= SAF + SHF + ALF

SAF		SHF		ALF				
Slope Angle (°)	Factor	Slope Height (m)	Factor		Factor			
				Adjacent Land	Only slope	Slope and water course	Slope and unstable land	S+WC+UL
<15	0	<3	-1(1)	-ve	0	0	0	0
15-25	1	3-10	0	flat	0	1	0	1
25-35	2	>10	1	+ve	1	2	1.5	2
>35	3							

Figure 7-8 Calculation of BV for a cohesive slope

Assessment Values

The SSHI assessment calculation for observations appears to be based on a simple additive concept. The more that indicates either actual or incipient problems with any given slope the greater the cumulative score. Herein attempt is made to prevent a possibility of double accounting for any set of observable states. For example surface water being observed can be the result of blocked drains it is therefore reasonable to take only the 'worst' of either the extent of water on the slope or the state of any drainage system.

A geotechnical engineer would expect that any derived Base Value (which in essence relates to the potential for long term problems) would correlate with where greater slope distress is observed and also with the rapidity with which the instability develops. The Base Value and its relation to Observations is discussed in a subsequent section of this report.

Movement Assessment (MA)

Movement is the most direct evidence of slope problems. In fact all other evidence presented below is really indicative of a long term problem that has not, as yet, presented itself in an obvious way. Some movement will require immediate action if the railway is to remain in use, such as an obvious track displacement. Other forms will need to be interpreted as to how soon this may lead to making a section of track unusable. The generalised algorithm utilises the same general forms of visual movement have previously been identified in the SSHI algorithm (Fig.7.9).

 Copyright © MAINLINE Consortium

Movement Assessment (MA)

M1	M2 Track Heave	Toe Bulge	Crest Slump	Mid-slope Hummocky	Toe Debris
Track Heave	4	0	0	0	0
Toe Bulge	4	2	0	0	0
Crest Slump	5	3	1	0	0
Mid-slope Hummocky	4	2.5	2	1	0
Toe Debris	4	2	2	1.5	1

Note: Scores not increased when more than 2 features present. Take highest score from assessment where more than one score applicable

Figure 7-9 Movement assessment

Surface Water Assessment (SWA)

Water can both be visible on the slope or be indicated by other obvious signs. This type of feature, as with surface cracking, is a function of the time of year the observation is undertaken and the state of the current or recent weather. Consequently the observer must sensibly account for this variation in the observation recorded; not over-emphasising water during inclement weather nor underplaying it during a dry spell (Fig.7.10).

Surface Water Assessment (SWA)

SW1	SW2 Surface Flow	Erosion channels	Marshy ground	Toe ponding	Toe fines accumulation	Crest erosion
Surface Flow	2	NA	NA	NA	NA	NA
Erosion channels	2.5	1	NA	NA	NA	NA
Marshy ground	2.5	1.5	1	NA	NA	NA
Toe ponding	2.5	1.5	1	0.5	NA	NA
Toe fines accumulation	2.5	1.5	1	1	0.5	NA
Crest erosion	3	2	1.5	1.5	1.5	1

Figure 7-10 Surface water assessment

Drainage Assessment (DA)

Drainage requirements for any slope are a function of a number of factors:

- Is there a likelihood of surface flow, usually from surrounding ground?
- Is the slope generally granular, so drains have limited benefit?
- Is the groundwater table likely to be close to the slope face?
- If soils are interbedded then perched water tables may develop, which could seep on to the slope face; interception of these seepages is beneficial
- Prevent groundwater day lighting at the bottom of the slope by installing toe drains

The consequence of the above is that the requirement for, and the extent of, drainage is case specific. Where drains are employed, when they become partially blocked or inoperative, the consequences can be significant. Drains when blocked potentially act as

 Copyright © MAINLINE Consortium

mini reservoirs, continually feeding water into a slope, even during dry periods. Consequently there is a strong possibility that any blocked drains will accelerate any tendency for a slope to degrade or fail (Fig.7.11).

Drainage Assessment (DA)

	D2				
D1	Competent	Crest blocked	Slope blocked	Toe blocked	No drains
Competent	-1 (1)	NA	NA	NA	NA
Crest blocked	0.5	1 (2)	NA	NA	NA
Slope blocked	0.5	1.5 (2)	0.5	NA	NA
Toe blocked	0.5	1	1	0.5	NA
No drains	NA	NA	NA	NA	1

(1) If ALF >0, Otherwise 0

(2) If Adjacent Land slope +ve, Otherwise reduce by 0.5

Figure 7-11 Drainage assessment

Vegetation Assessment (VA)

It is recognised that a slope that has properly managed vegetation can have a beneficial effect on maintaining longevity of the asset. Two specific elements are (Fig.7.12):

- Grass covering : During wet periods the grass cover retards any surface water flow, limiting erosion. In dry periods cover can limit cracking of the ground due to evaporation and desiccation; subsequently rainfall can readily enter the ground through the cracks, generate a shallow perched water table and so lead to increased likelihood of a shallow soil translation or localised failure.

- Trees and bushes : The root systems developed by larger scale vegetation can act to reinforce the deposits within a metre or two of the surface of a slope, thereby increasing resistance to any potential downslope movement. However an uncontrolled growth of this larger form of vegetation can, in the long term, give rise to uprooting of trees; brought about by high winds and/or low root penetration in slopes with only limited organic soil cover.

Vegetation Assessment (VA)

	V2					
V1	Slope cracked (>3mm)	Slope bare/sparse	Abundant grass	Occasional trees	Frequent trees	Tilted trees
Slope bare/sparse	1	0.5	NA	NA	NA	NA
Abundant grass	0.5	NA	-1 (1)	NA	NA	NA
Occasional trees	1	0.5	-1 (1)	0	NA	NA
Frequent trees	1.5	1	1	1	1	NA
Tilted trees	2	2	2	2.5	2.5	2

(1) If MA ≥2, Otherwise 0

Note: Scores not increased when more than 2 features present. Take highest score from assessment where more than one score applicable

Figure 7-12 Vegetation assessment

 Copyright © MAINLINE Consortium

Burrowing Assessment (BA)

The existence of large areas of sloping ground, as exhibited by cut slopes, makes them ideal locations for animals such as rabbits, foxes and badgers to excavate their burrows. Unfortunately burrowing, particularly at the toe of a slope, leads to local undermining of the face and eventually local downslope movement. The SSHI algorithm uses burrowing input parameters related to UK wildlife (rabbits, foxes and badgers)and which may not be the same in all parts of Europe. Therefore more general burrowing observation categories have been proposed for this algorithm.

Construction Activity Assessment (CAA)

Any earthwork is susceptible to the effects of other activities that take place in the vicinity. The most immediately obvious is stockpiling of spoil above a cutting, or excavating at its toe. Both of these options will reduce the overall stability of a slope (Fig.7.13).

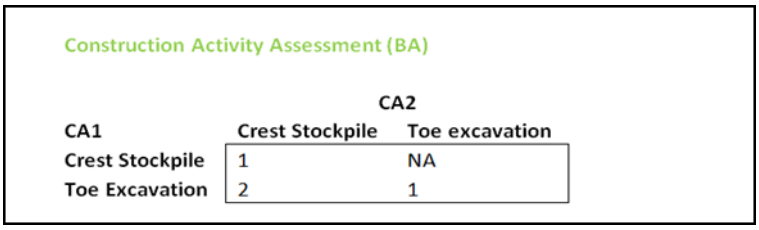

Figure 7-13 Construction activity assessment

Previous Remediation Assessment (PRA)

Inevitably some slope suffering varying degrees of distress will have already had remedial treatment. This may be to address stabilisation of the entire slope, or only to address a localised issue. The observer should examine the form of works that have been undertaken, their overall effectiveness and whether the consequences of a detrimental feature (though still evident) have been nullified by the remediation employed:

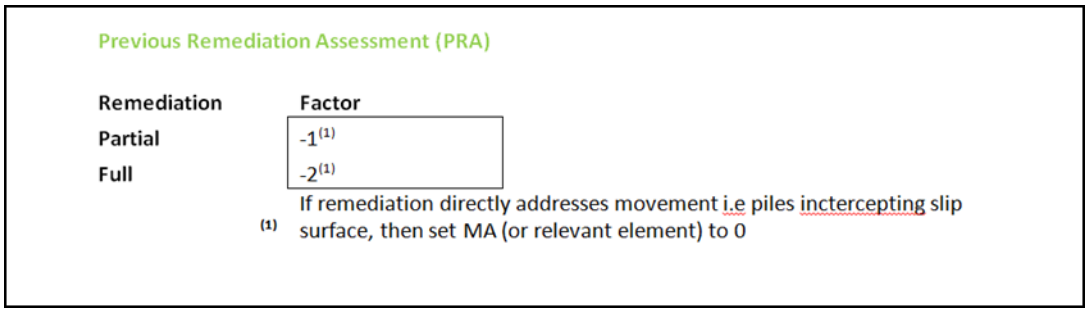

Figure 7-14 Remediation assessment

Assessment Value (AV) calculation

For a cohesive slope, the assessment parameters described in the preceding sections combined using the algorithm shown in Fig.7.15.

 Copyright © MAINLINE Consortium

Slope Assessment Value (SAV)

SAV = [MA OR VA](1) + [SWA OR DA] (2) + CAA + BA(3) + PRA

(1) If VA = -1, then reduce MA by 1. Highest of MA or VA to be taken
Take highest of SWA or
(2) DA
(3) Burrowing scores should also be looked at in isolation as this necessitates very specific intervention
(4) Either adopt value, or if remediation directly addresses a a specific element, reduce that to 0 (see PRA tab)

Figure 7-15 Slope assessment

Overall slope stability calculation

It can be sensibly argued that the overall assessment of a slope should be primarily based on the field observations captured in the Assessment Value (AV). However, when considering the long term liability that any given slope presents to the operator, consideration should be given to the original condition of the as constructed slope; this equates to its Base Value (BV), as defined within this report. The reasoning behind this suggested philosophy is that the AV relates to a point in time, not having been evaluated based on time since construction nor on the catalogue of any historical activity on or near the slope; except those items such as remediation, where there is an evident legacy. The BV is really a predictive operator, in that it is derived from elements of the slope that were evident when the slope was constructed. It is in effect a quantitative assessment of potential for failure sometime in the future; in a design sense a higher BV between one slope and another equates to a lower Factor of Safety of the as constructed slope. This philosophy is in line with the philosophy adopted in SSHI which combines potential and actual (observed) failure scores in the overall slope assessment calculation.

In line with this philosophy and to account for both the observed state of the slope (AV) and its original projected tendency to show signs of instability (BV), the overall Stability Value (SV) at time of assessment is described as expressed in Fig.7.16.

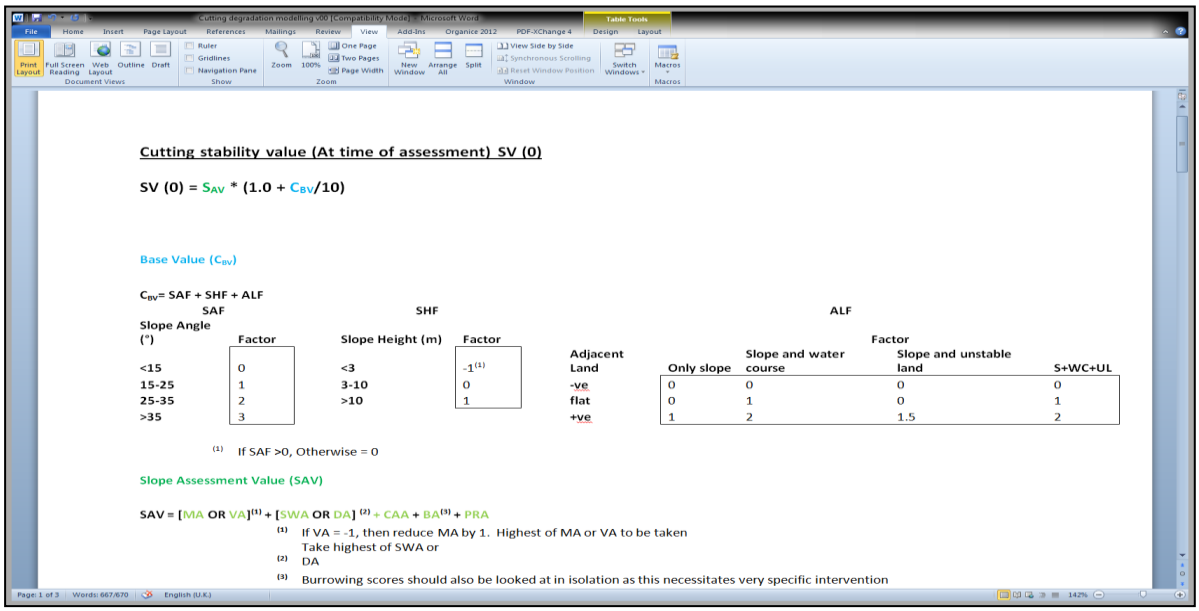

Cutting stability value (At time of assessment) SV (0)

SV (0) = S_{AV} * (1.0 + C_{BV}/10)

Base Value (C_{BV})

C_{BV}= SAF + SHF + ALF

SAF

Slope Angle (°)	Factor
<15	0
15-25	1
25-35	2
>35	3

SHF

Slope Height (m)	Factor
<3	-1(1)
3-10	0
>10	1

ALF

Adjacent Land	Factor: Only slope	Slope and water course	Slope and unstable land	S+WC+UL
-ve	0	0	0	0
flat	0	1	0	1
+ve	1	2	1.5	2

(1) If SAF >0, Otherwise = 0

Slope Assessment Value (SAV)

SAV = [MA OR VA](1) + [SWA OR DA] (2) + CAA + BA(3) + PRA

(1) If VA = -1, then reduce MA by 1. Highest of MA or VA to be taken
Take highest of SWA or
(2) DA
(3) Burrowing scores should also be looked at in isolation as this necessitates very specific intervention

Figure 7-16 Stability value assessment

7.3 Deterioration Modelling

Once a condition rating method such as the SSHI/RSHI or an alternative scoring system has been developed and implemented it is possible to undertake deterioration modelling by observing and predicting how the defined condition scores change over time. The modelling approach adopted might be probabilistic or deterministic and the selected approach will depend upon the level of uncertainty involved in the process and input parameters. A brief discussion of the two modelling approaches is provided below, and examples of each are presented in sections 7.3.2 and 7.3.3. The most appropriate approach for the MAINLINE cuttings model is then identified in chapter 7.3.4

7.3.1 Probabilistic and deterministic modelling approaches

A deterministic process or model is one which will always lead to the same outcome given the same set of inputs. With full knowledge of the inputs it is possible to say with 100% certainty what the outcome will be.

A probabilistic process or model is one whose outcomes can vary even when provided with the same set of inputs. There may be some uncertainty in the inputs and some aspects of the process may be 'hidden'. Rather than predicting a definite outcome one is reduced to calculating the probabilities of each of the possible outcomes occurring.

Intuitively it would be preferable to describe everything in a deterministic way as knowing what is going to happen with 100% certainty is more useful than simply knowing a set of probabilities. This is particularly true when attempting to model the whole life performance of a single asset rather than a population of many assets. The end user of the MAINLINE LCAT will require a tool that supports decision making on a structure by structure basis, and for this purpose probabilistic outputs are less useful.

However in practice it is often impossible to form a complete and accurate description of all of the relevant inputs and processes. In this instance adopting a deterministic point of view would be misleading, and the probabilistic point of view becomes the most fruitful. Many of the processes that are important in the subject of asset management involve uncertainty; not least the extent to which an asset's condition will deteriorate over time cannot be predicted with 100% certainty.

There are benefits and limitations to each of these deterioration modelling approaches, which presents a challenge in selecting the most appropriate technique. In the following sections the probabilistic approaches formerly used by SKM and Network Rail are discussed, and a potential deterministic approach is presented.

7.3.2 Probabilistic cutting deterioration models developed by SKM and NR

Network Rail (NR) have been collecting SSHI and RSHI data for their earthworks for approximately 10 years, and have therefore chosen to pursue probabilistic deterioration modelling techniques based on deterioration trends observed by analysis of past condition data. The following sections will report on the probabilistic deterioration modelling work that Network Rail have commissioned.

 Copyright © MAINLINE Consortium

Civil Engineering CP5 Cost Modelling (CeCost) (SKM 2012a-b)

As part of the CeCost CP5 Project SKM have worked with Network Rail to develop deterioration models for a range of asset types, including soil and rock cuttings. These models are used to predict how the condition of these assets will change over time, and so to determine the volume and timing of corresponding interventions, based on a defined intervention policy set by Network Rail. These models are probabilistic and based on analysis of historical SSHI/RSHI data. They can be used at individual asset level, or can be set up to run for a whole population of assets. The key features of the cutting deterioration models developed by SKM for NR in 2012 are discussed below.

Soil Cutting deterioration model (based on SSHI) (SKM 2012a)

The deterioration models incorporate 3 condition sub models (Fig.7.17) as follows:

- Whole Slope - The first four failure modes in the SSHI system (Rotational, Translational, Earthflow and Washout) are modelled together as the 'Whole Slope' condition. This is because they are implemented in largely the same way within the algorithm.

- Burrowing - animal activity is modelled separately as it is different but important in its own right. By modelling burrowing separately in this way, the need for specific burrowing interventions can be more accurately predicted.

- Drainage – the condition of slope drainage is also modeled separately to aid prediction of drainage intervention requirements.

In order to calculate overall classification of an earthwork the model also track two other characteristics:

- Potential Score – made up of a drainage component (modelled in the drainage sub model) and a non-drainage component

- Slope Height Factor – in line with the earthworks factor, this can be 1, 1.3 or 1.6 and remains fixed for a given section of cutting.

Five data inputs are required for the models: Actual Score, Potential Score, Slope Height Factor, Burrowing Condition, Drainage Condition. These inputs come from inspection data, and represent the current condition of the cutting.

The data inputs are banded into condition vectors within each sub model:

- The starting condition values of each of these modelled parameters are multiplied by corresponding degradation matrices in order to predict the change of condition over time (Markov chain process).

- The deterioration matrices identify the probability that assets in each starting condition state will remain in that condition state or deteriorate to a worse condition over a defined period of time, in this case a 5 year period.

 Copyright © MAINLINE Consortium

- Deterioration matrix values were derived via an analysis by Network Rail; historic condition examination data was assessed and any assets found to feature more than one exam over time were used to generate frequency distributions illustrating how the various scores changed over time. An over view of the the derivation of the deterioration Matrices is provided in Fig.7.18, and full details can be found in (SKM 2012a).

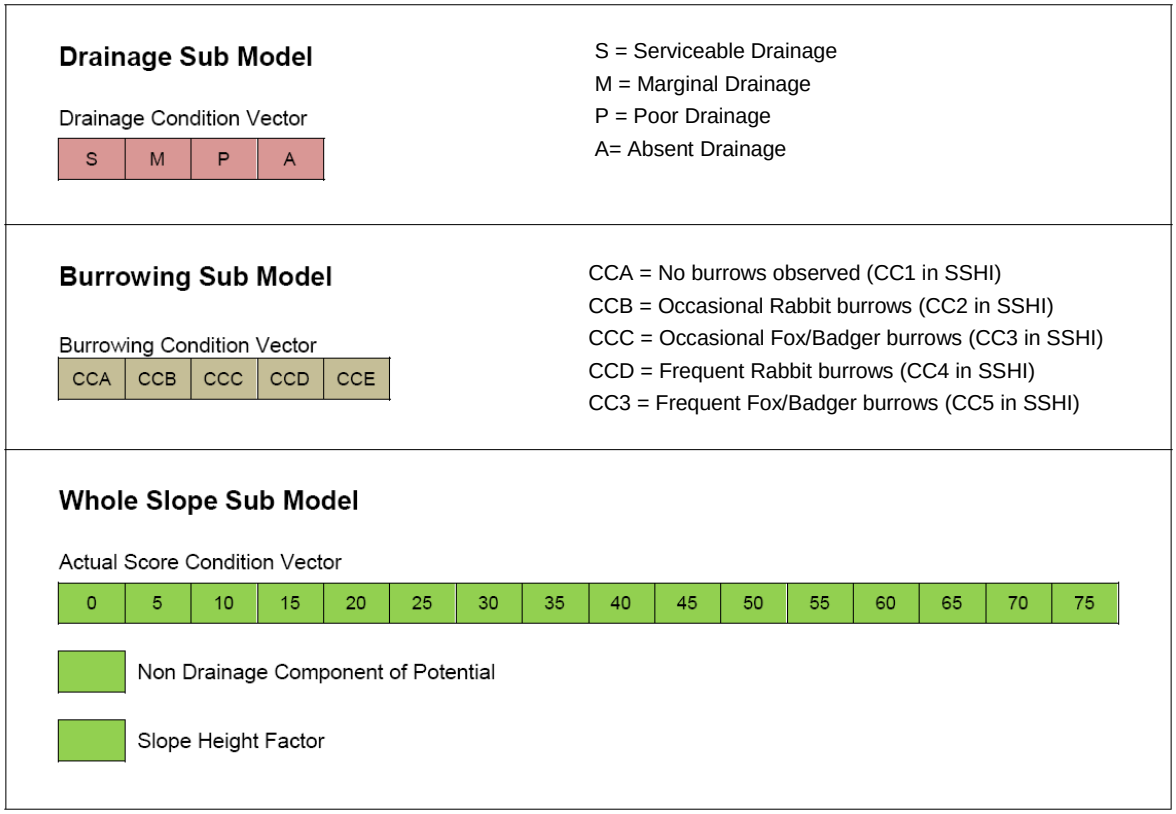

Figure 7-17 Soil cutting Condition Sub Models, Condition Vectors and Other Modelled Characteristics

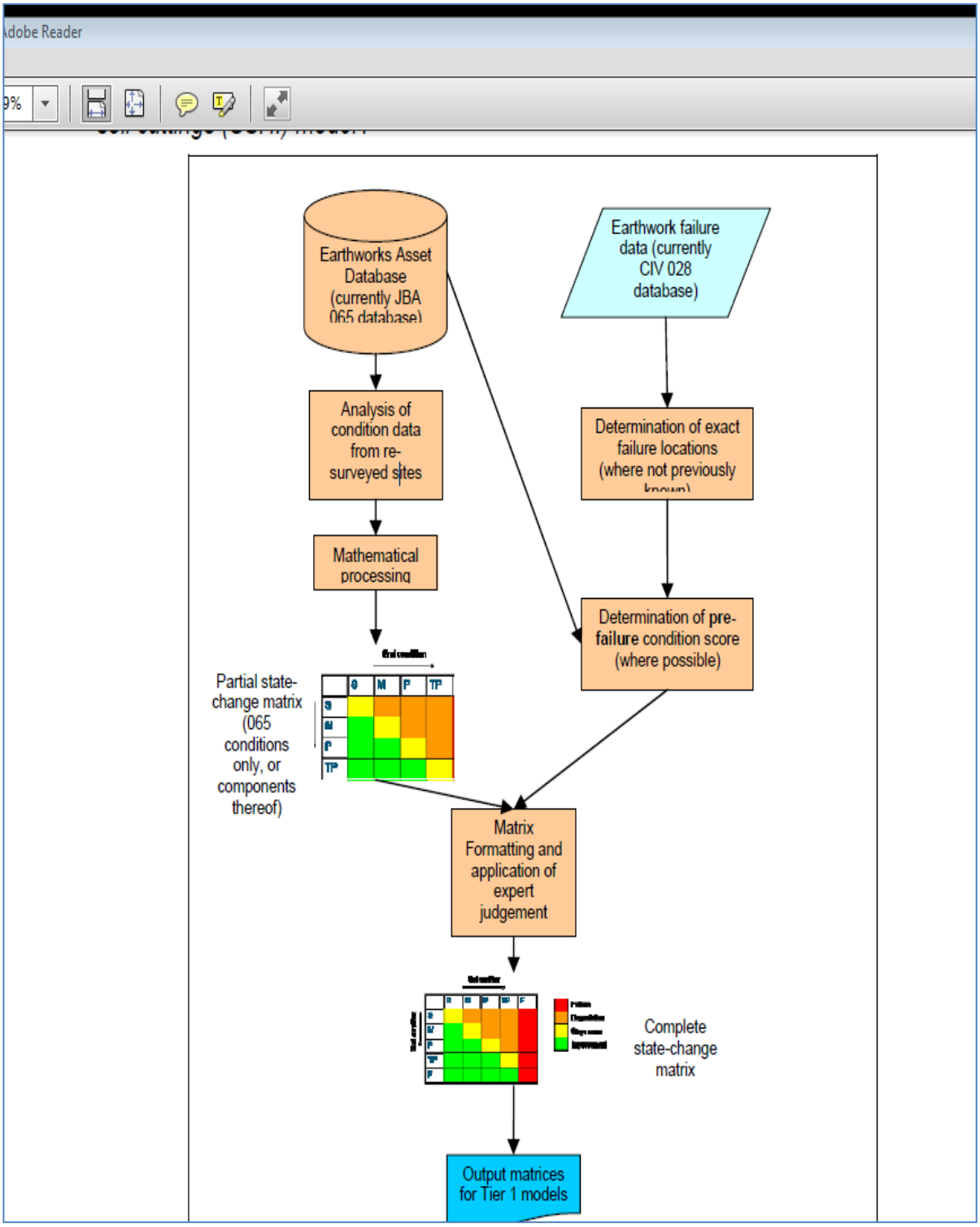

Figure 7-18 Network Rail Analysis of earthwork asset state change matrix

Sample probabilistic deterioration matrices for the 3 condition sub models are provided in Fig.7.19.

 Copyright © MAINLINE Consortium

Start State	End State 0	5	10	15	20	25	30	35	40	45	50	55	60	65	70	75
0	0.932	0.000	0.008	0.000	0.010	0.00	0.014	0.005	0.000	0.000	0.000	0.000	0.000	0.000	0.000	0.000
5	0	0.915	0.006	0.010	0.010	0.01	0.010	0.011	0.010	0.010	0.000	0.000	0.000	0.000	0.000	0.010
10	0	0	0.907	0.000	0.015	0.01	0.014	0.018	0.010	0.010	0.000	0.005	0.000	0.000	0.000	0.007
15	0	0	0	0.903	0.011	0.01	0.010	0.011	0.010	0.010	0.000	0.010	0.010	0.000	0.000	0.010
20	0	0	0	0	0.930	0.01	0.013	0.008	0.000	0.000	0.000	0.010	0.006	0.000	0.000	0.007
25	0	0	0	0	0	0.88	0.018	0.021	0.010	0.008	0.010	0.012	0.012	0.010	0.000	0.016
30	0	0	0	0	0	0	0.862	0.030	0.013	0.014	0.009	0.018	0.015	0.010	0.010	0.021
35	0	0	0	0	0	0	0	0.842	0.022	0.021	0.015	0.020	0.019	0.017	0.010	0.036
40	0	0	0	0	0	0	0	0	0.814	0.031	0.023	0.028	0.025	0.020	0.015	0.043
45	0	0	0	0	0	0	0	0	0	0.798	0.031	0.036	0.028	0.020	0.019	0.069
50	0	0	0	0	0	0	0	0	0	0	0.795	0.046	0.031	0.030	0.014	0.084
55	0	0	0	0	0	0	0	0	0	0	0	0.894	0.035	0.020	0.010	0.042
60	0	0	0	0	0	0	0	0	0	0	0	0	0.853	0.040	0.025	0.082
65	0	0	0	0	0	0	0	0	0	0	0	0	0	0.843	0.028	0.130
70	0	0	0	0	0	0	0	0	0	0	0	0	0	0	0.791	0.209
75	0	0	0	0	0	0	0	0	0	0	0	0	0	0	0	1.000

Figure 4 – Sample Actual Score 5 year deterioration matrix

Start State	End State S	M	P	A
S	0.65	0.25	0.10	0.00
M	0	0.60	0.40	0.00
P	0	0	1.00	0.00
A	0	0	0	1.00

Figure 5 – Sample Drainage 5 year deterioration matrix

Start State	End State CCA	CCB	CCC	CCD	CCE
CCA	0.974	0.021	0.00	0.00	0.00
CCB	0	0.984	0.00	0.01	0.00
CCC	0	0	0.975	0.022	0.00
CCD	0	0	0	1.00	0.00
CCE	0	0	0	0	1.00

Figure 7-19 Sample Soil cutting 5 year degradation matrices for Slope, Drainage and Burrowing.

Rock Cutting deterioration model (SKM 2012b)

The rock cutting deterioration modelling is based on the following input data items from the RSHI surveys:

- The overall RSHI score - split into 12 overall rock slope condition bands (RS-bands)
- 3 Drainage data fields – ‘Groundwater Seepage’, ‘Surface water flow’, and ‘Drainage problem’ which are combined to give 12 possible drainage condition bands (DR-bands)
- Together, the RS-band and DR-band are used to define an asset condition.
- Deterioration between the 12 RS states and 12 DR states is input by the user into deterioration matrices, in a similar way to the SSHI modelling process. An example RSHI deterioration matrix is shown in Fig.7.20.

 Copyright © MAINLINE Consortium

Deteriorate FROM:	Deteriorate TO: 1	2	3	4	5	6	7	8	9	10	11	12
1	94%	5%	1%	0%	0%	0%	0%	0%	0%	0%	0%	0%
2	0%	94%	5%	1%	0%	0%	0%	0%	0%	0%	0%	0%
3	0%	0%	94%	5%	1%	0%	0%	0%	0%	0%	0%	0%
4	0%	0%	0%	94%	5%	1%	0%	0%	0%	0%	0%	0%
5	0%	0%	0%	0%	94%	5%	1%	0%	0%	0%	0%	0%
6	0%	0%	0%	0%	0%	94%	5%	1%	0%	0%	0%	0%
7	0%	0%	0%	0%	0%	0%	94%	5%	1%	0%	0%	0%
8	0%	0%	0%	0%	0%	0%	0%	94%	5%	1%	0%	0%
9	0%	0%	0%	0%	0%	0%	0%	0%	94%	5%	1%	0%
10	0%	0%	0%	0%	0%	0%	0%	0%	0%	94%	5%	1%
11	0%	0%	0%	0%	0%	0%	0%	0%	0%	0%	95%	5%
12	0%	0%	0%	0%	0%	0%	0%	0%	0%	0%	0%	100%

Figure 7-20 Example rock cutting deterioration matrix 0

The derivation of the deterioration probabilities for rock cuttings was undertaken by Network Rail via the same process described above.

Asset Level Modelling (Halcrow Tier 2/3 modelling)

The same probabilistic approach to deterioration modelling was applied in the Tier 2/3 model which is being developed for use as a decision support tool which can be used to test the outcomes of various defined intervention options on a single asset. This has been developed in an Excel spreadsheet which has probabilistic deterioration matrices embedded within it. A screenshot from the degradation tab of the tool is provided in Fig.7.21.

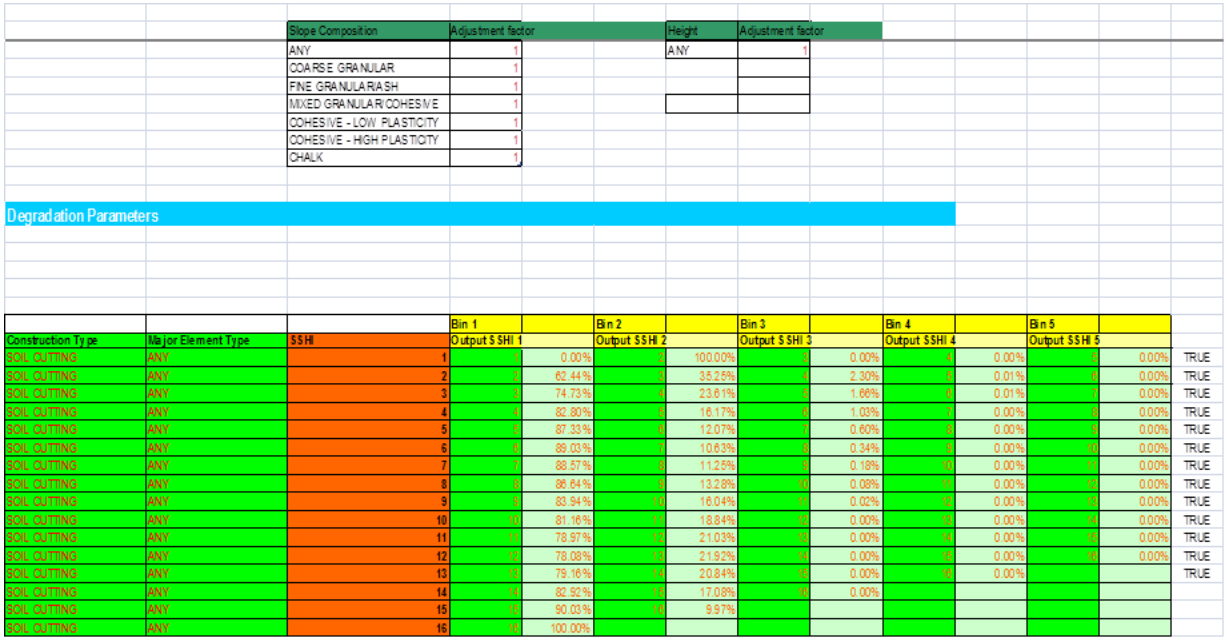

Figure 7-21 Degradation tab screen shot from the Network Rail Tier 2/3 model

 Copyright © MAINLINE Consortium

7.3.3 A proposed approach to deterministic deterioration modelling

As discussed above, the probabilistic deterioration modelling approach based on historical data has been favoured for cuttings in the past as it deals with the uncertainties and complexities surrounding the processes involved. However this approach has the following limitations which should be acknowledged:

- The model is based on previously observed deterioration trends, and assumes they will be projected into the future. This may not be a valid assumption as cutting deterioration trends are closely linked with climate change effects, and may therefore change significantly in the future.

- The reliability of the deterioration model is limited by the quality; quantity and time span of existing data records. As such, the outputs of the model need to be validated and checked against the experience and knowledge of geotechnical engineers, case studies and the latest research.

- As discussed above, the output of a probabilistic model consists of a set of probabilities rather than one defined outcome. Interpretation of a set of probabilities can be cumbersome and difficult, and the usefulness of such outputs can be particularly limited when modelling at single asset level rather than across a large number of assets.

The following section refers back to the factors used to derive the Assessment Value (AV) in the generalised algorithm presented in Section 7.2.4, and proposes a deterministic method for modelling degradation of a soil cutting. It attempts to predict how the overall condition score will change over a defined time period, based on the range of parameters that were observed at the last inspection. The proposed deterioration rates are based on engineering judgement, and an understanding of the deterioration mechanisms that are in action. The numerical values given for the degradation rate of specific feature are somewhat arbitrary, but are provided to give some indication of relative effects on degradation rate of the different input parameters. The factors are in line with the SSHI input parameters, and so expected deterioration trends discussed here could also be used to validate observed trends in SSHI data sets.

In addition, a discussion is provided on how the on- going effects of climate change may also affect rates of slope degradation. It is projected that climate change is likely to more seriously increase the degradation rates of only some of the elements discussed herein.

Slope Movement

All the forms of slope movement that are identified in the algorithm are evidence that the slope, either in part or in full, has failed. This indicates that at some point, either at the time of the observation or earlier, the factor of safety of the slope has fallen below one. As soil properties are stable (in all but exceptional circumstances) instability is likely to have resulted from something like prolonged rainfall, leading to a rise in groundwater levels. By inference the feature identified and on-going downslope movement will be affected by climate change, where this leads to increased rainfall.

Regardless of any worsening weather patterns, where a slope has shown signs of movement, at some point, the likelihood is this will re-occur. It is also probable that a change

 Copyright © MAINLINE Consortium

in slope geometry, brought about by the movement that has occurred, will also have increased the tendency for soils to creep downslope. In simple terms, if nothing else, soil will gradually move to and accumulate at the base of the slope. The point at which this impedes trains is a function of the rate of accumulation and the proximity of the track to the base of the slope (cess).

Taking the above into consideration it can be surmised that degradation rates, relate to this form of slope distress, will be relatively rapid.

The more severe the signs of movement observed, the faster the anticipated deterioration rate.

Relating this back to the generalised algorithm, it might be expected that the condition score would increase by the following factors over 10 years Observed movement factor – 0 – Degradation rate +0.5 over 10 years (if BV > +1) +1 – Degradation Rate +1 over 10 years +2 or greater – degradation Rate +1 over 5 years

Surface Water

Evidence of surface water inevitably leads to the conclusion that erosion of the slope will occur on an on-going basis, even if erosion was not visible when the observations on the slope were made.

Slopes showing any indication of surface water at time of assessment would be expected to deteriorate faster than those showing no signs surface water.

Again it is also inevitable that where climate change leads to increase in rainfall intensity and/or quantity rates of erosion will be accelerated. Without any measures put in place, such as drainage, the consequence is debris accumulation at the base of the slope and possibly increased flooding. Rates of degradation clearly relate to the frequency and volume of water traversing the slope face.

Increasing rainfall intensity and/or quantity will lead to faster deterioration rate, and therefore predictions in expected changes in these factors due to climate change should be considered.

Relating this back to the generalised algorithm, it might be expected that the condition score would increase by the following factors over 10 years Surface flow and erosion channels – Degradation rate +1 over 10 years Toe fines accumulation – Degradation rates +1 over 10 years Crest erosion and toe flooding – degradation rates +0.5 over 10 years Marshy ground – degradation rates +0.5 over 15 years

 Copyright © MAINLINE Consortium

Drainage

The benefits of good drainage are that surface water is intercepted before flowing onto the slope face or captured on its way down the face. For groundwater, drainage suppresses the possibility of this forming a surface expression, by means of marshy ground or seeping from a perched water table (often caused by interbedding of deposits).

A slope with present and functioning drainage is expected to deteriorate more slowly than a slope with no drainage.

However when this drainage becomes blocked, as discussed previously, the effects of water can be even more pronounced than if drainage had not been there in the first place; by effectively acting as water reservoirs feeding the slope.

If drainage is present but blocked, the deterioration rate could be expected to be faster than if there is no drainage present.

In relation to climate change the benefits of good drainage become even more pronounced, as the more aggressive nature of increased rain intensity and volume are suppressed by intercepting the flows.

If rainfall intensity and frequency increases as a result of climate change effects than the retarding effect of drainage on deterioration is expected to become more significant.

Overall probable rates of slope degradation can be designated as follows:
Comprehensive drainage system, in good working order - +0.5 over 30 years
No drainage system - +1 over 20 years
Crest drains blocked - +1 over 10 years
Toe and face drains blocked - +0.5 over 10 years

Vegetation

Vegetation, particularly abundant grass cover, is very effective in suppressing erosion and drying out of surface soils. Bare bare ground on the other hand is readily susceptible to erosion, cracking and generation of shallow perched water tables.

Slopes with abundant grass or occasional trees and bushes might be expected to deteriorate more slowly than slopes with no vegetation cover.

The main problem will occur as the larger vegetation continues to grow and cannot be sustained through shallow root systems in sloping ground; as discussed in the section on vegetation observations.

Slopes with abundant trees might be expected to deteriorate more rapidly.

The presence of tilted trees on a slope is an indication that movement has already occurred, and deterioration could be expected to occur even more rapidly.

 Copyright © MAINLINE Consortium

Slopes with tilted trees are expected to deteriorate the more rapidly than slopes with any other vegetation cover.

Suggested rates of degradation are: Bare ground - +1 over 10 years Abundant grass - +0.5 over 30 years Occasional trees and bushes - +0.5 over 20 years Abundant trees - +1 over 10 years Trees tilted - +1 over 5 years

Burrowing

Inevitably, unless fencing or nettering is introduced or the animals are removed from the site, the extent of burrowing is likely to increase with time, thus increasing the deterioration rate.

A slope with burrows will deteriorate more quickly than one without any burrows.

A suggested rate is: Degradation rate +1 in 10 years

Construction Activity

The weather and environmental factors in general are amenable to some form of statistical evaluation. Human activity such as construction works on or adjacent to the slope however, is not. This presents some difficulty in predicting the impact of these factors on long term deterioration trends. For example there might at some point in the future be a period of activity, such as digging a trench, followed by an extended hiatus – however the timing, duration, location and extent of the works is impossible to predict, particularly when it may be undertaken by parties outside of the asset owner's organisation.

To account for the long term effect of past construction activity observations on deterioration is thereby fraught with difficulty. Idealistically one can assume that if work has been observed at the time of the examination, it will remain unaltered, for example a spoil heap on top of the slope. Realistically the spoil heap will get bigger, or be removed; a trench may be open but later filled in; a hole may be dug at the slope base sometime in the future. Pragmatically one can say that if activity has occurred adjacent to a slope then it is likely something else will happen in the future, conversely where no activity has occurred there is a good likelihood nothing will occur in the future.

A slope with observed construction activity might be expected to deteriorate more quickly than a slope without any observed construction activity.

On this simplistic basis the following is proposed: Construction activity observed – Degradation rate is +1 over 10 years No construction observed – Degradation rate is 0

Previous Remediation

Any previous remediation is accounted for in the overall slope assessment score. Deterioration is not tied to a remediation but to the elements related to overall slope

 Copyright © MAINLINE Consortium

performance, described above. Therefore any observations relating to previous remediation works are not expected to be directly correlated with deterioration rates.

7.3.4 Most suitable approach for cutting deterioration modelling

The previous sections have looked at both probabilistic and deterministic modelling approaches that might be adopted for cuttings. Following assessment of the options, it is judged by the authors of this chapter, in consultation with the D5.5 participants that the most appropriate approach to take forward into the MAINLINE LCAT will be the simplified algorithm with deterministic approach to modelling deterioration. The numerical deterioration rates suggested in this chapter will be refined by means of analysis of historical data.

Effect of climate change on cutting deterioration rates

It is clear from the research undertaken so far that there is a strong link between cutting stability and climatic events; in particular rainfall, and that as a result deterioration rates are likely to be sensitive to climate change effects. It is acknowledged however that there is a high degree of uncertainty surrounding climate change predictions, and that the changes are predicted to vary between regions. Research by the Intergovernmental Panel on Climate Change (IPCC) indicates that the following trends might be observed across Europe for the period 2070 – 2099:

- Extreme weather events, including storms, extreme precipitation and resulting floods are expected to increase in likelihood and severity.
- It is expected that annual average precipitation will increase in northern and north central Europe while it will decrease in southern Europe.
- Extremes of daily precipitation are very likely to increase in northern Europe.
- Baltic regions - more frequent and stronger winter storms
- The changes in average temperature and precipitation are expected to be gradual over a long time period, and will affect different climate zones within Europe quite differently.

As can be seen from Fig.7.22, the extent of climate change effects, and therefore the extent of their impact on cutting deterioration, is expected to vary across Europe.

 Copyright © MAINLINE Consortium

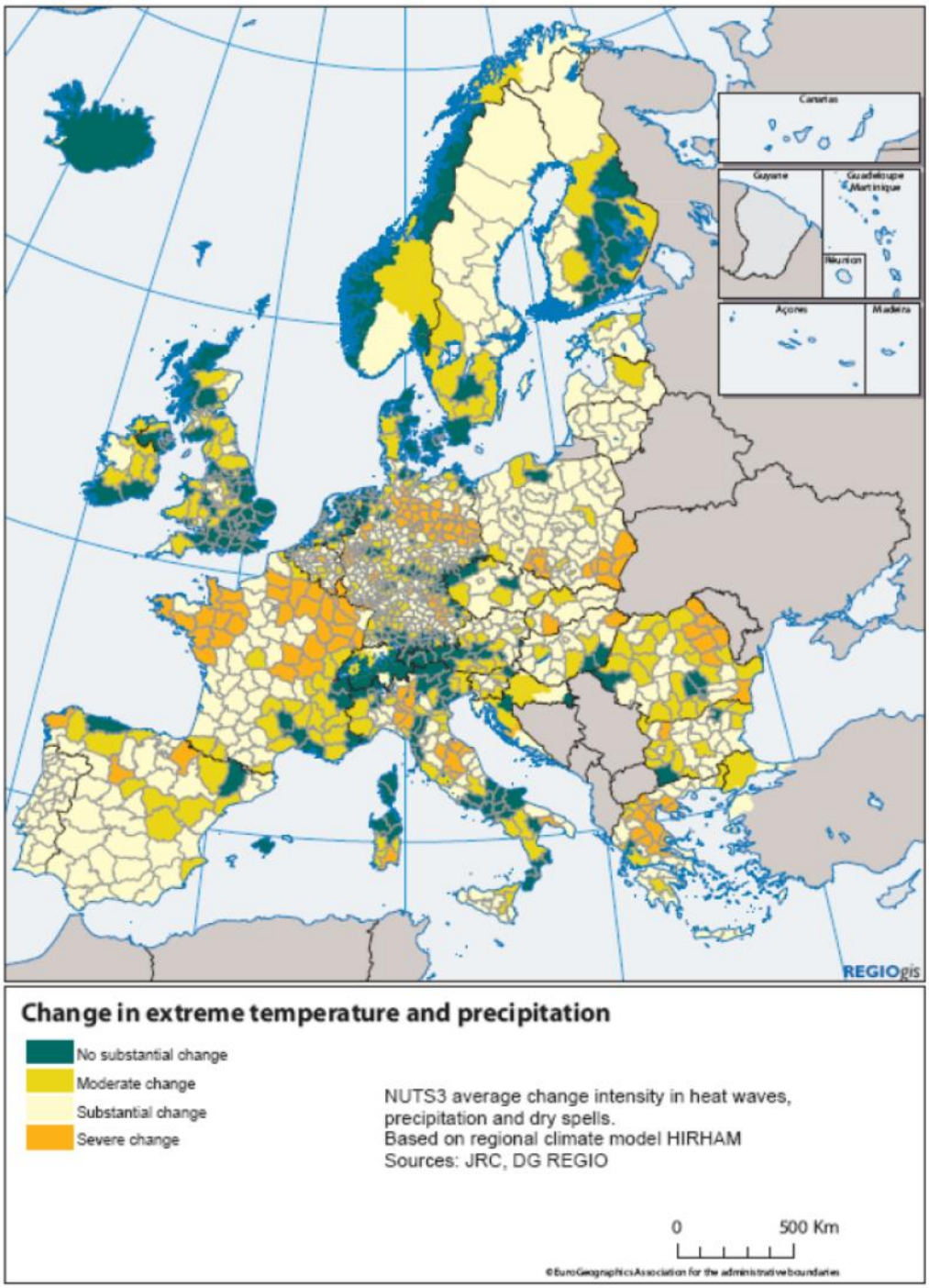

Figure 7-22 Extent of climate change effects

In December 2012 The Geological Society published a volume of papers entitled Earthworks in Europe (Geotechnical Society 2012) which includes two papers on the links between the stability of earthworks and climate change effects. An overview of the content of these papers is provided below

G J Macdonald et al explore the relationship between soil moisture deficit (SMD) and earthwork slope failures. They present research indicating that soil slope instability may be associated with rapid changes in SMD, and suggest that if climate change causes more extreme weather patterns in the future then rapid changes in SMD could become more

 Copyright © MAINLINE Consortium

frequent, resulting in more frequent slope failures. Graphs of UK case study data are provided, giving an initial indication of the correlation between SMD and slope movement.

A second paper by D G Toll et all describes an experimental facility that has been set up to provide field measurements for use in calibrating numerical models of soil responses to climatic changes. A full scale embankment (representative of a UK highway or rail asset) was built and subjected to a climate control system designed to impose different climate change scenarios. Pore water pressures have been monitored since 2007, and will continue to be monitored into the future to gain a better idea of longer term effects. The results from experimental research such as this might be incorporated into the deterioration model in order to predict the effect of climatic trends than have not been observed in the past.

Availability of historical data for model validation
The proposed modelling approach utilizes the same condition data that is collected by Network Rail using the SSHI algorithm. As such historical SSHI data (available for the past 10 years in the UK) could be used for the validation of this modelling approach (though the input data would need to be extracted and fed through the proposed alternative algorithm)

It is not known what form of data exists in other parts of Europe. This will need to be investigated in the next D2.3. An attempt had been made to develop a model that is generic and flexible enough to be adapted to suit a range of input data types.

7.4 Modelling the Effect of Interventions

7.4.1 Literature Review

CIRIA C591 Infrastructure Cuttings
The wide variety of possible material properties and slope angles mean that an extensive range of remedial treatments and preventative techniques are required for the maintenance of cuttings. The CIRIA report divides the range of available cutting interventions into two categories:

- Hard techniques – structural techniques that are visually obvious
- Soft techniques – those that are visually less intrusive and which improve the strength or other properties of the ground such as its drainage capability.
- Details of specific available techniques, including diagrams can be found in the CIRIA report. An overview of these techniques is presented in Table 7.12.

 Copyright © MAINLINE Consortium

Table 7-12 Summary of remedial treatment and preventative techniques for cuttings (CIRIA C591)

Technique	Rock or soil method		Remedial or preventative		Hard or soft		Emergency or permanent		Comments
	R	S	R	P	H	S	E	P	
Regrading and toe berms	●	●	●			●	●	●	Simple solution, may require toe berm structure to keep within existing land
Reinforced/strengthened fills		●	●			●		●	Reinforced soil methods widely used
Stabilised fills			●			●		●	Lime and lime-cement methods increasing in use
Granular replacement		●	●			●		●	Historically popular for repair of shallow slips on highways
Gravity walls and gabions	●	●	●		●		●	●	Normally used at cutting toe with regrading. Gabions can be used for emergency works
Piled walls		●	●		●			●	Includes bored and minipiles, pali-radice and sheetpiles. Piles can be used as base support for walls
Ground anchors and mini piles for wall support		●	●		●			●	Provide lateral support to walls
Soil nails		●	●	●		●		●	Popular method but may require wayleaves if cutting is boundary line
Ground anchors, rock bolts and dowels	●			●	●			●	Can be used to provide local or overall cutting support but wayleaves may be required
Dentition and buttressing	●			●	●			●	Effective method for enhancing local stability
Dowel piles		●	●			●		●	Access and equipment for installation may be significant
Netting and meshing	●			●		●		●	Used to control rather than prevent rockfall
Catch fences	●			●	●			●	Reduces impact of rockfall. Maintenance required
Benching, ditches and rock traps	●			●		●		●	Suitability depends on slope angle and space at toe of cutting
Rockfall shelters	●			●	●			●	Provides high level of protection from rockfall
Alarm and warning systems	●	●				●	●	●	Low cost but may not prevent closure of infrastructure
Internal drainage	●	●	●	●		●		●	Installation can be difficult
Slope drainage	●	●	●	●	●	●		●	Important feature of cuttings to prevent erosion
Toe drainage	●	●	●	●		●		●	Check that construction will not undermine cutting stability
Membranes, eg sprayed concrete	●	●	●	●	●		●	●	Can be used to prevent water ingress/ ravelling of loose surfaces
Vegetation	●	●	●	●		●		●	Use of green solution becoming increasingly more important. Reduces negative aesthetic impact of cutting
Maintenance methods	●	●	●	●		●	●	●	Maintenance essential to all cuttings

 Copyright © MAINLINE Consortium

Table 7-13 Principal advantages and limitations of remedial treatment and preventative techniques for cuttings

Technique	Advantages	Limitations	Suitable conditions
Regrading and toe berms	Simple and effective measure and immediate effect	Sometimes difficult to achieve within site boundaries	All soil and rock conditions
Reinforced/ strengthened fills	Steep slopes can be achieved	Requires excavation past failed zone to get sufficient length for basal grid	Soil reinforcement chosen to suit fill type. Sufficient room for temporary excavations
Stabilised fills	May be possible to reuse failed soils	Often requires excavation of failed soils. Environmental issues with lime and cement dust	Lime and lime cement for generally inorganic clays
Granular replacement	Well proven technique for shallow and deeper soil failures. Simple to design and supervise	Cost of importing suitable fill may be high. Disposal of excavated material required. Requires considerable excavation beyond shallow rupture surface	All soil conditions although typically used in high plasticity clays. Temporary works stability needs to be considered
Gravity walls and gabions	Positive structural solutions and can provide long-term solution	Costs can be high for gravity walls and plant required may require closure of infrastructure	All ground types
Piled walls	Positive structural solution. Can provide local or overall stability solution. Scope for creating additional space at toe	Requires mechanical equipment and temporary works requirements can be extensive	Most soils and softer rock slopes
Ground anchors and mini piles for wall support	Can provide high lateral support forces to walls	Require specialist installation methods	Soils where high friction forces possible
Soil nails	Cost effective solution becoming more popular	Access platforms required for steep cuttings as mechanical equipment used	Most effective in granular soils and low plasticity clays/soft rocks
Ground anchors, rock bolts and dowels	Proven technology providing positive support	Access can be difficult and should be considered when developing schemes. Wayleaves may be required	All rock cuttings
Dentition and buttressing	Simple and cost-effective in providing local support to unstable rock masses	Access should be considered. Provides local support only	Hard rock cuttings
Dowel piles	Can provide stability to slope problems	High installation cost. Stabilisation not immediate	Applied to deep soil slope failures
Netting and meshing	Simple cost-effective solution	Requires inspection and repair for damage. Does not prevent failure and ravelling of slopes	Fractured rock cuttings and rocks susceptible to weathering
Catch fences	Helps minimise risk to infrastructure users	Does not prevent rockfall and limit on size of rocks that can be restrained. Maintenance and damage repair expected	Rock cuttings where rockfall failure prevention methods not possible
Benching, ditches and rock traps	Simple and effective method of containing/reducing speed of rockfall	Requires maintenance and regular cleaning. Excavation may be difficult and expensive	Rock cuttings where slope angle permits benching
Rock fall shelters	Positive structural solution. Provides high level of safety	High cost and must be designed for high impact loadings	Heavily trafficked infrastructure cuttings where prevention methods are not possible
Alarm and warning systems	Low cost providing early warning	Will not prevent failures but only provide warning. Possible disruption to infrastructure	All cutting types
Internal drainage	Reduces and controls groundwater levels and flow through face	Requires maintenance. Can be difficult to install	Slopes where water has a significant influence on stability
Slope drainage	Simple to install	On steep slopes can have negative visual impact	All cutting types
Toe drainage	Simple to install and reduces risk of erosion at cutting toe	Installation may have an effect on cutting stability in soil slopes	All cutting types
Membranes, eg sprayed concrete	Used for erosion control or as a part of structural solution	Can mask underlying problems and may have unacceptable visual impact	Most soil and rock conditions
Vegetation	Aesthetically pleasing and enhancement of soil stability near surface of slope	Not suitable in all environments and can mask underlying problems. Can present a safety/ maintenance liability. Consider root damage in rock slopes	Success dependent on plant selection, soil type, orientation and maintenance
Maintenance methods	Prolong life of cuttings	Can have significant effect on whole-life costs. Consider safety risks to maintenance personnel	All cuttings

 Copyright © MAINLINE Consortium

The CIRIA guide also presents the main advantages, limitations and suitable conditions for each technique, as shown in Tab.7.13.

It is usually necessary to use a combination of techniques in order to stabilise or remediate a cutting. The CIRIA guide identifies the following list of main considerations when selecting individual or combinations of interventions:

- safety
- maintaining traffic operation
- applicability to soil or rock and groundwater conditions
- access, temporary works and ease of construction
- location of infrastructure boundary relative to cutting face
- initial cost and long-term maintenance requirements
- design life and performance requirements
- environmental, aesthetic and sustainability issues.

Review of the Effect of Interventions on Earthwork Condition Rating (Network Rail, 2012)

Definition of Intervention Categories and Types

In 2012 Network Rail commissioned a study into the effect of various intervention types on the Condition Rating (SSHI/RSHI) of earthworks. A report was produced on the findings of this study.

The report identifies the categories of interventions for soil cuttings given in Table 7.14.

Table 7-14 Soil Cutting Intervention Categories as defined in the NR Intervention Study

Renewal Interventions	All defects and indicators of instability and poor drainage are removed. Full length of cutting is remediated (at NR this is broken down into 100m lengths)
Refurbish Interventions	Remedial works are limited to the defective area only All defects are removed Indicators of instability are not removed Drainage works are not included
Maintenance works	Drainage condition is improved, though drainage enhancements are not included Maintenance works can cover full length of cutting

 Copyright © MAINLINE Consortium

The typical types of soil cutting intervention used at Network Rail are shown in the Intervention Matrix in Fig.7.23. This is a risk matrix which shows which intervention is likely to be applied to a particular cutting, depending upon its current condition (Serviceable, Marginal, Poor or Top Poor) and the asset criticality.

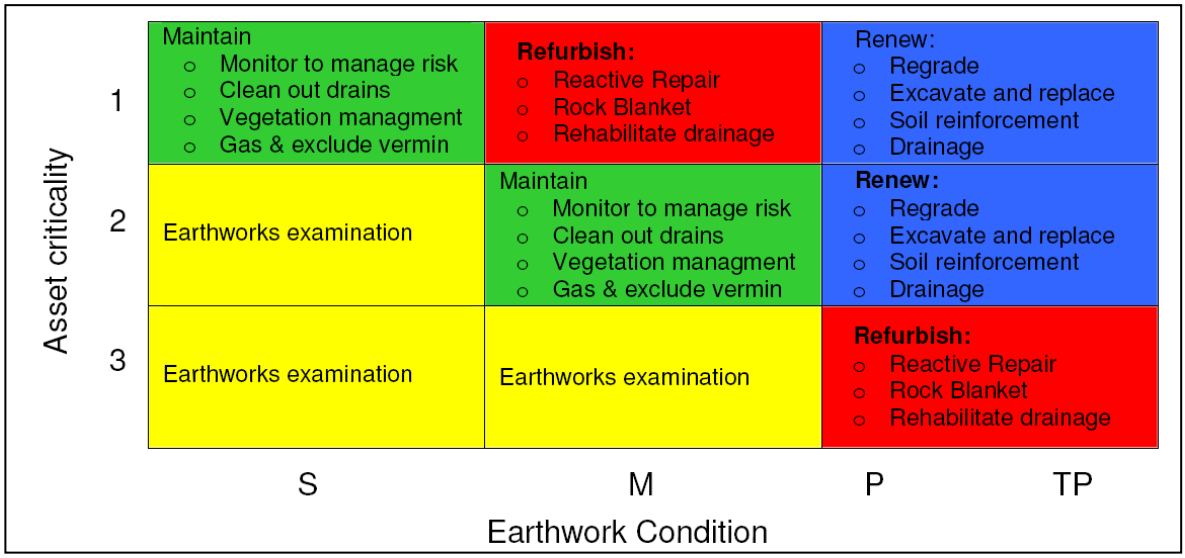

Figure 7-23 Simplified Network Rail Soil Cutting Intervention Matrix (Intervention Study)

As can be seen in Fig.7.23, interventions within the Renewal Category are split into 4 types, based on their effect on the SSHI algorithm:

- Regrade – altering the slope geometry
- Excavate and replace – altering the slope composition
- Soil reinforcement (e.g. soil nailing and pile stabilisation) - reinforcing the existing slope without altering geometry or composition. Soil reinforcement solutions may be significantly different in engineering principles, however they affect they SSHI algorithm in the same way.
- Drainage works – improvements to drainage issues only.

 Copyright © MAINLINE Consortium

Table 7-15 Rock Cutting Intervention Categories as Defined in the NR Intervention Study

Renewal Interventions	Removal of all vegetation on slopes. Removal of drainage problems, Reduction of surface water and groundwater seepage by 1. If cess present depth increased by 0.5m. Removal of material from previous failures. The potential for further failures removed. Reinforcement 100%, Total hazards treated 100%, Effectiveness of remedial works 100%.
Refurbish Interventions	Removal of all vegetation on slopes. Removal of drainage problems. If cess present depth increased by 0.5m. Removal of material from previous failures. Reinforcement 50%, total hazards treated increase by 50%, Effectiveness of remedial works increase by 50%.
Maintenance Interventions	Removal of vegetation on slopes. Removal of drainage problems. If cess present depth increased by 0.5m. o Removal of material from previous failures.

The Network Rail Intervention Study also identifies categories and types of rock cutting interventions. Because the RSHI condition rating system is more directly affected by the scope of remedial works undertaken, a simpler approach could be taken to categorising rock cutting intervention categories, as shown in Tab.7.15.

Typical intervention techniques within each category are shown in the rock cuttings intervention matrix in Fig.7.24.

 Copyright © MAINLINE Consortium

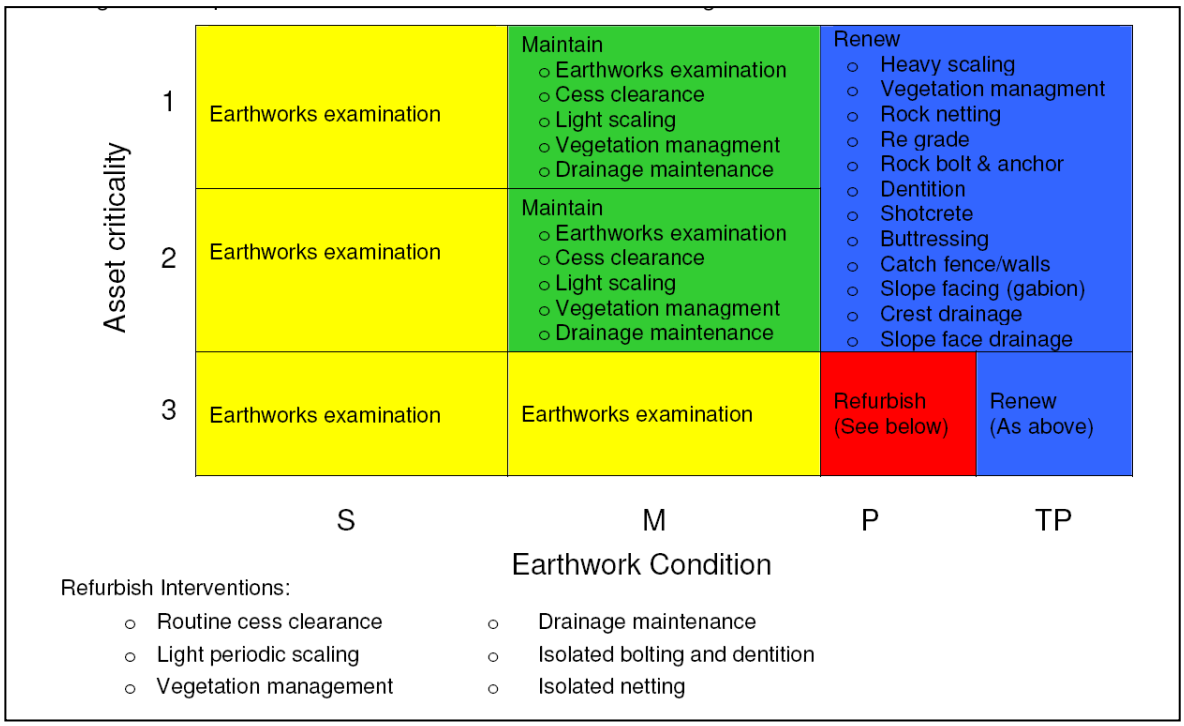

Figure 7-24 Simplified Network Rail Rock Cutting Intervention Matrix (Intervention Study)

The rock cutting intervention techniques within each category fall into 4 generic types, based upon which failure mechanism it is related to, as shown in Tab.7.16.

Table 7-16 Intervention Types for Rock Cuttings (NR Intervention Study)

Failure Mechanism	Intervention Type		
	Renew	Refurbish	Maintain
Planar	Type 1	Type 5	Type 9
Wedge	Type 2	Type 6	Type 10
Toppling	Type 3	Type 7	Type 11
Ravelling	Type 4	Type 8	Type 12

7.4.2 Approach to quantifying the effect of interventions

In order to quantity the effect of interventions on deterioration rate it is necessary to consider the following (task 2.3):

- The immediate benefit of Interventions – i.e. reduce deterioration rate, condition freeze or condition improvement,
- The rate of deterioration asset following the end of the intervention design life.

Fig.7.25 presents a preliminary intervention effect matrix.

 Copyright © MAINLINE Consortium

Preliminary intervention effect matrix *for soil cuttings*

		Condition Assessment Parameters (SKM Proposed algorithm for cohesive cuttings)										
		Base values				Assessment Values						
	Input name	Soil Type	Slope Angle Factor	Slope Height Factor	Adjacenet Land Factor	Movement	Vegetation	Surface Water	Drainage	Burrowing	Construction Activity	Previous Remediation
	Input code	ST	SAF	SHF	ALF	MA	VA	SWA	DA	BA	CA	PR
Interventions	Regular Earthworks Examinations	0	0	0	0	0	0	0	0	0	0	0
	Ground Investigation	0	0	0	0	0	0	0	0	0	0	0
	Monitor to manage risk	0	0	0	0	0	0	0	0	0	0	0
	Clean out drains	0	0	0	0	0	0	X	X	0	0	X
	Vegetation management	0	0	0	0	0	X	0	0	0	0	X
	Gas and exclude vermin	0	0	0	0	0	0	0	0	X	0	X
	Reactive isolated slope repair	0	0	0	0	X	X	X	0	X		X
	Rehabilitate drainage	0	0	0	0	0	0	X	X	0	0	X
	Full slope regrade	0	X	X	0	X	X	X	0	X	0	X
	Excavate and replace	X	X	X	0	X	X	X	0	X	0	X
	Soil reinforcement	X	0	0	0	X	X	X	0	X	0	X
	Install new drainage	0	0	0	0	0	0	X	X	0	0	X

Key

X	Condition uplift effect to be applied to input parameter (numerical values to be determined following further development of the model)
0	No anticipated effect on assessment parameter

Figure 7-25 Example of intervention Matrix

7.5 Conclusion

7.5.1 Scope and limitations

Applicable to cohesive cuttings – will be rolled out to granular/interbedded following review and comments from other IMs around Europe

This model builds upon on extensive research undertaken by Network Rail in the development of the SSHI algorithm and incorporates additional experience and engineering judgement from SKM. However input has been limited to that of UK partners with largely UK experience, and review and comments from other European IMs and geotechnical experts will enhance the quality and reliability of the model produced.

7.5.2 Areas for further work

1) Validation with historical data

The assessment input parameter weightings and intervention uplift effects have been derived based on Network Rail's experience and research, as well as geotechnical input from SKM. These will need to be validated with past data in order to validate and refine the assigned values,

2) Extend modelling technique to granular, interbedded and rock cuttings

3) Incorporation of the model into the D5.5 LCAT

4) Incoporating monitored data

Ideally a degradation model would be designed to allow for either type of input parameter. If monitored values became available a more detailed level of modelling could be unlocked that could make use of this data. The level of uncertainty is reduced when monitored values are available rather than just observations. And therefore the confidence in the predicted deterioration could be improved by using this typeof input data.

 Copyright © MAINLINE Consortium

7.6 References

Babtie Group (2003), “Development of the Soil Slope Hazard Index and Associated Algorithm”

Geotechnical Society (2012), “Geology Special Publication No. 26 – Earthworks in Europe”, T.A. Radford (Ed), Geological Society of London, UK.

Kelemen A. et al (2009), “The Climate Change Challenge for European Regions”, European Commission, Brussels

McMillan P., Manley G., (2003), “Rail rock slope risk appraisal”, International Conference on “Maintenance & Renewal of Permanent Way; Power & Signalling; Structures & Earthworks”, 30th April - 1st May 2003, London, UK.

ML-1.1 (2013), “Benchmark of new technologies to extend the life of elderly rail infrastructure”, Deliverable 1.1 – Mainline project

ML-2.1 (2012), “Degradation and performance specification for selected assets”, Deliverable 2.1 – Mainline project.

ML-4.1 (2013), “Report on assessment of current monitoring and examination practices in relation to degradation models”, Deliverable 4.1 – Mainline project

ML-5.5 (2013),” Prototype for a Life Cycle Assessment Tool (LCAT) “ Deliverable 5.5 – Mainline project.

SKM (2012a), “Civil Engineering CP5 Cost Modelling (CeCost) – Embankments and soil cuttings (SSHI) Model, Model Functionality”

SKM (2012b), “Civil Engineering CP5 Cost Modelling (CeCost) – Rock cuttings (RSHI) Model, Model Functionality”

TRL (2000), “Rock Engineering guides to good practice: rock slope medial and maintenance work”, P McMilan, A J Harber and I M Nettleton (Eds), Project Report PPR555

 Copyright © MAINLINE Consortium

8. Corrosion and coatings (Surrey)

8.1 Introduction

Corrosion has major implications in relation to the long-term safety and management of metallic structures, such as steel railway bridges. Several types of corrosion damage have been identified in literature. Their occurrence and the subsequent rate of progression depend on several factors and their interactions; the majority of these factors are associated with the exposure conditions (e.g. relative humidity, temperature, atmospheric pollution, etc) and the type of protection system applied on the exposed surfaces. Modelling the long-term deterioration due to corrosion is a vital constituent of any bridge management system, since they can be used to rationalize the allocation of resources for the inspection, maintenance and repair of deteriorating metallic bridges.

The fundamental mechanisms involved in metallic corrosion and the types of corrosion damage are discussed in sections 8.1.1 and 8.1.2. The influence of exposure conditions (including prescriptive classification of exposure environments) on the corrosion process is reviewed in section 8.2. and a classification scheme is presented for the available corrosion models. Emphasis is given to the use of dose response functions (DRF) for predicting time-dependent corrosion damage. Corrosion test results are summarised and deterioration time-profiles developed using the available corrosion models are presented. The available corrosion protection systems are reviewed in section 8.3 and a framework for the classification of coating deterioration models is presented in section 8.4.

8.1.1 Basics of metallic corrosion

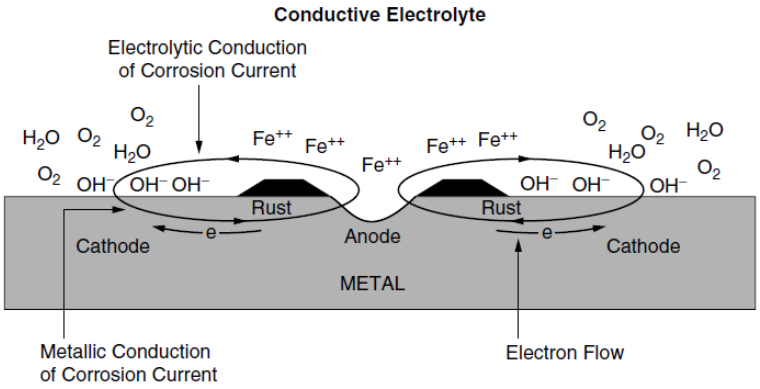

Metallic corrosion is an electrochemical process which characterised by the formation of anodes and cathodes on the metal surface as shown in Fig.8.1.

Figure 8-1 Mechanism of electrochemical corrosion (Hare 2006).

Corrosion occurring at the anode causes the dissolution of metal (i.e. metal ions go into solution):

$$M = M^{n+} + ne \quad (8.1)$$

For the case of iron/steel the anodic reaction is given by:

$$Fe \rightarrow Fe^{2+} + 2e \quad (8.2)$$

 Copyright © MAINLINE Consortium

At the cathodes, in neutral and alkaline conditions, oxygen and water react with the free electrons released at the anode to form hydroxyl ions:

$$2H_2O + O_2 + 4e = 4OH^- \quad (8.3)$$

In acidic conditions the cathodic reaction is given by Equation 4.

$$O_2 + 4H^+ + 4e = 2H_2O \quad (8.4)$$

The hydroxyl ions produced at the cathode react with the free ferrous ions which result in the formation of ferrous hydroxide. Eventually, the formation of corrosion products (i.e. rust) takes place due to the oxidation of the ferrous hydroxide; this is described by:

$$4Fe + 3O_2 + 2H_2O = 2Fe_2O_3H_2O \quad (8.5)$$

Based on the corrosion mechanism described above the following observations can be made in relation to the corrosion process:

- Corrosion occurs only at the anode; no corrosion occurs at the cathode.
- Corrosion process requires the simultaneous presence of water and oxygen.

8.1.2 Types and extent of corrosion damage

Several types of corrosion have been identified by the literature (Landolfo et al. 2010), which can be broadly classified based on the extent of the deterioration (i.e. local vs. uniform corrosion deterioration); these are summarized as follows (Fig.8.2):

- Uniform corrosion
- Pitting corrosion
- Crevice corrosion
- Erosion corrosion
- Cavitation corrosion
- Galvanic corrosion
- Fatigue corrosion

 Copyright © MAINLINE Consortium

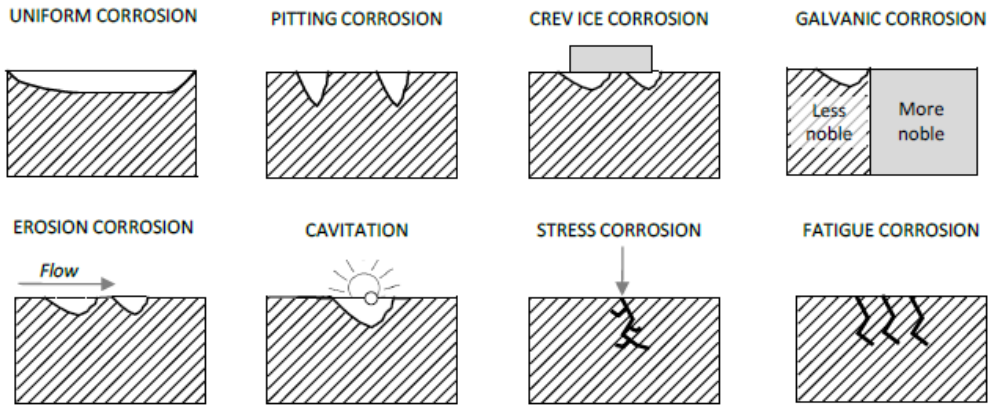

Figure 8-2 Types of corrosion (adapted from Landolfo et al. 2010).

The type and rate of corrosion damage is related to specific exposure conditions such as microbial and bacterial corrosion, gaseous corrosion, marine corrosion, underground corrosion and atmospheric corrosion (Sorensen et al. 2009, Landolfo et al. 2010). The possible outdoor exposure conditions are schematically depicted in Fig.8.3.

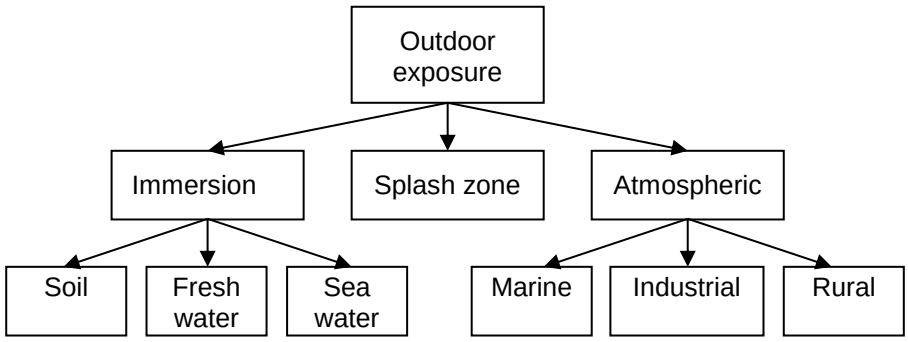

Figure 8-3 Outdoor exposure conditions (adapted from Sorensen et al. 2009).

This report primarily focuses on the modelling of corrosion damage caused by outdoor exposure due to harsh atmospheric conditions (e.g. atmospheric pollution caused by industrial activity, high Cl^- concentrations in coastal exposure, etc.). There are also several studies on modelling corrosion damage under immersed and splash zone (marine) exposure conditions which are not examined in this report (e.g. Melchers 2003, Melchers and Jeffrey 2008). Reference is made, however, to other exposure types where necessary.

8.1.3 Protective coatings

Corrosion deterioration caused by adverse exposure conditions can have a significant influence on the structural performance of metallic structures, such as steel highway and railway bridges. The cost associated with corrosion damage in many cases represents a significant portion of a nation's GDP (Almeida 2005). A number of phenomena are associated with the corrosion process, including (e.g. Greenfield and Scantlebury 2000):

- The anodic and cathodic reactions
- The formation of conductive pathways for ions and electrons

 Copyright © MAINLINE Consortium

Several types of systems are available for the protection of steel structures against corrosion, including organic, inorganic and metallic coatings, enclosure systems etc. In many cases, coatings provide corrosion protection to the substrate metal by interfering/hindering the phenomena associated with corrosion initiation and propagation. These systems provide a means of preventing/ controlling – in the long-term – the occurrence and rate of corrosion damage in the substrate metal. The different coating types – which can are typically consist of multiple layers applied to exposed metallic surfaces – are summarised as follows (de Wit et al. 2011):

- Metallic coating systems
- Inorganic (non-metallic) coatings (e.g. conversion layers)
- Organic coating systems
- Duplex coating systems (e.g. system consisting of metallic and/or organic layers)

The selection of a suitable corrosion protection system should take into account the following aspects (Almeida 2005): a) surface preparation, b) quality of products and environment, c) application process and d) Environmental conditions during application/curing. Ideally, the selection of a suitable coating should be based on the anticipated exposure conditions for the structure's particular location. In some cases, coating appearance (aesthetical reasons) can be a decisive factor regarding its composition (Sangaj and Malshe 2004). However, the cost associated with the corrosion protection of steelwork is of significance importance when selecting a protective system, since in many cases coating deterioration will determine the time of maintenance (Kuroda et al. 2003). The environmental impact and the associated costs are aspects which are likely to be relevant under the continuously tightening environmental regulations. Hence, the selection of a suitable protective system requires consideration of these aspects.

The protective coatings themselves degrade with time; the rate of deterioration is often determined by the harshness of the exposure conditions. The long-term performance – and consequently service life – of a coating, however, is affected by other factors such quality of workmanship during its application, accidental damage, inadequate specification and unexpected changing exposure conditions (e.g. increased pollution, climate change).

In practice, the condition of protective coatings is usually assessed through visual inspection which is part of a generic condition assessment procedure. Visual inspection, alone, can lead to inconsistent assessments and potentially conservative scoring of coating condition. Furthermore, the potential causes of coating damage found during visual inspection are not considered. The availability of a coating performance model would enable the more rational assessment and prioritization of inspections/repairs.

The main coating types, their resistance and corresponding deterioration mechanisms are reviewed in sections 8.3 and 8.4 and a framework for the modelling of the time-dependent performance of deteriorating coatings is presented. Areas where further research is needed are identified and discussed.

 Copyright © MAINLINE Consortium

8.2 Corrosion damage

Modelling of corrosion damage is an important task within the context of planning the long-term maintenance/rehabilitation works. It is generally accepted that the process of atmospheric corrosion is determined by the synergistic action of several influencing factors, including parameters associated with the exposure conditions (e.g. temperature, relative humidity, atmospheric pollution and salinity) as well as the material type (BS EN ISO 9223 & 9224 2012).

Corrosion damage is commonly assessed in terms of weight loss or thickness loss. On this basis, a number of corrosion damage models – which involve varying levels of complexity and accuracy – have been proposed in literature. The results of corrosion tests – e.g. using the standard specimens of BS EN ISO 9226 (2012c) – are expressed either as a mass loss per unit area or as a thickness loss over time, given by:

$$C_m = \frac{\Delta m}{At} \tag{8.6}$$

$$C_t = \frac{\Delta m}{A\rho t} \tag{8.7}$$

where, C_m and $C_t$are the rates of corrosion expressed in mass loss and micrometers per year, respectively, Δm is the mass loss (g), A is the surface area (m^2), t is the exposure time (years) and ρ is the metal density (for steel ρ = 7.86 g/cm^3).

8.2.1 Influencing parameters

The corrosivity of an atmosphere in a particular geographical location is mainly determined by two groups of factors: (a) climate factors (e.g. temperature and relative humidity) and (b) levels of atmospheric pollutants (e.g. sulphur dioxide and airborne salinity). Other atmospheric pollutants which adversely influence corrosion are including ozone, nitrogen oxides and particulates (BS EN ISO 12944 1998); their effects on corrosion, however is relatively small. Furthermore, the position of an element within a structural system has an effect on the microclimate which develops around it and hence its location affects the corrosion process (BS EN ISO 12944 1998, Tamakoshi 2006). In general, metallic structural elements exposed to open-air are more susceptible to corrosion damage compared to covered elements (Tamakoshi 2006).

Atmospheric corrosion involves the presence of a thin layer of moisture (i.e. electrolyte) of the exposed steel surface which is an important rate controlling factor (Evans 1981, Kucera 1988, BS EN ISO 12944 1998). Test results have shown that increasing relative humidity (RH), condensation and atmospheric pollution accelerate the corrosion process. Figure 8.4 shows the effect of SO_2 on the corrosion losses on (a) steel and (b) zinc specimens.

 Copyright © MAINLINE Consortium

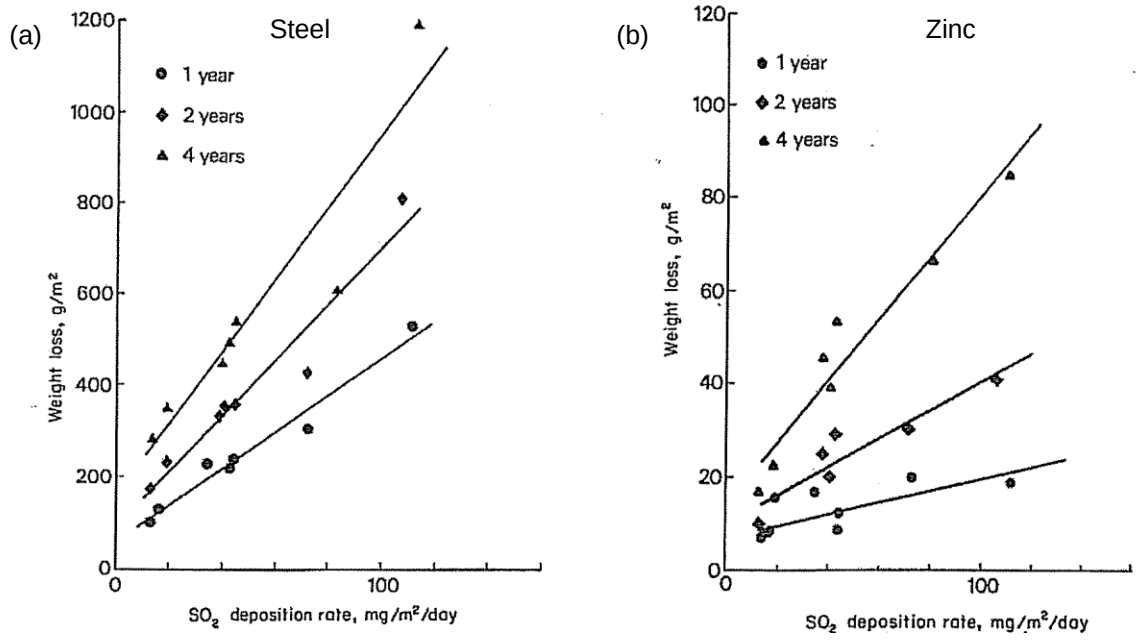

Figure 8-4 Effect of SO2 deposition rate on corrosion losses in temperate conditions (Kucera 1988): (a) Steel specimens and (b) Zinc specimens.

High corrosion activity is observed for values of RH > 80% and T > 0°C. The influence of RH, which can be also expressed as the time of wetness (Tidblad et al. 2000), becomes significant in very cold or dry climates (Kucera 1988). When exposed to polluted environments, corrosion may take place at much lower values of RH. Among the influencing factors, the atmospheric pollutant SO_2 (associated with the combustion of fossil fuels) is often considered as the factor with highest effect on corrosion rate (Kucera 1988). However, the effect of atmospheric pollution (SO_2, airborne salinity) on the rate of corrosion reduces as a function of distance from the emitting source as shown in Fig.8.5.

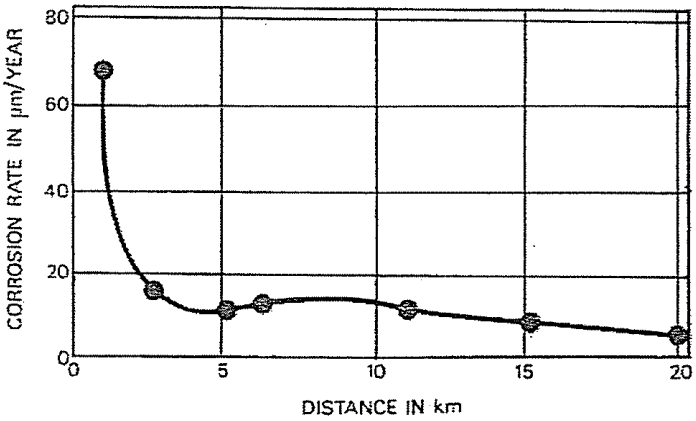

Figure 8-5 Effect of distance from industry emitting SO2 on corrosion rate (adapted from Kucera 1988).

 Copyright © MAINLINE Consortium

8.2.2 Atmospheric corrosivity classification

These observations led to the development of a codified framework for the classification of exposure environments in relation to atmospheric corrosivity and the provision of guiding values for the corrosivity categories. The relevant (international) standards are BS EN ISO 9223 (2012a) and BS EN ISO 9224 (2012b). In BS EN ISO 9223 (2012a) six categories of atmospheric corrosivity are defined (Tab.8.1) A description of the typical expected conditions for each category is also provided in this table.

Table 8-1 Description of categories of atmospheric corrosivity (extracted from Appendix C of BS EN ISO 9223:2012).

Corrosivity category[a]	Corrosivity	Typical environments — Examples[b]	
		Indoor	Outdoor
C1	Very low	Heated spaces with low relative humidity and insignificant pollution, e.g. offices, schools, museums	Dry or cold zone, atmospheric environment with very low pollution and time of wetness, e.g. certain deserts, Central Arctic/Antarctica
C2	Low	Unheated spaces with varying temperature and relative humidity. Low frequency of condensation and low pollution, e.g. storage, sport halls	Temperate zone, atmospheric environment with low pollution (SO_2 < 5 µg/m³), e.g. rural areas, small towns Dry or cold zone, atmospheric environment with short time of wetness, e.g. deserts, subarctic areas
C3	Medium	Spaces with moderate frequency of condensation and moderate pollution from production process, e.g. food-processing plants, laundries, breweries, dairies	Temperate zone, atmospheric environment with medium pollution (SO_2: 5 µg/m³ to 30 µg/m³) or some effect of chlorides, e.g. urban areas, coastal areas with low deposition of chlorides Subtropical and tropical zone, atmosphere with low pollution
C4	High	Spaces with high frequency of condensation and high pollution from production process, e.g. industrial processing plants, swimming pools	Temperate zone, atmospheric environment with high pollution (SO_2: 30 µg/m³ to 90 µg/m³) or substantial effect of chlorides, e.g. polluted urban areas, industrial areas, coastal areas without spray of salt water or, exposure to strong effect of de-icing salts Subtropical and tropical zone, atmosphere with medium pollution
C5	Very high	Spaces with very high frequency of condensation and/or with high pollution from production process, e.g. mines, caverns for industrial purposes, unventilated sheds in subtropical and tropical zones	Temperate and subtropical zone, atmospheric environment with very high pollution (SO_2: 90 µg/m³ to 250 µg/m³) and/or significant effect of chlorides, e.g. industrial areas, coastal areas, sheltered positions on coastline
CX	Extreme	Spaces with almost permanent condensation or extensive periods of exposure to extreme humidity effects and/or with high pollution from production process, e.g. unventilated sheds in humid tropical zones with penetration of outdoor pollution including airborne chlorides and corrosion-stimulating particulate matter	Subtropical and tropical zone (very high time of wetness), atmospheric environment with very high SO_2 pollution (higher than 250 µg/m³) including accompanying and production factors and/or strong effect of chlorides, e.g. extreme industrial areas, coastal and offshore areas, occasional contact with salt spray

NOTE 1 Deposition of chlorides in coastal areas is strongly dependent on the variables influencing the transport inland of sea salt, such as wind direction, wind velocity, local topography, wind sheltering islands outside the coast, distance of the site from the sea, etc.

NOTE 2 Extreme effect by chlorides, which is typical of marine splash or heavy salt spray, is outside of the scope of this International Standard.

NOTE 3 Corrosivity classification of specific service atmospheres, e.g. in chemical industries, is outside of the scope of this International Standard.

NOTE 4 Surfaces that are sheltered and not rain-washed in marine atmospheric environments where chlorides are deposited and cumulated can experience a higher corrosivity category due to the presence of hygroscopic salts.

NOTE 5 A detailed description of types of indoor environments within corrosivity categories C1 and C2 is given in ISO 11844-1. Indoor corrosivity categories IC1 to IC5 are defined and classified.

[a] In environments with expected "CX category", it is recommended that the atmospheric corrosivity classification from one-year corrosion losses be determined.

[b] The concentration of sulfur dioxide (SO_2) should be determined during at least one year and is expressed as the annual average.

 Copyright © MAINLINE Consortium

BS EN ISO 9223 (2012a) suggests that the classification should be based on 1-year test results (Tab.8.2). Alternatively, where test results are not available, this standard provides dose response functions (i.e. models which predict the corrosion loss as a function of climatic and atmospheric pollution variables) for different metals, which allow the atmospheric corrosivity classification based on environmental information. The dose response functions (DRF) of are discussed in more details later.

Table 8-2 Corrosion rates for the 1st year of exposure for different corrosivity categories (extracted from BS EN ISO 9223:2012).

Corrosivity category	Corrosion rates of metals r_{corr}				
	Unit	Carbon steel	Zinc	Copper	Aluminium
C1	g/(m²·a)	$r_{corr} \leq 10$	$r_{corr} \leq 0,7$	$r_{corr} \leq 0,9$	negligible
	µm/a	$r_{corr} \leq 1,3$	$r_{corr} \leq 0,1$	$r_{corr} \leq 0,1$	—
C2	g/(m²·a)	$10 < r_{corr} \leq 200$	$0,7 < r_{corr} \leq 5$	$0,9 < r_{corr} \leq 5$	$r_{corr} \leq 0,6$
	µm/a	$1,3 < r_{corr} \leq 25$	$0,1 < r_{corr} \leq 0,7$	$0,1 < r_{corr} \leq 0,6$	—
C3	g/(m²·a)	$200 < r_{corr} \leq 400$	$5 < r_{corr} \leq 15$	$5 < r_{corr} \leq 12$	$0,6 < r_{corr} \leq 2$
	µm/a	$25 < r_{corr} \leq 50$	$0,7 < r_{corr} \leq 2,1$	$0,6 < r_{corr} \leq 1,3$	—
C4	g(m²·a)	$400 < r_{corr} \leq 650$	$15 < r_{corr} \leq 30$	$12 < r_{corr} \leq 25$	$2 < r_{corr} \leq 5$
	µm/a	$50 < r_{corr} \leq 80$	$2,1 < r_{corr} \leq 4,2$	$1,3 < r_{corr} \leq 2,8$	—
C5	g/(m²·a)	$650 < r_{corr} \leq 1\,500$	$30 < r_{corr} \leq 60$	$25 < r_{corr} \leq 50$	$5 < r_{corr} \leq 10$
	µm/a	$80 < r_{corr} \leq 200$	$4,2 < r_{corr} \leq 8,4$	$2,8 < r_{corr} \leq 5,6$	—
CX	g/(m²·a)	$1\,500 < r_{corr} \leq 5\,500$	$60 < r_{corr} \leq 180$	$50 < r_{corr} \leq 90$	$r_{corr} > 10$
	µm/a	$200 < r_{corr} \leq 700$	$8,4 < r_{corr} \leq 25$	$5,6 < r_{corr} \leq 10$	—

NOTE 1 The classification criterion is based on the methods of determination of corrosion rates of standard specimens for the evaluation of corrosivity (see ISO 9226).

NOTE 2 The corrosion rates, expressed in grams per square metre per year [g/(m²·a)], are recalculated in micrometres per year (µm/a) and rounded.

NOTE 3 The standard metallic materials are characterized in ISO 9226.

NOTE 4 Aluminium experiences uniform and localized corrosion. The corrosion rates shown in this table are calculated as uniform corrosion. Maximum pit depth or number of pits can be a better indicator of potential damage. It depends on the final application. Uniform corrosion and localized corrosion cannot be evaluated after the first year of exposure due to passivation effects and decreasing corrosion rates.

NOTE 5 Corrosion rates exceeding the upper limits in category C5 are considered extreme. Corrosivity category CX refers to specific marine and marine/industrial environments (see Annex C).

The standard BS EN ISO 9223 (2012a) provides a classification for individual climatic and atmospheric pollutants using ranges of values. For example, Table 8.3 provides a classification of the environment based on the deposition rate or concentration of SO_2.

 Copyright © MAINLINE Consortium

Table 8-3 Classification based on different SO2 ranges (extracted from BS EN ISO 9223:2012).

Deposition rate of SO_2 mg/(m²·d)	Concentration of SO_2 µg/m³	Level
$P_d \leq 4$	$P_c \leq 5$	P_0 Rural atmosphere
$4 < P_d \leq 24$	$5 < P_c \leq 30$	P_1 Urban atmosphere
$24 < P_d \leq 80$	$30 < P_c \leq 90$	P_2 Industrial atmosphere
$80 < P_d \leq 200$	$90 < P_c \leq 250$	P_3 Highly polluted industrial atmosphere

NOTE 1 Methods of determination of sulfur dioxide (SO_2) are specified in ISO 9225.

NOTE 2 The sulfur dioxide (SO_2) values determined by the deposition, P_d, and volumetric, P_c, methods are equivalent for the purposes of this International Standard. The relationship between measurements using both methods can be approximately expressed as: $P_d = 0{,}8\,P_c$. This conversional factor is based on the deposition rate measurements on alkaline surfaces.

NOTE 3 For the purposes of this International Standard, the sulfur dioxide (SO_2) deposition rate and concentration are calculated from continuous measurements during at least one year and are expressed as the annual average. The results of short-term measurements can differ considerably from long-term values. Such results are only used for guidance.

NOTE 4 The ranges given cover common levels in individual types of atmospheres. Extreme values are listed in Table B.2.

8.2.3 Deterioration modelling

Prediction of the time-dependent deterioration due to corrosion damage is an important aspect in any bridge management system. The development of corrosion models requires the systematic gathering of data for the factors associated with the exposure conditions and the corresponding corrosion losses in the exposed specimens. In general, data obtained through field exposure of test specimens allows assessing the harshness of the exposure conditions associated with a particular location. Equally important is the role of experimental data from field exposure tests for the development and validation of accurate corrosion models. In general, results from corrosion tests performed in the lab should be cautiously interpreted since they may differ remarkably with field exposure results. Nonetheless, the ability to carefully control individual parameters in lab-based corrosion studies allows the sensitivity of these parameters to be rationally established.

Table 8-4 Proposed model classification.

	Description	Modelling approach		Comments
		Deterministic	Probabilistic	
Level 1	Empirical models. Effect of all influencing factors (i.e. exposure conditions, metal type, etc.) are taken into account through fixed model constants	✓	×	Model coefficients are associated with very high uncertainty. Available statistical properties may not be reliable and hence not suited for probabilistic analysis. Questionable model transferability.
Level 2	Empirical models which directly relate the rate of corrosion to specific exposure variables (see section 2.3.2.1). These models are known as dose response functions (DRF).	✓	✓	These models rely on the data availability of atmospheric pollutants and climatic parameters in a particular area. Suitable for probabilistic analysis when sufficient data for the exposure conditions is

 Copyright © MAINLINE Consortium

				available.
Level 3	Simulation-based mechanistic models (e.g. Roberge et al. 2002). They may involve advanced simulation techniques (e.g. CFD) to predict airflow patterns to determine rate of pollutant mass transfer on the exposed surfaces.	✓	×	Predicted results depend on modelling assumptions. Insufficient input data for practical applications, especially for probabilistic analysis.

Proposed model classification

Modelling the rate and amount of corrosion loss can be considered in different levels of various complexity and accuracy. Table 8.4 provides a summary of the proposed classification for modelling atmospheric corrosion.

This report primarily focuses in Level 2 models due to their potential use in practical applications using either a deterministic or probabilistic approach; however, a brief description of Level 1 models is also provided. It should be noted that the development and validation of corrosion models largely depends on the amount and type of available experimental data.

Models for atmospheric corrosion

When the exposure conditions are simply classified as rural, urban, industrial, marine, etc. and no other information is provided regarding the exposure conditions, corrosion can be modelled using a range of values which represent expected corrosion losses following a specific time period of exposure. Simple regression models can be also used to model corrosion as a function of time. In these models, the effects of all the influencing factors (i.e. exposure conditions and material type) on the rate and amount of corrosion loss are accounted by the model as constant coefficients. A number of models have been proposed in literature for the calculation of long-term corrosion loss due to atmospheric exposure. Among them, the most well-known is the power model given by the following equation (Feliu et al. 1993a, b, Haagenrud and Henriksen 1996, Radomski 2002, Sharifi and Paik 2011):

$$C(t) = At^B \tag{8.8}$$

where, $C(t)$ is the average loss of thickness after t years of corrosion and parameters A and B are experimentally determined coefficients obtained through regression analysis on test results in different environmental exposure conditions. Hence, the influence of the exposure environment (i.e. climatic factors and levels of atmospheric pollutants) and metal type is considered by selecting suitable values for coefficients A and B. Table 8.5 provides both the mean and coefficient of variation (COV) of coefficients A and B for carbon and weathering steel in relation to three different exposure classifications. Fig. 8.6 shows the thickness losses vs. time predicted using the mean values for A and B. (Table 8.5) in Eq. 8.8 (Level 1 model) for carbon steel in environments with dissimilar corrosivity.

 Copyright © MAINLINE Consortium

Table 8-5 Statistical properties of A and B for different exposure classifications (e.g. Radomski 2002, Sharifi and Paik 2011).

Parameters	Carbon steel		Weathering steel	
	A ($\times 10^{-3}$ mm)	B	A ($\times 10^{-3}$ mm)	B
Rural environment				
Mean value, μ	34	0.65	33.3	0.498
Coefficient of variation, σ/μ	0.09	0.10	0.34	0.09
Coefficient of correlation, ρ_{AB}	Not available	–	–0.05	–
Urban environment				
Mean value, μ	80.2	0.593	50.7	0.567
Coefficient of variation, σ/μ	0.42	0.40	0.30	0.37
Coefficient of correlation, ρ_{AB}	0.68	–	0.19	–
Marine environment				
Mean value, μ	70.6	0.789	40.2	0.557
Coefficient of variation, σ/μ	0.66	0.49	0.22	0.10
Coefficient of correlation, ρ_{AB}	–0.31	–	–0.45	–

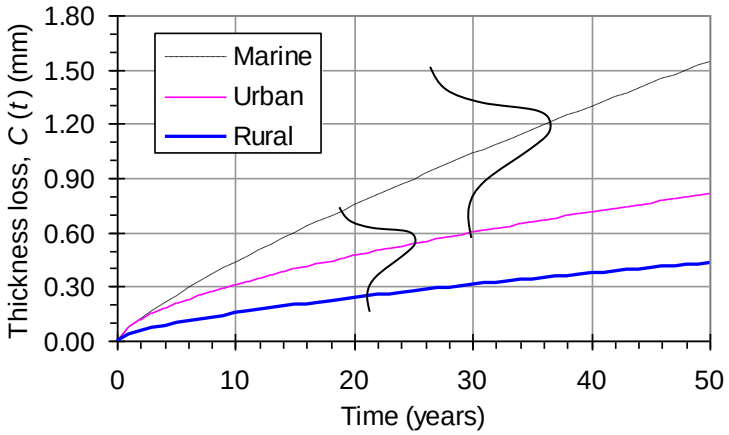

Figure 8-6 Predictions of Eq. 8 (Level 1 model) for carbon steel in different environments using mean values for A and B.

An obvious limitation of Eq.8.8 is its inability to consider separately the impact and future evolution of each of the climatic and atmospheric variables, which in-turn (individually and synergistically) determine the exposure conditions of the structure. Furthermore, Table 8.5 indicates that coefficients *A* and *B* are associated with high uncertainty. The effect of the several influencing parameters which determine the exposure conditions are considered implicitly through *A* and *B* and hence it is not possible to individually examine each of the influencing parameters on the observed variability associated with the progress of corrosion. Eq.8.8 may give inaccurate estimates of corrosion damage when used in conditions dissimilar to the ones used for its calibration (Klinesmith et al. 2007). To overcome the limitations imposed by Eq.8.8 attempts have been made to develop models which directly relate the climatic and atmospheric variables to the rate of corrosion (e.g. Feliu et al. 1993a, b, Haagenrud and Henriksen 1996, Klinesmith et al. 2007, BS EN ISO 2012a, b). These models, which are known in literature as dose response functions (DRF), are discussed next.

 Copyright © MAINLINE Consortium

Dose response functions

Dose response functions are mathematical functions which relate explicitly several exposure variables (e.g. temperature, relative humidity, atmospheric pollution, etc.) with the observed corrosion losses following a certain time period. In most cases, corrosion loss is quantified in terms of metal thickness or mass loss (see Eqs.8.6-7).

Many functions have been proposed during the past five decades; many of them, however, involve limitations which do not allow their practical application. A comprehensive review on the early stage development of DRFs is provided by (Haagenrud and Henriksen 1996 and Klinesmith et al. 2007). In this section, the DRFs which appear to be generally applicable for a wide range of metal types and exposure conditions are only presented. It should be noted that – in general – these models use average annual values for the input climatic and atmospheric pollution variables.

DRFs of Feliu et al. (1993a and 1993b)

Dose response functions for several materials (i.e. carbon steel, aluminium, zinc and copper) were developed by Feliu et al. (1993a, 1993b). In their studies corrosion loss evolves with time according to Eq.8.8 in which coefficients *A* and *B* are calculated from DRFs. For carbon steel the DRFs for *A* and *B* are given by:

$$A = 33 + 57.4\mathrm{Cl} + 26.6\mathrm{S} \tag{8.9}$$

$$B = 0.57 + 0.0057(\mathrm{Cl})(\mathrm{T}) + 7.7\times10^{-4}\mathrm{D} - 1.7\times10^{-3} \tag{8.10}$$

where, Cl is the annual average concentration of chloride (mg/dm^2/d), S is the annual average concentration of sulphur dioxide (mg/dm^2/d), T is the annual average temperature (^{o}C) and D is the annual number of rainy days. The reliability of Eq.8.10 (coefficient *B*) is questionable since a poor correlation (*R* = 0.40) is observed between its predictions and the experimental data (Feliu et al. 1993b).

DRFs of Klinesmith et al. (2007)

Klinesmith et al. (2007) using the ISO CORRAG tests results for various locations in 12 countries, developed the DRF model given by Eq.8.11 for four different metals. This model allows the calculation of the time-dependent thickness loss (μm) due to corrosion considering the effect (and evolution) of the different climatic and atmospheric variables:

$$C(t) = At^B\left(\frac{\mathrm{TOW}}{C_1}\right)^D\left(1+\frac{\mathrm{SO_2}}{E}\right)^F\left(1+\frac{\mathrm{Cl}}{G}\right)^H e^{J(\mathrm{T}+T_0)} \tag{8.11}$$

where, TOW is the time of wetness (h/year), SO_2 is the sulphur dioxide concentration (μg/m^3), Cl is the chloride deposition rate (mg/m^2.d), C_1 = 3800 h/year (mean value), E = mean of measured values of SO_2, G = 50, T is the air temperature (^{o}C), T_0 = 20 ^{o}C and coefficients *A, B, D, F, H* and *J* are tabulated in Table 8.6 for different types of metals and specimen types used.

 Copyright © MAINLINE Consortium

Table 8-6 Coefficients A, B, D, F, H, J in Equation 11 for various metal and specimen types (Klinesmith et al. 2007).

Materials	Types of specimens	Coefficients					
		A	B	D	F	H	J
Carbon steel	Flat	13.4	0.98	0.46	0.62	0.34	0.016
	Helix	19.7	0.05	0.46	0.62	0.34	0.016
Zinc	Flat	0.16	0.36	0.24	0.82	0.44	0.05
	Helix	0.26	0.05	0.24	0.82	0.44	0.05
Copper	Flat	0.46	0.15	0.02	0.38	0.46	0.02
	Helix	0.78	0.22	0.02	0.38	0.46	0.02
Aluminum	Flat	0.094	0.05	0.23	1.14	0.42	0.01
	Helix	0.27	0.05	0.23	1.14	0.42	0.01

DRFs of BS EN ISO 9223 & 9224 (2012)

BS EN ISO 9223 (2012a) provides DRFs for steel, zinc, copper and aluminium which can be used to calculate coefficient *A* (1st year of corrosion) in Eq.8.8 (or Eq.8.13 for *t*> 20 years) as a function of several environmental and atmospheric variables. For steel the DRF of BS EN ISO 9223:2012 is given by Eq.8.12:

$$A = 1.77\mathrm{SO}^{0.52}\exp\left(0.02\mathrm{RH} + f_{St}\right) + 0.102\mathrm{Cl}^{0.62}\exp\left(0.033\mathrm{RH} + 0.04\mathrm{T}\right) \qquad (8.12)$$

where, SO is the average annual deposition of SO_2 (mg/m^2.d), RH is the average annual relative humidity (%), Cl is the average annual deposition of Cl^- (mg/m^2.d) and T is the annual (average) temperature (^{o}C). BS EN ISO (2012b) suggests the use of Eq.8.8 for time periods up to 20 years. Beyond the initial 20 years of corrosion the maximum corrosion attack can be estimated using Equ.8.13:

$$C\left(t > 20\right) = A\left[20^B + B\left(20^{B-1}\right)\left(t - 20\right)\right] \qquad (8.13)$$

where, *A* is calculated from Eq.8.12 and *B* depends on the material type. Table 8.7 provides the statistical properties of coefficient *B* (i.e. mean and standard deviation) for different metals (i.e. carbon steel, zinc, copper and aluminum). The *B* value suggested by BS EN ISO for carbon steel in Table 8.7 has been obtained for the steel composition given in Table 8.8. The value of B can be calibrated for steel of different compositions using Eq.8.14:

$$B_a = 0.569 + \sum b_i w_i \qquad (8.14)$$

where, B_a is the alloy specific value of coefficient *B*, $b_i$is a multiplier (Tab.8.9) associated with the ith alloying element involved in the formation of corrosion products (i.e. rust layers) and $w_i$is mass fraction of the *i*th alloying element.

 Copyright © MAINLINE Consortium

Table 8-7 Statistical properties of coefficient B (BS EN ISO 9224 2012b).

Metal	**Mean, μ_B**	**Standard deviation, σ_B**
Carbon steel	0.523	0.0260
Zinc	0.813	0.0300
Copper	0.667	0.0295
Aluminum	0.728	0.0395

Table 8-8 Steel composition used for the estimation of B in Table 8.7 (extracted from BS EN ISO 9224 2012b).

Element	**Composition mass fraction (%)**
Carbon	0.056
Silicon	0.060
Sulphur	0.012
Phosphorus	0.013
Chromium	0.020
Molybdenum	0.010
Nickel	0.040
Copper	0.030
Niobium	0.010
Titanium	0.010
Vanadium	0.010
Aluminum	0.020
Tin	0.005
Nitrogen	0.004
Manganese	0.390

Table 8-9 Values of bi for different alloying elements in Eq. 14 (BS EN ISO 9224 2012b).

Element	**b_i**
C	-0.084
P	-0.490
S	1.440
Si	-0.163
Ni	-0.066
Cr	-0.124
Cu	-0.069

The mean value of *B* for zinc in Table 8.7 has been estimated using pure zinc (BS EN ISO 9224 2012b). The corrosion performance of zinc under atmospheric exposure is highly

 Copyright © MAINLINE Consortium

affected by its composition. Zinc alloys exposed to the atmosphere are generally associated with higher values of *B* compared to pure Zinc. Eq.8.8 is likely to underestimate the rate of corrosion in zinc exposed to atmospheres with high concentrations of SO_2. BS EN ISO 9224 suggests to use $B = 1$ (linear corrosion rate) for zinc exposed to atmospheres highly polluted with SO_2.

The corrosion model of BS EN ISO 9223 & 9224 (2012a, b) is very useful in estimating the rate of corrosion based on specific exposure conditions for an area (i.e. SO_2, T, etc.) through coefficient *A* (Eq.8.12). However, the influence of long-term changes of exposure conditions (due to climate change and/or increase/decrease in the concentrations of atmospheric pollutants) on the rate of corrosion cannot be considered since coefficient *B* remains constant irrespectively of the exposure conditions.

Development of deterioration profiles

Field data

A large number of studies are available in literature reporting results from corrosion tests performed under field exposure conditions. Fig.8.7a-b summarize corrosion rate (i.e. annual corrosion loss) tests results for the UK and internationally, respectively. A trend emerges in the exposure results of Fig.8.7a (UK based tests) despite the high variability; as the harshness of the exposure conditions increases also the corrosion rate increases. In the test results of Fig.8.7b a very high variability is observed. This highlights the difficulty in comparing results from different studies performed under similar (but different) exposure conditions with specimens of varying composition. Although these results are very useful in assessing the corrosiveness of different environments, their limited time periods (i.e. < 10 years) over which the experiments were performed do not allow the long-term estimations of corrosion losses. Such data, however, can be useful in assessing the corrosion models (e.g. Eq.8.12).

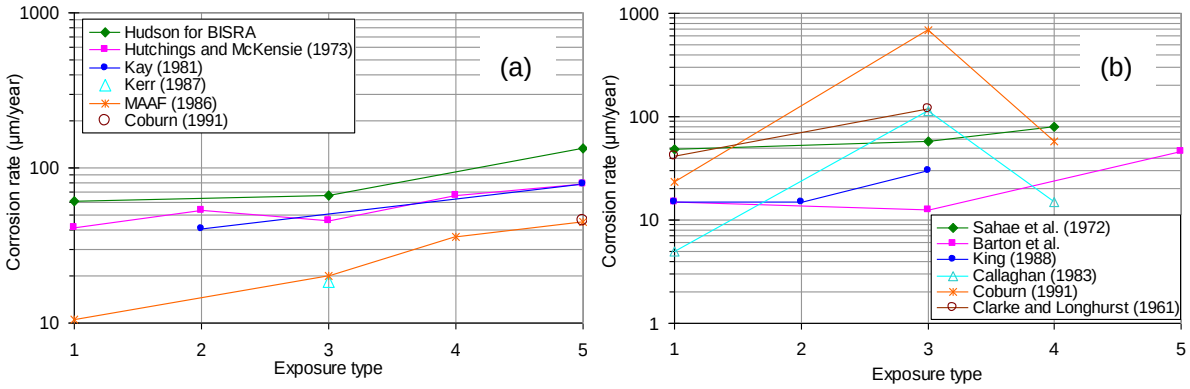

Figure 8-7 Summary of corrosion tests results for: (a) the UK and (b) internationally (Gascoyne and Bottomley 1995). X-axis: 1=Rural/urban, 2=light industrial, 3=marine, 4=industrial/marine, 5=high industrial. For raw data see Tables 8-17 and 8-18 in Appendix A.

Time-profiles using dose response functions

The corrosion models presented in the previous sections can be used to develop deterioration profiles for exposed steel elements under various exposure conditions. As an

example, Figs.8.8a-d show the effects of different climatic and atmospheric variables on the long-term predictions of corrosion thickness losses for steel calculated using the DRF of Klinesmith et al. (2007) given by Eq. 11. The input values for the exposure variables used in these figures are typical values suggested in BS EN ISO 9223 (2012a). By comparing the figures it is evident that atmospheric pollution (i.e. SO_2 concentration) and airborne salinity have the greatest impact on the long-term rate of corrosion. Figure 8.9 schematically depicts the potential extension of DRFs (Level 2 models) to a probabilistic framework by using suitable distributions for the input variables associated with the exposure conditions (i.e. temperature, relative humidity, SO_2 and Cl^-).

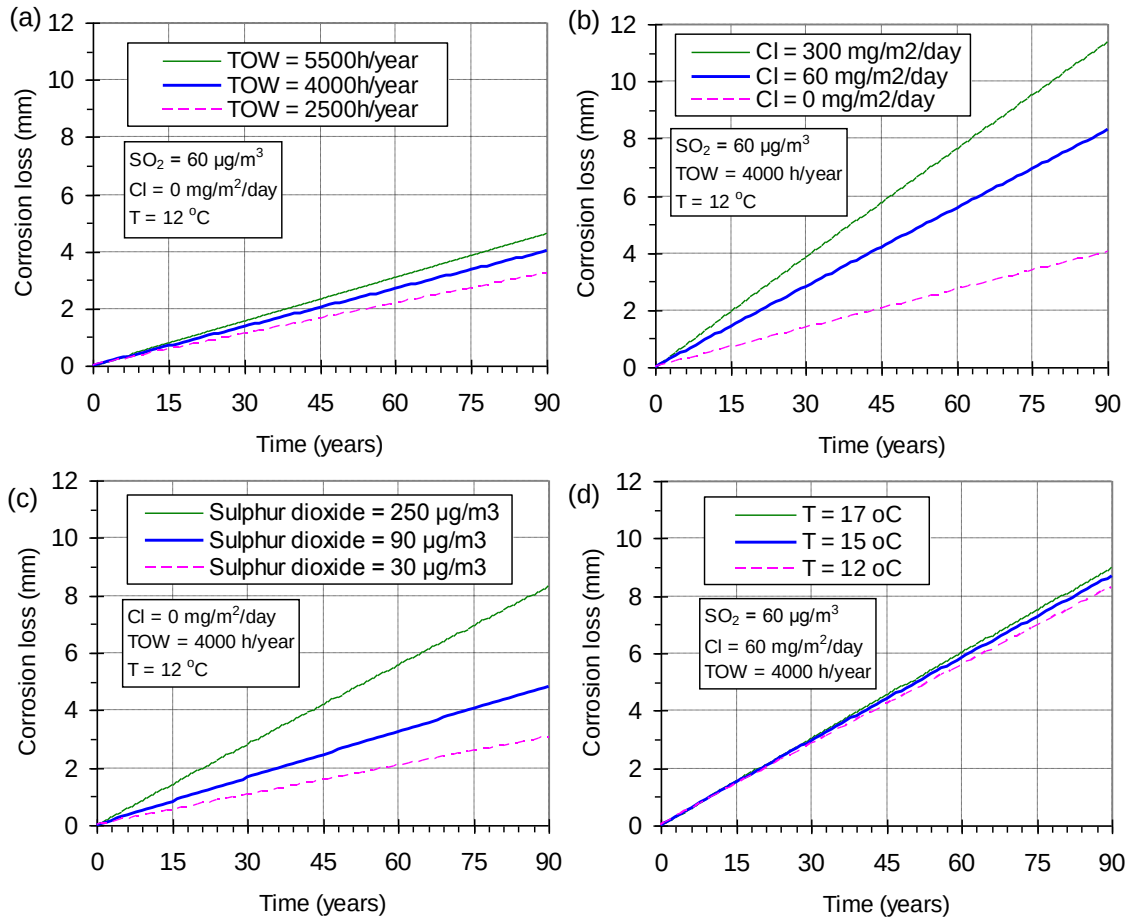

Figure 8-8 Effect of varying climatic and atmospheric parameters on the corrosion losses for steel with time, predicted using Equation 11: (a) time-of-wetness (TOW), (b) Cl deposition rate, (c) SO2 concentration and (d) Temperature. Variable ranges from BS EN ISO 9223 (2012a).

 Copyright © MAINLINE Consortium

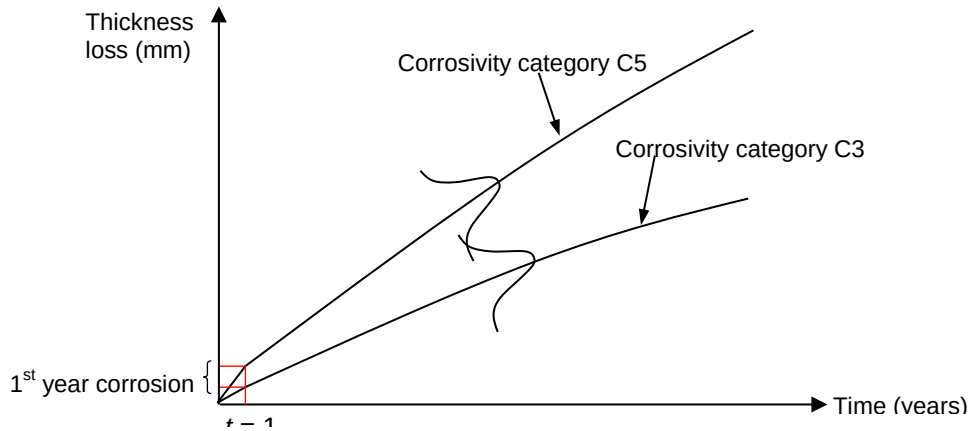

Figure 8-9 Development of deterioration profiles using DRFs (Level 2 models). Input from the corrosivity classification of BS EN ISO 9223 (2012a), see Tables 8.1-3.

8.3 Corrosion protection systems

Corrosion damage in metallic structures such as steel railway bridges is responsible for a number of physical and mechanical (i.e. structural) effects. The initiation and accumulation of corrosion damage on structures in service can cause significant losses of safety and reliability (i.e. increase of uncertainty associated with structural performance). Modern codes of practice provide prescriptive guidance for corrosion design (e.g. Eurocode 3 suggests a corrosion allowance for steel elements which cannot be inspected) as well as recommendations on the use of protective systems for corrosion control, such as protective coatings applied on the exposed steel surfaces, enclosure systems (BS EN 2005, BS EN ISO 12944, BD 1996), etc. The characteristics and performance of the available coating systems are discussed in a separate report.

8.3.1 Coating composition

Organic coatings

The main constituents of organic coating layers are the binder, the pigment and the solvent. Additionally, fillers and additives are commonly used to add specific properties to the final coating, such as impact and abrasion resistance, UV absorption, fire-resistance and volume increase (de Wit et al. 2011).

The binder is used to create the matrix of the coating on which other constituents are added. The physical and chemical properties of the coating are determined by its density and composition (de Wit et al. 2011). The main difference between organic and inorganic coating layers is in the composition of their binder. Epoxy-based binders are commonly used for organic coatings, while silicate binders are used in inorganic coatings (Keijman 1999). Table 8.10 summarises the generic types of paints based on their binder.

The pigment is used to improve the effectiveness of the coating system against corrosion and to colour the coating for architectural purposes. For example in galvanic pigments which incorporate metallic particles (e.g. zinc dust), the zinc particles in the coating will corrode (i.e. coating becomes the anode of an electrochemical cell) while the substrate metal is protected by becoming the cathode (Hare 2006).

 Copyright © MAINLINE Consortium

The addition of the solvent enables the homogeneous mixing of the binder with the other constituents of the coating by reducing the viscosity of the binder. This enables the application of the coating as a smooth continuous film onto the metallic surface (de Wit et al. 2011).

Table 8-10 Summary of commonly used binders (CORUS 2004).

Binder		**System cost**	**Tolerance of poor surface**	**Chemical resistance**	**Solvent resistance**	**Water resistance**	**Overcoating after aging**	**Comments**
Black coatings (tar based)		Low	Good	Moderate	Poor	Good	Very good with coatings of same type	Limited to black or dark colours. May soften in hot conditions.
Alkyds		Low-medium	Moderate	Poor	Poor-Moderate	Moderate	Good	Good decorative properties. High solvent levels.
Acrylated rubbers		Medium-high	Poor	Good	Poor	Good	Good	High build films that remain soft & are susceptible to sticking.
Epoxy	Surface tolerant	Medium-high	Good	Good	Good	Good	Good	Suitable for a range of surface and coatings*.
Epoxy	High performance	Medium-High	Very poor	Very Good	Good	Very Good	Poor	Susceptible to chalking in UV light.
Urethane & polyurethane		High	Very poor	Very Good	Good	Very Good	Poor	Can be more decorative than epoxies.
Organic silicate & inorganic silicate		High	Very poor	Moderate	Good	Good	Moderate	May require special surface preparation.

The coating system is built-up by adding several compatible layers one on top of another. Hence, a wide range of coating systems can be produced since the composition and thicknesses of the individual layers can vary. The first layer which is placed in direct contact with the substrate metal is the primer. Primers are often enriched with corrosion inhibitive pigments (e.g. zinc rich epoxy) to provide sacrificial protection. The intermediate coat layers are used to obtain the required thickness of the coating system. The function of the topcoat (or finish) layer is twofold; firstly, it provides the initial resistance from the external environment and secondly, it determines the aesthetical appearance (e.g. colour, gloss, etc.) of the coated surface. An example of a multicoat system which incorporates a zinc rich epoxy primer is shown in Fig.8.10.

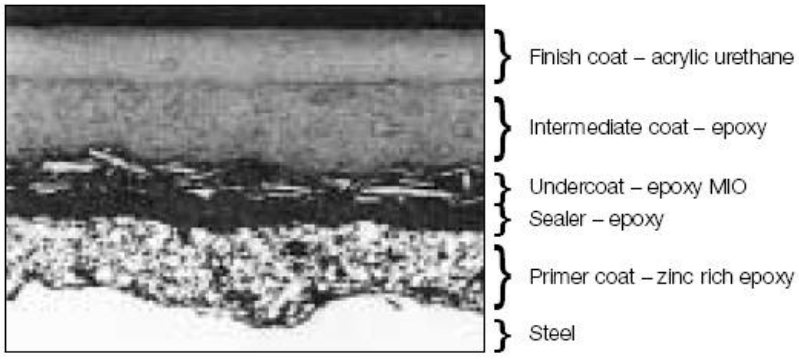

Figure 8-10 Typical section of multilayer protective coating system with zinc enriched epoxy primer (CORUS 2004).

 Copyright © MAINLINE Consortium

In the United Kingdom, guiding standards exist for the specification of coating systems and their application on metallic highway and railway bridges. Corrosion protection of railway bridges using/ protective coatings and sealants are covered by standards NR/GN/CIV/002, NR/L3/CIV039 and NR/L3/CIV/040 (see NR 2009a, b and c) published by Network Rail, which is the asset owner and also holds the responsibility for maintenance. These Network Rail standards provide a number of alternative coating systems for new structures (N-series coating systems) and maintenance/repair of existing structures (M-series coating systems). The selection of a suitable protective system is closely related to the anticipated exposure conditions (classification of exposure conditions is based on BS EN ISO 12944-2). The majority of the protective coating systems for new construction are based on a duplex (hybrid) metallic-organic coat composition. Maintenance coatings suggested in NR/L3/CIV/040 for the re-application/repair of existing metallic structures are summarised in Table 8.11.

Tables 8.12 and 8.13 provide recommendations on coating system selection for patch repairs and full replacement of coatings, respectively. The former is based on the existing coating system while in the case of full replacement the selection of coating system is based on the exposure conditions.

Table 8-11 Examples of coating systems for existing metallic structures (NR 2009a).

System name	Title	Substrate	Coats (Stripe coats omitted)			
			A	B	C (Intermediate)	D (topcoat)
M20	Protective system for existing structures using epoxy	Existing iron or steel blast-cleaned to a surface standard Sa2½ and a surface profile mean peak to valley height of 70 to 100µm	Select primer with a min dft of 50µm; - blast primer for damp surfaces - epoxy blast primer - zinc rich epoxy blast primer	Select primer from the following: - high solids epoxy primer with min dft 100µm - epoxy intermediate coat with min dft 125µm	Epoxy intermediate coat with min dft 125µm	Select from the following and use min dft of 50µm: - anti-graffiti paint – polyurethane coloured finish - acrylic urethane topcoat - polysiloxane topcoat
M21	Protective system for existing structures using epoxy glass flake	Existing iron or steel blast-cleaned to a surface standard Sa2½ and a surface profile mean peak to valley height of 70 to 100µm	Epoxy blast primer with min dft 25µm		Epoxy glass flake intermediate coat with min dft 400µm	Select from the following and use min dft of 50µm: - anti-graffiti paint – polyurethane coloured finish - acrylic urethane topcoat - polysiloxane topcoat
M24	Patch repair of aged alkyd and acrylated rubber systems on existing structures using a durable	Existing iron or steel with aged alkyd protective system spot blast-cleaned to a surface standard Sa2½ and a surface profile mean peak to valley height of	Surface tolerant epoxy primer with min dft 100µm		High build surface tolerant epoxy undercoat with min dft 100µm	Select from the following and use min dft of 50µm: - acrylic urethane topcoat - polysiloxane topcoat

 Copyright © MAINLINE Consortium

	two pack protective system	70 to 100µm or cleaned using power or hand tools to surface standard St3				

Table 8-12 Systems for the patch repair of existing coating (NR 2009a).

Existing paintwork	**Recommended systems (in accord with surface condition)**
Aged Alkyd	M24, M34
Urethane Alkyd MIO	M24, M34
Epoxy pitch	M26.3, M34
Bitumen	M27.4
Chlorinated/acrylated rubber	M24
Epoxy/polyurethane	M20, M24, M34
Epoxy glassflake	M21, M34
Anti-graffiti	M29.2
Sub surface	Patch repairing not generally permitted

Table 8-13 Systems for complete recoating (NR 2009a).

Environment as defined in BS EN ISO 12944-2	**Recoating systems (to accord with surface condition)**	
	Recommended	Acceptable
C2 (external)	M20, M24	M21, M34
C3	M20, M24	M21, M34
C4	M20, M21	M34
C5	M20, M21	M20, M34
lm2	Consult specialist	-
Sub surface	N6	
C2 (internal)	M24	M34

The mechanisms of corrosion resistance as well as the time-dependent deterioration of organic coatings are both discussed in later parts of this report.

Metallic coatings

Metallic coatings can provide excellent long-term corrosion protection to metallic structures in a range of harsh exposure conditions (e.g. marine environment). The two most commonly used methods for the application of metallic coatings on structural elements are the hot-dip galvanizing and thermal spraying (CORUS 2004).

The former method requires the immersion of the cleaned steel element in a fluxing agent prior to its contact with molten zinc at around 450^{o}C (CORUS 2004). During this process, the

zinc reacts with the steel to create an intermediate layer of Zn/Fe alloys (see Fig.8.11a). The outer layer of the coating is pure zinc. The specifications of coatings produced using hot-dip galvanizing are based on BS EN ISO 1461.

When applying a metallic coating using thermal spraying, either zinc or aluminium. A heated spray gun (oxygas flame or electric arc) is fed with the metals in powder or wire form and the subsequently the melted metal is blown onto the metallic surface using a compressed air jet (CORUS 2004). The repeated deposition of metal particles, with size 10-120μm, leads to coating formation. In this case, the sprayed metal does not react with the substrate metal and thus no alloy is produced as shown in Fig.8.11b. In thermal spraying, the appropriate surface preparation is important since the bond between the metallic coating and the substrate metal is primarily mechanical. In UK, standard BS EN 22063 provides guidance on the use of thermal spraying aluminium or zinc coatings.

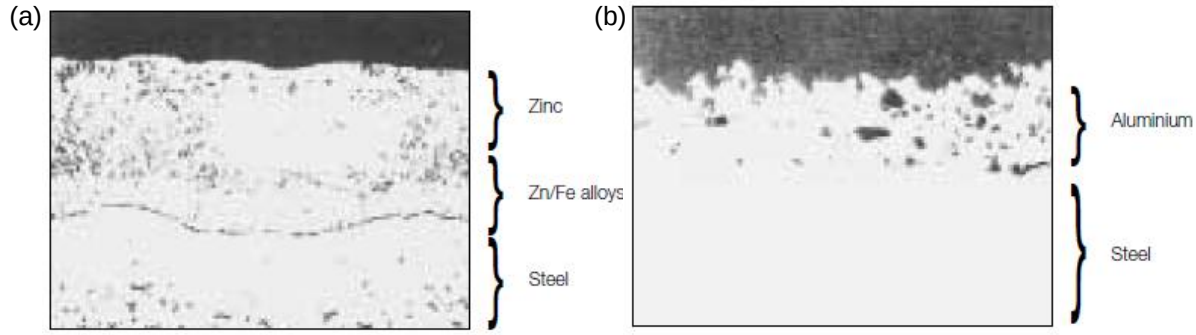

Figure 8-11 Metallic coatings on steel substrate (CORUS 2004): (a) Hot-dip galvanizing and (b) thermally sprayed aluminium.

A duplex (hybrid) coating is produced when an additional protective coating (e.g. organic coating) is applied on the top of a thermally sprayed coating. These are discussed in the next section.

Duplex and hybrid coating systems

Duplex and hybrid coating systems are not uncommon when superior long-term corrosion protection is required. Typically, duplex coating systems consist of a metallic coating applied directly on the prepared substrate metal followed by subsequent organic coating layers. In this way, the pores of the metallic coating are sealed using the organic coating, which adds additional protection against the ingress of corrosive species. Figure 8.12 shows an example of a duplex coating system.

Figure 8-12 Example of high performance duplex coating system on steel substrate (CORUS 2005).

Table 8-14 Protective coating systems for new steel bridges (CORUS 2005).

Ref. number	Title	Surface preparation and profile	Coats and thicknesses (stripe coats omitted)				Estimated cost £/m^2 (2001)
			A	B	C Intermediate coat	D Topcat	
N1	Thermally sprayed metal/ epoxy	Sa 3 75 to 100µm	Aluminium or zinc 100µm	Epoxy sealer 25µm max.	Either; HS epoxy primer, epoxy MIO epoxy intermediate 150µm min.	Either; polyurethane, acrylic urethane, epoxy acrylic, flouropolymer or polysiloxane 50µm min.	22
N2	Epoxy glass flake	Sa 2½ 75 to 100µm	Epoxy blast primer 25µm min.	-	Epoxy glass flake 400µm min.		19+
N3	Polyester glass flake		Epoxy blast primer 25µm min.	-			21+
N4	Epoxy MIO		Epoxy blast primer 50µm min. or zinc rich epoxy blast primer 50µm min.	(a) High solids epoxy primer 100µm. or epoxy MIO inter. Coat 125µm min.	Epoxy MIO intermediate coat 125µm min. (if previous coat (a)) otherwise: epoxy intermediate coat 100µm min.		16
N5	Elastoplastic urethane		Epoxy blast primer 25µm min.	-	Elastomeric polyurethane 1000µm min.		18

Table 8.14 compares the recommended duplex coating system (N1) with other coating systems for new steel railway bridges in the UK.

Hybrid coatings systems, consisting of metal alloys or two dissimilar metallic coating layers, have been proposed. For instance, Kuroda et al. (2006) reported results from a long-term experimental program thermally sprayed coatings including a hybrid alloy coating consisting of 87% Zinc and 13% Aluminium. Their results showed that this coating performed well in marine environment even when unsealed. A thermally spayed two layer Zinc-Aluminium hybrid coating system was tested by (Salas et al. 2012). In their coupons, a layer of Zinc was applied as a primer directly onto the steel surface and an aluminium layer was used as a topcoat with/without applied sealer. Their results, which demonstrated the excellent corrosion resistance properties of this coating system, revealed that the use of sealer further improves the coating performance.

 Copyright © MAINLINE Consortium

In UK, duplex coating systems (i.e. metallic-organic) are recommended for new steelwork irrespectively of the structure's exposure conditions (NR/GN/CIV/002). The use of hybrid metallic-metallic coatings is generally recommended for marine environments. In general, the main drawback of duplex and hybrid coating systems is their relatively higher initial cost. However, the anticipated reduced need for both maintenance/repair and the minimized service disruption of the structure can offset the initial additional costs.

8.3.2 Resistance mechanisms

Organic, metallic and duplex (hybrid) coatings protect the substrate metal through several resistance mechanisms which interfere with the anodic and cathodic reactions in the cell and the transport of species (e.g. ions) to the substrate surface. In general, the resistance mechanisms of the different protective systems can be used to classify coating in the following groups (e.g. Greenfield and Scantlebury 2000, Hare 2006, de Wit et al. 2011):

- Barrier coatings
- Inhibitive coatings
- Sacrificial coatings

Organic coatings

Organic coating systems, depending on their composition can be classified within any of the three coating types. Irrespectively of the protective mechanism that an organic coating provides to the metal, the maintenance of good adhesion with the substrate is a prerequisite for successful corrosion protection.

Barrier coatings

It is generally accepted that even very dense coatings cannot halt the water/moisture diffusion through their bulk (de Wit et al. 2011). The use of impermeable coatings can restrain the diffusion of oxygen needed for the reactions at the cathode. The principal resistance mechanism of barrier coatings, however, relies on the suppression of ions diffusion through the coating to the substrate surface (e.g. Hare 2006, Sorensen et al. 2009, de Wit et al. 2011). This causes an increase in the electrical resistance of the water near the substrate (i.e. current flow between the anode and the cathode is halted), see Fig.8.13.

 Copyright © MAINLINE Consortium

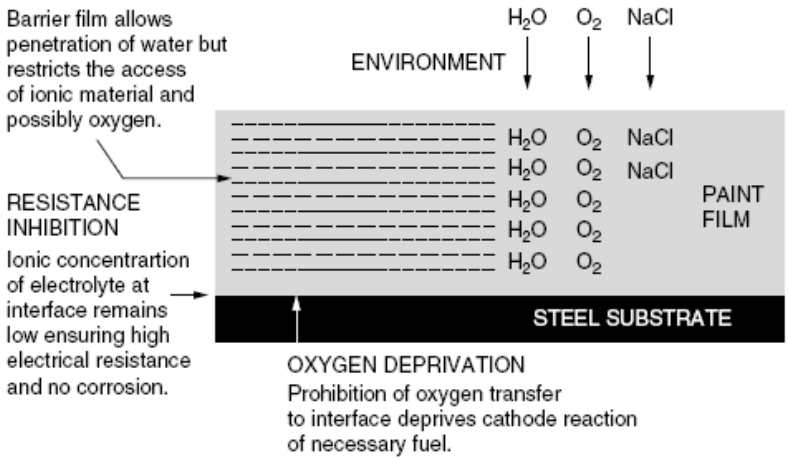

Figure 8-13 Protection mechanism of barrier coatings (adapted from Hare 2006).

The effectiveness of a barrier coating is determined by its thickness and the composition of its binder (Sorensen et al. 2009). To increase the electrical resistance and improved adhesion in immersed conditions the composition of barrier coatings includes non-hydrophilic constituents and lamella pigments (Hare 2006). Furthermore, increasing the thickness of barrier coatings reduces the delamination of both intact and defective coatings. Barrier coating can be used in conjunction with cathodic protection.

Inhibitive coatings

The principal resistance mechanism of inhibitive coating systems relies on its ability to promote the formation of an insoluble passive film on the metal substrate. For this reason they mainly applied as the primer layer of a coating system since the formation of the passive film requires that its constituents reach the substrate (Sorensen et al. 2009). The primer layer is enriched with pigments which release oxidizing ions and other passivating agents when dissolved in aqueous environment near the substrate, see Fig.8.14.

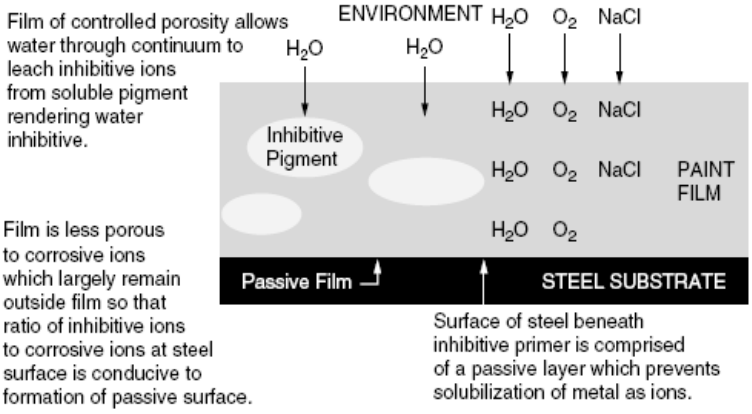

Figure 8-14 Protection mechanism of inhibitive coatings (adapted from Hare 2006).

Careful selection of the binder and the inhibitive pigment is required to avoid the rapid exhaust of the inhibitive ions provided by the pigment and reduce blistering (Hare 2006). Coating permeability has an important role in ensuring that moisture required for the dissolution of the inhibitive pigment; however, too permeable coatings may enable the easier

transport of aggressive agents (e.g. cl, sulphates) to the metal surface. The compositions of inhibitive coatings often include among others oils, alkyds, epoxy esters, epoxies and latex primers (Hare 2006). Inhibitive coatings are often used in environments with high atmospheric corrosiveness (e.g. industrial environments).

Sacrificial coatings

Sacrificial coatings protect the substrate metal through the mechanism of galvanic corrosion. The metal (powder) in the coating becomes the anode while the substrate metal becomes the cathode. A requirement for protecting metals through sacrificial coatings is that the metal particles in the coating are in contact with the substrate metal. Hence, this coating type is applied solely as the primer layer of a coating system (Sorensen et al. 2009). Commonly used sacrificial coatings systems incorporate a highly pigmented zinc-rich primer, with pigment volume concentrations (PVC) close to the critical PVC (Hare 2006, Sorensen et al. 2009). The formation of zinc corrosion products provides further protection to the substrate metal through the additional barrier action against the ingress of aggressive species. Figure 8.15 schematically depicts the protective mechanism of sacrificial coatings.

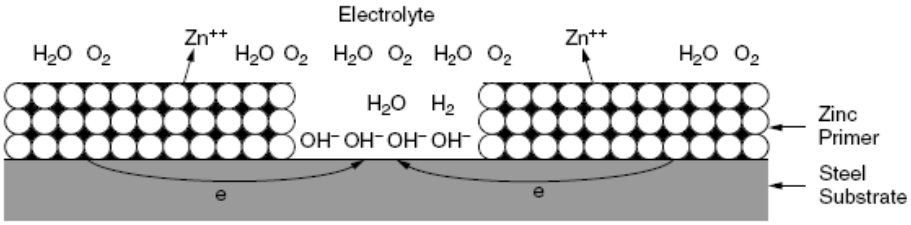

Figure 8-15 Protection mechanism of sacrificial coatings (adapted from Hare 2006).

In neutral environments, zinc-rich coatings are often used without the use of a topcoat. In contrary, in corrosive environments (e.g. highly acidic or alkaline), increase corrosion protection can be obtained by the over-coating of organic zinc-rich primers with barrier topcoats.

Metallic coatings

Metallic coatings protect the substrate metal through sacrificial cathodic protection together with barrier action. The metallic coating, typically zinc in hot-dip galvanizing or aluminium in thermal sprayed coatings, acts as the anode of an electrochemical cell. It follows that the substrate metal becomes the cathode. Hence, through this mechanism, the metallic coating sacrificially corrodes protecting the substrate. The formation of zinc or aluminium corrosion products provides additional barrier protection against corrosive species reaching the substrate. Several studies have demonstrated the excellent long-term corrosion protection properties of metallic coatings (e.g. see Kuroda et al. 2003 and 2006). In turn, the reduced maintenance requirements and the potential environmental benefits of using metallic coatings can offset the potentially higher initial cost associated their use.

 Copyright © MAINLINE Consortium

8.4 Coating deterioration

8.4.1 Influencing factors

Deterioration of in-service coatings is affected by several factors associated with the following stages:

- Coating specification (for anticipated exposure conditions)
- Application period (surface preparation, application, curing)
- Environmental exposure (after application, includes accidental damage)

Hence, the deterioration of coating systems is a complex phenomenon due to the large number of variables involved. The presence of defects within a coating system (e.g. caused by defective material or post-application accidental damage) generally accelerates the deterioration process which eventually leads to the occurrence of a failure mode (i.e. substrate steel is no longer protected). The most common failure mode is the loss adhesion, for instance due to blistering or cathodic delamination, between the coating and the substrate metal. Other failure criteria of coatings which did not fail prematurely (e.g. premature adhesion loss) may include the time needed for the consumption of the active ingredients of inhibitive and sacrificial coatings (i.e. inhibitive pigment, consumption of zinc dust, etc.).

The potential defects and failure modes associated with protective coatings are discussed in section 8.4.2.

8.4.2 Defects and failure mechanisms of protective systems

The prime function of a coating system is to protect the substrate metal from corrosion and in some cases to provide the require appearance to the structure. Often, the aesthetical appearance of a coated metal surface can be compromised by extensive defects or deterioration of its protective coating. This report focuses on the deterioration of coatings in relation to their protective capabilities against corrosion. More specifically, the end of service life of the coating is denoted as the time from its application up to the moment that the substrate metal is no longer protected against corrosion. It should be noted that although compromised appearance and loss of corrosion protection are generally coupled processes, there are cases that a coating may fail prematurely without any noticeable visual damage (Bayliss and Deacon 2002).

Typically, the service life of a coating system is expressed through an expected time-period. The actual time of failure is highly uncertain due to the variability in surface preparation, coating quality (e.g. quality control during application), the constantly changing exposure conditions (i.e. local microclimate) as well as unexpected factors such as accidental damage. A number of defects and failure modes have been identified for protective coatings, e.g. (Greenfield and Scantlebury 2000, Delplancke et al. 2001, Bayliss and Deacon 2002, Sorensen et al. 2009). The presence of defects in general leads to a reduced service life for the coating (i.e. time required to attain a failure mode is reduced). The starting point of developing these defects can be traced to several sources, for instance substrate contamination due to poor quality surface treatment, inadequate curing of the applied coating

 Copyright © MAINLINE Consortium

and accidental damage. The main defects often observed in organic coating together with a brief description are summarised in Table 8.15.

Table 8-15 Summary of defects and failure modes of protective coatings.

Defect/failure mode	Time of occurrence	Description
Bacterial/fungal attack	After coating application	Coating constituents provide nutritional source for bacteria/fungi. Leads to premature loss of corrosion protection.
Bleeding	During/after coating application	Movement of intermediate coat leads to the staining of the Topcoat.
Blooming	After coating application	Forms on glossy surfaces and mainly affects the aesthetical appearance (loss of gloss and dulling of colour). Caused by increased humidity during curing. Blooming can affect the integrity of the coating system (reduced adhesion between layers) although coating system continues to protect the substrate. It can be treated using a suitable solvent.
Chalking	After coating application	Formation of friable, powdery layer on the coating. Caused by the degradation of the binder, particularly when exposed to UV-attack (e.g. sun rays) and moisture (e.g. dew condensation). The composition of the binder affects the rate of disintegration.
Cissing/crawling/ fisheyeing	During application	Develops due to poor application of the coating. Areas of the substrate fail to be wetted properly by the wet paint. Paint retreats resulting in holes or attenuated films. The source of this defect is often the poor surface cleaning from oils, grease or silicones, prior to the application of the coating or erroneous selection of solvent type.
Cobwebbing	During application	Development of thin strings during the spraying of fast-drying coatings. This defect is attributed to the very fast evaporation of the solvent (e.g. due to high temperature).
Cracking	After coating application	In general, cracking develops due to internal stresses exceeding the coating's tensile strength. Cracking is affected by the application and curing of the coating. Coatings containing solvents are more frequently affected. The following terminology is used to distinguish the different cracking types (adapted from Bayliss and Deacon 2002): *Hair cracking*: Random fine cracks which do not penetrate the topcoat, *Checking*: Fine cracks which do not penetrate the topcoat and they create a pattern, *Cracking*: Cracks that penetrate at least one coat which may lead to complete failure, *Crazing*: Similar to checking type with deeper and wider cracks, *Crocodiling*: Pattern similar to a crocodile's hide; similarities with crazing, *Mud cracking*: pattern appears as dried-out mud. This cracking type affects very thick (inorganic) zinc silicate coatings.
Failure to cure two-part materials	During application	Coatings which dry-out without the addition of the catalyst are generally softer than properly mixed and cured coatings. The mixed coating may have a reduced pot life, not sufficient for its proper application. Curing of two-pack epoxies is compromised at low temperatures (i.e. $<5^{o}$C).
Dry spray	During application	Paint particles fail to produce a uniform coating due to insufficient wetness. Instead, a powdery layer is produced. This defect is observed when fast-drying materials (e.g. two pack epoxies) are sprayed from far distance to the surface of substrate metal. Strong winds can also cause this type of defect.

 Copyright © MAINLINE Consortium

Fading	After coating application	Colour change of the coating following UV-exposure. It is cause by the degradation of coloured pigments or dyes.
Lifting/ pulling up	During application	Softening and expansion of a previously applied coating caused by the application of a new paint with strong solvents. Can be prevented by using compatible solvents and by ensuring that the previously applied layer is sufficiently dry and harden.
Orange peel	During application	Coating appears to have a texture similar to the skin of an orange. This defect is caused by improper spray application (e.g. low air pressure, incorrect distance, etc). In some cases coating reapplication may be required.
Pinholes	During application and drying	Pinholes are caused by trapped air/gas bubbles which burst causing small craters in wet paint film and fail to be cover within the drying period of the coat.
Pinpoint rusting	During/after coating application	Pinpoint rusting appears as isolated spots of rust and they are caused by uncoated high peaks in the metal surface which started to corrode. It is often observed to occur in patterns which indicate its potential dependence of surface-preparation or coating application. In some cases this defect can be treated with additional sanding down and coating application.
Runs and sags	During/after coating application	Downward movement of paint film on a flat surface due to paint collection at surface irregularities such as cracks or holes. The surrounding has set while the excessive coating flows. This defect type affects mainly the appearance of the coating.
Saponification	N.A.	Decomposition of an oil-containing binder by reaction with alkali and water. This defect type is observed on immersed coatings used together with cathodic protection (CP).
Skin curing	During application	The occurrence of this defect results in a softer than expected coating. This defect occurs when the outer coating surface is cured at a faster pace than the remaining bulk of the coating, for instance under direct strong sunlight or forced heating of the top surface. It affects more coatings in which chemical reactions are involved in the curing process. It can affect coatings which cure by oxidation or evaporation. It can be observed in cases that the temperature of the substrate steel is significantly lower than the temperature on the top of the coating.
Spot-blast boundary breakdown	During application / maintenance	Spot-blasting for cleaning during the application of maintenance coating can damage the adjacent old paint causing a reduced adhesion (often the damage is not visible). This increases the vulnerability of the coating to moisture, aggressive species and eventually leads to blistering.
Thickness faults	During/after coating application	This defect is often observed at the edges of steel sections where the actual coating thickness can be up to 60% less than required thickness. Other locations where this defect may occur are including nuts, bolts, weld areas etc.
Uneven gloss	After coating application	Appears in the form of patches on glossy surfaces. This defect develops due to moisture in the film, temperature fluctuations during application, poor sealing of a porous substrate, etc.
Undercutting/ Filiform corrosion	After coating application	Corrosion which develops laterally under the coating. Often this type of failure mechanism initiates at an existing defect or at places where corrosion products were not properly removed before the coating application. The development of this failure mode is affected by the adhesion properties of the coating. Filiform corrosion also occurs under organic coatings; the main difference with undercutting is that it appears as long filaments at the edges of an existing defect.

 Copyright © MAINLINE Consortium

Wrinkling	During application	It occurs during the drying stage of the application. Observed especially in thick oil-based paints. The outer surface of the film cures by atmospheric oxidation, while lower layers cure at a much slower pace.
Delamination	After coating application	Initiates at an existing defect which becomes the anode in an electrochemical cell. For more details see section *Coating delamination*
Blistering	After coating application	Associated with undamaged coatings. Migration of ions through conductive pathways. Blistering usually is associated with the alkaline environment at blister front causing the loss of bond at the coating-substrate interface (cathodic blistering). Rate controlling parameter is the transport of ions to the cathode. For more details see section *Blistering of organic coatings*

The most commonly observed as well as severe failure modes of organic coatings are development of blistering and cathodic delamination. These are discussed in the following sections. Filiform corrosion is also an important failure mode of organic coatings; this, however, is commonly observed in coated aluminium components (Sorensen et al. 2009). For this reason it is not further discussed in this report.

Coating delamination

Cathodic delamination is a commonly observed failure mode of organic coatings with inherent or induced defects. Corrosion initiates at the defect forming corrosion products which potentially block the pores. As a result, the area where the coating is damaged becomes the anode while cathodes develop at the edges of the defect. The alkaline environment (pH > 12 due to hydroxyl ions) at the cathodic areas at the substrate is responsible for the bond loss at the coating-substrate interface. The formation of insoluble corrosion products promotes the separation of anodes and cathodes. The propagation of corrosion depends on the nature of the corrosion products which in turn control the rate of oxygen transport to the anode and cathode. If the rate of oxygen transport through the coating (near the defect edges) is higher than the rate of oxygen transport through the corrosion products, then the deterioration mechanism is by cathodic delamination. In the case that the opposite occurs, the failure mechanism is due to anodic undermining. The rate controlling parameter in this failure mechanism is the diffusion rate of cations required for charge neutralization of the cathodically produced hydroxyl ions. A similar deterioration mechanism for coatings with no apparent defects known as blistering has been identified; this is discussed next.

Blistering of organic coatings

The development of blisters is typically associated with coatings where no defect is visible. The possible mechanisms involved in this type of failure mode are including expansion due to swelling, gas inclusion or osmotic processes (Sorensen et al. 2009). Among these mechanisms, osmotic processes have been shown to be the most significant mechanism in blistering. Blister development has been observed to have the following characteristics (Greenfield and Scantlebury 2000):

- The higher the osmotic pressure of the immersion liquid, the smaller the amount of blistering.

 Copyright © MAINLINE Consortium

- The chlorides concentration in the liquid within blisters developed under seawater immersion conditions is lower than that of the seawater. The liquid within the blister has been found to be alkaline.

- No corrosion is observed under these blisters.

- A relation has been observed between the location of the blisters and the nearby corrosion sites.

Further research revealed that the following three types of blistering exist (Greenfield and Scantlebury 2000):

1. Osmotic blistering

2. Anodic blistering

3. Cathodic blistering

Among the different types of blistering, the most extensively examined is cathodic blistering. This failure mode is caused by the alkaline environment at cathodic areas at the substrate which is responsible for the bond loss at the coating-substrate interface as well as the development of osmotic pressure. Nguyen et al. (1995) proposed a conceptual model for cathodic blistering, as shown in Fig.8.16, for coatings with no visible defects. According to their model, the following sequential steps lead to the formation of cathodic blistering (see numbers in Fig.8.16):

1. Formation of conductive pathways due to low crosslink density or hydrolysis and dissolution caused by water attack at hydrophilic areas. These areas eventually interconnect with each other.

2. The conductive pathways allow the transportation of ions to the substrate surface.

3. Anodes develop on the substrate metal at the base of the conductive pathways.

4. Cathodes develop at the vicinity of the conductive pathways.

5. The presence of defects and pores in coating-metal interface or conductive pathways in the coating allow the migration of (sodium) ions to the cathodic sites which is needed for charge neutralization.

6. The alkalinity of the sodium hydroxides (NaOH) at the cathodic areas causes the loss of bond at the coating-metal interface (i.e. cathodic delamination).

7. Water is transported through the coating to the cathodic areas due to osmotic pressure gradients caused by presence of hydroscopic sodium hydroxides.

8. Development and possible coalesce of blisters. This eventually may lead to complete delamination.

 Copyright © MAINLINE Consortium

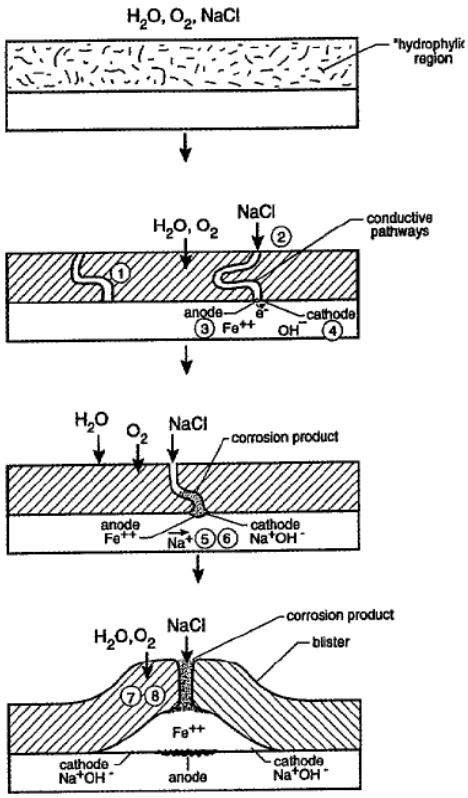

Figure 8-16 Cathodic blistering in coatings with no defects (Nguyen et al. 1995).

It has been observed that the presence of Cl^- has a significant effect on the rate of formation of the first oxide layer (Nguyen et al. 1995). Furthermore, experimental evidence suggests that cathodic blisters are observed only when pores and coating defects are exposed to electrolytes. The high permeability of organic coatings to water and oxygen implies that coating deterioration do not depend on these parameters. It has been shown that the transport of ions through the coating is the main cause of coating deterioration (Nguyen et al. 1995).

8.4.3 Deterioration modelling

Influencing factors

The preceding literature review on the available coating types, resistance mechanisms and failure modes revealed that coating performance is determined by the combined action of several influencing factors. These factors can be associated with the exposure conditions (e.g. levels of atmospheric pollution) as well as the coating itself (e.g. coating type, thickness, quality, etc.). In general, the development of models to predict coating performance requires direct or indirect consideration of the following parameters:

- Coating's chemical and physical characteristics, including its principal resistance mechanism (e.g. barrier, inhibitive or galvanic action).

- The anticipated exposure conditions, including levels of individual climatic and atmospheric variables for a particular location.

Other aspects which may need consideration when developing a model are the quality of both surface preparation and coating curing.

Model types

Performance modelling can be considered at several levels of complexity and accuracy. In this report the simplest form of model to describe the performance of a protective coating system is denoted as Level 1 model. The modelling level increases together with the complexity of the model. It is interesting to note that currently in practice, coating

performance is estimated using Level 1 models (i.e. expected service life provided by the coating manufacturer). In general, the following four modelling levels can be defined:

- In Level 1 models either a single value or a range of values is available for the expected service life of a coating system for a particular environmental exposure (e.g. service life is roughly 10 years for industrial environmental exposure). It should be noted that the exposure conditions are determined by several climatic and atmospheric variables. In Level 1 models no quantitative information is available on the influence individual factors on coating performance.

- In Level 2 models (or advanced Level 1) the basic statistical properties of the coating's service life available (i.e. mean and standard deviation). When the distribution type is also known then these models are denoted as Advanced Level 2 models. Although these models can take into account the performance variability, no functional relationship between the coating performance and the several influencing parameters is established.

- Level 3 models include mathematical functions which define the basic relationship between coating performance and a set of influencing variables (e.g. temperature, humidity, coating thickness, etc.). These phenomenological models are generally known as dose response functions (DRF). Advanced Level 3 models include DRFs where the statistical properties of the influencing (input) factors are known. It follows that the statistical properties of the coating performance can be obtained using, for instance, simulation techniques (e.g. Monte Carlo simulation).

- Level 4 include analytical/theoretical and simulation-based (e.g. CFD) models. These models describe mathematically the fundamental mechanisms involved in the actual deterioration process. Hence, these are very useful when the interpretation of experimental data is required. Their application, however, in practice is generally limited due to the type of input data required (in many cases such data can be measured only in carefully prepared lab specimens).

Development of time-profiles

In general, the development of time-profiles in both Level 1 and Level 2 models requires data on coating performance gathered by regular inspection at certain time-intervals (e.g. every year or every a few years inspection). This in turn would allow capturing the performance profile of the coating. In Levels 3 and 4 models, the rate of deterioration is determined by the levels of the input values. For instance, the annual relative humidity or the annual deposition rate of chloride on the coated surface is both important deterioration rate-controlling variables. Hence, the development of time-profiles using Level 3 and Level 4 models requires monitoring of such variables for the particular location of a structure. An equally important aspect in modelling coating performance is the spatial characteristics of the deterioration (i.e. spread of damage on a coated surface). The various (idealised) processes involved in coating deterioration are schematically depicted in Figure 8.17.

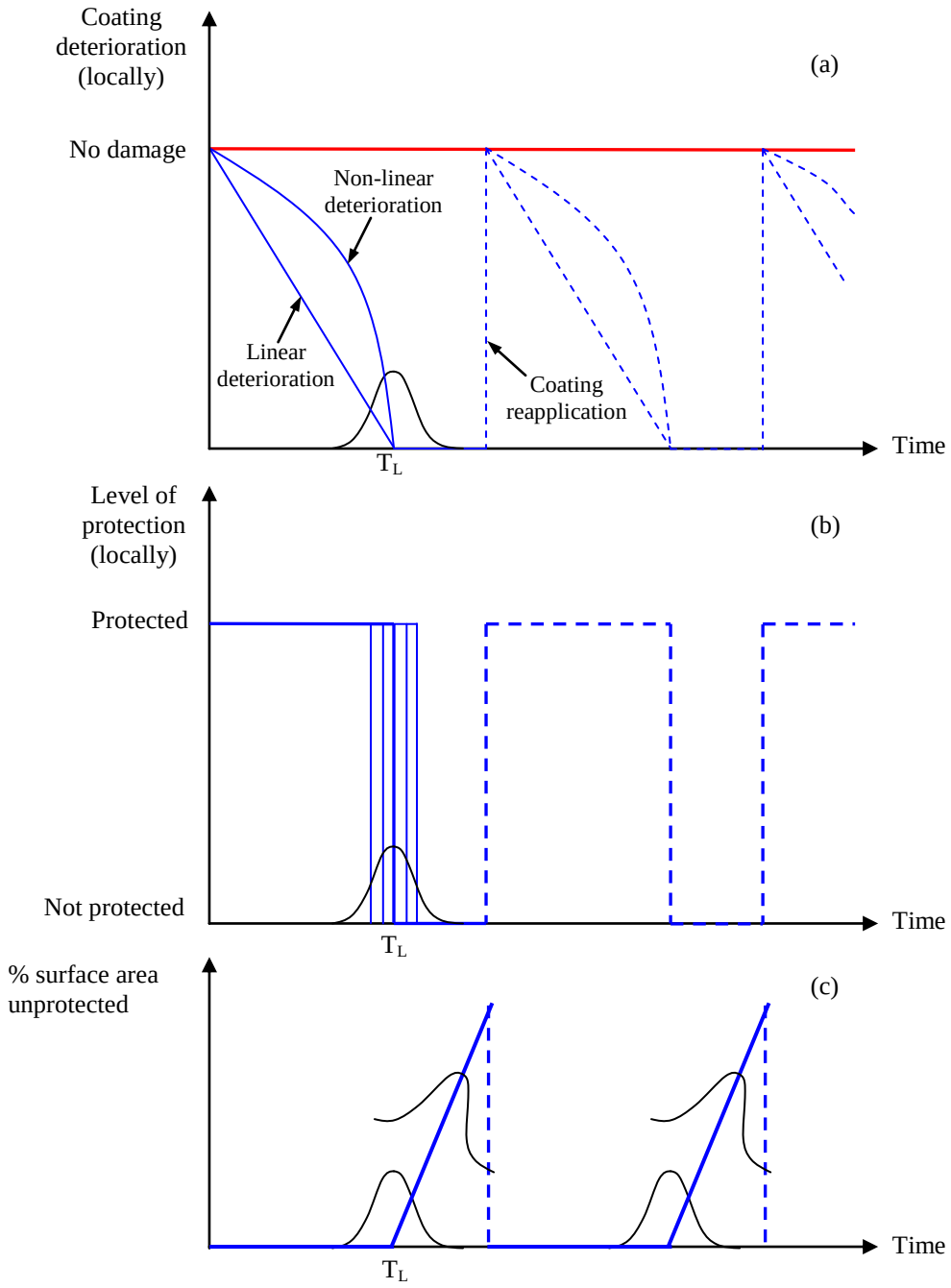

Figure 8-17(a) Coating performance at material level, (b) Time when substrate metal is not-longer protected and (c) evolution of % unprotected area with time.

Organic coatings

As previously discussed, organic coatings usually protect the substrate metal through one of the three distinctive mechanisms (barrier, inhibitive or galvanic coatings). This implies that the coating has failed when the protective mechanism is no longer active. For example in inhibitive coatings, failure could be denoted as the time when the concentration of active pigment ingredients has been consumed to a value which is below a minimum threshold value. Similarly, in zinc-rich coatings, the sacrificial consumption of zinc will eventually lead

 Copyright © MAINLINE Consortium

to inadequate protection against corrosion. Although, in both cases, coating failure is due to the exhaustion of the coating's vital ingredients, premature failure may occur due to blistering/delamination. In general, the performance of a coating system can be assessed at material (local) level. However, the spatial characteristics of coating deterioration are of paramount importance in bridge assessment. Hence, ideally a model should capture both local coating performance and extent of damage on a coated surface. In some cases the inability to predict the location of coating deterioration increases the complexity of the modelling process. For instance, at present it is not possible to predict with any certainty the location of blister formation in intact organic coatings (Sorensen et al. 2009).

Level 2 models could be developed using the available inspection data on the performance of organic coatings. Whether, the development of such model will fall within the Level 2 or Advanced Level 2 group of models depends on the amount and quality of the inspection data. For instance, ideally the availability of inspection records from several bridges exposed to similar exposure conditions and protected by the same type of coating would allow the development of an Advanced Level 2 model. In practice, however, this might not be possible. Furthermore, the statistical properties of coating performance (e.g. area over which protection is lost) would need to be adjusted for different classes of exposure conditions (i.e. rural, urban, industrial-marine) and workmanship quality (e.g. poor, good excellent) during the coating application, including surface preparation and curing.

The development of Level 3 models (i.e. DRF) could be attractive when the assessment of specific exposure variables on coating performance is required. However, the generalization of a Level 3 model it would not be recommended to dissimilar coatings (e.g. different compositions and thicknesses, etc.) than the coating used for its derivation. The development of such a model requires the systematic monitoring of several parameters (e.g. climatic and atmospheric parameters) as well as coating performance; it is unlikely that such data is currently available.

A Level 4 model is required to describe adequately the main mechanisms and processes of coating deterioration during exposure. The mathematical models, in this case have a physical meaning (as opposed to phenomenological models). Pommersheim, Nguyen and Hubbart (Pommersheim et al. 1994, Nguyen et al. 1995) developed analytical models for the blistering processes in organic coatings. Their models are very useful in improving the understating of the fundamental mechanisms involved in the blistering/delamination process of organic coatings at a local level. The spatial characteristics of this deterioration type over a coated surface are not examined by their model. Furthermore, in practice an organic coating may fail due to other failure mechanisms such as the consumption of the coating's active corrosion inhibitive ingredients (e.g. sacrificial consumption of zinc powder).

The preceding discussion indicates that Level 2 or Advance Level 2 models seem to be the most likely candidate models for estimating the performance of organic coatings. This is due to the difficulty in obtaining realistic value ranges for the variables associated with the development and input of Level 3 (or above) models. Another limitation, which hinders at present the use of Level 3 and Level 4 models in practice, is the impossibility to predict a priory the failure mode of a particular coating, since this is a function of a large number of variables and their interactions.

 Copyright © MAINLINE Consortium

(a)

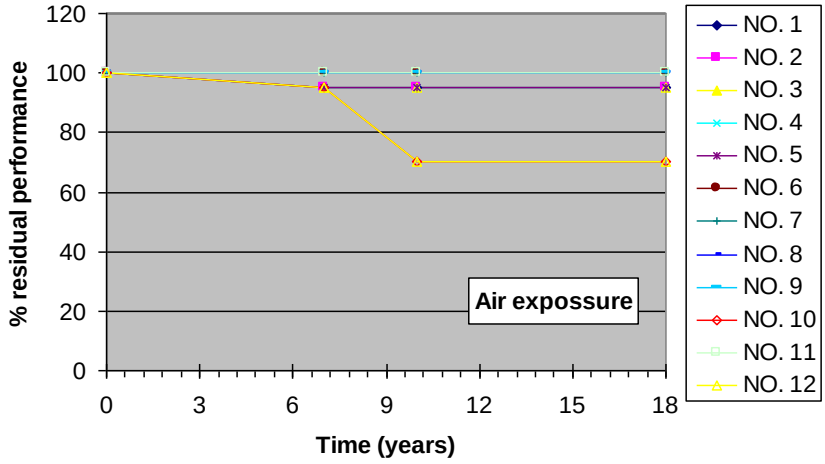

(b)

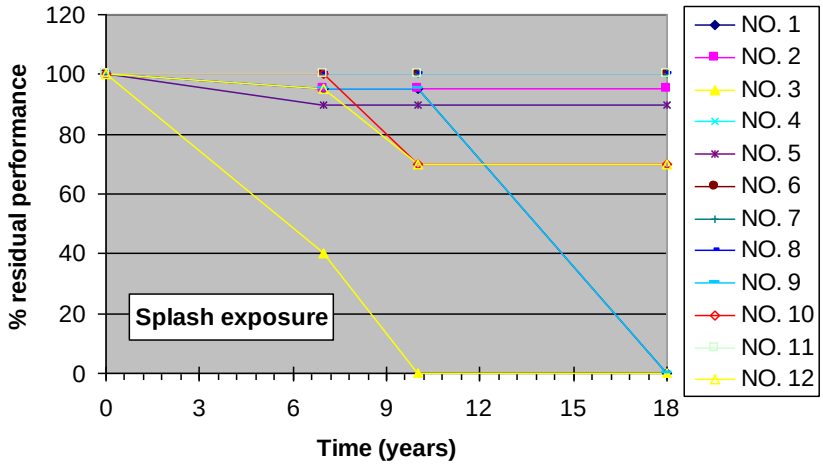

(c)

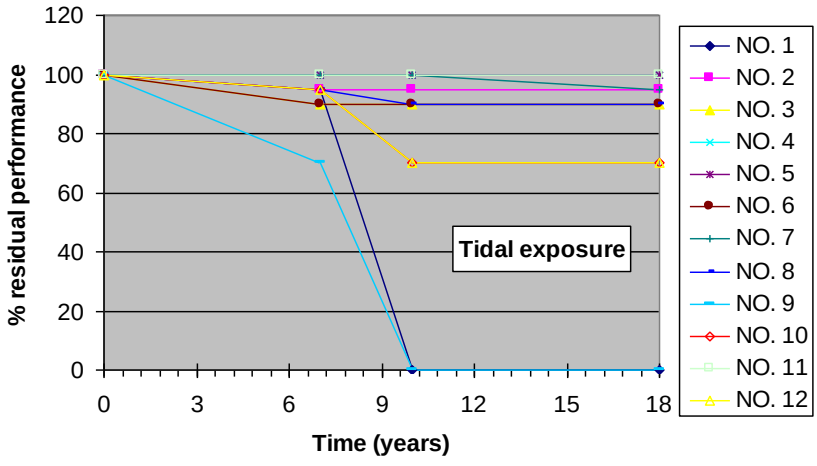

Figure 8-18 Performance evolution of thermally sprayed metallic coatings after 18 years of exposure for different exposure conditions: (a) sea-air, (b) splash zone and (c) tidal zone. [data from (Kuroda et al. 2006) assuming A=100%, B=90%, C=70%, D=40% and E=0%].

 Copyright © MAINLINE Consortium

Metallic coatings

A similar situation is observed for metallic coatings, where currently Level 1 models are generally used. Figure 8.18 shows an example of (Level 1) time-profiles for several metallic and hybrid coatings after 18 years of continuous exposure with inspections carried at 7, 10 and 18 years, for details on the composition of the different metallic coatings see (Kuroda et al. 2006). Three classes of exposure were examined; atmospheric, splash zone and tidal zone for all the 12 coatings examined.

Level 2 models and time profiles could be developed using the available inspection data from bridges with similar coatings and exposure conditions. Similarly to organic coatings, the amount and quality of the available data are significant for model development.

As previously discussed, metallic coatings protect the substrate by means of sacrificial corrosion. In the case of metal corrosion the fundamental relationships between the factors which determine the exposure conditions (e.g. temperature, relative humidity, atmospheric pollution, etc.) and the deterioration process of aluminium or zinc are generally available (Feliu et al. 1993a, b, BS EN ISO 2012a, b). This implies that potentially the performance of metallic coatings could be modelled using Level 3 models (i.e. dose response functions, DRF), provided that no other failure mode denotes the end of service life (e.g. loss of adhesion). The DRFs of (BS EN ISO 2012a, b) have been developed using results from exposure tests on aluminium and zinc coupons. Hence, it remains to examine whether the available dose response functions for aluminium and zinc can be directly used as Level 3 models for estimating the long-term performance of the corresponding metallic coatings.

8.5 Intervention strategies

The main causes of deterioration in metallic bridges are corrosion, fatigue/cracking and permanent deflections/distortions caused by extreme or accidental loading (e.g. impact). The selection of a suitable intervention strategy largely depends on the characteristics of a particular bridge with consideration to be given to the following (ICE 2008, NR 2009a, b and c):

- Material type (e.g. cast/wrought iron, steel)
- Type and severity of damage (e.g. corrosion, fatigue, etc.)
- Anticipated exposure conditions
- Construction form (cast, welded, bolted or riveted) and degree of redundancy
- Costs related with closure and traffic diversion
- Services passing through the structure

 Copyright © MAINLINE Consortium

Table 8-16 Repair/maintenance methods for metallic bridges

Type of action	Comments	Indicative references
Increase/restore protection system against corrosion (coating application)	This may involve patch repairs or in cases of extensive coating deterioration complete coating replacement. In some cases alternative corrosion protection systems (e.g. bridge enclosure) might be used. For indicative costs of protective coating systems see Table 8-14 but note that these apply to initial rather than repeat coatings.	NR (2009a, b and c), BD (1996)
Strengthening/repair using conventional materials	Addition of steel plates by welding or rivets, replacement of missing parts (e.g. rivets).	Reid et al. (2001) Agocs et al. (2005)
Strengthening using novel materials, e.g. fibre reinforced polymers (FRP) systems	FRP plates are externally bonded to the (treated) metal surface using epoxy resin. The FRP plates can contain carbon, glass or aramid fibres. The fibres can have a uniaxial, biaxial or multi-axial orientation.	Cadei et al. (2004)
Repair/management of fatigue damage	Increase of steel area to reduce stress ranges (e.g. using doublers or splices), grinding, alteration of weld geometry, elimination of discontinuities, etc.	FHWA (2013)

Notes: In most cases, surface preparation is required prior to the application of the aforementioned repair/ maintenance methods. More details on the specific requirements for each method can be found in the references provided.

Several approaches have been presented in literature for the optimization of intervention strategies bearing in mind the safety of the structure (Das 1997, Yanev 2007). This section focuses on the repair/maintenance methods, summarised in Table 8.16, which can be part of an intervention strategy, for metallic bridges affected by corrosion and/or fatigue damage.

The use of the methods summarised in Table 8.16 is twofold; (a) they can be used to restore the structure's condition to its original level (or even exceed it) and (b) provide a means of mitigating the corrosion process (halt/decelerate material loss) or the damage accumulation (e.g. due to fatigue).

8.6 Summary

This report provides a review on the corrosion modelling of metallic structures exposed to environments of varying atmospheric corrosivity. Initially the basic mechanisms involved in the corrosion process are reviewed. The factors with the highest influence on atmospheric corrosion and the exposure classification are discussed with reference to the provisions of current international standards and published experimental results. A framework for the classification of corrosion models is presented, with emphasis given to the use of dose response functions (DRF) for predicting time-dependant corrosion losses as a function of

several atmospheric pollutants and climatic factors. Commonly used protective coating systems for steel structures are reviewed. Initially the composition and main resistance mechanisms associated with the different types of organic and metallic coatings are discussed. A summary is provided on the defects and failure mechanisms commonly observed in organic and metallic coatings and a framework for the deterioration modelling of protective coatings is provided.

- The main conclusions of this report may be summarised as follows:

- Three levels of modelling have been identified for the long-term modelling atmospheric corrosion damage.

- Dose response functions (Level 2 models) appear to be the most suitable. DRF models – which explicitly relate several exposure variables to observed thickness losses due to corrosion – can be used either deterministically or be part of a probabilistic framework.

- Sacrificial organic and metallic coatings are amongst the most commonly used corrosion protection systems on steel structures.

- A number of failure mechanisms are associated with the different coating types; this depends, however, on coating type and exposure conditions. The pre-existing defects also have an adverse effect on coating service life.

- A very limited number of models are available for the modelling of coating performance. However, a number of experimental techniques are available (e.g. electrochemical impedance spectroscopy), which could be used to quantify the evolution of coating performance under varying exposure conditions (e.g. see Bos 2008, Sekine et al. 2002).

- The development of time-profiles on coating performance requires consideration of both the deterioration at a local (material) level as well as the evolution of the time-dependent spread of damage.

- The high uncertainty associated with the performance of coating systems subject to varying exposure conditions could be taken into account using probabilistic-based modelling.

8.7 References

Agocs, Z., Ziolko, J., Vican, J., Brodniansky, J. (2005), “Assessment and refurbishment of steel structures”, Spon Press, ISBN 0-415-23598-7 (UK).

Almeida, M.E.M. (2005), “Minimisation of steel atmospheric corrosion: updated structure of intervention”, Progress in Organic Coatings 54:81-90.

BD. (1996), “BD 67/96, Part 7: Enclosure of Bridges”, Design Manual for Roads and Bridges Volume 2: Highway Structures: Design (Substructures and special structures), Materials, Section 2: Special Structures, The Highways Agency, UK.

Bos, W.M. (2008), “Prediction of coating durability – Early detection using electrochemical methods”, PhD Thesis, Delft University of Technology, The Netherlands.

BS EN ISO. (1998). “BS EN ISO 12944-2. Paints and varnishes – corrosion protection of steel structures by protective paint systems – part 2: Classification of environments”, BSI

BS EN ISO. (2012a). “BS EN ISO 9223:2012. Corrosion of metals and alloys – Corrosivity of atmospheres – Guiding values for the Corrosivity categories”, BSI.

BS EN ISO. (2012b). “BS EN ISO 9224:2012. Corrosion of metals and alloys – Corrosivity of atmospheres – Classification, determination and estimation”, BSI.

BS EN ISO. (2012c). “BS EN ISO 9226:2012. Corrosion of metals and alloys – corrosivity of atmospheres – determination of corrosion rate of standard specimens for the evaluation of corrosivity”, BSI.

BS EN. (2005). “BS EN 1993-1-1:2005. Eurocode 3. Design of steel structures – Part 1-1: General rules and rules for buildings”, BSI

Cadei, J.M.C., Stratford, T.J., Hollaway, L.C., Duckett, W.G. (2004), “C595: Strengthening metallic structures using externally bonded fibre-reinforced polymers”, CIRIA report, London, ISBN 0-86017-565-2.

CORUS.(2004), “The prevention of corrosion on structural steelwork”, Corus Construction & Industrial, UK.

CORUS.(2005), “Corrosion protection of steel bridges”, Corus Construction & Industrial, UK.

Das, P.C. (Ed.). (1997), “Safety of bridges”, Thomas Telford Publishing, ISBN 0727725912.

de Wit, J.H.W., van der Weijde, D.H., Ferrari, G. (2011), “Organic coatings”, in Corrosion Mechanisms in Theory and Practice, 3rd Edition, Marcus P. (Ed), CRC Press, pp.863-905.

Delplancke, J.L., Berger, S., Lefebvre, X., Maetens, D., Pourbaix, A., Heymans, N. (2001), “Filiform corrosion: interactions between electrochemistry and mechanical properties of the paints”, Progress in Organic Coatings 43:64-74.

Evans, U.R. (1981), “An introduction to metallic corrosion”, 3rd Edition, Edward Arnold (Publishers) Limited, ISBN 0-7131-2758-9.

Feliu, S., Morcillo, M., Feliu, S. Jr. (1993a). “The prediction of atmospheric corrosion from meteorological and pollution parameters – I. Annual corrosion”, Corrosion Science 34(3), 403-14.

Feliu, S., Morcillo, M., Feliu, S. Jr. (1993b). “The prediction of atmospheric corrosion from meteorological and pollution parameters – II.Long-term forecasts”, Corrosion Science 34(3), 415-22.

FHWA.(2013), “Manual for the repair and retrofit of fatigue cracks in steel bridges”, FHWA Publication No.FHWA-IF-13-020, US Department of Transportation, Federal Highway Administration.

 Copyright © MAINLINE Consortium

Gascoyne, A., Bottomley, D. (1995), “Atmospheric corrosion rates of railway bridge structures”, Report No.LR-MSU-084, Issued by Scientifics for the British Rail Research, British Railways Board.

Greenfield, D., Scantlebury, D. “The protective action of organic coatings on steel: a review”, The Journal of Corrosion Science and Engineering, Vol. 3, Paper 5, 2000.

Haagenrud, S.E., Henriksen, J.F. (1996). “Degradation of built environment–review of cost assessment model and dose-response functions”, Durability of Building Materials and Components 7(1), Sjostrom (Ed.).

Hare, CH. (2006). “Corrosion and its control by coatings”, in Coatings Technology Handbook, Taylor & Francis Group, 102, 1-9.

Hutchins, J.S., McKenzie, M. (1973), “Characterisation of bridge locations by corrosion and environmental measurements – first year results”, Rept No.LR550, Transport and Road Research Laboratory, UK.

ICE. (2008), “ICE Manual of Bridge Engineering”, 2nd edition, Parke, G. &Hewson, N. (editors), Thomas Telford, ISBN 9780727734525.

Keijman, J.M. “Inorganic and organic coatings – the difference”, in PCE’ 99 Conference: Achieving quality in coatings work: the 21st Century challenge, Brighton, England.

Kim, I.T., Itoh, Y. (2005), “An acceleration-cyclic corrosion test of coating systems for steel bridges”, in 4th International Conference on Advances in Steel Structures, Vol. 2, Shanghai, China.

Klinesmith, D.E., McCuen, R.H., Albrecht, P. (2007). “Effect of environmental conditions on corrosion rates”, Journal of Materials in Civil Engineering, 19(2), 121-29.

Kuroda, S., Kawakita, J., Takemoto, M. (2006), “An 18-year exposure test of thermal-sprayed Zn, Al, and Zn-Al coatings in marine environments”, Corrosion 62(7):635-47

Landolfo, R., Cascini, L., Portioli, F. (2010). “Modeling of metal structure corrosion damage: a state of the art report”, Sustainability, 2, 2163-75; doi:10.3390/su2072163.

Melchers, R.E. (2003). “Probabilistic models for corrosion in structural reliability assessment – part 1: empirical models”, Journal of Offshore Mechanics and Arctic Engineering, 125, 264-71.

Melchers, R.E., Jeffrey, R.J. (2008). “Probabilistic models for steel corrosion loss and pitting of marine infrastructure”, Reliability Engineering and System Safety, 93, 423-32.

Nguyen, T., Hubbard, J.B., Pommersheim, J.M. “Unified model for the degradation of organic coatings on steel in a neutral electrolyte”, Journal of Coatings Technology, 1996;68(no.855):45-56.

NR. (2009a), “NR/GN/CIV/002: The use of protective coatings and sealants”, Guidance Note, Network Rail, London.

 Copyright © MAINLINE Consortium

NR. (2009b), “NR/L3/CIV/039: Level 3 – Specification for the assessment and certification of protective coatings and sealants”, Network Rail, London.

NR. (2009c), “NR/L3/CIV/040: Level 3 – Specification for the use of protective coating systems”, Network Rail, London.

Perez, C., Collazo, A., Izquierdo, M., Merino, P., Novoa, X.R. (1999).“Characterisation of the barrier properties of different paint systems. Part I. Experimental set-up and ideal Fickian diffusion”, Progress in Organic Coatings 36:102-108.

Pommersheim, J.M., Nguyen, T., Zhang, Z., Hubbard, J.B. (1994).“Degradation of organic coatings on steel: mathematical models and predictions”, Progress in Organic Coatings 25:23-41.

Radomski, W. (2002), “Bridge rehabilitation”, Imperial College Press.

Reid, I.L.K., Milne, D.M., Craig, R.E. (2001), “Steel bridge strengthening – a study of assessment and strengthening experience and identification of solutions”, Thomas Telford, ISBN 0727728814.

Roberge, P.R., Klassen, R.D., Haberecht, P.W. (2002). “Atmospheric corrosivity modelling – a review”, Materials and Design, 23:321-30.

Salas, O., de Tincon, O.T., Rojas, D., Tosaya, A., Romero, N., Sanchez, M., Campos, W. (2012), “Six-year evaluation of thermal-sprayed coating of Zn/Al in tropical marine environments”, International Journal of Corrosion, Volume 2012, Article ID 318279.

Sangaj, N.S., Malshe, V.C. (2004), “Permeability of polymers in protective organic coatings”, Progress in Organic Coatings 50:28-39.

Sekine, I., Yuasa, M., Hirose, N., Tanaki, T. (2002), “Degradation evaluation of corrosion protective coatings by electrochemical, physicochemical and physical measurements”, Progress in Organic Coatings 45:1-13.

Sharifi, Y., Paik, J.K. (2011). “Ultimate strength reliability analysis of corroded steel-box girder bridges”, Thin-Walled Structures, 49:157-66.

Sorensen, P.A., Kiil, S., Dam-Johansen, K., Weinell, C.E. (2009), “Anticorrosive coatings: a review”, J. Coat. Technol. 6(2):135-76.

Tamakoshi, T., Yoshida, Y., Sakai, Y., Fukunaga, S. (2006). “Analysis of damage occurring in steel plate girder bridges on national roads in Japan”, 22nd US-JAPAN Bridge Engineering Workshop, Seattle, WA.

Tidblad, J., Mikhailov, A.A., Kucera, V. (2000). “Model for the prediction of the time of wetness from average annual data on relative air humidity and air temperature”, Protection of Metals, Vol. 36, No. 6, pp. 533-40.

Yanev, B. (2007), “Bridge Management”, John Wiley & Sons, INC., ISBN 0471691623.

8.8 Appendix A

Table 8-17 Surveys of corrosion rates for various exposures in the UK.

Reference	Sample type	Environment	Location	Exposure period (years)	Corrosion rate (μm/year)
Hudson for BISRA (1931, 1934-1936, 1939)	Ingot iron samples exposed vertically	Rural/Suburban	Godalming	1	48
			Llanwrtyd Wells		64
			Teddington		71
		Marine	Brixham		53
			Calshot		79
		Industrial	Motherwell		97
			Woolwich		102
			Sheffield		137
			Frodingham		163
			Derby		173
Hutchings and McKensie (1973)	Hot rolled mild steel and low alloy steel on bridge structures	Industrial	Tinsley	1	79
		Industrial/Marine	Billingham		66
		Light industrial	Loudwater		53
		Urban/Marine	Portishead		46
		Rural	Silverdale		41
Kay (1981)	Mild steel panels	Industrial	Manvers	2	79
		Light industrial	Derby		51
			Wolverhampton		30
Kerr (1987)	Corrosion survey on Tay bridge	Marine/ Estuarine	East facing	2	15
			West facing		15
			Underside		25
MAAF (1986)	Zinc samples divided in 8 categories	Rural (categories 1-3)	N.A.	Data collected during 1969-73	6-15
		Coastal (cat. 3-4)			15-25
		Industrial (cat. 6-8)			36-53
		Industrial/ marine (cat. 6)			36
Coburn (1991)	Carbon steel	Industrial	N.A.	1-2 years	46

Note that data and bibliographical information of the references provided can be found in (Gascoyne and Bottomley 1995)

 Copyright © MAINLINE Consortium

Table 8-18 Surveys of corrosion rates for various exposures internationally.

Reference	Sample type	Environment	Location	Exposure period (years)	Corrosion rate (μm/year)
Sahae et al. (1972)	Variety of steel	Coastal	Japan	1	58
		Urban			56
		Coastal/Industrial			79
		Rural			41
Barton et al.	N.A. (tests performed in Russia)	Heavy industrial	Usti na Labe	5	46
		Coastal	Sarafovo		15
			Batumi		10
		Urban	Orgovan		15
			Zvenigorod		15
King (1988)	Test panels for four metals exposed to a 2km grid.	Severe marine (<0.5km from the sea)	Coastal area of Melbourne, Australia	2	30
		Mild industrial			15
		Rural (typically 10km from the sea)			15
Callaghan (1983)	Various metals including mild steel tested in South Africa)	Rural	Pretoria	10	5
		Industrial	Sasol		15
		Severe Marine	Durban		38
			Walvis Bay		84
			Bluff		218
Coburn (1991)	Corrosion rates on carbon steel determined by weight loss	Marine	North America	1-2	295-1067
		Industrial			30-84
		Urban			20-23
		Rural			23-28
Clarke and Longhurst (1961)	Steel panels	Coast	Nigeria	N.A.	119
		Town			42

Note that data and bibliographical information of the references provided can be found in (Gascoyne and Bottomley 1995)

 Copyright © MAINLINE Consortium

9. Tunnels (Surrey/SETRA)

9.1 Introduction

Tunnels are important infrastructure assets which provide access to otherwise inaccessible locations, such as mountainous areas or underground, assisting the economic development of a country. Well-designed tunnels have a number of environmental benefits such as protection of the natural environment (i.e. flora and fauna), energy/fuel economy due to shortened trips and decongestion of busy areas (Ireland et al. 2007). There are several types of tunnels including unreinforced and reinforced concrete (pre-cast segmental, cast in-situ, sprayed concrete), masonry (brick, stone block) and metal lined tunnels. Also unlined tunnels exist. The alternative methods of tunnel construction (e.g. cut and cover, etc.) are beyond the scope of this report and are not discussed herein; a comprehensive review can be found in (CIRIA 2009).

Several phenomena are associated with the degradation of a tunnel's performance over time, including geotechnical (incl. seismic loading) related degradation, deterioration of the tunnel lining material, accidental damage (e.g. fire, blast, etc.) and vandalism or terrorism (Inokuma and Inano 1996, Long et al. 2011, Wang 2010, Sandrone and Labiouse 2011, CIRIA 2009). The structural failure of a tunnel can be associated with serious socio-economic consequences including, loss of life, service disruption, need to re-route and loss of revenue from sensitive goods (e.g. food products). Damage and disruption of services which pass through the tunnel may also occur (e.g. water mains, cables, etc.). Furthermore, neighbouring structures may be affected (e.g. damage in structures located within the zone of influence of the tunnel). As a result, the structural assessment of deteriorating tunnels plays an important role in maintaining continuous safety levels (in and out of the tunnel) and prioritizing any necessary remedial works.

The deterioration mechanisms, and their impact on performance, of concrete and masonry tunnels are discussed in this report. Tunnel deterioration may occur due to geotechnical/geological related phenomena or due to material deterioration (e.g. corrosion of reinforced concrete linings) of the tunnel itself. In this report, the types of deterioration observed in different tunnel types are discussed in section 2, with emphasis given to material deterioration in concrete tunnels.

9.2 Deterioration types

The type and extent of deterioration of a tunnel is determined by both the location (surrounding geological conditions, groundwater, etc.) and material type (masonry, concrete). Typical lining defects are schematically depicted in Figure 9.1. The deterioration associated with geotechnical/geological phenomena is discussed in section 9.2.1, while the deterioration associated with the lining material of concrete and masonry tunnels is discussed in section 9.2.2.

 Copyright © MAINLINE Consortium

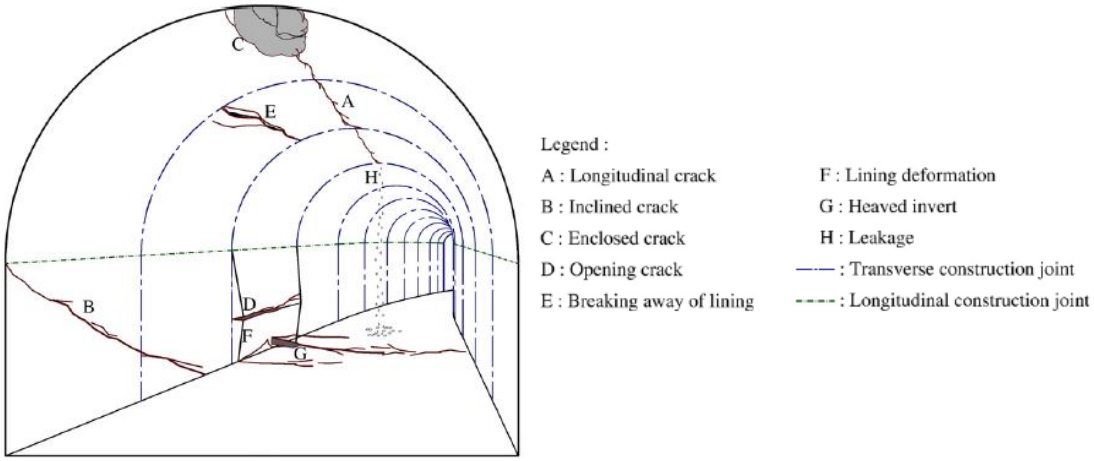

Figure 9-1 Defects observed on linings (adapted from Wang 2010).

Table 9.1 summarises the main cause of tunnel deterioration reported by tunnel inspectors internationally. This table is concerned with road tunnels (no such data was found exclusively for railway tunnels). Consequently, some differences can be expected between the observed deterioration of road and railway tunnels in relation to the operational conditions.

Table 9-1 Main causes affecting tunnel deterioration in different countries (Sandrone and Labiouse 2011).

		Country						
		Switzerland	France	Italy	UK	USA	Japan	South Africa
Construction and geotechnical conditions	Age	×	×			×	×	
	Material quality	×	×				×	
	Construction faults			×				×
	Geological conditions	×	×	×	×	×	×	
	Hydrogeological conditions	×	×	×	×	×		×
Environment	Temperature	×		×	×	×	×	
	Humidity	×		×	×	×	×	×
	Frost, ice formation, freeze and thaw cycles	×	×	×	×	×	×	×
	Biological attack (mushrooms, micro-organisms)	×	×					×
Operation	Traffic	×		×	×	×		×
	Pollution (corrosive atmosphere, ventilation system)	×	×	×		×		×
	De-icing salts	×		×	×	×		
	Fires					×		
	Accidents							

 Copyright © MAINLINE Consortium

9.2.1 Geotechnical related deterioration

Groundwater

Groundwater can affect both the effective properties of the surrounding ground as well as the durability of the tunnel itself (e.g. ingress of aggressive groundwater through a concrete lining can lead to sulfate attack). For instance, groundwater can be responsible for the loss of shear strength on rock joins and bedding planes (CIRIA 2009). This can cause the transfer of load on the tunnel lining. The potential effects of groundwater which may influence the performance of a tunnel may be summarised as follows (CIRIA 2009):

- Settlement of sidewall footing due to ground softening.
- Additional loading due to swelling of clays and marls.
- Attack by aggressive groundwater. Water penetrating through cracks can lead to sulfate attack and corrosion.
- In masonry-lined tunnels, the chemical action (e.g. sulfate attack) or water ingress can cause the wash out of inter-ring mortar causing ring separation (see Fig. 9.4).
- Loss of shear strength on rock joints and bedding planes.
- Development of voids by the dissolution of limestone/outwash of fines. This leads to loss of lining confinement.
- Reduced resistance against inward movement of side walls

Ground and rock movements

Movements of the ground adjacent to the tunnel lining (e.g. due to instability of neighbouring slopes) can cause pressure built-up which may lead to lining distortion (Wang 2010). Several factors are responsible for ground movements; these, however, are largely depending on the type of soil or rock. For instance, rock movements may take place along faults, shear zones and joints (CIRIA 2009). Water flow may cause erosion and undermining of the lining. The loading exerted by a porous soil onto the lining may change as a result of changes its water saturation. For instance, clays may expand when exposed to air and water which can lead to an increased pressure and distortion of the lining (CIRIA 2009).

These phenomena in conjunction with poor workmanship, such as inadequate packing of the lining, can affect the load distribution exerted by the ground onto the lining. In some cases, this can lead to concentrated pressure applied onto the tunnel lining (as opposed to a desirable uniform distribution of pressure).

The above discussion indicates that the ground conditions, including its mechanical properties, may change with time causing changes in the loading applied on the tunnel. Changes in the stress distribution (within the lining) may cause crushing, cracking, heaving, bulging and shearing of the tunnel lining (CIRIA 2009). For instance, differential loading or settlement of the tunnel can lead to the development of shear cracking, while increased lateral pressure may cause the formation of cracks on the side walls of the tunnel.

The lining failure mode can be established by the patterns and texture of the observed cracking/fractures. Three types of lining fractures are identified; these are longitudinal,

 Copyright © MAINLINE Consortium

circumferential and diagonal cracking (see also Fig.9.1).Among them, longitudinal cracking – caused by changes in loading and foundation capacity or ring separation – is the most serious type and it is associated with progressive lining failure which can result in partial or total collapse. Figure 9.2 shows the main types of lining distortion in masonry-lined tunnels.

In a recent study, Wang (2010) examined the development of cracking due to shear deformation of the lining caused by slope instability in the vicinity of the tunnel. In this study, the observed cracks on a lining were characterized (i.e. spatial distribution, texture and appearance of the cracks) in relation to the direction of slope movement. It should be noted that cracking and spalling of lining material may occur due to material deterioration, for instance under freeze-thaw conditions or due to rebar corrosion; material deterioration is discussed in more detail in section 9.2.2.

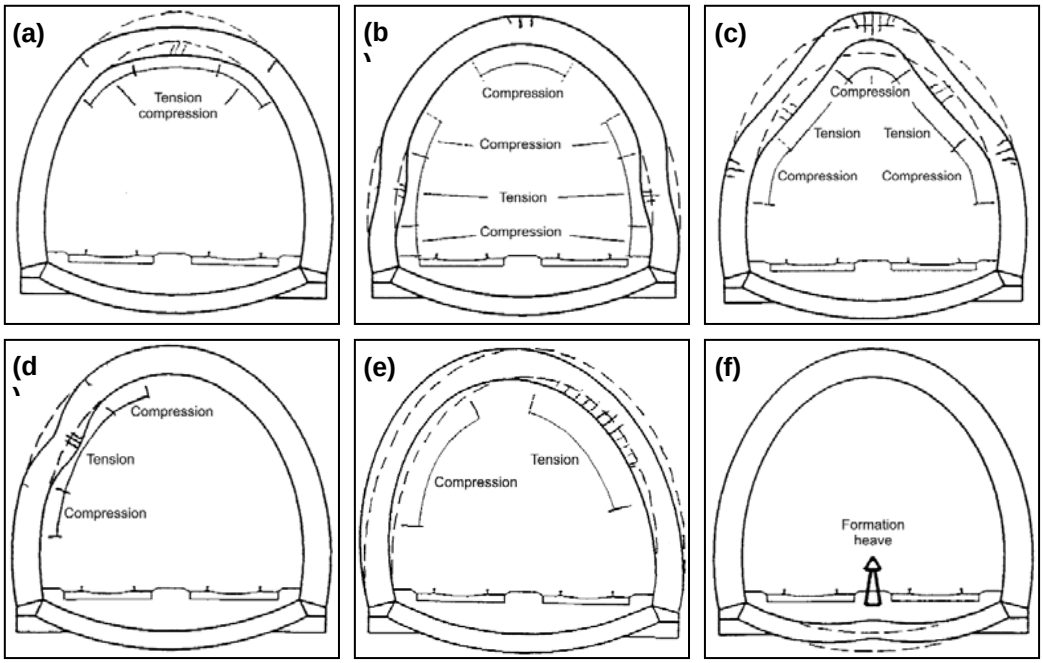

Figure 9-2 Types of lining distortion in masonry-lined tunnels (adapted from CIRIA 2009).

9.2.2 Material deterioration

Material deterioration refers to adverse changes in the properties of the lining material due to internal or external influences (e.g. loss of mechanical properties, loss of material area, etc.). The main causes of material deterioration in masonry-lined and concrete-lined tunnels are discussed in the next sections.

Masonry lined tunnels

Table 9.2 provides a summary of the main deterioration causes in masonry-lined tunnels, together with a brief description for each of them. It is interesting to note that most of these deterioration mechanisms are associated with the presence of water (examples are given in Fig.9.3-4).

 Copyright © MAINLINE Consortium

Table 9-2 Causes of deterioration in masonry-lined tunnel (adapted from CIRIA 2009).

Deterioration mechanism	Consequences
Freeze-thaw cycling	Where masonry is persistently wet and exposed to repeated freeze-thaw cycles, this can cause spalling of masonry units and mortar loss from joints. it is most likely in masonry at or near to portals or open shafts, which are likely to be subject to a greater number of freeze-thaw cycles (Fig.9.3).
Physical salt weathering	Transport and precipitation of salts can cause softening, crumbling, flaking blistering and laminar spalling of mortar and masonry units.
Sulfate attack	This generally an expansive reaction between sulfates (present in groundwater, soil and rock) and components of the cement matrix of mortar causing its deterioration into a flaky, crumbly non-structural material. sulfate attack may also affect bricks and some types of stone with similar results
Leaching and corrosive attack	The mortar's calcium hydroxide and calcium carbonate components are particularly vulnerable to attack by acidic water, and their loss creates secondary porosity that can weaken materials and in turn aggravates the effects of other agents like freeze-thaw. In anaerobic conditions, particularly in tunnels carrying sewage, corrosive hydrogen sulphide may be produced. Leaching may result in staining and whitish deposits on masonry surfaces.
Biological attack	Tree roots can cause serious damage to the structural fabric of the tunnels and even tens of metres below the ground surface. Other plants can disrupt masonry at portals. Smaller organisms that may be found in damp areas of the tunnel fabric can cause deterioration by increasing porosity and facilitating leaching, and by other mechanisms. The microbial anaerobic conditions can lead to low pH resulting in attack of grout, concrete and metal.
Repair with unsympathetic materials	The use of overly-hard mortar can lead to masonry units losing their faces and edges. The use of overly-hard masonry units in repairs can damage adjacent original fabric. Use of impermeable materials can increase saturation and redirect moisture into other components or part of the structure, accelerating their deterioration. Corrosion of ferrous elements can cause spalling of adjacent masonry.
Expansion and contraction (thermal, wetting and drying cycles)	This can result in internal fracture of the units and spalling and loss of mortar from the joints.
Moisture saturation	Units are vulnerable to environmental agents that cause deterioration. The nature and extent of saturation is a function of the type and amount of porosity. Movements of moisture can result in washout of fines from particulate materials, e.g. from the ground behind the lining, causing weakening and instability.
Ground movements	The development of additional stresses or change in stress distribution due to ground movement can lead to cracking or loosening of masonry units, which in extreme cases can lead to loss of structural integrity of the lining (Fig.9.4).
Cyclic loading and fatigue effects	Cyclic loading such as from repeated passage of vehicles or trains principally affects the invert of tunnel structures, unless they are near-surface. There is little information available on the effects of this action and fatigue exhibited by masonry linings, but research carried out by Cardiff University of Cardiff (Roberts et al. 2006) indicates that this does occur and could potentially be of structural importance.

 Copyright © MAINLINE Consortium

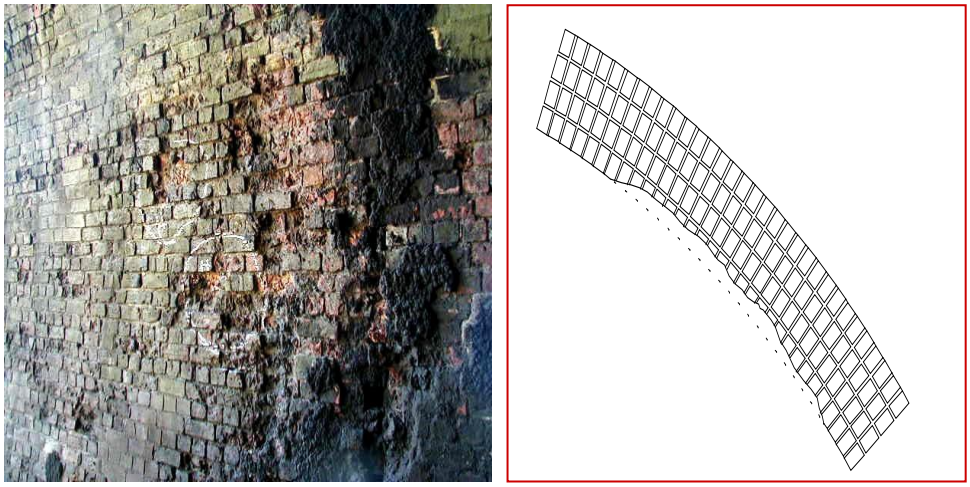

Figure 9-3 Example of material loss in brick tunnel linings caused by freeze-thaw attack (with permission from Network Rail): photograph of the deteriorated masonry lining and sketch depicting the residual cross- section of the damaged lining.

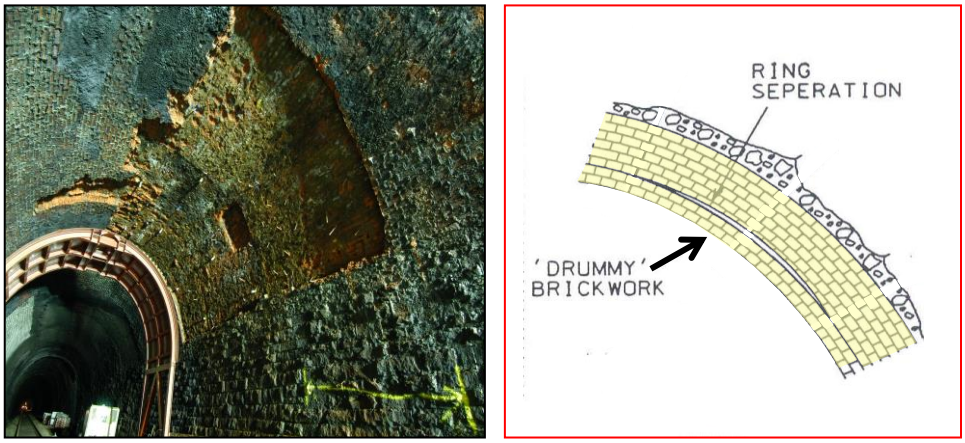

Figure 9-4 Example of ringseparation (with permission from Network Rail): photograph of the deteriorated lining and sketch depicting the portion of the lining thickness affected by ring separation.

Concrete lined tunnels

Table 9.3 provides a summary of the main deterioration causes in concrete-lined tunnels, together with a brief description for each of them. A more detailed discussion is given in the following sections. It should be noted that, in some cases, the occurrence of one type of deterioration may cause the initiation of another. For instance, sulfate attack can cause concrete cracking and material disintegration which may result in a reduced corrosion protection of the embedded reinforcing bars (Corral-Higuera et al. 2011).

 Copyright © MAINLINE Consortium

Table 9-3 Principal causes of deterioration in concrete-lined tunnels

Deterioration mechanism	Consequences
Sulfate attack	Reaction between sulfates (present in groundwater, soil and rock) and components of the cement matrix of mortar causing its deterioration into a flaky, crumbly non-structural material. For more details see below.
Freeze-thaw attack	Concrete is a porous material which is able to absorb and retain moisture. Deterioration takes place when saturated or near saturated concrete is subjected to freeze-thaw cycles. There are two damage types associated with freezing and thawing action; these are (a) surface scaling and (b) internal cracking. For more details see below.
Alkali-aggregate reactions (AAR)	AAR refers to reactions which occur between the alkaline content of the cement paste and some aggregate types, the two main types of AAR being Alkali-silica reaction (ASR) and Alkali-carbonate rock-reaction (ACR). ASR can only occur when the concrete has high alkali content in the cement paste, reactive aggregates have been used and water is present. For more details see below.
Reinforcement corrosion	The alkaline nature of concrete promotes the formation of the thin oxide film which protects the embedded steel from corrosion (i.e. steel passivation). Once the steel is depassivated, e.g. due to the carbonation of the concrete cover, a number of physical effects take place, including loss of steel area, concrete cracking and spalling, impaired mechanical reinforcing bar and bond properties. For more details see below.

Nowadays, it is generally known which concrete properties are required for specific environmental exposure. This information is included in standards such as EN 206-1 (see reference BS EN 2000) together with national complementary requirements. Eurocodes prescribe cover layers based on expected service lives in different exposure conditions. However, long-term exposure conditions may differ significantly from the initially assumed exposure conditions.

Sulfate attack

In this deterioration mechanism, the sulfates react with constituents of the hardened cement (i.e. calcium aluminate hydrates) to form gypsum ($CaSO_4 \cdot 2H_2O$) or ettringite ($3CaO \cdot Al_2O_3 \cdot 3CaSO_4 \cdot 31H_2O$), e.g. (Neville 2004, Long et al. 2011). Sulfate attack can also lead to the formation of thaumasite; in this case external sulfates react with calcium silicate hydrates (CSH) to form thaumasite ($CaSiO_3 \cdot CaCO_3 \cdot CaSO_4 \cdot 15H_2O$). This is classified as a different type of sulfate attack and it is not further discussed in this report (Crammond 2003, Neville 2004, Long et al. 2011). Formation of ettringite is not harmful before decades have passed and the cement paste is leached.

Sulfate attack takes place when an external source of sulfates is present in solution which comes in direct contact with concrete (Neville 2004). An external source of sulfates is often the direct contact of concrete with groundwater in gypsum-bearing soils as well as clays and mudstones (CIRIA 2009). Sulfate may be also present from not natural deposits in brownfield sites previously occupied by (chemical-related) factories (Neville 2004). In contrast, an

 Copyright © MAINLINE Consortium

internal source of sulfates is the use of aggregates which contain sulfates; this leads to expansion when water has access. Besides gypsum in aggregates, an internal form of sulfate attack known as Delayed Ettringite Formation (DEF) may show up if concrete has been heated to more than 65 ^{o}C during curing/early hardening. This is a serious deterioration mechanism for massive structures (but not so common) which shows up when water has access.

The expansive nature of the reactions in sulfate attack (i.e. volume increase) leads to cracking, concrete softening and material disintegration; these eventually adversely affect the mechanical properties of concrete, i.e. loss of stiffness, strength, ductility and its durability (Long et al. 2011). In some cases, penetration of sulfate attack damage throughout the entire section has been observed (CIRIA 2009). The extent (i.e. intensity and rate) of sulfate attack on concrete, however, is determined by several factors, including among others the solubility (dry salts will not react with concrete), the continuity (i.e. static vs. flowing water) and concentration of sulfate-containing water (Neville 2004) as well as the composition of the concrete itself (e.g. Lee et al. 2005). Finally, sulfate attack should not be confused with physical salt weathering which leads to a different type of material deterioration as opposed to the chemical process of sulfate attack (Neville 2004).

Freezing and thawing (Frost attack)

Concrete is a porous material which is able to absorb and retain moisture. Deterioration takes place when saturated or near saturated concrete is subjected to freeze-thaw cycles (CIRIA 2009). There are two damage types associated with freezing and thawing action (Kosior-Kazberuk 2012); these are including surface scaling and internal cracking. The complex processes involved in the freeze-thaw mechanism can be summarised as follows (e.g. Bazant et al. 1988, Hasan et al. 2004):

- Ice forms on the concrete surface at temperatures below 0^{o} C. Following the freezing initiation, the pore solution will freeze at the freezing point. This causes hydraulic pressure to develop due to unbalanced thermodynamic equilibrium.

- Unfrozen pore solution in small pores begins to flow towards the frozen solution in larger pores and subsequently freezes as well. Internal shrinkage and additional hydrostatic pressure develop due to the internal solution (water) redistribution. The water redistribution is identified as a key factor in the development of damage during the frost cycles.

- The higher thermal expansion of ice – in comparison to the thermal expansion of concrete – is responsible for the higher amount of ice contraction at low temperatures. Through this mechanism, additional empty space is available and filled with unfrozen water from the smaller pores which also freezes. Under thawing conditions, tensile stresses develop in the concrete due to the expansion of the ice (i.e. ice expands more than concrete) leading to internal cracking.

- The formation of cracks causes an increase of concrete's saturation when these are filled with additional water in temperatures above 0^{o}C.

Internal cracking of concrete caused by freezing and thawing action is responsible for reductions in stiffness and strength of concrete both in compression and tension (e.g. Ueda et al. 2009, Hanjari et al. 2011). Furthermore, cracking due to freeze and thaw may lead to

 Copyright © MAINLINE Consortium

concrete spalling and, hence, a reduction of the lining thickness. If internal cracking or delamination through the thickness of lining or wall takes place, this will accelerate with time. In reinforced concrete, frost damage of the concrete has an adverse effect on the bond properties of the embedded reinforcing bars (Hanjari et al. 2011). Concrete cracking and spalling adversely affect the durability of the lining, increasing the possibility of reinforcement corrosion occurrence. This type of damage is commonly observed in concrete located near portals and shafts due to the high temperature fluctuations at these locations (CIRIA 2009). Freeze-thaw damage is sometimes seen in combination with ASR, resulting in a double-effect (accelerated).

Alkali-aggregate reactions (AAR)

Alkali-aggregate reactions (AAR) were initially presented by Stanton in the 1940's (Stanton 1940). They refer to reactions which occur between the alkaline content of the cement paste and some aggregate types (Swamy 1992). The two main types of AAR are Alkali-silica reaction (ASR) and Alkali-carbonate rock-reaction (ACR); in this report the discussion is limited to ASR. ASR involves the reaction of the alkaline hydroxides in the cement with the siliceous minerals in the aggregates. As a result of this reaction, an alkali silica gel forms able to absorb large amounts of water, which in turn leads to the development of expansive stresses. The following conditions are required for ASR to take place (Swamy 1992):

- The concrete should have high alkali content in the cement.
- The aggregate should contain a reactive form of silica, i.e. Opal (amorphous), chalcedony (crystalline, fibrous) and tridymite (crystalline).
- Water should be present.

Generally, ASR will not occur if any of these requirements is not met; the converse is also valid. This enables the development of strategies for the management of structures prone to ASR. It has been suggested that a certain proportion of the reactants leads to the maximum expansion; this is known as the "pessimum proportion" (Swamy 1992). For example, 3-5% Opal content in aggregates is sufficient to cause maximum expansion. The value of this critical content increases for aggregates of lower reactivity.

Corrosion of steel in concrete

The high alkalinity of concrete assists the formation of an insoluble oxide layerat surface of the embedded steel reinforcements. This mechanism, which protects the steel reinforcements from corrosion, is known as steel passivation (Broomfield 1997, Glass and Buenfeld 2000). Corrosion of the embedded steel will occur if this oxide film becomes unstable, i.e. steel depassivation. Carbonation and chloride attack are identified as the main causes, responsible for the destabilization of the passive oxide film (Broomfield 1997). In both mechanisms, the aggressive species (i.e. Cl^-, CO_2) diffuse through the pores and existing cracks of concrete and eventually reach the steel; this period during which no corrosion damage is observed is known as corrosion initiation.

Carbonation: In carbonation, carbon dioxide and the alkaline hydroxides react in the concrete. Calcium carbonate is produced by the reaction of carbonic acid (H_2CO_3) with calcium hydroxide (H_2CO_3 forms through the dissolution of CO_2 in water), see Equation 9.1.

 Copyright © MAINLINE Consortium

$$H_2CO_3+Ca(OH)_2 \rightarrow CaCO_3+2H_2O \quad (9.1)$$

Calcium hydroxide is associated with high pH values in the pore solution (around 12-13) and its consumption due to carbonation can cause pH to reduce to values below 10 (Broomfield 1997). As a result of this mechanism, the protective oxide film becomes unstable and the steel is no longer protected against corrosion. The main factors influencing the carbonation process are the thickness of the concrete cover, the permeability and alkalinity of concrete, the relative humidity and temperature and the concentration of carbon dioxide (Broomfield 1997). Carbonation-induced corrosion usually affects large parts of the reinforcing bars causing a fairly uniform loss of steel area. The accumulation of corrosion products at the steel-concrete interface over time results in cracking of the concrete cover in a direction parallel to the longitudinal axis of the affected reinforcements.

Chloride attack: Chlorides attack the thin oxide protective layer causing localised steel section loss. During this process the chlorides are not consumed but they act as a catalyst during the depassivation process (Broomfield 1997). The depassivation mechanism due to chloride attack is shown in Fig.9.5.

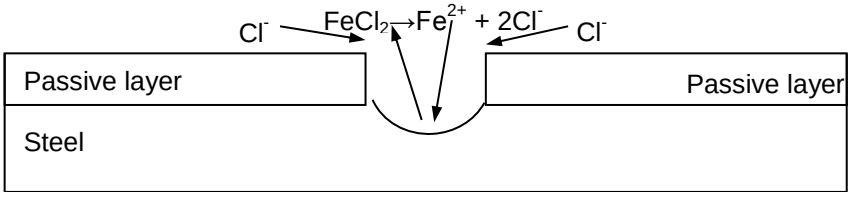

Figure 9-5 Chloride induced depassivation (Broomfield 1997).

Chloride-induced corrosion is characterized by the formation of pits, i.e. small anodic areas. The most common sources of chlorides in concrete are (a) cast-in chlorides and (b) chlorides from external sources. Cast-in chlorides are chlorides added to the concrete mix in the form of set accelerators (e.g. calcium chloride), the use of sea water or contaminated aggregates (Broomfield 1997). Chlorides from external sources are transported to the depth of the steel by means of capillary sorption and diffusion through a network of interconnected pores in the concrete (Martin-Perez et al. 2001a). When a critical chloride concentration is exceeded, the passivation layer on the steel surface becomes unstable (Broomfield 1997, Ann and Song 2007). The critical chloride concentration is commonly assessed using the chloride to hydroxyl ratio. Corrosion is observed for chloride to hydroxyl ratios exceeding 0.6; this is a Cl- concentration of 0.4% and 0.2% by cement weight for cast-in chlorides and external chlorides, respectively (CTRE 2006, Ann and Song 2007).

Process and effects of corrosion in RC: Corrosion is often modelled as a two-stage process (Fig.9.11) including (a) time to corrosion initiation and (b) corrosion propagation. Steel depassivation denotes the beginning of the propagation stage. Once corrosion enters the propagation stage, a number of physical changes initiate at the affected reinforcing bars, the surrounding concrete and their bond due to the built-up of corrosion products (i.e. rust) at the steel-concrete interface; this causes physical and mechanical damage to the concrete (e.g. concrete cracking, loss of strength, etc.). This may eventually lead to loss concrete section and bond between steel and concrete. The irregular loss of steel area has a negative effect of the mechanical properties of the affected reinforcements (e.g. loss of ductility). The effects of uniform and localised corrosion in RC and their interrelations are schematically shown in Fig.9.6.

 Copyright © MAINLINE Consortium

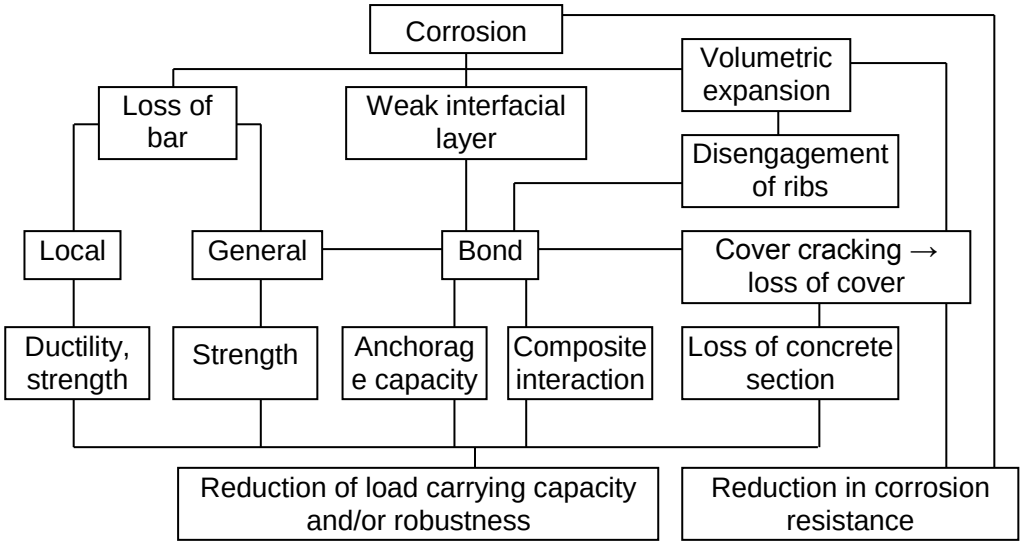

Figure 9-6 The effects of corrosion in RC (FIB 2000).

Pitting corrosion, which is associated with localised stress concentrations due to the highly localised section loss, can cause significant reductions of strength and ductility in the reinforcing bars (Cairns et al. 2005, Du et al. 2005a, b).Its extent and spatial distribution are generally difficult to characterize, potentially leading to safety risks in severely affected structures.

9.3 Deterioration modelling

9.3.1 Time-dependent tunnel performance

Figure 9.7 shows a number of different scenarios of tunnel performance over time. The performance of the tunnel may suddenly deteriorate following the occurrence of a serious accident (e.g. explosion followed by fire), as shown in Figure 9.7. Tunnel performance may also deteriorate gradually without any sudden damage incurred (e.g. fire). The causes of this gradual performance deterioration for masonry and concrete lined tunnels have been briefly reviewed in section 9.2. In this section, the available models for quantifying the effects of the different types of deterioration on tunnel performance are discussed, with emphasis given to material deterioration in concrete lined tunnels.

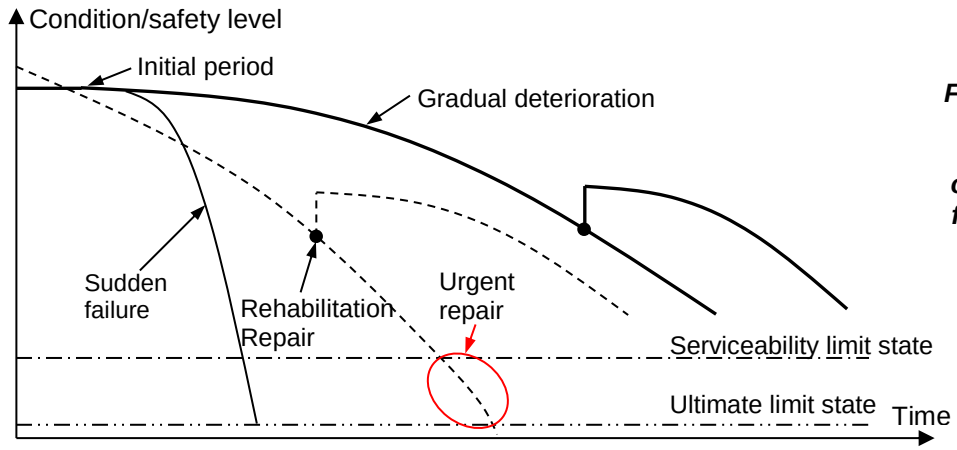

Figure 9-7 Examples of performance profiles of tunnels over time (modified from Sandrone and Labiouse 2011).

9.3.2 Geotechnical related deterioration

Geotechnical related deterioration refers to the damage induced to the tunnel lining caused by changes in the stress distribution for instance due to instability of neighbouring slopes, ground settlement, etc. Furthermore, water movements in the soil can have a significant effect on the type and rate of tunnel deterioration (e.g. groundwater can promote the occurrence of sulfate attack in concrete and masonry linings). Modelling of geotechnical related deterioration of tunnels can be very complex especially in cases that the composition and characteristics of the ground are not constant along the length of the tunnel. Assessing the performance of a tunnel in relation to the geological conditions (and how these may change with time) requires the use of soil mechanics principles; see e.g. (Graig 2007). Generally, assessment methods involve the use of appropriate soil-structure numerical models, which attempt to capture the changes in tunnel loading as a result of ground/soil movement and deterioration, e.g. (Youakim et al. 2000).

9.3.3 Modelling of material deterioration in concrete lined tunnels

Corrosion of steel in concrete

As previously mentioned, the process of corrosion of steel in concrete is commonly idealised as a two stage process, namely initiation and propagation. In general, the corrosion initiation stage can be idealised as a diffusion process, for instance using Fick's second law of diffusion as originally proposed by Collepardi et al. (1972), and has been the prevailing basis for development of different models for service life estimations (e.g. see Duracrete 2000, FIB 2006).

Once the corrosion process has entered the propagation stage, a number of physical effects occur gradually which are responsible for the loss of area and mechanical properties of steel and concrete and their interaction (i.e. bond). Several studies have investigated the influence of corrosion on the material and bond properties, e.g. (Almusallam 2001, Palsson and Mirza 2002, Fang et al. 2004, Du et al. 2005a, b, Cairns et al. 2005, Lundgren 2007, Val and Chernin 2009, Kashani et al. 2013, etc.). Based on these studies, models have emerged – which allow the quantification of the corrosion effects on the material and bond properties – that can be used in the performance assessment of corroding RC structures, e.g. (Coronelli and Gambarova 2004, Stewart 2012, Kallias and Rafiq 2013).

A gradual loss of reinforcement yield strength and ductility for increasing corrosion amounts has been observed experimentally, e.g. (Du et al. 2005a, b). Equation 9.2 can be used to quantify the reduction of yield strength with increasing corrosion damage (Stewart 2009):

$$f_y^D = \left[1.0 - \alpha_{y1}\left(A_{pit}/A_{stnom}\right)100\right] f_{y0} \tag{9.2}$$

where, f_{y0} and f_y^D are the original and reduced yield strengths, respectively, A_{stnom} is the initial cross-sectional area, α_{y1} = 0.005 (Du et al. 2005a) and A_{pit} is the area of the pit. The pit configuration of Figure 9.8 can be used to estimate A_{pit}, as a function of maximum pit depth, $P_{max}$and initial rebar diameter, d_b, see Equations 9.3–9.6.

 Copyright © MAINLINE Consortium

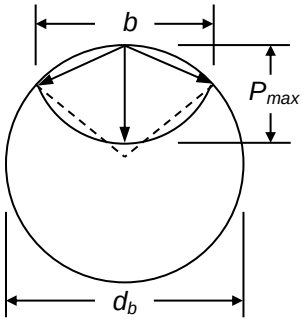

Figure 9-8 Pit configuration (Stewart 2009).

$$A_{pit}(t) = \begin{cases} A_1 + A_2 & P_{\max} \le d_b/\sqrt{2} \\ A_{stnom} - A_1 + A_2 & d_b/\sqrt{2} < P_{\max} \le d_b \\ A_{stnom} & P_{\max} \ge d_b \end{cases} \quad (9.3)$$

$$A_1 = 0.5\left[\theta_1\left(\frac{d_b}{2}\right)^2 - b\left(\frac{d_b}{2} - \frac{P_{\max}^2}{d_b}\right)\right] \quad (9.4a)$$

$$A_2 = 0.5\left[\theta_2 P_{\max}^2 - b\frac{P_{\max}^2}{d_b}\right] \quad (9.4b)$$

$$b(t) = 2P_{\max}(t)\sqrt{1-\left[\frac{P_{\max}(t)}{d_b}\right]^2} \quad (9.5)$$

$$\theta_1 = 2\arcsin\left(\frac{b}{d_b}\right) \quad (9.6a)$$

$$\theta_2 = 2\arcsin\left(\frac{b}{2P_{\max}}\right) \quad (9.6b)$$

P_{max} can be estimated from values of uniform corrosion and a pitting factor $R_{pit} = P_{max}/P_{av}$ with R_{pit}ranging between 4 to 8 (Gonzalez et al. 1995). $P_{av}$is the uniform loss of rebar radius (mm) after t years and it can be calculated using Equation 9.7.

$$P_{av} = 0.0116 i_{cor} t \quad (9.7)$$

where, i_{cor} (μA/cm^2) is the corrosion current (i.e. rate of corrosion).

It has been observed experimentally that increasing corrosion damage has a negative effect on the ductility of the affected reinforcements, e.g. (Almusallam 2001, Cairns et al. 2005, Du et al. 2005b, Alexopoulos et al. 2007, Kashani et al. 2013). Different experimental configurations, specimen geometries (e.g. plain and ribbed reinforcing bars) and methods to speed-up corrosion were used in these studies. For example, Equation 9.8 (Du et al. 2005b) can be used to calculate the residual ductility of corroding reinforcing bars in terms of a gradual reduction of ultimate rebar strain, ε_u^D, for increasing corrosion damage.

$$\varepsilon_u^D(t) = \left[1 - \alpha_{y2} Q_{cor}(t)\right] \varepsilon_0 \quad (9.8)$$

where, α_{y2} is an experimental coefficient, ε_0 is the initial (uncorroded) ultimate strain and $Q_{cor}$is the % loss of steel area given from Equation 9.9. Du et al. (2005b) proposed the conservative value α_{y2} = 0.05 to be used in assessment. This value is somewhat conservative for deformed reinforcing bars embedded in concrete, in this case α_{y2}= 0.037 (Du et al. 2005b).

$$Q_{cor}(t) = \left[1 - \frac{A_{st}^D(t)}{A_{stnom}}\right] 100 \quad (9.9)$$

with,

$$A_{st}^D(t) = \pi\left[r_0 - P_{av}(t)\right]^2 \quad (9.10)$$

where,$A_{st}^D(t)$ and A_{stnom} are the remaining and the original area of the corroding reinforcing bars, respectively.

Concrete microcracking and cracking occurs due to the build-up of corrosion products at the steel-concrete interface. This mechanism is known to have a negative effect on the mechanical properties of the concrete (e.g. loss of strength). Coronelli and Gambarova (2004) proposed a model which can be used to calculate the residual strength of concrete in compression for a given level of corrosion loss in the reinforcing bars.

Corrosion also affects the bond performance of the affected reinforcing bars with concrete. Low amounts of corrosion, prior to the development of longitudinal cracking cause an increase of bond strength between the corroding reinforcing bars and concrete (FIB 2000). Bond performance begins to deteriorate upon the formation of visible longitudinal cracking along the length of the corroding reinforcing bar. Several empirical and numerical models have been proposed for the quantification of the residual bond properties (e.g. Rodriguez et al. 1994, Lundgren 2005, Lundgren 2007, Val and Chernin 2009).

Sulfate attack

The formation of ettringite and thaumasite, both associated with sulfate attack and involving expansive reactions, lead to concrete becoming a loose mass, as well as cracking and spalling (Brueckner et al. 2012).

Two important parameters (other than concrete composition) affecting the rate of concrete deterioration due to external sulfate attack are the water composition and the flow characteristics. In a recent study, it was found that the sulfate content of groundwater was up to 4 g/l (Leemann and Loser 2011). However, no information of water flow was provided and the assumption was made that flow is likely to be determined by the meteorological conditions.

A mechanistic model, proposed by Atkinson and Hearne (cited by Clifton et al. 1999), enables the prediction of the rate of degradation (i.e. sulfate attack rate) in concrete under continuous immersion in sulfate solutions, namely

 Copyright © MAINLINE Consortium

$$R = X_{spall} \Big/ T_{spall} = \frac{E\beta^2 c_s C_o D_i}{\alpha_o \tau (1-\nu)} \quad (9.11)$$

where, X_{spall} is the spalled layer thickness, T_{spall} is the time required for a layer to spall, E is the modulus of elasticity of concrete, β is the linear strain caused by one model of sulfate ions reacted with $1m^3$ of concrete, c_s is the sulfate ion concentration in the bulk solution (assumed constant), C_o is the concentration of reacted sulfate ion from the solution present as ettringite, D_i is the intrinsic diffusion coefficient of sulfate ions, $\alpha_o = 1$ is a roughness coefficient for the fracture path, τ is the fracture surface energy of the concrete and ν is the Poisson's ratio. The deterioration model of Equation (9.11) is based on the following assumptions (Clifton et al. 1999):

- Sulfate ions diffuse into concrete from the surrounding environment.
- Expansive reactions are taking place between the sulfate ions and the aluminium (e.g. C_3A) in concrete.
- Magnesium ions are absent in the solution.
- Stresses develop in the surface layers which in turn lead to cracking and spalling of the affected concrete.
- The affected layer of the reacted material is distinctively separated from the unaffected (inner) concrete mass.

In a more recent study (Brueckner et al. 2012) the rate of deterioration due to thaumasite formation was found to be up to 1.8mm/year for widely used concrete mixes. The rate of deterioration was shown to be affected by the concrete mix design and type of solution. For the concrete mixes examined, an initiation period of six months was observed during which deterioration was not evident. Recent experimental results (Zhang et al. 2013) confirmed the importance of w/c ratio on the observed expansion and damage of concrete due to sulfate attack; as the w/c increases, both expansion and damage also increased. Furthermore, it was observed that the presence of chlorides in the sulfate solution has a beneficial effect on the observed damage; the higher the chloride concentration in the solution the lower the observed expansion and damage (Zhang et al. 2013). In their study, an expansion model was presented for concrete exposed to chloride-sulfate environments.

The expansive reactions involved in sulfate attack lead to cracking and material disintegration which in turn are responsible for loss of strength and durability. The available models (e.g. Equation 11) are able to predict the extent of sulfate attack (i.e. intensity and rate). It is anticipated that cracking and material softening will affect the residual mechanical properties of concrete (i.e. residual stiffness and strength). The models for external sulfate deterioration, however, do not provide information regarding the evolution of material properties with time. One approach to consider the damage during the structural assessment of deteriorating tunnels due to sulfate attack is to ignore the resistance of the concrete in the damaged zones. This is likely to be a conservative assumption since damaged concrete may still exhibit some resistance (e.g. Lee et al. 2005, Leemann and Loser 2011, Hartell et al. 2011). Alternatively, if more information is available on the residual material properties of sulphate-damaged concrete, these values should be used in assessment (instead of completely ignoring the damaged zones). The type and depth of attack can be obtained

through experimental testing of concrete cores. The attacked layer should be disregarded when lack of cohesiveness is observed. For specific concrete and exposure conditions, it may be possible to evaluate directly a relatively simple time-dependant relation from examination results, provided they have been collected consistently for a relatively long time period.

Freeze-thaw attack

Frost attack has an adverse effect on the durability, the mechanical properties of the affected concrete and the bond properties of steel reinforcing bars in frost-damaged concrete (Bazant et al. 1988, Matsumoto et al. 2001, Hasan et al. 2004, Hasan et al. 2008, Ueda et al. 2009, Hanjari et al. 2011, Hanjari et al. 2013).

A number of models have been proposed to quantify the effect of freezing and thawing processes on the durability (i.e. development of cracking) of concrete structures (e.g. Bazant et al. 1988, Matsumoto et al. 2001). In these studies, freezing and thawing action is modelled as a coupled heat-moisture transfer process. Bazant et al. (1988) modelled the movement of water in concrete during the freeze and thawing phenomenon as a double diffusion process, considering both macroscopic and local diffusion. In their model, the temperature distribution (i.e. heat conduction) is calculated considering the latent heat of freezing. It follows that their model allows predicting the development of stresses in the concrete resulting from the freezing-thawing action (i.e. pore pressures) and the externally applied loads. Matsumoto et al. (2001) presented closed form expressions for the freeze-thawing process considering the equilibrium relation of moisture (i.e. unfrozen water) for temperatures greater than 0^oC. In the presence of ice, the liquid (i.e. unfrozen) water content is a function of the local temperature. However, freezing will not take place when the chemical moisture potential is less than the critical chemical moisture potential irrespectively of the temperature (i.e. this applies also for temperatures below 0^o C). These relations were taken into account by Matsumoto et al. (2001) using equilibrium relations between the unfrozen water, the chemical potential of moisture and the temperature.

These models are useful in assessing the cracking behaviour and durability of concrete caused by frost attack. However, the adverse effects of freeze-thawing on the residual properties (i.e. strength, stiffness, etc.) of frost damaged concrete were not quantified by these studies.

A number of studies (Hasan et al. 2004, Hasan et al. 2004, Hasan et al. 2008, Ueda et al. 2009, Hanjari et al. 2011, Hanjari et al. 2013) presented models for the quantification of the effects of frost damage (i.e. irreversible tensile deformations and cracking in concrete) on the residual mechanical properties of concrete and the steel-concrete bond (for the case of reinforced concrete). These models can be used to consider the changes in material (e.g. loss of concrete stiffness and strength) and bond properties caused by freezing-thawing action in the analysis of frost-damaged concrete structures.

An elasto-plastic and fracture model for frost-damaged concrete in compression was developed in an early study by (Hasan et al. 2002, cited by Hasan et al. 2004). The limitations of the stress-strain constitutive model for frost-damaged concrete included its inability to consider the irreversible tensile deformation and fracture due to freezing-thawing action. Furthermore, the computation of the stress-strain relationship required as input the compressive strength of the damaged concrete (e.g. through experimental testing of core sampling). To eliminate these drawbacks, a fracture parameter was introduced to this model,

 Copyright © MAINLINE Consortium

by the same authors in a later study (Hasan et al. 2004), to account for the effect of freezing-thawing damage (i.e. cracking) on the initial stiffness (this fracture parameter is independent from the fracture parameter related to the effect of applied loading).

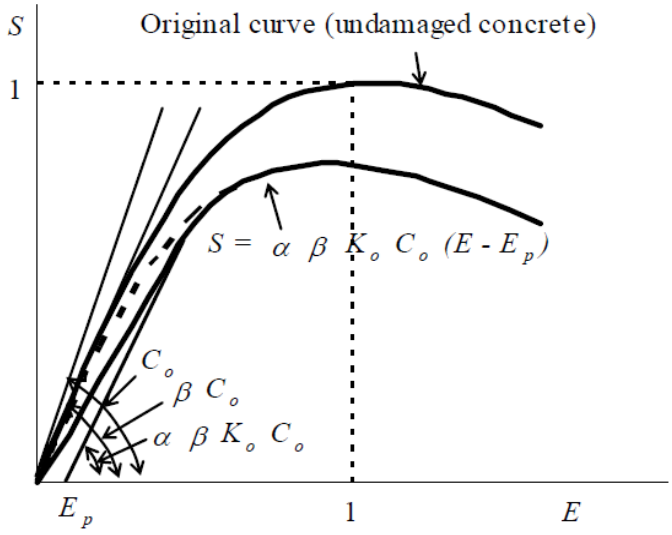

Figure 9-9 Equivalent stress-equivalent strain relationship of undamaged and freeze-thaw damaged concrete (Hasan et al. 2004).

In their formulation, the fracture parameter associated with freeze-thaw damage is a function of the remaining expansion of concrete (Hasan et al. 2004). The stress-strain model, which is schematically depicted in Figure 9.9, is defined in terms of the mechanical equivalent stress-equivalent strain relationship given by Equation 9.12:

$$S = \alpha\beta K_o C_o \left(E - E_p\right) \tag{9.12}$$

where, α is the effective factor (Equation 9.13), β is the fracture parameter associated with frost damage (Equation 9.14), S is the equivalent stress, E is the equivalent strain, K_o is the fracture parameter associated with loading, C_o is the initial stiffness and E_p is the equivalent plastic strain (Equation 9.15).

$$\alpha = e^{-1.70E_{pf}} e^{1.70E_{pf}^{0.15}E_{\max}^{0.85}} \text{ for} E_{max}<E_{pf}\text{, otherwise } \alpha = 1 \tag{9.13}$$

$$\beta = e^{-0.45E_{pf}\left(1-e^{-30E_{pf}}\right)} \tag{9.14}$$

$$E_p = E_{\max} - a\left(1-e^{-bE_{\max}}\right) \tag{9.15}$$

where,

$$a = \frac{20}{7} - 2.10E_{pf} + 0.34E_{pf}^2 \tag{9.16a}$$

$$b = 0.35 + 0.25E_{pf} + 0.18E_{pf}^2 \tag{9.16b}$$

 Copyright © MAINLINE Consortium

where,$E_{pf}$and E_{max} are the equivalent plastic strain associated with frost damage and the maximum equivalent strain, respectively.

The parameters required as input by this model include the measured plastic strains caused by freeze-thaw damage and the compressive strength and corresponding strain (at peak) for the undamaged concrete. Hasan et al. (2004) acknowledged that a step forward will be to develop a model for predicting the plastic strains associated with frost damage from temperature histories. In a later study by the same authors (Hasan et al. 2008), their previous model was expanded to consider the effect of fatigue loading. Their results indicated that fatigue strength reduces faster in frost-damaged concrete compared to undamaged concrete.

Ueda et al. (2009) developed a mesoscale model to study the compressive and tensile behaviour of frost-damaged concrete. Their model was based on a 2D rigid body spring model (RBSM) approach, in which frost damage is taken into account by means of zero strength elements and mesoscale plastic strains (due to frost-damage). In this modelling level, concrete is represented by the explicitly modelling of the aggregates, the mortar and the interfacial transition zones between them. The model requires as input values of measured plastic strains caused by freeze-thaw action. Although the results of their study demonstrated the validity of their model, is it likely that the high computational cost involved will render this approach unsuitable for large structures (for instance a tunnel structure).

More recently, Hanjari et al. (2011) used splitting test results and inverse analysis to model the tensile stress – crack opening relation (σ-w) of frost damaged concrete using a bi-linear approximation as shown in Figure 9.10. In this model, the estimated variables are the tensile strength f_t, the elastic modulus E, the fracture energy G_F and the coefficients α_1, α_2 and b_2 (see Figure 9.10). This model is likely to be useful input for finite element analysis for the modelling of the softening (post-peak) behaviour of frost-damaged concrete.

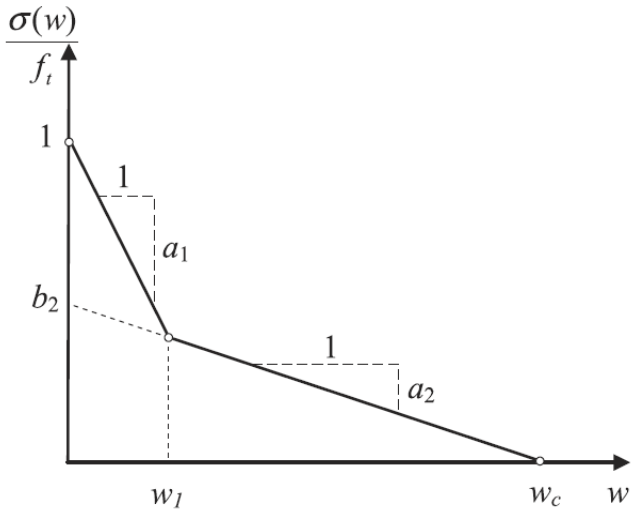

Figure 9-10 Bi-linear stress – crack opening model (Hanjari et al. 2011).

A stress-strain model for frost-damaged concrete in compression was presented by Hanjari et al. (2013). Their model was based on the σ-ε model of Thorenfeld et al. for undamaged concrete in compression, which was modified to account for the effects of frost damage on the mechanical properties (see Equations 9.17 – 9.19).

$$\sigma_{cc} = f_{cc}^{d}\left(\frac{\varepsilon}{\varepsilon_{cc}^{d}}\right)\left(\frac{n}{n-1+\left(\frac{\varepsilon}{\varepsilon_{cc}^{d}}\right)^{nk}}\right) \tag{9.17}$$

with

$$n = \frac{E_c^d}{E_c^d - E_0^d} \tag{9.18}$$

and

$$k = \begin{cases} 1 & \text{for } 0 < \varepsilon < \varepsilon_{cc}^{d} \\ 0.67 + \frac{f_{cc}^{d}}{62} & \text{for } \varepsilon > \varepsilon_{cc}^{d} \end{cases} \tag{9.19}$$

where, $\varepsilon_{cc}{}^{d}$ is the strain at maximum stress and it is estimated from experimental data, $E_c{}^{d}$ is the secant elastic modulus and $E_0{}^{d}$ is the tangential elastic modulus of the frost-damaged concrete.

It should be noted that although these models are very useful in quantifying the effect of a certain damage level caused by freeze-thaw action on the performance of concrete structures, at present no time-dependent model was found in the literature for predicting the residual material properties of frost-damaged concrete over time (i.e. following periods of freeze and thawing action).

Alkali-aggregate reactions (AAR)

At present no time-dependent model is found in the literature for concrete degradation by AAR due to a large variety in reactive aggregate types, concrete quality and water access to the structure. A high number of references exist of testing under accelerated conditions with varying results of expansion - however, these are difficult to be correlated to in-situ conditions and residual load bearing capacity.

9.3.4 Modelling of material deterioration in masonry lined tunnels

Very few physically based models exist for material deterioration in masonry lined tunnels. Some recent attempts were made to adapt models developed for freeze-thaw damaged concrete, assuming that the underpinning behaviour of masonry is similar (porous material), see (Bozinovski et al. 2011). In the absence of models for deteriorating masonry (i.e. brick-mortar system), the alternative is to develop empirical condition-based degradation profiles using field inspection data; this will be explored within deliverable D2.3 of the project.

 Copyright © MAINLINE Consortium

9.4 Evolution of deterioration

9.4.1 Concrete lined tunnels

Steel corrosion in concrete

As previously mentioned, steel corrosion in concrete is often modelled as a two stage process as shown in Figure 9.11. Hence, the development of deterioration-time profiles requires consideration of the relevant physical effects of corrosion associated with the propagation period; these can be modelled using the models described in previous sections. The propagation stage, however, is not usually allowed to develop much due to the rapidly increasing repair costs. Typical measures for corrosion control in practice involve the use of cathodic protection or the removal of chloride infected cover layer (or carbonated layer) and its replacement with sprayed or new repair concrete.

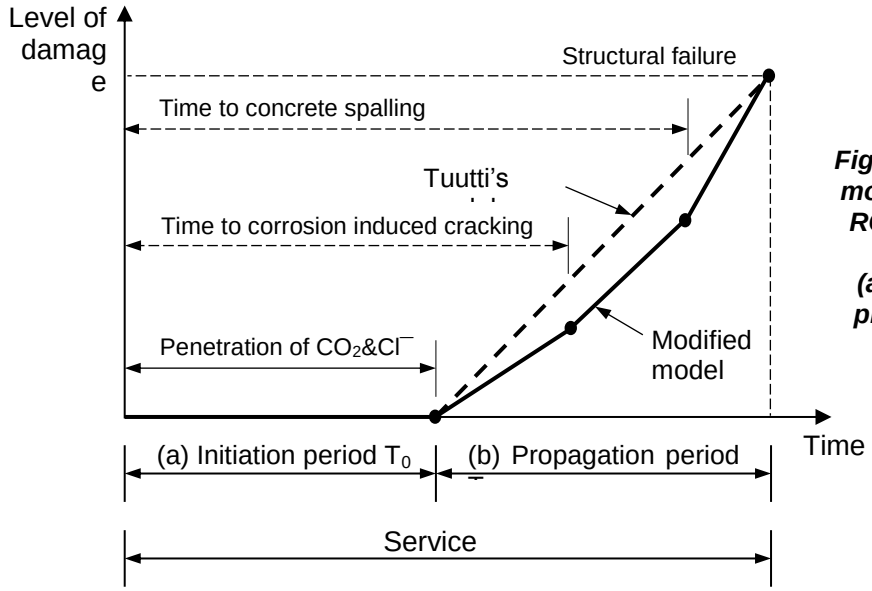

Figure 9-11 Service-life models of a corroding RC structure (Otieno 2011): (a) Initiation and (b) propagation stages.

Hence, the development of deterioration-time profiles requires consideration of the relevant physical effects of corrosion associated with the propagation stage; these can be modelled using the models described in the next sections.

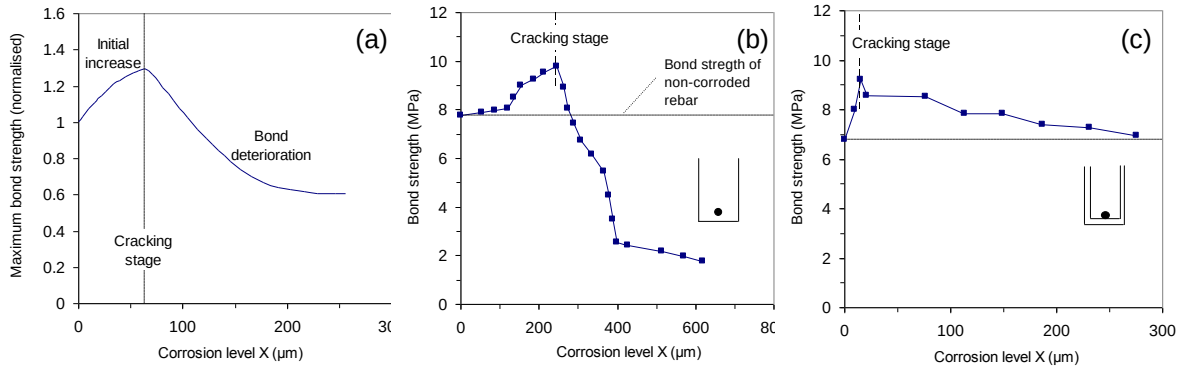

Figure 9-12 Evolution of bond strength for increasing corrosion levels (Berra et al. 2003): (a) as per (FIB 2000); (b) in unconfined concrete and (c) in concrete confined using steel stirrups.

 Copyright © MAINLINE Consortium

As an example, Figures 9.12a to 9.12c show the evolution of bond strength for increasing steel corrosion losses under varying degrees of confinement. It should be noted that the properties of reinforced concrete as well as the corrosion process itself are both associated with significant uncertainties. Hence, the development of performance profiles for corroding RC linings within a probabilistic framework is highly desirable.

Sulfate attack

Sulfate attack causes cracking and disintegration of concrete. This leads to loss of stiffness and strength over time. As previously discussed, no models are at present available for predicting the evolution of sulfate-damaged concrete with time. Experimental results from several studies (e.g. Lee et al. 2005, Hartell et al. 2011, Diab et al. 2012) indicate that the amount and rate of losses in mechanical properties of sulfate-damaged mortars and concrete are affected by the composition of the concrete (including *w/c* ratio) as well as the sulfate solution (e.g. concentration of sulfates). For example, Hartell et al. (2011) quantified experimentally the effect sulfate attack on the strength of concrete cylinders. A number of parameters were investigated in their study, including the effect of partial immersion to sulfate solution and the *w/c* ratio of the concrete. The control specimens were immersed in limewater. Figures 9.13 and 9.14 show their compressive and tensile load test results, respectively. Their results indicate that (as expected) both the compressive and tensile loads decrease for increasing water to cement ratios. The results in Figure 9.13 indicate that for mixes with low *w/c* ratio the compressive capacity of the specimens remained unaffected by sulfate exposure. For higher values of *w/c* ratios, an initial increase of load capacity is observed during the first 6-months of exposure. Beyond this initial period, compressive resistance deteriorates rapidly for the mixes of higher *w/c* ratios, with a reduction of more than 50% observed at the end of the 24-month exposure. Experimental results of sulfate-damaged mortars can be seen in Figures 9.18-19.

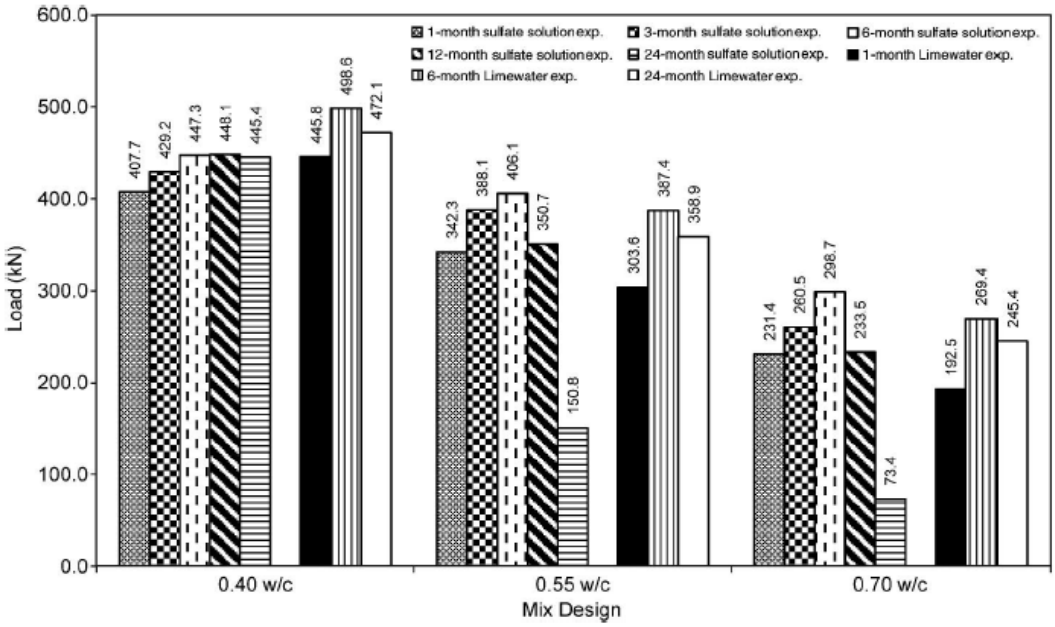

Figure 9-13 Compression load test results of (Hartell et al. 2011) for cylinders exposed to sulfate solutions.

 Copyright © MAINLINE Consortium

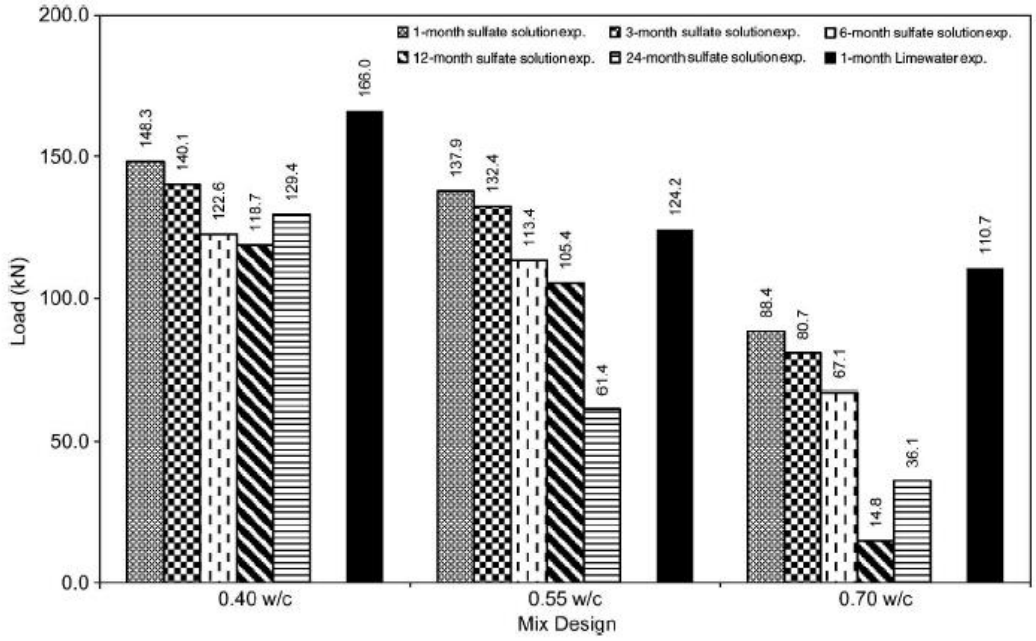

Figure 9-14 Tensile (splitting) load test results of (Hartell et al. 2011) for cylinders exposed to sulfate solutions.

The results in Figure 9.14 indicate that the tensile strength of sulfate-exposed cylinders is only moderately affected for concrete mixes with low w/c ratios. For higher w/c ratios (i.e. *w/c* = 0.55 and 0.70) a gradual reduction of tensile load is observed. In all cases shown in Figure 12 no initial increase of tensile load is observed. In these studies, no results are presented regarding the residual stiffness and ductility of the sulfate exposed concrete.

The results from these experimental studies indicate that a suitable model for predicting the evolution of mechanical properties of sulfate-damage concrete should consider a wide range of variables, including – among others – concrete composition, exposure duration and solution composition. As pointed out by Neville (2004), most research (and hence knowledge) on sulfate attack of concrete is based on laboratory based experiments and sulfate attack on concrete under (actual) field conditions remains unclear. Furthermore, the variables and processes involved in sulfate attack are likely to be associated with high variability. As a result, a desired feature of a model for predicting the influence of sulfate attack on mechanical properties of concrete is likely to be its ability to be used within a probabilistic framework.

Finally, it should be noted that in the case of reinforced concrete, cracking and spalling due to sulfate attack may allow the initiation of rebar corrosion. In this case, corrosion damage should also be considered in the structural assessment.

Freeze-thaw attack

The accumulation of damage (e.g. cracking) caused by cycles of freezing and thawing is responsible for the loss of strength and stiffness of concrete. As previously discussed, no models are at present available for predicting the evolution of mechanical properties of frost-damaged concrete with time. The experimental results from the available experimental studies indicate that as the number of freezing and thawing cycles increases the observed losses in stiffness and strength of concrete and bond strength of embedded reinforcing barsalso increase, for example see Figures 9.15 to 9.17.

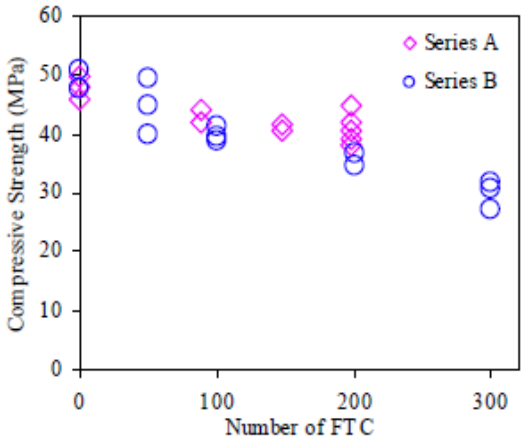

Figure 9-15 Evolution of concrete compressive strength with increasing number of freezing and thawing cycles (FTC) based on the experimental results of (Hasan et al. 2004). Series A and B correspond to the different concrete mixes used in their study.

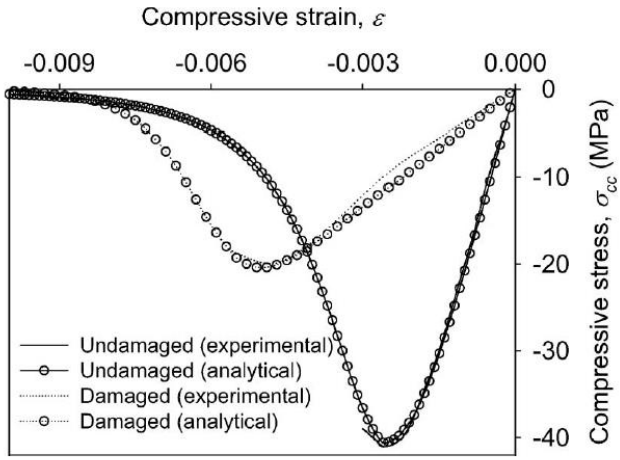

Figure 9-16 Stress – strain behaviour in compression of undamaged and frost damaged (50% reduction of compressive strength) concrete (Hanjari et al. 2013). Note that freeze-thaw cycles were continued until the desired reduction of compressive strength was obtained.

The models presented in section 9.3 are potentially useful in estimating the residual properties of concrete (e.g. σ-ε relationship of damage concrete) for a specific level of frost damage. However, these models do not provide any information on how frost damage develops over time. Furthermore, the available experimental results have been obtained in laboratory conditions. Hence, their use for assessing frost-damaged concrete in actual (field) exposure conditions is unproven and, if necessary, should be done with caution.

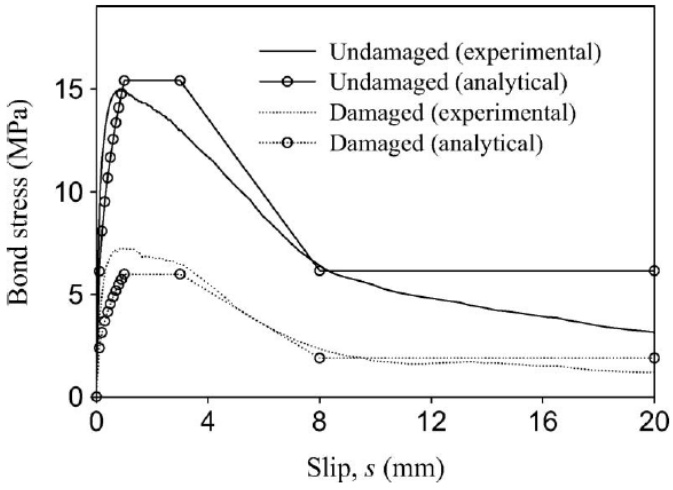

Figure 9-17 Bond stress – slip curves for reinforcing bars in undamaged and frost-damaged (50% reduction of compressive strength) concrete (Hanjari et al. 2013). Note that freeze-thaw cycles were continued until the desired reduction of compressive strength was obtained.

 Copyright © MAINLINE Consortium

9.4.2 Masonry lined tunnels

Sulfate attack

Similarly to concrete (see section 9.4.1) sulfate attack causes cracking and disintegration of the mortar. The masonry bricks (and some types of stone) can be also affected by sulfate attack. This leads to loss of stiffness and strength over time. At present no models are available for predicting the performance evolution of sulfate-damaged mortars with time. Experimental results from several studies (e.g. Lee et al. 2005) indicate that the amount and rate of losses in mechanical properties of sulfate-damaged mortars and concrete are affected by the composition of the mortar (including w/c ratio) as well as the sulfate solution (e.g. concentration of sulfates). For example, Figure 9.19 shows the evolution of compressive strength in sulfate-damaged OPC mortars with time for different types of sulfate solutions (Lee et al. 2005). Figure 9.20 shows the evolution of mortar compressive strength over time for mortars where various amounts of silica fume have been added. It is interesting to note that in all cases, an initial increase of mortar compressive strength is observed in these figures.

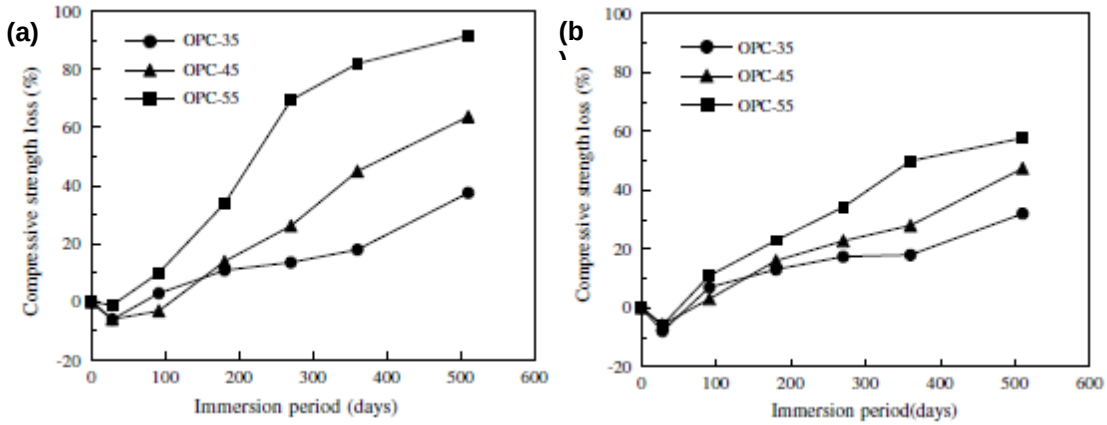

Figure 9-18 Evolution of compressive strength in sulfate-damaged OPC mortars with different w/c ratios (Lee et al. 2005): (a) 5% sodium sulfate solution and (b) 5% magnesium sulfate solution.

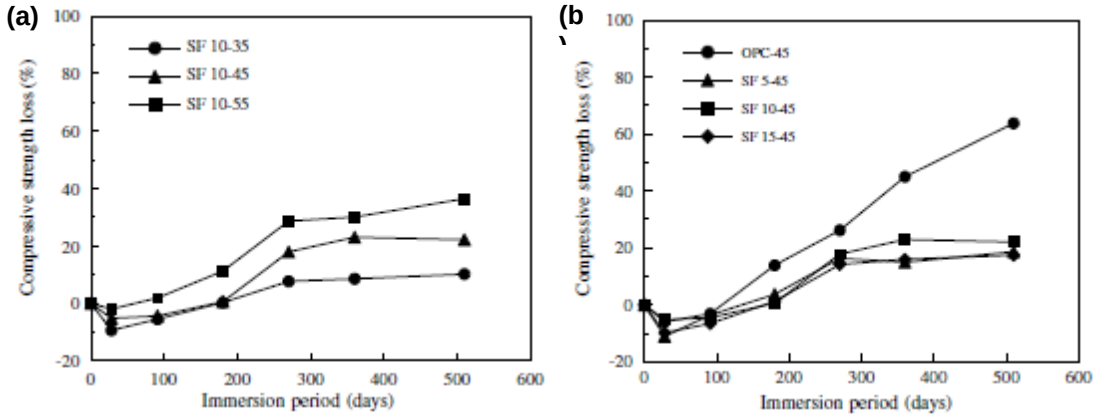

Figure 9-19 Evolution of compressive strength in sulfate-damaged mortars (in 5% sodium sulfate solution) with silica fume and varying w/c ratios (Lee et al. 2005): (a) 10% SF and (b) w/c ratio = 0.45.

 Copyright © MAINLINE Consortium

9.5 Repair and rehabilitation of concrete

Repair or rehabilitation of (reinforced) concrete involves treatment, after defects have occurred, to restore the structure to an acceptable condition. Defects cause some compromise in condition or function relative to the original, and this generally means that a process or processes have resulted in movement, loss of material, and/or loss in materials properties.

Repairs are therefore mostly reactive, and initiated when evidence of deterioration becomes apparent. The objective of repair can be defined as being to restore or enhance one property such as durability, structural strength, function or appearance. Rehabilitation refers to bringing degradation under control to enable a structure to continue to serve its intended purpose. This can be either repairing to bring concrete back to a state similar to the original, or using methods to arrest deterioration processes to enable on-going service. The literature appears to make little or no differentiation between ‘repair’ and ‘rehabilitation’.

ENV 1504-9 (2008)presents the following definitions:

- Defect: an unacceptable condition that may be in-built or may be the result of deterioration or damage.
- Protection: a measure that prevents or reduces the development of defects.
- Repair: a measure that corrects defects.

According to the deterioration mechanisms presented in Section 9.4.3, once it has been agreed that repairs are needed to meet the remaining life required of a structure, the types of repair that may be appropriate can be selected. However, there is a large range of options dependant on what the repair is meant to do, and how long it is to last. The purpose of a concrete repair in tunnel system can be one of, or combinations of, the following:

- to restore structural integrity,
- to arrest deterioration,
- to prevent future deterioration,
- to restore integrity of sealed system e.g. waterproofing,
- aesthetic appearance.

It is generally accepted that repair materials should be selected to provide the best compromise of the properties required, and may be further influenced by the funding available, availability of materials, and technical or other constraints such as application techniques and environment of working.

Tuutti (1999) states that when selecting a repair, the behaviour and properties of different materials, and how different parameters affect service life, must be understood. Failure to appreciate these factors can cause detrimental effects to a structure by the repair process, such as an increase in corrosion activity caused the formation of incipient by anodes. Areas of intense corrosion, found in structures prior to repair, have an incidental protective effect on

the surrounding steel even if the concrete is chloride contaminated, and therefore incipient anodes can develop into new corrosion sites after the intense corrosion site is repaired.

Concrete deterioration in tunnels and concrete lining may be caused by various factors including: water Infiltration, corrosion from embedded metal, thermal effects, loading conditions, and poor workmanship. As concrete deteriorates, proper repairs shall help to avoid further degradation of the structure.

9.5.1 Crack and spall repair of concrete

The repair of concrete delaminations and spalls in tunnels has traditionally been performed by the form–and–pour method for the placement of concrete, or by the hand application of cementitious mortars that have been modified by the addition of polymers. Both of these methods are not well suited for tunnels that are in continuous daily operation. This daily operation usually permits the tunnel to be out of service for very short periods of time. Therefore, the repair process must be rapid, not infringe on the operating envelope of the daily traffic and be a durable long–term monolithic repair.

Today, the repair of concrete structural elements is performed typically by two methods: the use of hand applied mortars for small repairs and the use of shotcrete for larger structural repairs. In either case the preparation of the substrate is the same, only the type of material differs.

Preparation of concrete

The surface preparation for concrete repair requires removal of all unsound concrete by either the use of chipping hammers or the use of hydro–demolition. Unsound concrete is removed to the full depth of the unsound concrete. In cases where chipping hammers are used it has been found that limiting the size of the hammers by weight is the best way to control over excavation. The use of hydro–demolition requires testing on site, at the beginning of the project to determine what pressures are required to excavate the unsound concrete without removing the sound substrate. Hydro–demolition should not be used in areas that house electrical equipment, cables, or other mechanical equipment that may be effected by the excavation process.

After the unsound concrete is removed, any leaking cracks or construction joints must be sealed prior to the application of the reinforcing steel coatings and the shotcrete. This sealing should be performed using a chemical grout suitable for the type and magnitude of the leakage. In general single component polyurethane grouts are the most successful in effectively sealing most tunnel leaks.

Preparation of steel

Once the unsound concrete has been removed, reinforcing steel must be cleaned and if a loss of section is evident the damaged reinforcing steel must be removed and replaced. All rust and scale must be removed from the reinforcing steel and any exposed steel liner sections or other structural steel elements. The cleaning is generally to a white metal commercial grade cleaning. Once cleaned the reinforcing steel is to be evaluated for loss of section and if the loss of section is greater than 30% an analysis must be performed. If the results of the analysis indicate that the lining does not have adequate strength with the remaining reinforcing steel, then the damaged steel must be replaced. After the steel has

 Copyright © MAINLINE Consortium

been cleaned a coating must be placed on the steel to protect the steel from accelerated corrosion due to the formation of an electrolytic cell. Numerous products exist for this purpose, including epoxy and zinc rich coatings. Zinc rich coatings are better suited for this application due to the fact that they do not form a bond–breaker as do many epoxies. This is important since these materials are applied by the use of a paint brush and it is difficult to prevent the concrete surface from being accidentally coated.

Repairs

Small shallow spalls are repaired by the use of a polymer modified hand patch mortar. Hand patch mortar is a pre-packaged polymer modified mortar that is applied in different lifts. Other than small repairs which utilize the repair mortars, the most commonly used material is shotcrete (or specifically pre-packaged polymer modified fibrous shotcrete).

Shotcrete Repairs

There are two processes for the application of shotcrete: Dry Process and Wet Process. Both processes have been in use for many years and are equally applicable for use in tunnel rehabilitations. The wet process creates little dust and is applicable for use in tunnels when partial tunnel closures allow traffic inside the tunnel during the repair work. The dry process creates extensive dust and is not suitable for partial tunnel closures due to limited visibility created by the dust. Once the reinforcing and structural steel elements have been cleaned and coated, welded wire mesh is to be placed over the area to be shotcreted. The wire mesh is attached to the existing reinforcing and to the substrate by specific devices.

9.5.2 Structural Injection of Cracks

Cracking is the most common defect found in concrete tunnel liners. While most of the cracks are a result of thermal activity, there are cracks that are a result of structural stresses that were not accounted for in the design. It is important to note that cracks also occur as a result of shrinkage and thermal stresses in the tunnel structure. Cracks that exhibit thermal stresses should not be structurally rebonded since they will only move and re–crack. However, structural cracks that occur as a result of structural movement, such as settlement and are no longer moving should be structurally rebonded. Any crack being considered for structural rebonding must be monitored to assess if any movement is occurring. A structural analysis of the tunnel lining should be performed to ascertain if the subject crack requires rebonding.

There are three types of resin typically available for injection of structural cracks in tunnels: vinyl ester resin, amine resin and polyester resin. Vinyl ester resin is the common type of resin used for bridge repair work and is usually not suited for tunnel work since most cracks in tunnels are damp or wet. The vinyl ester resin will not bond to surface saturated concrete and will not structurally rebond a damp or moist crack. However, if the crack is totally dry during the injection process this epoxy will provide a suitable rebonding of the concrete. Amine and polyester resins are best suited for the structural rebonding of cracks in tunnels. Both resins are unaffected by moisture during installation and will bond surface saturated concrete. Cracks with flowing water must be carefully injected and the manufacturer's advice must be obtained to ensure proper installation of the resin.

 Copyright © MAINLINE Consortium

9.5.3 Segmental Linings Repair

Segmental lining can be made up of either, precast concrete, steel or cast iron. A segmental liner is usually the primary liner of a tunnel. The segments are either bolted together or keyed. The only segmental liners that are keyed are the precast liners. The most common problems with segmental liners is deformation of the flanges in the case of steel and cast iron liners and corner spalling of precast concrete segments. The spalling of precast segments and deformation of the flanges of steel/cast iron segments usually occurs at installation or as a result of impact damage from vehicles. In addition the rusting through of the liner plate of steel/cast iron segments occasionally occurs.

The repair of spalls in precast concrete liner segments is performed by the use of a high performance polymer modified repair mortar which is formed to recreate the original lines of the segment. In the event the segment gasket is damaged the gasket's waterproofing function is restored by the injection of a polyurethane chemical grout. Damaged bolt connections in precast concrete liner segments are repaired by carefully removing the bolt and installing a new bolt, washer, waterproof gasket and nut. The bolts are to be torqued to the original specification and checked with a torque wrench.

The repair of steel/cast iron liners varies according to the type of liner material. Steel is weldable while cast iron is not. Common defects in these types of liners are deformed flanges and penetration of the liner segment due to rusting. Deformed flanges can be repaired by reshaping the flanges with hammers or heat. Holes in steel liner segments can be repaired by welding on a new plate. Bolted connections often have galvanic corrosion which is caused by dissimilar metal contact and often require the entire bolted connection to be replaced. When the bolted connection is replaced a nylon isolation gasket is used to prevent contact between the high strength bolt and the liner plate. Repairs to cast iron liner segments is similar to those for steel. However, since cast iron cannot be welded the repair plate for the segment is installed by brazing the repair plate to the cast iron or drilling and tapping the liner segment and bolting the repair plate to the original liner segment. In some instances it is easier to fill the area between the flanges with shotcrete.

9.5.4 Quality of concrete repair

Concrete repair implies integration of the new material with old concrete in order to form a composite system capable of enduring exposure to service loads, environment and time. Successful repair should enable uniform behaviour and performance of multi-layer system as a monolithic one. What makes this goal difficult are differences in age, properties and performance of two materials.

After placing the repair material, the bond starts to develop in the contact area between two materials. This results in gradual building up restraint of the overlay in the contact zone. On the other hand, as a consequence of hydration and drying, repair material tends to shrink. Since the movement is restrained by already hardened concrete substrate, stresses start to increase in the repair material. These stresses, induced by differential shrinkage between drying repair material and old concrete substrate, are considered to be main cause of premature failure of repair (Li 2009; Heinemann 2012). Differential shrinkage damage depends on many factors, some of which are the age of concrete, temperature gradients, moisture variations, matching properties of repair and substrate, boundary conditions (restraints), magnitude of induced stresses, strain capacity, etc. A number of analytical models for bonded overlays subjected to differential shrinkage have been developed

(Beushausen and Alexander 2007; Zhou, Ye & al. 2008; Denarié, Silfwerbrand & al. 2011). By experimental examination (Denarié, Silfwerbrand et al. 2011), relaxation was found to be very important as it releases approximately 40-50% of tensile overlays stresses induced by shrinkage.

Depending on the achieved properties and mutual interaction between two materials, stresses can be differently distributed and give different outcome in overall repair system. If the repair material is too strong compared to the original concrete, there is higher probability of debonding. Additionally, by increasing the bond strength, the debonding mechanism is delayed, but the level of constrain and therefore cracking tendency in repair material is enhanced.

Repair patch dimensions, such as area and thickness, can also have an influence on the performance of repair (Bissonnette, Courard& al. 2011). Large repairs tend to crack more easily than smaller repairs. Thickness is also likely to influence the bond stress by thickness dependent shrinkage (Courard 2010). What has to be determined and examined is how large the influence is of each of these two different mechanisms of damage on the likelihood of a bond failure. In other words, if a certain amount of damage is inevitable, which mechanism is more dangerous regarding overall performance of the repair.

Considering all stated, crucial parameters for achieving reliable performance and durability of the repair are compatibility of properties of repair material and concrete substrate and sufficient bonding mechanism and bond properties at the interface (Luković& al, 2012).

Compatibility

Compatibility is a balance between deformational, physical, chemical, electrochemical and aesthetic properties between a repair material and existing substrate which needs to ensure that repair system withstands stresses induced by restrained volume change, chemical and electrochemical effects without premature deterioration (Vaysburd and Emmons 2004, 2006). Otherwise, incompatibility may result in initial tensile stresses that either crack the repair material or cause debonding at the interface. Dimensional compatibility, which includes drying shrinkage, thermal expansion, creep, and modulus of elasticity, is the most significant component. Important matching properties of concrete substrate and repair material are stated.

Bond strength and bonding mechanism in transition zone

Parameters that affect bond strength and bond development at the interface between concrete substrate and repair material are adhesion force and moisture transport.

Adhesion

According to the European Standard (EN1504-10:2004), bond is defined as the adhesion of the applied product or system to the concrete substrate. In that aspect, adhesion can be considered as a fundamental issue in repair of concrete structures (Czarnecki 2008). In the European Standard for repair (EN1504-3:2005), it is stated that tensile bond strength should be at least 2 MPa for structural and 1 MPa for non- structural repairs. Properties of both repair material and concrete substrate, as well as exposure conditions, have an influence on achieved adhesive strength in repair system (Czarnecki 2008). Very important step in achieving sufficient level of adhesion is appropriate surface preparation of concrete

 Copyright © MAINLINE Consortium

substrate. The first step should be identification of unsound/contaminated concrete, and its removal. After that different surface treatment are applied in order to clean the surface and accomplish appropriate roughness of concrete substrate: hammering, sandblasting, hydrojetting, scarifying, acid- etching, shotblasting. It has to be noted that some of the impacting methods such as jack hammering can induce microcracking and surface damage which "easily outweighs the benefits of an increased roughness" (Courard 2000; Bissonnette, Nuta& al. 2008). Adequate fluidity and workability are paramount properties of the repair material which influence the developing adhesion force. Lower viscosity, lower contact angle and higher superficial tension of the repair material enable faster spreading, penetration into the waviness profile of the concrete substrate and higher interaction area between two materials. As a viscosity of repair material increases in time, it is very important to enable contact between repair material and original concrete as soon as possible (Bissonnette, Courard & al. 2011).

Adhesion and, therefore, strength and integrity of the bond depend not only on physical and chemical characteristics of the repair material and concrete substrate, but also on the environmental conditions that the repaired structure is exposed to. Temperature and relative humidity of the environment have great influence on initial saturation level of concrete substrate. There is a widespread agreement to promote the "saturated substrate with dry surface" as one of the best compromises for achieving good surface preparation (Bissonnette, Courard & al. 2011). Curing period of repair patches, which has not been thoroughly examined and usually is neglected, is very important for achieving good adhesion.

In order to gain higher adhesion, Portland cement grout, latex modified Portland cement grout, and epoxy resins are sometimes used as a bonding agents. But this implies than sometimes instead of one potential weak zone, two interfaces might be created. That is why Bissonnette, Courard & al. (2011) stated that the use of bonding agents should normally be avoided. In addition, it has to be noted that application of different chemical substances cannot be the substitution for poor and inadequate workmanship.

Moisture transport

Sun, Ye et al. (2005) stated that microstructure of cement based materials could be described by the following parameters: degree of hydration, volume fraction and distribution of the total solid phase and the pore phase. These microstructural properties dominate further development of mechanical properties of cement based materials.

Interface zone presents a weak link in a repaired structure. The interface between old and new concrete is very similar to bond between aggregates and cement paste. Therefore, well known phenomenon called the "wall effect" could be expected at the interfacial zone between repair material and concrete substrate. One of the reasons for existence of this layer with high porosity can be explained by the loose packing of cement particles. Also, the concentration of small particles in the interfacial zone makes it possible that the degree of hydration in this zone is higher than in the bulk paste (Van Breugel 1991). The addition of ultra-fines like silica fume and fly ash was found to be beneficial in a way of reducing porosity and therefore increasing micro-hardness in this weak zone. But, what makes the interface between the repair material and the concrete substrate more complex than interfacial zone between aggregate and cement paste, is the sorptivity of unsaturated concrete substrate. In other words, aggregates are usually impermeable, whereas concrete substrate is porous material which absorbs water from initially fully saturated repair material. Consequently,

 Copyright © MAINLINE Consortium

development of microstructure and mechanical properties in repaired systems is additionally affected by moisture transport between the two materials.

After placing of the repair material, it starts hardening. Its microstructure starts forming and process is driven by hydration. This causes continuous changes in phases present in the repair material. Due to a continuous change of pore structure with age and wide range of pore sizes present in cement paste, migration of moisture within concrete is more complex than in most other porous media. Moisture transport is driven by difference in moisture content between repair material and surface, and between repair material and concrete substrate. Water will move from areas with higher to areas with lower water concentrations. What complicates the problem is that the diffusion coefficient, which determines the rate of transport, is dependent on moisture content in pore structure. In the literature, it is found that the diffusion coefficient decreases by about 10 to 20 times when passing from 90% to 60% pore humidity (Bažant and Najjar 1972). The diffusion coefficient of a concrete substrate is, therefore, dependent on the moisture content and the already formed pore structure of the hardened concrete, while the diffusion coefficient of the repair material is dependent on the moisture content and on-going hydration which causes continuous change of the pore structure. But, diffusion affects the rate of cement hydration as it decreases the water amount available for further hydration process and slows down reaction. Initial water cement ratio in bulk repair material also decreases. Although, this can be beneficial, as the bond strength may increase, for low water to cement mixtures, there might not be enough water for further hydration. This may significantly affect the quality of the repair.

By resolving moisture movement through new and old concrete, degree of hydration, local water-cement ration and pore structure at the interface can be determined. This way the key factor regarding bonding mechanism between concrete substrate and repair material would be obtained, giving useful information regarding quality and development of the bond. According to present literature review, microstructure properties and development at the interface are not investigated thoroughly.

9.5.5 Influence of repair actions

It is clear that to achieve the goal of more durable repaired concrete structures, practitioners must use techniques and procedures that are appropriate for the deterioration mechanism(s), environmental conditions and structural circumstances which exist for the specific structure or part of the structure under consideration. There is also a need to take a wider and longer term view upon these matters. Unfortunately, at the moment a short- term ‘first cost’ focus is generally being taken by most owners of buildings and structures, rather than a longer-term ‘remaining life’ perspective which overall might be more efficient and effective from a wider financial and sustainability viewpoint. This is often done for well-understood, but unfortunate, reasons and is commonly in response to severe financial pressures and limitations upon budgets available for maintenance and remedial works.

It is postulated that the through-life management of concrete structures could be improved by (Matthews 2007, Matthews, Sarkkinen & al 2007):

- Early intervention, before damage is visible.
- Proactive monitoring and maintenance in support of this.
- Correct diagnosis of the problem and mechanism(s) causing the deterioration.

 Copyright © MAINLINE Consortium

- Effective intervention systems for preventative and remedial treatments.

Indeed, it is critical that a wider and more sustainable perspective is taken upon the creation of new structures and for the through-life care and management of existing structures. These issues are central to the philosophy and concepts behind the approach outlined in the CONREPNET project (2001).

Figure 9.15 illustrates the underlying concept, taking the situation of steel reinforcement embedded in the concrete and the circumstances leading to corrosion. This assumes that a sufficient concentration of oxygen and moisture is present to facilitate corrosion. A very simple two-stage linear corrosion model (after Tuutti - 1999) has been adopted. This is portrayed by the orange line in Fig.9.20. In the early life of the structure (the initiation phase), the ingress of aggressive species occurs through the cover concrete (e.g. carbon dioxide, chlorides). After some time, the surface of the reinforcement becomes depassivated permitting corrosion to begin. The corrosion propagation phase is entered and corrosion products are produced, with cracking of the concrete and spalling following at some later time. The diagram also illustrates when visible damage is likely to occur in this process. It will be seen that this is relatively late, only becoming apparent sometime after the fundamental deterioration (which leads eventually to damage, possibly years later) has taken place.

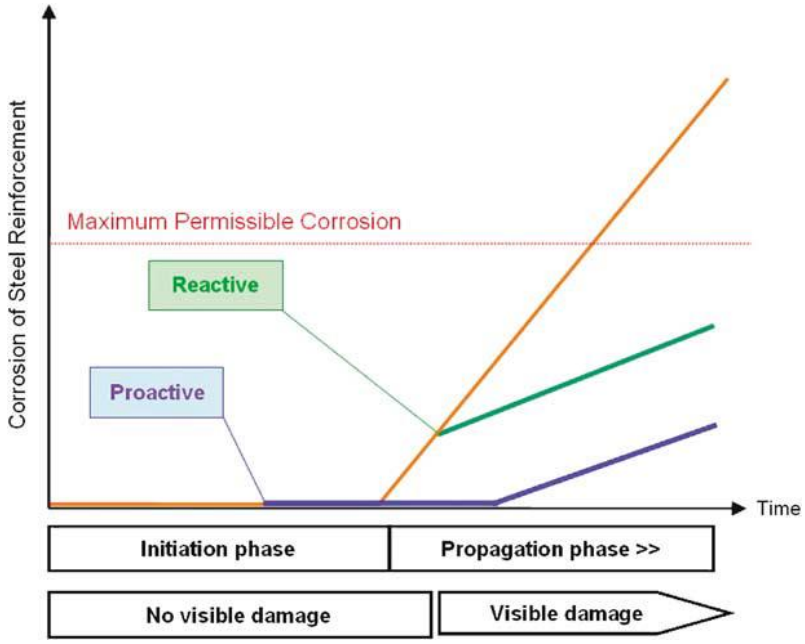

Figure 9-20 Reactive and proactive approaches to the maintenance of structures suffering from reinforcement corrosion (Matthews 2007)

Reactive maintenance is likely to be instigated only when visible indications appear (eg cracking or spalling of concrete), with an intervention being made to slow the rate of deterioration and extend the useful service life of the structure. This response is illustrated by the green line in Fig.9.21. Proactive maintenance, such as the early application of a coating to slow the ingress of the aggressive species, could potentially delay the onset of corrosion and extend the useful service life. Such action would be undertaken during the initiation phase and is portrayed by the blue line in Figure 9.21.

The implementation of these concepts is illustrated in Figure 9.21, which presents a time-line representation of the two alternative philosophies. The green line portrays the variation in

 Copyright © MAINLINE Consortium

performance with time when a reactive strategy is followed. The blue line symbolises the potentially much smaller variation in performance with time associated with the adoption of a proactive strategy. The plot includes a notional indication of their respective costs. The periods of disruption associated with each approach are also indicated by similarly coloured vertical dashed lines. A number of shorter periods are likely to be required for the proactive approach, compared with a significantly longer period for the greater amount of work involved in the reactive repairs.

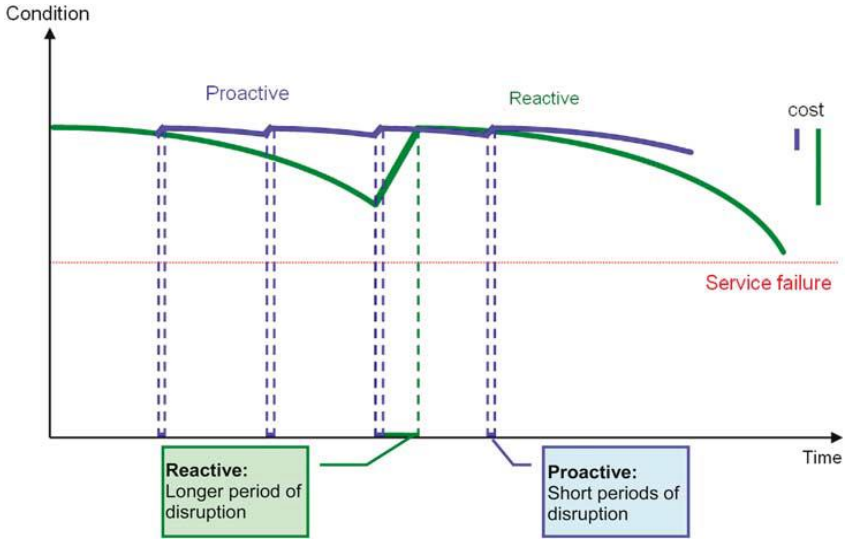

Figure 9-21 Alternative approaches to the management and maintenance of structures (CONREPNET 2007)

It is clear that both strategies assume that the condition is fully restored, as far as the right repair techniques have been successfully applied.

9.6 Concluding remarks

This report provides a review of the most commonly observed deterioration mechanisms of masonry and concrete tunnels. The available models which can be used to quantify the different types of deterioration on tunnel performance are reviewed with emphasis given to concrete lined tunnels. The conclusions of this report may be summarised as follows:

- The types of tunnel deterioration can be grouped as geotechnical related deterioration and material related deterioration. A third group is related to degradation due to accidental damage (including fire); this however is beyond the scope of this report.

- Geotechnical related deterioration is related to changes in the ground conditions adjacent to the tunnel, for instance changes in the stress distribution due to slope instability.

- Reinforcement corrosion and frost damage (due to freezing and thawing cycles) are commonly observed material-related deterioration mechanisms in concrete tunnels. These deterioration mechanisms are responsible for the loss of mechanical properties of mortars and concrete due to cracking development and material disintegration.

 Copyright © MAINLINE Consortium

- The development of deterioration-time profiles in relation to sulfate attack requires knowledge of the soil composition and concrete characteristics (e.g. through the analysis of sampled soil and concrete cores).

- Similarly, the development of deterioration-time profiles with respect to freeze-thaw action requires understanding of temperature variations in relation to the quality of concrete mixes used.

- A number of models are available for estimating the residual mechanical properties of sulfate and frost-damaged concrete; however, they do not provide information on how degradation develops over time.

- In the absence of deterioration models for masonry lined tunnels, the use of field inspection data will be explored in relating changes of condition with time.

For concrete linen, the chapter presents the influence of repair/rehabilitation interventions and their consequences on the deterioration profile as long as the intervention are correctly performed.

9.7 References

Alexopoulos, N.D., Apostolopoulos, C.A., Papadopoulos, M.P., Pantelakis, S.G. (2007), “Mechanical performance of BStIV grade steel bars with regard to the long-term material degradation due to corrosion damage”, Construction and Building Materials 21:1362-1369.

Almusallam, A.A. (2001), “Effect of degree of corrosion on the properties of reinforcing steel bars”, Construction and Building Materials 15(8):361-368.

Ann, K.Y., Song, H.W. (2007), “Chloride threshold level for corrosion of steel in concrete”, Corrosion Science 49:4113-33.

Bažant Z., Najjar L. (1972), “Nonlinear water diffusion in nonsaturated concrete”, Materials and structures 5(1): 3-20.

Bazant, Z.P., Chern, J.C., Rosenberg, A.M., Gaidis, J.M. (1988), “Mathematical model for freeze-thaw durability of concrete”, J. Am. Ceram. Soc. 71:776-783.

Berra, M., Castellani, A., Coronelli, D., Zanni, S., Zhang, G. (2003), “Steel-concrete bond deterioration due to corrosion: finite-element analysis for different confinement levels”, Magazine of Concrete Research 55(3):237-247.

Bertolini, L., Elsener, B., Pedeferri, P., Polder, R. (2004), “Corrosion of steel in concrete: Prevention, diagnosis, repair”, Wiley-VCH, ISBN 3-527-30800-8.

Beushausen H. D., Alexander M. (2007), “Performance of concrete patch repair systems”, Advances in Construction Materials: 255-262.

Bissonnette B., Courard L. & al (2011), “Bonded cement-based material overlays for the repair, the lining or the strengthening of slabs or pavements”, State-of-the-art report of the RILEM Technical Committee 193-RLS, Springer Verlag.

 Copyright © MAINLINE Consortium

Bissonnette B., Nuta A. & al (2008). Concrete repair and interfacial bond: Influence of surface preparation, CRC.

Bozinovski, Z.L., Lahdensivu, J., Vesikari, E. (2011), “Degradation modes and models for masonry structures”, in Chapter 2, State-of-the-Art Report on Deterministic and Probabilistic Degradation Models: Degradation Models for Service Life Design, Summary Report of the Cooperative Activities of the COST Action 25, Sustainability of Constructions – Integrated Approach to Life-time Structural Engineering, Volume 2, pp. 69-80.

Broomfield, J.P. (1997), “Corrosion of steel in concrete: Understanding, investigation and repair”, E&FN SPON, ISBN 0-419-19630-7.

Brueckner, R., Williamson, S.J., Clark, L.A. (2012), “Rate of the thaumasite form of sulfate attack under laboratory conditions”, Cement & Concrete Composites 34:365-369.

BS EN. (2000), “BS EN 206-1:2000. Concrete – Part 1: Specification, performance, production and conformity”, BSi.

Cairns, J., Plizzari, G.A., Du, Y., Law, D.W., Franzoni, C. (2005), “Mechanical properties of corrosion-damaged reinforcement”, ACI Materials Journal 102(4):256-264.

Chung, L., Najm, H., Balaguru, P. (2008), “Flexural behaviour of concrete slabs with corroded bars”, Cement & Concrete Composites 30:184-93.

CIRIA. (2009), “Tunnels: inspection, assessment and maintenance”, C671, CIRIA, ISBN: 978-086017-671-8, London.

Clifton, J.R., Frohnsdorff, G., Ferraris, C. (1999), “Standards for evaluating the susceptibility of cement-based materials to external sulfate attack”, Materials Science of Concrete – Sulfate Attack Mechanisms, Special Volume (Proceedings from Seminar on Sulfate Attack Mechanisms, Quebec, Canada, October 5-6, 1998), American Ceramic Society, pp.337-355.

CONREPNET (2001), “CONREPNET. Thematic network on performance-based remediation of reinforced concrete structures”, GTC1-2001-43067, European Commission.

Coronelli, D., Gambarova, P. (2004), “Structural assessment of corroded reinforced concrete beams: modelling guidelines”, Journal of Structural Engineering 130(8):1214-24.

Collepardi, M., Marcialis, A., Turriziani, R. (1972), “Penetration of chloride ions into cement pastes and concretes”, Journal of the American Ceramic Society 55(10):534-535.

Corral-Higuera, R., Arredondo-Rea, S.P., Neri-Flores, M.A., Gomez-Soberon, J.M., Almeraya-Calderon, F., Castorena-Gonzalez, J.H., Almaral-Sanchez, J.L. (2011), “Sulfate attack and reinforcement corrosion in concrete with recycled concrete aggregates and supplementary cementing materials”, International Journal of Electrochemical Science 6:613-621.

Courard L. (2000), “Parametric study for the creation of the interface between concrete and repair products”, Materials and structures 33(1): 65-72.

 Copyright © MAINLINE Consortium

Crammond, N.J. (2003), “The thaumasite form of sulfate attack in the UK”, Cement & Concrete Composites 25:809-818.

CTRE. (2006), “Evaluation of corrosion resistance of different steel reinforcement types”, Center for Transportation Research and Education (CTRE), Bridge Engineering Center, Iowa State University, CTRE Project 02-103.

Czarnecki L. (2008),”Adhesion–A challenge for concrete repair”, CRC.

Denarié E., Silfwerbrand J. (2011), “Structural behaviour, bonded cement-based material overlays for the repair, the lining or the strengthening of Slabs or Pavements: 81-106.

Diab, A.M., Awad, A.E.M., Elyamany, H.E., Elmoaty, A.E.M.A. (2012), “Guidelines in compressive strength assessment of concrete modified with silica fume due to magnesium sulfate attack”, Construction and Building Materials 36:311-318.

Du, Y.G., Clark, L.A., Chan, A.H.C. (2005a), “Residual capacity of corroded reinforcing bars”, Magazine of Concrete Research 57(3):135-147.

Du, Y.G., Clark, L.A., Chan, A.H.C. (2005b), “Effect of corrosion on ductility of reinforcing bars”, Magazine of Concrete Research 57(7):407-419.

Duracrete. (2000), “DuraCrete: Probabilistic performance based durability design of concrete structures”, DuraCrete Final Technical Report, The European Union – BriteEuRam III, Contract BRPR-CT95-0132, Project BE95-1347, Document BE95-1347/R17.

EN1504-10 (2004), “Products and systems for the protection and repair of concrete structures - Definitions - Requirements - Quality control and evaluation of conformity - Part 10: Site application of products and systems and quality control of the works”.

EN1504-1 (2005), “Products and systems for the protection and repair of concrete structures - Definitions, requirements, quality control and evaluation of conformity - Part 1: Definitions”.

EN1504-3 (2005), “Products and systems for the protection and repair of concrete structures - Definitions, requirements, quality control and evaluation of conformity - Part 3: Structural and non-structural repair”.

EN1504-9 (2008), “Products and systems for the protection and repair of concrete structures- Definitions, requirements, quality control and evaluation of conformity- Part 9: General principles for the use of products and systems”.

Fang, C., Lundgren, K., Chen, L., Zhu, C. (2004), “Corrosion influence on bond in reinforced concrete”, Cement and Concrete Research 34:2159-2167.

FIB. (2000), “Bond of reinforcement in concrete, State-of-art report”, fib bulletin 10, Federation Internationale du Beton, prepared by Task Group Bond Models, Lausanne.

FIB. (2006), “Model code for service life design”, fib Bulletin No. 34, ISBN: 978-2-288394-074-1.

 Copyright © MAINLINE Consortium

Glass, G.K., Buenfeld, N.R. (2000), “Chloride-induced corrosion of steel in concrete”, Prog.Struct.Engng Mater. 2:448-58.

Gonzalez, J.A., Andrade, C., Alonso, C., Feliu, S. (1995), “Comparison of rates of general corrosion and maximum pitting penetration on concrete embedded steel reinforcement”, Cement Conc Res, 25(2):257–264.

Graig, R.F. (2007), “Graig’s soil mechanics”, Seventh edition, Spon Press.

Hanjari, K.Z., Kettil, P., Lundgren, K. (2013), “Modelling the structural behaviour of frost-damaged reinforced concrete structures”, Structure and Infrastructure Engineering 9(5):416-431.

Hartell, J.A., Boyd, A.J., Ferraro, C.C. (2011), “Sulfate attack on concrete: Effect of partial immersion”, Journal of Materials in Civil Engineering 23(5):572-579.

Hasan, M., Okuyama, H., Sato, Y., Ueda, T. (2004), “Stress-strain model of concrete damaged by freezing and thawing cycles”, Journal of Advanced Concrete Technology 2(1):89-99.

Hasan, M., Ueda, T., Sato, Y. (2008), “Stress-strain relationship of frost-damaged concrete subjected to fatigue loading”, Journal of Materials in Civil Engineering 20(1):37-45.

Inokuma, A., Inano, S. (1996), “Road tunnels in Japan: deterioration and countermeasures”, Tunnelling and Underground Space Technology 11(3):305-309.

Ireland, T.J., Rock, T.A., Hoyland, P. (2007), “Planning and design of the A3 Hindhead tunnel, Surrey, UK”, in Underground Space – the 4th Dimension of Metropolises, Bartak, Hrdina, Romancov&Zlamal (eds), Taylor & Francis Group, London, ISBN 978-0-415-40807-3.

Kallias, A.N., Rafiq, M.I. (2013), “Performance assessment of corroding RC beams using response surface methodology”, Engineering Structures 49:671-685.

Kashani, M.M., Crewe, A.J., Alexander, N.A. (2013), “Nonlinear stress-strain behaviour of corrosion damaged reinforcing bars including inelastic buckling”, Engineering Structures 48:417-429.

Kimura, S., Kitani, T., Koizumi, A. (2012), “Development of performance-based tunnel evaluation methodology and performance evaluation of existing railway tunnels”, Journal of Transportation Technologies 2:113-128.

Kosior-Kazberuk, M. (2012), “Effects of interaction of static load and frost damage mechanism of concrete elements”, Journal of Sustainable Architecture and Civil Engineering 1(1):40-45.

Lee, S.T., Moon, H.Y., Swamy, R.N. (2005), “Sulfate attack and the role of silica fume in resisting strength loss”, Cement & Concrete Composites 27:65-76.

Leemann, A., Loser, R. (2011), “Analysis of concrete in a vertical ventilation shaft exposed to sulfate-containing groundwater for 45 years”, Cement & Concrete Composites 33:74-83.

 Copyright © MAINLINE Consortium

Li V. C., Horii H. (2000), Repair and retrofit with engineered cementitious composites, Engineering Fracture Mechanics 65(2-3), 317-334.

Long, G.C., Xie, Y.J., Deng, D.H., Li, X.K. (2011), “Deterioration of concrete railway tunnel suffering from sulfate attack”, J. Cent. South Univ. Technol. (Springer), 18:881-888.

Luković M., Ye G., van Breugel K (2012), “Reliable concrete repair: A critical review”, International Conference Structural Faults and Repair, Edinburgh, Scotland, UK, 3-5 July 2012.

Lundgren, K. (2005), “Bond between ribbed bars and concrete. Part 2: The effect of corrosion”, Magazine of Concrete Research 57(7):383-95.

Lundgren, K. (2007), “Effect of corrosion on the bond between steel and concrete: an overview”, Magazine of Concrete Research 59(6):447-61.

Ma, K.L., Long, G.C., Xie, Y.J. (2012), “Railway tunnel concrete lining damaged by formation of gypsum, thaumasite and sulfate crystallization products in southwest China”, J. Cent. South Univ. 19:2340-2347, (Springer).

Malumbela, G., Alexander, M., Moyo, P. (2009), “Steel corrosion on RC structures under sustained service loads – A critical review”, Engineering Structures 31:2518-25.

Martin-Perez, B., Pantazopoulou, S.J. (2001b), “Effect of bond, aggregate interlock and dowel action on the shear strength degradation of reinforced concrete”, Engineering Structures 23:214-27.

Martin-Perez, B., Pantazopoulou, S.J., Thomas, M.D.A. (2001a), “Numerical solution of mass transport equations in concrete structures”, Computers & Structures 79:1251-64.

Matthews 2007, “Achieving durable repaired concrete structures: a performance-based approach”, Proceedings of the Institution of Civil Engineers, Structures & Buildings 160, Issue SB1, 1–12

Matthews S.L., Sarkkinen M., Morlidge J. R (2007), “Achieving durable repaired concrete structures: Adopting a performance-based intervention strategy”, IHS BRE Press, Watford, UK.

Matsumoto, M., Hokoi, S., Hatano, M., “Model for simulation of freezing and thawing processes in building materials”, Building and Environment 36:733-742.

Neville, A. (2004), “The confused world of sulfate attack on concrete”, Cement and Concrete Research 34:1275-1296.

Otieno, M.B., Beushausen, H.S., Alexander, M.G. (2011), “Modelling corrosion propagation in reinforced concrete structures – A critical review”, Cement & Concrete Composites 33:240-5.

Palsson, R., Mirza, M.S. (2002), “Mechanical response of corroded steel reinforcement of abandoned concrete bridge”, ACI Structural Journal 99(2):157-162.

 Copyright © MAINLINE Consortium

Perez F., Bissonnette B. (2009), “Parameters affecting the debonding risk of bonded overlays used on reinforced concrete slab subjected to flexural loading”, Materials and structures 42(5): 645-662.

Rodriguez, J., Ortega, L.M., Casal, J. (1994), “Corrosion of reinforcing bar and service life of reinforced concrete structures: Corrosion and bond deterioration”, Proc. Int. Conf. on Concrete Across borders, Vol.2, pp.315-326.

Rodriguez J., Munoz R. (2006), “Manual REHABCON on concrete repair and rehabilitation, Concrete Repair, Rehabilitation and Retrofitting”, Taylor & Francis Group, London, ISBN 0415(39654):9.

Sandrone, F., Labiouse, V. (2011), “Identification and analysis of Swiss national road tunnels pathologies”, Tunnelling and Underground Space Technology 26:374-390.

Stewart, M.G. (2009), “Mechanical behaviour of pitting corrosion of flexural and shear reinforcement and its effect on structural reliability of corroding RC beams”, Structural Safety 31(1):19-30.

Stewart, M.G. (2012), “Spatial and time-dependent reliability modelling of corrosion damage, safety and maintenance for reinforced concrete structures”, Structure and Infrastructure Engineering: Maintenance, Management Life-Cycle Design and Performance 8(6):607-619.

Stanton, T.E. (1940), “Expansion of concrete through reaction between cement and aggregate”, Proc. ASCE 66:1781-1811.

Sun Z., Ye G. & al (2005), “Microstructure and Early-Age Properties of Portland Cement Paste - Effects of Connectivity of Solid Phases”, Materials Journal 102, 122-129.

Suput, J.S., Mladenovic, A., Cernilogar, L., Olensek, V. (2003), “Deterioration of mortar caused by the formation of thaumasite on the limestone cladding of some Slovenian railway tunnels”, Cement & Concrete Composites 25:1141-1145.

Swamy, R.N. (Ed.). (1992), “The alkali-silica reaction in concrete”, Van Nostrand Reinhold, ISBN 0-216-92691-2.

Tuutti K. (1999), “Repair Philosophy for Concrete Structures”, Proceedings of the international conference on concrete durability and repair technology, University of Dundee, Scotland, UK, 8-10 September 1999, 159-169

Ueda, T., Hasan, M., Nagai, K., Sato, Y., Wang, L. (2009), “Mesoscale simulation of influence of frost damage on mechanical properties of concrete”, Journal of Materials in Civil Engineering 21(6):244-252.

Val, D.V., Chernin, L. (2009), “Serviceability reliability of reinforced concrete beams with corroded reinforcement”, Journal of Structural Engineering 135(8):896-905.

Vaysburd A.H., Emmons P.H. (2006), “Concrete Repair- a Composite System: Philosophy, Engineering and Practice”, Restoration of Buildings and Monuments 12(5/6): 423.

 Copyright © MAINLINE Consortium

Vaysburd A. M., Emmons P.H. (2004)," Concrete repair technology-a revised approach is needed", Concrete international 26(1): 59-65.

Wang, T.T. (2010), "Characterizing crack patterns on tunnel linings associated with shear deformation induced by instability of neighboring slopes", Engineering Geology 155:80-95.

Yoon, S., Wang, K., Weiss, W., Shah, S. (2000), "Interaction between loading, corrosion, and serviceability of reinforcement in concrete", ACI Materials Journal 97(6):637-44.

Youakim, S.A.S., El-Metewally, S.E.E., Chen, W.F. (2000), "Nonlinear analysis of tunnels in clayey/sandy soil with a concrete lining", Engineering Structures 22:707-722.

Zhang, M., Chen, J., Lv, Y., Wang, D., Ye, J. (2013), "Study on the expansion of concrete under attack of sulfate and sulfate-chloride ions", Construction and Building Materials 39:26-32.

Zhao J. Song T. (2011), "Fiber-reinforced rapid repair material for concrete pavement", Advanced Materials Research 168: 870-874.

Zhou J., Ye G. & al (2008), "Modelling of stresses and strains in bonded concrete overlays subjected to differential volume changes", Theoretical and Applied Fracture Mechanics 49(2): 199-205.

Zuber, B., Marchand, J. (2000), "Modeling the deterioration of hydrated cement systems exposed to frost action, Part 1: description of the mathematical model", Cement and Concrete Research 30:1929-1939.

 Copyright © MAINLINE Consortium

10. Conclusions

This deliverable specifies relevant deterioration models for selected assets to be given special focus in the MAINLINE project and Work Package 5 for the application of the LCAT toolbox. These models will be introduced in the performance models as developed in deliverable D2.3.

Data for practical applications is not included in this deliverable and will be documented in the application cases of deliverable D5.5.

 Copyright © MAINLINE Consortium